Phys 2
SEP 29 1932

VOLUME 41 SECOND SERIES NUMBER 6

THE PHYSICAL REVIEW

PUBLISHED BY THE
AMERICAN INSTITUTE OF PHYSICS
INCORPORATED

UNDER THE EDITORIAL SUPERVISION OF THE
AMERICAN PHYSICAL SOCIETY

BOARD OF EDITORS
Managing Editor, JOHN T. TATE, University of Minnesota, Minneapolis
Assistant Editor, J. W. BUCHTA, University of Minnesota, Minneapolis
K. F. HERZFELD, A. W. HULL, F. W. LOOMIS, A. J. DEMPSTER, DAVID M. DENNISON
J. C. SLATER, R. C. GIBBS, E. O. LAWRENCE, J. H. VAN VLECK

SEPTEMBER 15, 1932

Faraday Effect with X-Rays – – – – – – – – – – – DAROL K. FROMAN 693
New Measurements of the Ranges of Alpha-Particles from Polonium, Uranium I and Uranium II with the Wilson Chamber – – – – – – – – – – – F. N. D. KURIE 701
Relativistic Thomas-Fermi Atom – – – – – M. S. VALLARTA AND N. ROSEN 708
Wentzel-Brillouin-Kramers Method of Solving the Wave Equation – – J. L. DUNHAM 713
Energy Levels of a Rotating Vibrator – – – – – – – – – J. L. DUNHAM 721
Rotational Analysis of Some CO_2 Emission Bands. Part I – – – – – R. F. SCHMID 732
Electronic Structures of Polyatomic Molecules and Valence. III. Quantum Theory of the Double Bond – – – – – – – – – – – – – ROBERT S. MULLIKEN 751
Production of Infrared Spectra with Electric Fields – – – – – – – E. U. CONDON 759
Impacts of Fast Electrons and Magnetic Neutrons – J. F. CARLSON AND J. R. OPPENHEIMER 763
Photoelectric and Thermionic Emission from Composite Surfaces – WAYNE B. NOTTINGHAM 793
Relation between the Electric and Diamagnetic Susceptibilities of Monatomic Gases – J. P. VINTI 813
Variation of the Principal Magnetic Susceptibilities of Certain Paramagnetic Crystals with Temperature – – – – – – – – – – – – – – – B. W. BARTLETT 818
Supersonic Dispersion and Absorption in CO_2 – – – – – – W. H. PIELEMEIER 833
Letters to the Editor – 838
Angular Distribution of Elastically Scattered Electrons in Mercury Vapour – F. L. ARNOT 838
Lower Limit for the Ground State of the Helium Atom – – – – – D. H. WEINSTEIN 839
Book Review – 840
Author Index to Volume 41 – – – – – – – – – – – – – – – – – – 841
Analytic Subject Index to Volume 41 – – – – – – – – – – – – – – 845
Current Literature of Physics

THE AMERICAN INSTITUTE OF PHYSICS INCORPORATED
11 EAST 38th STREET, NEW YORK, N. Y.

THE AMERICAN PHYSICAL SOCIETY

OFFICERS OF THE SOCIETY

President:	W. F. G. Swann	Bartol Research Foundation, Philadelphia, Pa.
Vice-President:	Paul D. Foote	The Gulf Companies, Pittsburgh, Pa.
Secretary:	W. L. Severinghaus	Columbia University, New York City
Treasurer:	G. B. Pegram	Columbia University, New York City
Editor:	John T. Tate	University of Minnesota, Minneapolis, Minn.
Local Secretary for the Pacific Coast:	L. B. Loeb	University of California, Berkeley, Calif.

THE PHYSICAL REVIEW

Published by the American Institute of Physics under the editorial supervision of the American Physical Society. Four volumes annually, six issues per volume.

First series. From July 1, 1893, to January 1, 1913, the Review was conducted by Edward L. Nichols, Ernest Merritt and Frederick Bedell, with the financial support of Cornell University. The first four volumes were issued annually; subsequent volumes, semi-annually; thirty-five volumes in all.

Second series. On January 1, 1913, the Review was transferred to the American Physical Society as announced on the first page of the new series which was then begun. Since then it has been conducted by a Board of Editors elected by the Society. Volumes 1-38 are semi-annual, beginning in January and July of each year from 1913 to 1931. Volumes 1-33 contain six issues each. Volumes 34-38 twelve issues. Beginning with Volume 39 there will be four volumes per year of six issues each.

Annual subscription, throughout the Postal Union, $12.00 in advance.

General index, 1893-1920, $4.00 in advance.

Back Volumes. Volumes 1-38, $9.00 per volume; Volume 39, $4.50; Back Numbers, $1.50 per copy for issues prior to July 1, 1929 (Vols. 1-33), $.75 per copy for issues subsequent thereto. Postage is free if remittance accompanies order; otherwise postage is extra. No bound volumes can be supplied. The Review offers to purchase a limited number of First Series, Vol. 1, No. 1 (at $2.00 each); Second Series, Vol. 7, No. 1, January 1916; Vol. 7, No. 2, February 1916; Vol. 7, No. 4, April 1916; and Vol. 7, No. 5, May 1916 (at $2.00 each).

Advertisements. Rates will be supplied on request. Copy for each number must be received two weeks prior to the dates of issue; old copy is used until new copy is received. Send electrotypes direct to printers, George Banta Publishing Co., Menasha, Wis.

Discount of ten percent is allowed to members of the American Physical Society on purchase of back numbers.

Changes of Address and Complaints of failure to receive the Review, in the case of members of the Physical Society, should be addressed to the Treasurer; in the case of other subscribers, to the Editorial Secretary. New copies can be sent free in response to complaints of non-delivery only if notice of non-delivery is received within three months of date of issue.

Manuscripts for publication should be submitted to the Editor, Physical Review, University of Minnesota, Minneapolis, Minn.

Proof and all correspondence concerning papers in process of publication should be addressed to the Editorial Secretary, American Institute of Physics, 11 East 38th Street, New York, New York.

Subscriptions, renewals, and orders for back numbers should be addressed to the Editorial Secretary, American Institute of Physics, 11 East 38th Street, New York, New York.

Entered at the post office at Menasha, Wis., as second class matter.
Acceptance for mailing at special rate of postage provided for in section 1103, Act of October 3, 1917, authorized September 6, 1926.

Second Series *September 15, 1932* *Vol. 41, No. 6*

THE

PHYSICAL REVIEW

The Faraday Effect with X-Rays

By DAROL K. FROMAN

Physics Laboratory, Macdonald College, McGill University

(Received July 19, 1932)

Voigt's theory for the rotation of the plane of polarization of light by a magnetic field is discussed and one of the equations used by W. Kartschagin and E. Tschetwerikowa who investigated the Faraday effect with x-rays transmitted through ferromagnetic materials, is shown to be inapplicable. The theory for the effect given by Drude is modified for the case of x-ray wave-lengths giving a rotation of $\chi = -2\pi\mu eIL/mc^2$ radians. μ is the refractive index, I is the intensity of magnetization, l the thickness of the material through wich the x-rays are transmitted. The other quantities have their usual meanings. Kartschagin and Tschetwerikowa found evidence suggesting a rotation in the case of x-rays. An experiment was performed which confirmed these suggestions and which checked the equation for χ given above well within the experimental error. The experimental error was large, but a rotation of the order of 10° was shown to occur for x-rays of wave-length 0.3A transmitted through 0.05 cm of iron in a field of 300 gauss.

INTRODUCTION

THE Faraday effect with x-rays has been studied by Kartschagin and Tschetwerikowa[1] using paraffin and iron in the magnetic field to produce a rotation of the plane of polarization. Their results were negative in the case of paraffin, but in the case of iron they say that their experimental results do not entirely justify the conclusion that a rotation exists but indicate a rotation of about 10°. They used iron of effective thickness about 0.01 cm in a magnetic field of 750 gauss. They compared their experimental results with Voigt's[2] theory which, under their experimental conditions, predicted a rotation of only 4′.

It is the purpose of this paper to discuss the applicability of Voigt's equation to paramagnetic materials; to modify the theory of Drude[3] for x-ray frequencies; to describe an experimental investigation on iron, indicating the differences between the method used and that of Kartschagin and Tschetwerikowa; and to compare the experimental results with the predictions of the two theories.

[1] W. Kartschagin and E. Tschetwerikowa, Zeits. f. Physik **39**, 886 (1926).

[2] W. Voigt, *Magneto- und Elektrooptik*, p. 130. Much of the fundamental work of this theory is due to H. Becquerel, C. R. **125**, 679 (1897).

[3] P. Drude, *The Theory of Optics*, Ch. VII.

Applicability of Voigt's Equation

On the basis of the electromagnetic theory Voigt deduces an equation for the rotation, χ, of the plane of polarization of light traversing a distance l of a material in the direction of an applied magnetic field of strength R_0, *viz:*

$$\chi = \lambda l R_0 e/mc^2 \cdot d\mu/d\lambda \tag{1}$$

where e, m, c and λ have their usual meanings and μ is the refractive index of the material. All quantities are in the C.G.S. system. This equation is not applicable to ferromagnetic materials since it is well known[4] that in this case χ is proportional to the intensity of magnetization and not to the magnetic field strength. Voigt himself points this out.[5] It does not suffice to substitute for R_0 the field produced by the magnetization alone, i.e., $4\pi I$ where I is the intensity of magnetization, since Eq. (1) is deduced on the assumption that the equations of motion of an electron in the medium under the action of the incident light and the applied magnetic field are:[6]

$$\begin{aligned} m\ddot{x} + h\dot{x} + kx - (eR_0/c)\cdot\dot{y} &= eX \\ m\ddot{y} + h\dot{y} + ky + (eR_0/c)\cdot\dot{x} &= eY \\ m\ddot{z} + h\dot{z} + kz &= eZ. \end{aligned} \tag{2}$$

In these equations the incident light travels in the direction of the magnetic field, h and k are the friction and elastic constants respectively and the other quantities have their usual meanings. Since eR_0/c cannot be replaced in these equations by $4\pi Ie/c$ it is not permissible to do so in Eq. (1).

As it is not known how to modify the magnetic force factors of Eqs. (2) for paramagnetic materials, the problem is attacked in a different way.

Modification of Drude's Theory for X-Rays

Drude assumes that a material contains rotating ions, electrons, whose magnetic moments may be alined, at least in paramagnetic materials, by the application of a magnetic field. The only effect of the electric field of a light wave is to displace the center of rotation of the electron if the natural frequency of the electron is far removed from that of the incident light. Thus the time rate of change of magnetic flux through a given area is composed of two parts, *viz:* the change which is produced directly by the magnetic vector of the light wave, and the change produced by the motion of the center of rotation of the electron due to the action of the light wave. Drude calculates these quantities and the corresponding current densities and substitutes directly in Maxwell's equations. On this basis he deduces the index of refraction and the rotation of the plane of polarization.

The index of refraction, μ, is given by:

$$\mu^2 = 1 + \sum_h \alpha_h n_h + \sum_k \beta_k n_k \tag{3}$$

[4] P. Drude, reference 3, p. 449.
[5] W. Voigt, reference 2, p. 20.
[6] W. Voigt, reference 2, p. 125.

where the subscripts h and k refer to nonconducting and conducting electrons respectively. n is the number of a particular type of electron per unit volume and α and β are functions of the properties of the medium and the period of the incident light. β is proportional to the square of the period and may be neglected in the case of x-rays since the frequency is very high. This approximation has been shown to be valid by experimental determinations of μ which agree within experimental error with Eq. (3), even for conductors, when β is put equal to zero. In this case h goes from 1 to the total number of different types of electrons present whether conducting or not.

Lorentz[7] also derives an expression for μ, namely:

$$\mu^2 = 1 + e^2/\pi m \cdot \sum_h n_h/(\nu_h^2 - \nu^2) \tag{4}$$

where e and m have their usual values, ν_h is the natural frequency of all of the n_h electrons and ν is the frequency of the incident light. Since the sums in Eqs. (3) and (4) are taken over the same range we can solve for α_h.

$$\alpha_h = e^2/\pi m(\nu_h^2 - \nu^2). \tag{5}$$

Drude also shows that the plane of polarization of plane-polarized light is rotated through an angle, χ, when a beam of light passes through a magnetized substance in a direction parallel to the magnetic field. χ is given by:

$$\chi = f\mu l/2c^2\tau^2 \tag{6}$$

where l is the thickness of the material traversed by the light, c is the velocity of light and $\tau = 2\pi\nu$. By convention χ is positive when the rotation is right-handed to an observer looking in the direction of the field. f is given by the equation

$$f = (1/c) \cdot \sum_h n_h'\alpha_h q_h/T_h + \sum_k n_k'\beta_k q_k/T_k. \tag{7}$$

Drude assumes that an electron of type h moves in an orbit of area q_h with a period T_h. n_h' is the effective number of electrons of this type per unit volume having their magnetic moments parallel to the external magnetic field. It is shown also that the number of lines of magnetic induction per unit area produced by these n_h' electrons is

$$M_h = 4\pi e q_h n_h'/cT_h. \tag{8}$$

The total flux per unit area is

$$4\pi I = \sum_h M_h \tag{9}$$

where I is the intensity of magnetization.

We may neglect the second sum in Eq. (7) as was done in Eq. (3) and combining Eqs. (7) and (8) we get

$$f = \sum_h \alpha_h M_h/4\pi e. \tag{10}$$

[7] H. A. Lorentz, *The Theory of Electrons*, 2nd Ed. p. 149.

It has been shown[8] that for x-rays we can neglect ν_h^2 compared to ν^2. Thus Eq. (4) becomes

$$\left.\begin{aligned} \mu^2 &= 1 - e^2n/\pi m\nu^2 \\ \text{or} \qquad \mu &= 1 - e^2n/2\pi m\nu^2 \end{aligned}\right\}. \tag{11}$$

This is the usual expression for μ.

Here $n = \Sigma_h n_h$ = the total number of electrons per unit volume and since μ differs only slightly from unity, the approximation in the second of Eqs. (11) is justified. Also Eq. (5) becomes

$$\alpha_h = -e^2/\pi m\nu^2. \tag{12}$$

Combining Eqs. (9), (10) and (12) we get

$$f = -\sum_h e^2 M_h/4\pi^2 em\nu^2 = -eI/\pi m\nu^2. \tag{13}$$

Substituting from Eq. (13) in Eq. (6)

$$\begin{aligned} \chi &= -\mu eII/2c^2\tau^2\pi m\nu^2 \\ &= -2\pi\mu eII/mc^2. \end{aligned} \tag{14}$$

It can be seen from Eq. (11) that $\mu < 1$ and α_h is negative. Consequently it appears that the sign of χ has a real significance in this case. For example, iron shows a positive rotation for visible light and in this range $\mu > 1$. Thus the quantity corresponding to α_h is positive for this region and χ is calculated as positive. The minus sign here indicates then that the rotation will be negative. The direction of rotation cannot be predicted for ordinary light from the magnetic properties of the substance but if the direction is known in one case and the calculated χ is of opposite sign in a second case, it is expected that the direction of rotation will differ in the two cases.

The work of several experimenters[9] has shown that the planes of electronic orbits are not rotated in a magnetic field but it may be pointed out that the deduction of Eq. (14) is independent of the mode of magnetization and depends only on the assumption that magnetization is an electronic effect.

It is interesting to note that χ is independent of the wave-length, λ, of the x-rays except in so far as μ is a function of λ. Since μ is very nearly unity for a wide range of x-ray wave-lengths, it is to be expected that χ will be approximately constant for all x-rays.

[8] H. A. Lorentz, reference 7.

[9] M. de Broglie, Le Radium **10,** 186 (1913).
K. T. Compton and E. A. Trousdale, Phys. Rev. **5,** 315 (1915).
A. H. Compton and Oswald Rognley, Phys. Rev. **16,** 464 (1920).
T. D. Yensen, Phys. Rev. **31,** 714 (1928).
J. C. Stearns, Phys. Rev. **35,** 1 (1930).
J. C. Stearns, Phys. Rev. **35,** 292 (1930).

The Experimental Arrangement

The general radiation of effective wave-length about 0.3A from a gas-filled x-ray tube was used in these experiments. This white radiation was about 10 percent polarized thus giving a much greater effective intensity than could be obtained by scattering. The arrangement of apparatus is shown in Fig. 1. The x-rays passed through holes in the pole pieces of an electromagnet, in a direction parallel to the magnetic field, and fell upon a cylindrical carbon scattering block which served as analyzer. The radiation scattered by the carbon block at right angles to the primary beam was detected by a photographic film bent into the shape of a cylinder having the same axis as the carbon block. The diameter of the cylindrical film holder was about 4 cm and of the block about 0.5 cm. The total distance from target to analyzer was about 25 cm. The holes in the pole pieces were just large enough to ensure

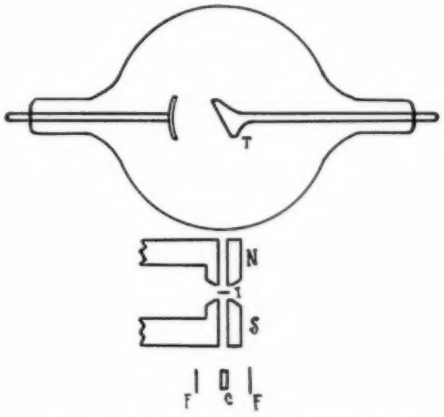

Fig. 1. Arrangement of apparatus. *T* is the target of the x-ray tube, *N* and *S* are the perforated magnetic pole pieces, *I* is the iron disk, *C* is the carbon analyzer and *F* is the photographic film.

uniform illumination over the scattering block. Any desired thickness of iron could be placed between the poles of the magnet.

The x-rays had a predominant polarization with the electric vector in the plane containing the stream of incident cathode rays at the target. The angle which this plane made with the straight line joining cathode and target depended upon the strength of the field produced by the magnet at the center of the x-ray tube. Thus a reversal of the magnetic field produced a rotation of the plane of predominant polarization even if there were no substance between the poles of the magnet. In order to eliminate this effect produced by the change in the direction of the cathode rays photographs were taken with different thicknesses of iron between the poles. The thickness of the iron was never changed enough to affect the magnetic field in the x-ray tube.

Photographs were taken with 0.05 cm and 0.075 cm of iron between the poles of the magnet with the field first in one direction and then in the other. A fixed lead stop between the scattering block and the film and just in front of the latter served to mark a constant angle with the axis of the x-ray tube

on the various films used. A microphotometer was used to measure the intensity on the film. As a continuously-recording microphotometer was not available the galvanometer deflections were read directly and the curves plotted. Fig. 2 shows two typical examples. These two curves represent the intensity arriving at the film after passing through 0.075 cm of iron in the magnetic field. Curve (1) was taken for the magnetic field in the direction of propagation of the x-rays and curve (2) with the field reversed. The angular displacement of one of these curves with respect to the other measures the combined effect of the magnetic field on the cathode rays and of any roation of the plane of polarization in transmission through the iron. The process was repeated using 0.05 cm of iron between the poles of the magnet. Since the effect on the cathode rays was the same as in the case for the thicker iron, any difference between the angular displacement of these curves and of those for 0.075 cm of iron measures the rotation of the plane of polarization produced by 0.025 cm of iron upon reversal of the magnetic field.

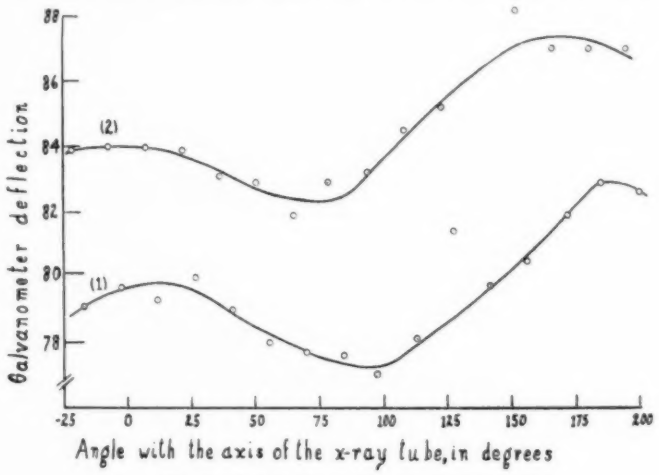

Fig. 2. Microphotometer curves.

Three sets of curves for each thickness of iron were obtained, the average displacements measured and the mean differences found.

The iron used was in the form of disks 0.025 cm thick and of diameter just greater than the holes in the pole pieces. On account of the difficulty of determining the magnetic properties of the iron and of estimating the demagnetizing effect of the free poles, a direct measurement of magnetization was made. As is well known[10] the force between two magnetic poles in contact is $2\pi I^2$ dynes per cm^2. The force required to separate one of the disks from the other two in the field was measured and the intensity of magnetization calculated. This was repeated with but two disks present. Mechanical difficulties rendered these results somewhat inaccurate but they are probably as precise as the measurement of angular displacements. The strength of the magnetic field producing magnetization was measured in order to test Voigt's equation.

[10] S. G. Starling, *Electricity and Magnetism*, p. 283.

If there is appreciable dispersion in the magnetic rotation the apparent percentage of polarization should be less with a magnetic field across the iron than without the field. That is, if the planes of polarization of different wave-lengths were rotated through different angles, the microphotometer curves would be flattened by the application of a field. No appreciable difference in the apparent percentage of polarization was obtained with the iron magnetized and not magnetized. Kartschagin and Tschetwerikowa did obtain a difference in this case but they were using the iron itself as the analyzing scatterer. They assumed that the effective thickness of iron traversed before scattering was equal to the thickness of iron which would absorb one-half of a primary beam of wave-length equal to the wave-length of maximum energy from their x-ray tube. Thus their primary rays travelled various distances in the direction of magnetization before analysis and a decrease in the apparent percentage of polarization is to be expected even if there is no dispersion.

TABLE I.

Trial	$\theta_1^\circ (l=0.05$ cm)	$\theta_2^\circ (l=0.075$ cm)	$\theta_2^\circ-\theta_1^\circ=\chi_2^\circ-\chi_1^\circ$	$\chi_2^\circ-\chi_1^\circ$	$\chi_2^\circ-\chi_1^\circ$
1	−4.3	−14.4	from experiment	from theory given in this paper	from Voigt's theory for nonferromagnetic materials
2	−4.3	−15.8			
3	−5.8	−15.8			
Average	−4.8	−15.3	−10.5	−14.0	-1.1×10^{-7}

In Table I θ_1 is the apparent rotation produced by a thickness of 0.05 cm of iron, and θ_2 by 0.075 cm, on reversal of the field. Both θ_1 and θ_2 include the effect of the field on the cathode rays. One might expect θ_1 to be much larger compared to θ_2. However the demagnetizing effect of the free poles is considerably reduced on increasing the thickness of the iron so that by Eq. (14) χ is increased by the increase of both l and I. The magnetic field was kept constant at 300 gauss. The intensity of magnetization measured 79 unit poles per cm² for 0.05 cm of iron and 97 unit poles per cm² for a thickness of 0.075 cm. $\theta_2-\theta_1$ is independent of any magnetic effect on the cathode rays. Values of χ were calculated for these two cases, χ_1 for 0.05 cm of iron and χ_2 for 0.075 cm of iron both from Voigt's theory (Eq. 1) and from Eq. (14). $\chi_2-\chi_1$ is given in Table I for comparison with $\theta_2-\theta_1$ as observed. $d\mu/d\lambda$ was calculated for Eq. (1) from Eq. (11). The minus sign indicates the direction of the rotation in the conventional manner.

CONCLUSIONS

The results given in the last three columns of Table I differentiate between the two theories in a striking and unmistakable way. Voigt's theory is certainly not applicable in this case. The comparatively large estimate of the rotation, 4′, made by Kartschagin and Tschetwerikowa in their case for Voigt's equation came about since their effective wave-length was near the K absorption level of iron. Thus their estimate of $d\mu/d\lambda$, based on the anomalous dispersion theory, was many times that given by Eq. (11). The effective fre-

quency used in the present experiments was certainly so much greater than any of the characteristic frequencies of iron that Eq. (11) contains no appreciable error.

It is very difficult to estimate the probable error in the experimental value of $\chi_2 - \chi_1$. After careful consideration of the various errors which may have entered due to the particular equipment used, and to the photographic method of measuring intensities, the author is forced to conclude that the results given here indicate only the correct order of magnitude of the effect. However it can be concluded with little doubt that the plane of polarization is rotated a few degrees under the conditions described. For these reasons no calculation of the Verdet constant has been made from the experimental results. It is greatly desired that accurate ionization-chamber measurements be made, using a much steadier source of x-rays than was available for this work, and it is hoped that such work, if not done elsewhere in the meantime, may be accomplished in this laboratory in the near future.

The author wishes to take this opportunity to thank Drs. W. and M. L. Rowles, and his wife, Ethel Froman, for their advice and assistance in the experimental part of this work.

New Measurements of the Ranges of Alpha-Particles from Polonium, Uranium I and Uranium II with the Wilson Chamber*

By F. N. D. KURIE†
Sloane Physics Laboratory Yale University

(Received July 5, 1932)

The Wilson cloud chamber method of range measurement described by the author in another paper has been applied to the α-particle ranges of polonium, uranium I, and uranium II. The polonium measurements were undertaken as a check on the method, but are in sufficiently good accord with previous results to stand alone. The range of polonium α-particles at 0°C and 760 mm is 3.690 ± 0.005 cm. The range of uranium I α-particles is 2.58 ± 0.015 cm and that of uranium II α-particles is 3.11 ± 0.01 cm. The polonium range is derived from 335 tracks while the uranium ranges are due to a total of 594 tracks. A method of separating the number-distance curves of the two uraniums is described which eliminates the uncertainty of finding the shorter range. The uranium data are in excellent agreement with the results of Laurence. This agreement is thought to be entirely fortuitous in so far as uranium I is concerned. The precision of Laurence's work is criticised.

INTRODUCTION

A PARALLEL beam of α-particles does not possess a sharp terminus, but the distances traversed by single particles before they can no longer be detected are governed by a probability law such that the number of particles stopping between x and $x+dx$ (the distance x being measured from the source) is given by the normal probability function $(1/\alpha\pi^{1/2}) \exp (x-l)^2/\alpha^2$, where α is a parameter called in this case the straggling coefficient. The distribution is symmetrical about l, the most probable range. There are many reasons why it is more desirable to use this range in other discussions, but experimental difficulties, however, have made it hard to assign precise values to it so one usually measures the extrapolated number-distance range defined by the following considerations. The number N of α-particles which pass beyond a given distance x is readily obtainable by integrating the normal function and is $N=(1/2)\{1-\text{erf } (x-l)/a\}$. This curve exhibits a sharply descending linear portion which on extrapolation meets the distance axis at R (the extrapolated number-distance range), where R is given by $R=l+\pi^{\frac{1}{2}}\alpha/2$. This may be written independently of α for short range particles, by making use of the data relating α to R given by Briggs.[1] Thus,

$$R = l + 4.2R^{1/2}\{1 - 1.51/R\}^{1/2}(10)^{-2}.$$

Another type of range is given by ionization current measurements, the interpretation of which is more obscure than that of the ranges derived sta-

* Part of a dissertation presented for the degree of Doctor of Philosophy at Yale University.

† Sterling Fellow.

[1] G. H. Briggs, Proc. Roy. Soc. **A118,** 594 (1928).

tistically from measurements on single particles. The relation between the ionization range and the number-distance range has recently been derived by Lewis and Wynn-Williams[2] on the basis of the ionization curve of a single α-particle. They deduce that the extrapolated number-distance range exceeds the extrapolated ionization range by 0.006 cm.

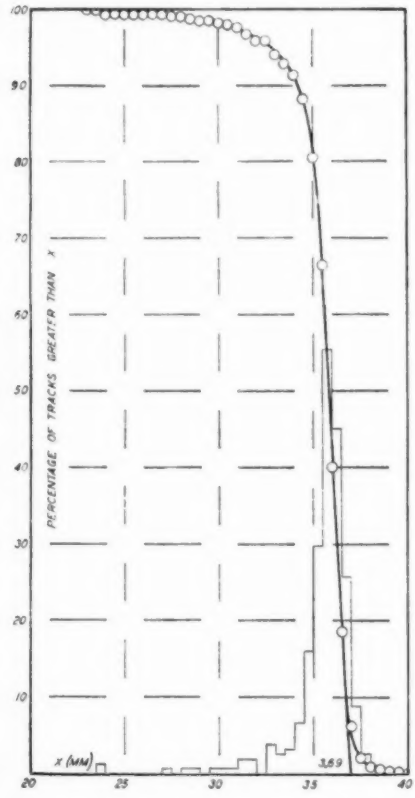

Fig. 1. Number-distance curve for polonium α-particles.

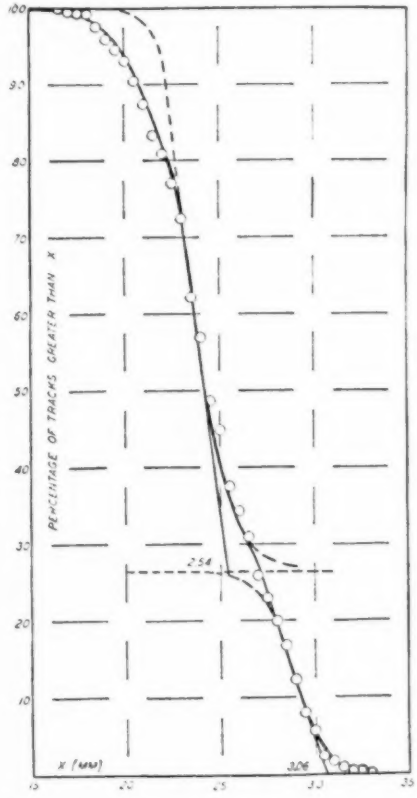

Fig. 2. Number-distance curve for uranium α-particles.

These remarks have been made with the view of helping to relieve some of the lack of uniformity in the interpretation given by different authors and texts to the phrase "the range of α-particles." In this paper the phrase will be taken to refer to the extrapolated number-distance range.

Polonium

The author has outlined in another paper[3] the procedure for obtaining the range of α-particles from weak sources. This briefly consists in taking two photographs of the tracks due to the α-particles in question formed in a large

[2] W. B. Lewis and C. E. Wynn-Williams, Proc. Roy. Soc. **A136,** 349 (1932).

[3] To be published in the Review of Scientific Instruments.

Wilson cloud chamber, and from them reconstructing a replica of the original track. This replica is measured and reduced to standard conditions (0°C, 760 mm). Because of the large size of the sources employed there are no slits or shutters; tracks are formed on ions of all ages. Those formed at constant density after an expansion are, however, much sharper than any others. That this sharpness can be used as a criterion for rejecting old tracks needs proof, and it was for that purpose that the range of polonium α-particles was examined.

The sources were prepared on silver wires, about 10 cm long and 0.001 inch in diameter, by deposition from a weakly acid (HCl) solution of polonium. It was found that with even the weakest of acid solutions there was a noticeable tarnish on the wire. It seemed likely that the only compound which might be formed would be silver chloride, which is soluble in ordinary hypo. A source deposited on a polished silver plate and showing the tarnish became perfectly clear on bathing it in hypo, without having lost any activity. A wire source after treatment with hypo gave a range 0.03 cm in excess of measurements before the treatment. The variation from source to source was never more than 0.01 cm, even with badly tarnished sources; after the hypo treatment was introduced the variation dropped below this value. All the sources used in the final measurements were bathed in hypo.

The results are shown in Fig. 1. The distribution curve of the ranges is shown in outline; it is drawn for $dx=0.05$ cm. The number-distance curve is plotted on a percentage scale, 100 percent corresponding to 335 tracks. Extrapolating the linear portion of this curve to the distance axis gives the range in the sense defined above, as $R_0=3.690\pm0.005$ cm at 0°C, 760 mm.

The limit of reliability is obtained by assigning to each column in the distribution histogram the error appropriate to the number of particles it contains. One gets thus two limiting histograms and so two limiting number-distance curves. The extreme extrapolated straight line portions of these meet the distance axis at R_0+p and R_0-p, where p is the limit of reliability.

This range corresponds to an extrapolated ionization range of 3.68 cm and to a mean range of 3.63 cm. The most reliable values of the polonium range are given in Table I. Those values marked with an asterisk were not measured directly but calculated by some relation of the form already mentioned.

TABLE I. *Range of polonium α-particles.*

Observer	Mean range	Extrapolated number-distance range	Extrapolated ionization range
Geiger[4]	—	—	3.72
I. Curie[5]	3.65	3.72	3.67
Harper and Salaman[6]	—	—	3.67
Lewis and Wynn-Williams[2]	3.61	—	3.65*
Kurie[7]	3.63*	3.69	3.68*

[4] H. Geiger, Zeits. f. Physik **8,** 45 (1921).
[5] I. Curie, Ann. de Physique **3,** 299 (1925).
[6] G. I. Harper and E. Salaman, Proc. Roy. Soc. **A127,** 175 (1930).
[7] This paper.

The results of the polonium measurements not only furnish a new value for the range of polonium α-particles but they show that the method of using the cloud chamber without slits or shutter for the α-particles does not hamper its precision.

Uranium

The two uraniums present a particularly difficult problem, being so weak that thick sources must be used. This leads to a broadening of the straggling curve and nearly masks the fact that the radiation from uranium is complex. Indeed, all the work up to 1910 gave uranium a single group of α-particles with a range between 2.7 cm and 3.4 cm.

Recently a number of attempts have been made to measure these two ranges more exactly. This has become very important in view of the difference between the ionization measurements of Geiger and Nuttall,[8] which gave ranges of 2.53 cm and 2.91 cm for uranium I and uranium II respectively, and the pleochroic haloe measurements of Gudden[9] which gave ranges of 2.68 cm and 2.76 cm for the same bodies.

The most notable effort is that of Laurence[10] who measured the ranges in a Wilson cloud chamber getting 2.59 cm and 3.11 cm. His work received corroboration from Rutherford[11] who showed by the scintillation method that the range of uranium II is not less than 3.06 cm, and from Ziegert[12] who found the number of ions produced per α-particle to correspond roughly to ranges of 2.7 cm and 3.1 cm.

Laurence's work, while representing a pronounced advance both in the technique of the Wilson chamber and in our knowledge of the range of uranium α-particles, nevertheless seems unsatisfactory and unconvincing as a precision measurement. The present work was undertaken because it was believed possible to avoid most of the assumptions and corrections used by Laurence.

This author has mentioned elsewhere that it is quite essential for precision that a cloud chamber be operated periodically at regular intervals; that the length of the interval be chosen with due regard to the thermodynamics of the chamber; that the illuminating arc be screened from the chamber until the moment of the expansion; and that the camera be properly synchronized with the expansion to prevent turbulences altering the lengths of the tracks.

The reasons which Laurence gives to prove that 98 percent of the tracks he photographed are formed at constant density are quite erroneous. Tracks of all ages are present in the chamber, those formed at constant density, however, being much sharper. This criterion of selection has already been mentioned above.

The corrections which Laurence was obliged to apply for the obliquity

[8] H. Geiger and J. M. Nuttall, Phil. Mag. [6] **23**, 439 (1912).

[9] B. Gudden, Zeits. f. Physik **26**, 110 (1924).

[10] G. C. Laurence, Trans. Nova Scotian Inst. Science **17**, 103 (1927); Phil. Mag. [7] **5**, 1027 (1928).

[11] Sir Ernest Rutherford, Phil. Mag. [7] **4**, 580 (1927).

[12] H. Ziegert, Zeits. f. Physik **46**, 668 (1928).

of the tracks to the chamber floor and for the heating of the gas in the chamber are difficult to estimate and have been avoided in the present work.

When one considers two superimposed number-distance curves it is clear, as is found for uranium, that the range of the shorter group is got by extrapolating the linear portion of the upper curve to the flat maximum of the lower curve (no-particle line of the upper curve). Unfortunately in uranium this flat maximum does not show up in the experimental curve. Instead of attempting to find its position Laurence has merely extrapolated the gentle curve of the uranium II particles until it cut the extended straight part of the uranium I section, calling their intersection the range of uranium I. A method will be described later which accomplishes the separation of the two curves and allows the shorter range to be got without such uncertain extrapolation.

Laurence's work, then, does not appear to be entirely unsusceptible to improvement. All possible improvements have been used in the present measurements.

The sources were prepared from uranium oxide (U_3O_8) by the method of McCoy[13] on a backing of mica 0.01 cm long, 1 cm wide and 0.001 inch thick. Subliming from an arc did not yield satisfactory sources; their weight and ionization currents did not check. That impurities are unavoidable in this respect is substantiated by Laurence's report that he got one track in 80 expansions from a source rougly four times as heavy as the ones here used which gave 0.6 tracks per expansion. This is much greater than can be explained on the basis of the relative sizes of the two cloud chambers.

The final results are shown in Fig. 2 in the form of a number-distance curve plotted on a percentage scale, 100 percent corresponding to 594 tracks. The curve consists of two portions, one pertaining to uranium I and the other to uranium II. The range of α-particles from uranium II (uncorrected for absorption in the source) is 3.06 cm.

The same data are shown in Fig. 3 plotted on probability paper, where the curve has reduced to three straight lines. The conclusion at once suggests itself that the midpoint M of the short connecting line gives the fraction of uranium II tracks. This idea was tested by constructing several two-component number-distance curves, whose relative proportions were known, distorting these by adding an excess of short range particles and plotting them on probability paper. The excess of short range particles was known from the work of Mlle. Curie and from the observations of the author in connection with the polonium measurements to be in the neighborhood of 10–15 percent of the total. The fractions of the two curves as got from the midpoint of the short connecting line were in all cases within 1 percent of their known values. We thus find the uranium group to constitute 26.5 percent of the total number of α-particles.

With this known we can now find the true number-distance curves to which the data best conform by making separate plots for uranium I and

[13] H. N. McCoy, Phil. Mag. [6] **11**, 176 (1906).

uranium II on probability paper. These true curves are shown dotted in Fig. 2.

The small fraction of uranium II tracks is due to the solid angle available for complete tracks in the cloud chamber being smaller for the long range particles than for the short range particles. A very rough calculation from the dimensions of the chamber has borne this out quantitatively.

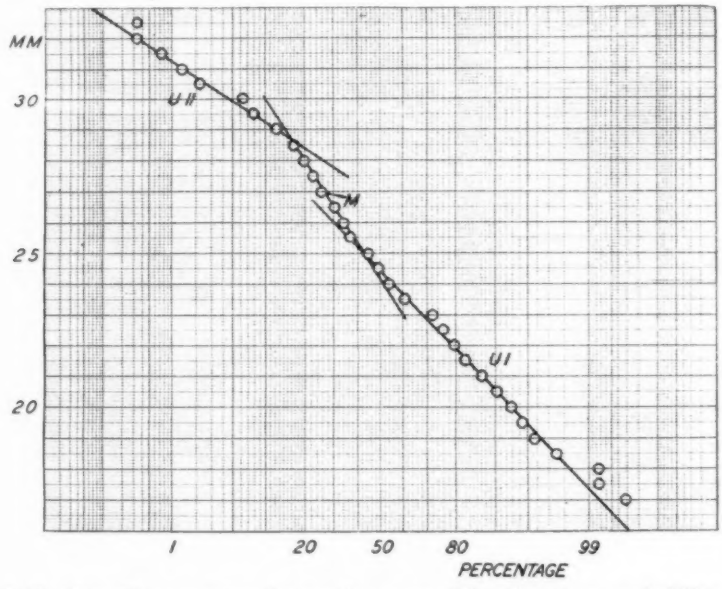

Fig. 3. Number-distance curve for uranium α-particles plotted on probability paper.

The correction for absorption in the source was calculated by Laurence in the paper discussed above. For sources of the thickness used in these measurements (of the order of 2 mg/cm^2) the correction is independent of the thickness and reduces to $\alpha\pi^{1/2}/2$, where α is the straggling coefficient. The straggling coefficients are 0.048 cm and 0.058 cm, respectively, for uranium I and uranium II, so that the corrections are 0.043 cm and 0.051 cm.

The final corrected ranges at 0°C and 760 mm are

$$R_{\mathrm{U\,I}} = 2.58 \pm 0.015 \text{ cm};$$

$$R_{\mathrm{U\,II}} = 3.11 \pm 0.01 \text{ cm}.$$

The limits of reliability have been calculated in the same manner as was done for polonium, but in addition the uranium I range is subject to an uncertainty due to the error in ascertaining the fractions of the two groups. This latter was estimated from the experiments with the fictitious curves to be 1 percent, corresponding to 0.006 cm in the range.

These results clearly agree with those of Laurence within the experimental error. This agreement is believed to be entirely fortuitous in so far as uranium I is concerned, for had the data been treated in the manner of Laurence a very much smaller value would have been obtained—nearer 2.50 cm than 2.59 cm.

The value of the half-life of uranium II as deduced from the range of its particles, assuming the Geiger-Nuttall law, is much smaller than that measured by Walling[14] and Collie.[15] When the range and Walling's value of λ is plotted on a Geiger-Nuttall graph of the uranium-radium series uranium II falls off the curve. The reason for this is not clear; the range seems to be sufficiently well established to lay the divergence to either a failure of the Geiger-Nuttall law or to inaccuracies in the experimental determinations of λ. The latter seems more probable since uranium I fits the slight curve (best form of the Geiger-Nuttall law) very well.

The author is greatly indebted to Professor Alois F. Kovarik, who suggested this problem, for the kind interest he showed and the friendly counsel he gave during the course of the experiments.

[14] E. Walling, Zeits. f. physik. Chem. **10,** 467 (1930).
[15] C. H. Collie, Proc. Roy. Soc. **A131,** 541 (1931).

The Relativistic Thomas-Fermi Atom

By M. S. VALLARTA AND N. ROSEN
Massachusetts Institute of Technology

(Received August 4, 1932)

The Thomas-Fermi equation determining the inner atomic potential and the charge distribution is generalized to take care of the relativistic change of mass with velocity. The relativistic equation is then solved numerically by means of a first order perturbation method and with the help of the differential analyzer. The solution is applied to the case of mercury and it is shown that while the atomic potential changes only slightly, the charge density is appreciably increased in the immediate vicinity of the nucleus and slightly decreased at larger distances.

THOMAS[1] and, independently, Fermi[2] have devised a valuable heuristic statistical method of finding the potential and the electron distribution around an atomic nucleus, in which the electrons are treated as if they formed an ideal gas obeying the Fermi-Dirac statistics. The charge density obtained in this manner, although admittedly not the actual one, is a sufficiently close approximation, at least for heavy atoms, that it can be successfully used in many problems, e.g., the calculation of x-ray scattering by heavy atoms and molecules.[3] It is a matter of some interest to investigate the modifications introduced in this atomic model by the relativistic variation of mass with velocity. While this correction may be expected to be negligible for most atoms, it becomes more appreciable as the atomic number increases because for very heavy atoms the electron velocities in the vicinity of the nucleus become high. For such atoms the electron density close to the nucleus may be appreciably changed by the relativity correction. In any case the latter is greatest just for those cases where the Thomas-Fermi distribution may be expected to be a good approximation to the actual one. Even for heavy atoms however, this correction is probabiy less important than the exchange correction. No satisfactory method of taking into account the exchange phenomenon has yet been devised and hence it will not be considered in the present paper.[4]

We proceed to derive the relativistic form of the Thomas-Fermi equation. Let V be the atomic potential and r the distance from the nucleus; then $V(r)$ satisfies the Poisson equation $\nabla^2 V = -4\pi\delta$ and the boundary conditions:

$$\lim_{r\to 0} V = Ze/r \quad \lim_{r\to\infty} V = 0 \tag{1}$$

[1] L. H. Thomas, Proc. Camb. Phil. Soc. **23**, 542 (1927).

[2] E. Fermi, Zeits. f. Physik **48**, 73 (1928).

[3] The literature in this connection is summarily reviewed by E. O. Wollan, Rev. Mod. Phys. **4**, 205 (1932).

[4] P. A. M. Dirac, Proc. Camb. Phil. Soc. **26**, 376 (1930).

where Z is the atomic number. The electron density δ in ordinary three dimensional space, taking into account spin and assuming that the electrons form a gas obeying the Fermi-Dirac statistics, is

$$-\delta = (2e/h^3)(4\pi p^3/3) \tag{2}$$

where e is the electron charge, h Planck's constant and p the momentum of the electrons having maximum energy. For a bound electron the energy E (sum of the kinetic and potential energies) is negative and its maximum value is zero. From the relativistic Hamiltonian

$$p^2 - (W+eV)^2/c^2 + m_0^2c^2 = 0 \tag{3}$$

where $W=E+m_0c^2$ is the total energy, m_0 the electron's rest mass and c the velocity of light in vacuum, we have, using the condition $E=O$ or $W=m_0c^2$ that

$$p^2 - e^2V^2/c^2 - 2m_0eV = 0. \tag{4}$$

Hence the electron density now becomes

$$-\delta = (2e/h^3)(4\pi/3)(2m_0eV + e^2V^2/c^2)^{3/2} \tag{5}$$

and from Poisson's equation

$$\nabla^2V = 4\pi(2e/h^3)(4\pi/3)\ (2m_0eV + e^2V^2/c^2)^{3/2} \tag{6}$$

which is the relativistic Thomas-Fermi equation.

To transform this equation into a simpler form we introduce so-called atomic units and the new variables $r=\alpha\rho$ and $V=\beta\phi$, where

$$\alpha = a_0/Z^{1/3} \qquad \beta = 9\pi^2eZ^{4/3}/128a_0 \tag{7}$$

and a_0 is the radius of the first Bohr circle. Eq. (6) now becomes

$$\frac{1}{\rho^2}\frac{d}{d\rho}\left(\rho^2\frac{d\phi}{d\rho}\right) = \phi^{3/2}(1 + \lambda\phi)^{3/2} \tag{8}$$

where

$$\lambda = e\beta/2m_0c^2 = 1.841 \times 10^{-5}Z^{4/3}. \tag{9}$$

Eq. (8) can now be solved by a first order perturbation method as follows: let $\phi=\phi_0+\lambda\phi_1$, then keeping first order terms we have

$$\phi^{3/2}(1 + \lambda\phi)^{3/2} \doteq \phi_0^{3/2} + (3/2)\lambda\phi_0^{1/2}\phi_1 + (3/2)\lambda\phi_0^{5/2}$$

and equating like powers of λ in (8) we obtain two equations:

$$\nabla^2\phi_0 = \phi_0^{3/2} \tag{10}$$

$$\nabla^2\phi_1 = (3/2)\phi_0^{1/2}(\phi_1 + \phi_0^2) \tag{11}$$

of which the first is the ordinary Thomas-Fermi equation whose numerical solution is known,[5] and the second is the equation for the relativistic correction.

To solve Eq. (11) we place $\phi_1 = F/\rho$ and obtain

$$d^2F/d\rho^2 = (3/2)\phi_0^{1/2}F + (3/2)\rho\phi_0^{5/2}. \tag{12}$$

The numerical value of the coefficients in this equation is calculated from the data of Bush and Caldwell.[5] The boundary conditions for the function F are immediately derived from the boundary conditions for V; they are simply that F vanishes both at zero and infinity. For small values of $\rho(\rho<0.1)$ the solution of (12) can be expressed in a power series, using the results of Baker.[6] The series expansion is found to be:

$$\begin{aligned} F = &-6\rho^{1/2} + C\rho - 5B\rho^{3/2} - 2\rho^2 + (3B^2/4 + 2C/5)\rho^{5/2} - 2B\rho^3 \\ &- (11/35 + 3B^3/56 + 3BC/35)\rho^{7/2} + \cdots \end{aligned} \tag{13}$$

where B is the negative slope of the Thomas-Fermi function $(B=1.5886)$[5,6] and C is a constant chosen so as to satisfy the boundary conditions for F. The numerical value of this constant as determined from the solution of Eq. (12) to be described below is $C=11.92$.

TABLE I.

ρ	$-F$	$-\phi_1$	ρ	$-F$	$-\phi_1$
0	0	∞	0.600	0.784	1.307
0.010†	0.490	49.0	0.704	0.725	1.032
0.030†	0.726	24.2	0.809	0.670	0.828
0.060†	0.878	14.62	0.913	0.621	0.681
0.080†	0.934	11.68	1.000	0.582	0.582
0.100	0.960	9.65	1.500	0.411	0.274
0.121	0.981	8.11	2.001	0.301	0.1505
0.142	0.994	7.00	3.00	0.1748	0.0583
0.163	0.999	6.13	4.00	0.1106	0.0277
0.180	1.001	5.57	5.00	0.0741	0.01482
0.204	0.999	4.90	6.00	0.0519	0.00865
0.309	0.958	3.11	7.00	0.0370	0.00568
0.413	0.898	2.175	8.00	0.0267	0.00334
0.517	0.834	1.612	9.00	0.0188	0.00209
			10.00	0.0123	0.00123

† Calculated from series expansion (13).

The numerical integration of Eq. (12) can be conveniently carried out in the differential analyzer, a machine for the solution of differential equations developed at this Institute by V. Bush.[7] The result of this integration is given in Table I and Fig. 1.

[5] References 1 and 2, also V. Bush and S. H. Caldwell, Phys. Rev. **38,** 1898 (1931).

[6] E. B. Baker, Phys. Rev. **36,** 630 (1930).

[7] V. Bush, Jour. Franklin Inst. **212,** 447 (1931). The authors take advantage of the present opportunity to thank Professor Bush and his assistants, Messrs. S. H. Caldwell, A. J. McLennan, S. D. Caldwell, J. F. Cummings, B. V. Holmes, and R. S. Jameson for their friendly help with the integration of this differential equation.

For the electron density we now have, from (5)

$$-\delta = (8\pi e/3h^2)(2m_0e\beta)^{3/2}\phi^{3/2}(1+\lambda\phi)^{3/2} \tag{14}$$

whereas for the same quantity calculated according to the Thomas-Fermi theory one has

$$-\delta_0 = (8\pi e/3h^3)(2m_0e\beta)^{3/2}\phi_0^{3/2} \tag{15}$$

hence for the ratio of the relativistic to the nonrelativistic charge density one obtains

$$\delta/\delta_0 = \phi^{3/2}(1+\lambda\phi)^{3/2}/\phi_0^{3/2}. \tag{16}$$

This ratio is appreciably different from, and greater than, unity at small distances from the nucleus; at large distances the ratio is very close to, but smaller than, unity. The total charge is of course the same in both cases.

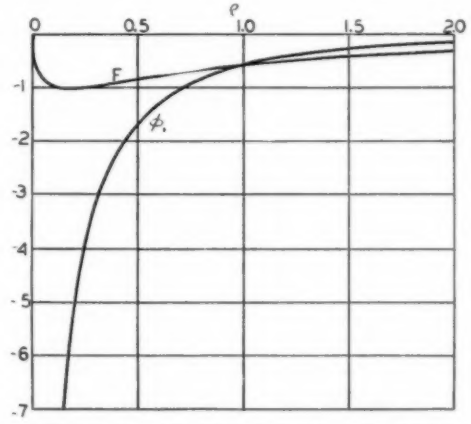

Fig. 1. Functions involved in relativity correction to Thomas-Fermi potential.

As an example let us take the case of mercury ($Z=80$). Here $\alpha=0.1225$Å and $\lambda=0.00635$. The value of the ratio (16) for different values of the distance

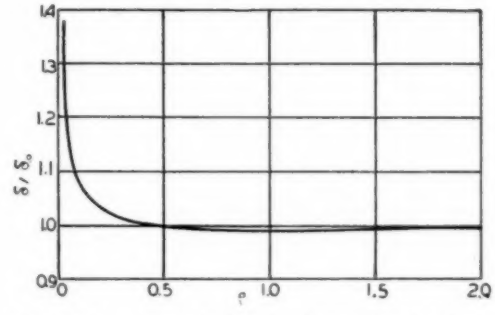

Fig. 2. Ratio of relativistic to nonrelativistic charge density for the mercury atom.

from the nucleus is given in Table II and plotted in Fig. 2. The relativistic and the nonrelativistic atomic potentials for mercury may be read off Table II. It is immediately seen that they are very nearly the same.

TABLE II.

ρ	r (X-units)	ϕ_0	ϕ	δ/δ_0
0.010	1.227	98.5	98.2	2.06
0.030	3.68	32.0	31.85	1.315
0.060	7.36	15.40	15.31	1.141
0.080	9.81	11.27	11.20	1.099
0.100	12.27	8.82	8.76	1.073
0.417	51.2	1.561	1.547	1.002
0.584	71.7	0.975	0.966	0.996
1.000	122.7	0.425	0.422	0.991
1.500	184.0	0.314	0.312	0.995
2.00	245.	0.244	0.243	0.996

The present investigation was suggested by Professor P. Debye to whom we wish to acknowledge our indebtedness.

The Wentzel-Brillouin-Kramers Method of Solving the Wave Equation

By J. L. DUNHAM
Harvard University

(Received May 11, 1932)

A more general treatment than has been available of the Wentzel-Brillouin-Kramers method of solving Schrödinger's equation for one degree of freedom is given. Wentzel's original energy-level condition is shown to be an asymptotic expression, good for large masses and large values of the quantum number. The connection between this method and that of Young is discussed. Finally the formulas are written in a form convenient for application to the calculation of energy levels from actual potential functions.

INTRODUCTION

THE Wentzel[1]-Brillouin[2]-Kramers[3] method of handling the wave equation (hereafter referred to as the W. B. K. method) is very well suited to the calculation of energy levels in heavy systems. This is evident from the fact that for such systems the Bohr theory levels fit the experimental facts rather well. Now these levels are the first approximation of the W. B. K. method, and hence we would expect it to give us rapidly converging results. Also such behavior is indicated by the correspondence principle, which predicts approximately classical properties for heavy systems as well as for high quantum numbers.

The usefulness of this method, however, has been limited by the fact that those treatments of it which have been rigorous have all been approximate, so that results of only a limited accuracy can be obtained. It is therefore the purpose of the present paper to extend the theory of the W. B. K. method to higher approximations, and to show that Wentzel's original generalization of the phase integral can be justified entirely. We shall also discuss the connection between this method and that of local momentum recently suggested by Young.[4]

Owing to the fact that Zwaan's[3] work on this subject is not very accessible we shall take up some of the points which he has discussed.

THE W. B. K. METHOD

The W. B. K. method of solving Schrödinger's equation is briefly as follows. Schrödinger's equation can usually be written

[1] G. Wentzel, Zeits. f. Physik **38,** 518 (1926).

[2] L. Brillouin, Comptes Rendus **183,** 24 (July 1926).

[3] H. A. Kramers, Zeits. f. Physik **39,** 828 (1926). See also A. Zwaan, Arch. Néerl. des Sciences **12,** 33 (1929), and L. A. Young and G. E. Uhlenbeck, Phys. Rev. **36,** 1154 (1930). For a good short account of Wentzel's presentation and some simple applications see Sommerfeld, Ergänzungsband, p. 158.

[4] L. A. Young, Phys. Rev. **38,** 1612 (1931) and **39,** 455 (1932).

$$d^2\psi/dx^2 + (8\pi^2 m/h^2)(E - V)\psi = 0. \tag{1}$$

Let

$$\psi = e^{(2\pi i/h)\int y\,dx}. \tag{2}$$

y is then determined by

$$(h/2\pi i)(dy/dx) = p^2 - y^2 \tag{3}$$

where $p^2 = 2m(E - V)$. We now expand y in a series;

$$y = y_0 + (h/2\pi i)y_1 + (h/2\pi i)^2 y_2 + \cdots. \tag{4}$$

Substituting this in Eq. (3) and equating the coefficients of different powers of h to zero separately, we find a set of equations to determine the y_n's. They are given by the recurrence formula

$$y'_{n-1} = -\sum_{m=0}^{n} y_{n-m} y_m, \qquad n = 0, 1, 2 \cdots \tag{5}$$

$$y_0 = \pm p, \tag{6}$$

from which we can obtain the y_n's by simple algebraic manipulation.

$$\begin{aligned} y_0 &= [2m(E - V)]^{1/2} \quad y_1 = V'/4(E - V) \\ y_2 &= -(1/32)(5V'^2 + 4V''(E - V))(2m)^{-1/2}(E - V)^{-5/2} \\ y_3 &= (1/128)(4V''''(E - V)^2 + 18V'V'''(E - V) + 15V'^3)m^{-1}(E - V)^{-4} \\ &\cdots\cdots\cdots\cdots\cdots\cdots\cdots\cdots\cdots\cdots\cdots\cdots \end{aligned} \tag{7}$$

So, if we know V, we can at once calculate ψ by means of Eqs. (7), (4) and (2). Eq. (4) can now be written

$$\begin{aligned} 2\pi i y/h = \pm\, & iB^{-1/2}(E - V)^{1/2} + V'/4(E - V) \\ & \pm (iB^{1/2}/32)(5V'^2 + 4V''(E - V))(E - V)^{-5/2} + \cdots \end{aligned} \tag{8}$$

where $B = h^2/8\pi^2 m$.

It is well known that this expression gives good approximations to y, and hence to ψ, when $(E - V)$ is fairly large. Obviously the same will be true in regions where the potential curve approaches some finite value asymptotically so that all of its derivatives vanish. Furthermore, if B is very small, at least the first few terms appear to converge rapidly. In fact it is known[4a] that this expression is asymptotically convergent both as B becomes small and as $|x|$ becomes large (if $\pm\infty$ are the boundaries of the region). That is to say, as we let B approach zero, the difference between the sum of the first n terms

[4a] See Zwaan, reference 3.

[5] For a discussion of asymptotic series see: W. B. Ford, "Studies on Divergent Series," Macmillan 1916, p. 22 and Chap. III; E. Borel, "Leçons sur les Series Divergentes," Gauthier-Villars 1928, p. 21. Also for applications to differential equations. J. Horn, Math. Ann. **52**, 271 (1899); and "Gewohn. Diff. Gleich." 1927, p. 188; L. Schlesinger: "Gewohnliche Differentialgleichungen," Vieweg 1922, p. 248. A very clear discussion of this subject is given by G. G. Stokes: "Math. and Phys. Papers." Vol. IV, pp. 77–109 and 283–298.

of Eq. (8) and the true value of y will be a small quantity of the order of $B^{n/2}$ for all values of n. A similar relation is true if, instead of letting B become small, we let $|x|$ become large. Consequently we can use a finite number of terms of Eq. (8) and, if B is small or $|x|$ large, this will give us a good approximation to y in spite of the fact that the series actually diverges.[5]

We shall find it convenient here to distinguish between two possible definitions of y. So far it has been defined as the solution of Eq. (3), but it could also be defined by means of Eq. (8). Now Eq. (8) has singular points where $E=V$, and in the neighborhood of those points it does not behave even approximately like the solution of Eq. (3), for we shall see later that the latter has no singularities on the real axis. Thus the two definitions are really different. We shall hereafter call the solution of Eq. (3), $\bar{y}$, to distinguish it from the quantity defined by Eq. (8), which we shall call plain y. For values of x such that $E \neq V$ the two definitions approach each other asymptotically as B approaches zero.

It should be noticed that y has two branches due to the fact that y_0 is given by the square root of p. All of the even numbered y_n's involve square roots, and the sign of the root is to be taken as the same as that in y_0. All of the odd numbered y_n's are single valued.

The Energy Level Condition

We turn now to a derivation of the energy level condition. Kramers[3] and Zwaan[3] have found the energy level condition using only the first two terms of Eq. (8). Their methods differed in that Kramers used another expansion for ψ to supplement Eq. (8) at points where it has singularities (i.e., where $E=V$), whereas Zwaan avoided such points by going around them in the complex plane. Kramers also pointed out that the earlier and more general work of Wentzel[1] was not rigorous, though his own work verified Wentzel's energy level condition as far as it went. This criticism of Wentzel's proof is entirely justified as we shall see, but it is possible to show that Wentzel's result is correct and can be used to find higher approximations to the energy level formula in some cases. It is this more general proof which shall be given in this paper.

In carrying out this proof we use essentially Zwaan's method instead of Kramers', as it lends itself more readily to work with higher approximations. The proof given here, however, differs considerably in details from that of Zwaan.

We use the definition of an energy level as a value of E for which ψ can be (a) single valued, (b) real on the real axis, and (c) bounded on the real axis. We shall follow the usual procedure of starting with a function which is zero at one of the boundaries and carrying it to the other boundary to find what conditions must be satisfied if it is to be zero there also. It will simplify matters if we restrict ourselves to a potential function having only one minimum on the real axis and hence, as we shall deal only with the discrete spectrum, only two points for which $E=V$.

For convenience we divide the real axis into three regions: I, II, and III.

Region I is to the left of both points where $E = V$, (i.e., Q and R, see Fig. (1), II is the region between these two points, and III is the region to the right of them.

We shall designate the two branches of y by the symbols y_a and y_b (these subscripts are not to be confused with the number subscripts in Eq. (4)). y_a is defined as that branch of y whose first term is positive imaginary in region I. Furthermore, we shall suppose the cut in the x plane to be the real axis between Q and R, and we require that in no integral shall the path of integration cross this cut.

The general solution of Eq. (1) will be of the form

$$\psi = c_a e^{(2\pi i/h)\int^x y_a dx} + c_b e^{(2\pi i/h)\int^x y_b dx}. \tag{9}$$

Now in order that ψ be bounded for $x = -\infty$, c_a must be zero since $i\int^x y_a dx$ becomes infinite for large negative values of x.[6] Consequently in region I ψ will have the form

$$\psi_{\mathrm{I}} = c_b e^{(2\pi i/h)\int_P^x y_b dx}. \tag{10}$$

Here c_b is to be determined by normalization. The choice of P_1, the initial point of integration, is arbitrary, c_b assuming different values for different choices of P. For simplicity we shall consider P to be in region I, thus making c_b real.

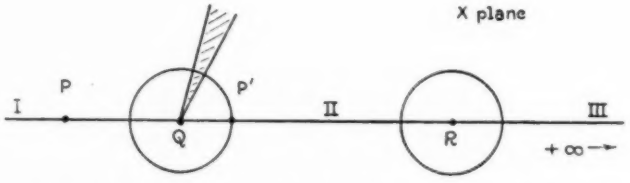

Fig. 1. Q and R are points where $E = V$. Region I is that part of the real axis to the left of Q, region II is between Q and R, and region III is to the right of R.

However, for ψ to have real values for points in region II, c_a *cannot* be equal to zero. Both terms will be needed there, because $\int ydx$ has complex values in region II and an expression of the form of Eq. (10) could not represent a real function. Consequently somewhere on the path from region I to region II (which we shall take so as to avoid the point Q at which $E = V$, and hence at which Eq. (8) has a singularity) it must be possible to change from an expression of the type of Eq. (10) to the more general form of Eq. (9). This sudden change in the coefficients of an asymptotic expression was first discussed by Stokes[5] and is a well-known phenomenon. It arises primarily from the fact that ψ has an essential singularity at infinity. If it did not it would not be necessary to resort to an asymptotic expression for its representation. Hence ψ may require different asymptotic representations for different paths to infinity.

[6] It will be noticed that the first term of Eq. (8) becomes the only important one near the boundaries of the region (here $-\infty$) since there either V becomes infinite or all its derivatives vanish. Also y is a pure imaginary in regions I and III, so that the exponents are real in these regions.

This change in the value of c_a can be looked at from the following point of view. For finite values of B and of x, Eq. (8) represents y only approximately. Hence Eq. (10) gives ψ in region I only to a certain degree of approximation, and similarly an expression of the form of Eq. (9) (with c_a suitably chosen) can represent ψ in region II only approximately. Now there must be some sector around Q (shown in Fig. 1 by the shaded area) where Eqs. (9) and (10) represent ψ with about the same accuracy. In this region it is immaterial which one we use, and we can consider the change in c_a as taking place there.

In order that ψ_{II} be real, c_a must be chosen as follows. Let

$$c_a = c_b e^{(2\pi i/h)\delta}. \tag{11}$$

Then

$$\delta = -\int_P^{P'} y_a dx - \left[\int_P^{P'} y_b dx\right]^* \tag{12}$$

where the asterisk denotes the complex conjugate. Then, since in region II, $y_a = -y_b^*$, we can write

$$\psi_{II} = c_b\left[e^{(2\pi i/h)\int_P^x y_b dx)^*/h} + e^{2\pi i/h\int_P^x y_b dx/h}\right]. \tag{13}$$

By a study of the integrals involved in δ it is not difficult to show that the same value of ψ_{II} is obtained by going around Q in either sense. That is to say, ψ_{II} is also single valued.

We proceed with the continuation of ψ into region III. In going around the point R we find by the same type of argument that c_a must change back to zero if ψ is to be bounded in that region. In region III y_a is the negative imaginary branch of y, and $i\int^x y_a dx$ becomes infinite for infinite x. So in region III we can easily make ψ bounded but the following relation must be satisfied in order to make it real.

$$(2\pi i/h)\int_P^x y_b dx = \text{real number} + \pi n i, \tag{14}$$

where x is now in region III and n is an integer. This can also be written

$$\int_P^x y_b dx + \left(\int_P^x y_b dx\right)^* = nh. \tag{15}$$

Now in Eq. (14) the path of integration went, say, above the points Q and R. In that case the complex conjugate of the integral is equal to the negative of the integral taken in the same direction but on a path going below Q and R.[7] Eq. (15) therefore becomes

$$\oint y dx = nh, \tag{16}$$

[7] This can be verified by using the fact that for real functions the conjugate of a function is the function of the conjugate argument. In applying this rule to square roots a change of branches must also be taken into account.

the path of integration being taken around region II, but including no singularities of y which lie off the real axis. In this equation it makes only a trivial difference if we use y_a instead of y_b.

Eq. (16) is also the condition that ψ be single valued in the sense that the same value of ψ is found no matter what the path of integration for $\oint y dx$ as long as it does not cross the cut QR.

We have shown that Eq. (16) is a necessary condition that E be a characteristic value of Eq. (1). The argument can easily be reversed to show that Eq. (16) is also a sufficient condition.

Wentzel's[1] original generalization of the Bohr phase integral is therefore justified, though the proof that we have given is more complicated than the considerations which Wentzel gave. However as Kramers[3] pointed out, a proof such as the one given above is necessary, because it shows the nature of Eq. (16) as essentially an asymptotic expression for the energy levels rather than an exact condition. Occasionally the series for $\oint y dx$ breaks off after a finite number of terms, in which case Eq. (16) gives exact values, but this does not occur generally.

Due to its asymptotic character, the series in Eq. (16) diverges for actual, finite values of B, and it can therefore be used to find energy levels only to a limited degree of approximation. The quality of the approximation is, in general, better for systems which are nearly classical than for those showing large quantum effects. This is not surprising since the first term of the energy level equation gives the classical Bohr theory.

The way in which the quality of the approximation depends on the presence of quantum effects is well illustrated by the case of a potential function with a sharp kink in it. This kink will give rise to characteristic quantum diffraction effects which would not be present if the kink were smoothed over. Suck a kink often arises from the presence of a singularity in the potential function near the real axis. If, in carrying the integral of Eq. (14) around Q and R we are forced to go near such a singularity, there will be a considerable part of the path for which Eq. (8) does not give a good approximation, and so the energy level formula will be relatively inaccurate.

We shall turn now to the connection between the methods of the present paper and the original work of Wentzel. His proof of Eq. (16) was based in part on a relation derived from Eq. (2), namely that $2\pi i\bar{y} = h\psi'/\psi$. Since wave functions are known to have n nodes in the region II, and since ψ' is not zero at these nodes, he inferred that $\bar{y}$ would have n simple poles in this region and that therefore the integral of $\bar{y}$ around these poles would be exactly nh. This argument, however, is not permissible because the ψ of Eq. (2) is not the characteristic solution. This is obvious since it requires a linear combination of such ψ's to represent the wave function in region II. In fact we can prove that $\bar{y}$ has no poles at all in the classical region of oscillation. (See below.)

Young[4] has recently developed a way of solving Eq. (1) which is very similar to the W. B. K. method. He introduces a quantity P, called the local momentum, which, on the real axis, is the real part of our function $\bar{y}$. Letting

$$\bar{y} = u + iv \tag{17}$$

where u and v are real functions of x, Eq. (3) separates into the following for real values of x.

$$hv'/2\pi = p^2 - u^2 + v^2 \tag{18}$$

and

$$hu'/2\pi = 2uv. \tag{19}$$

P is given by $hP = 2\pi u$, and Young has found that P has neither zero's nor poles on the real axis. It follows, since v is the logarithmic derivative of P, that v has no poles on the real axis either. Therefore $\bar{y}$ has no poles on the real axis.

How then can Eq. (16) be true? The answer to this has been given by Kramers.[3] Eq. (16) applies to the case in which we have expanded $\bar{y}$ in the series Eq. (4). This series converges asymptotically as B approaches zero for all values of x except those for which $E = V$. Such points are singular points in the expansion, and allow the integral in Eq. (16) to take on values different from zero. It should be noted that Eq. (16) tends asymptotically to zero as $B \to 0$ so that in the limit it behaves as if y had no poles. In other words, Eq. (16) refers to y and not to $\bar{y}$.

By a very simple analysis Young has derived an energy level condition in the form of a phase integral involving P, and it would be convenient if we could derive Eq. (16) directly from it, thus avoiding the use of asymptotic series and the like. Unfortunately this cannot be done because, as we have seen, the singularities which appear in the expansion for y (Eq. (8)), but which $\bar{y}$ does not possess, are essential for the usefulness of Eq. (16). Another difficulty, also connected with the asymptotic character of Eq. (8), is that though our expansion of y is purely imaginary in regions I and III, $\bar{y}$ must have a real component in those regions. This follows from the fact that P is nowhere zero. We must therefore conclude that the two methods use essentially different ways of representing the wave functions, and that there is no simple way of showing the equivalence of the results.

It is, however, worth noting that the two methods are complementary in that each has its own peculiar usefulness. Young's method brings out the physical significance of the situation very clearly, but is of limited use for actual computation because of the complicated differential equation from which P must be calculated. On the other hand, though the derivation of the W. B. K. energy level formula is rather long, it enables one to find energy levels by means of a very simple integration.

Simplification of the Formula

Having discussed the nature of Wentzel's energy level condition it remains only to put it in a more useful form. Using Eq. (8) we find that Eq. (16) is a series of integrals whose form is given by Eqs. (7). We shall consider them one by one.

The term in y_1 is the Bohr theory integral. It cannot be simplified until we know something more about V.

The term in y_1 gives us the half integer quantization. It has been discussed in all of the literature on the subject.

The term in y_2 adds something new. Integrating by parts we find:

$$(h/2\pi i)^2 \oint y_2 dx = (h/2\pi)^2 (2m)^{-1/2} \oint (5V'^2 + 4V'''(E-V))(E-V)^{-5/2} dx \tag{20}$$
$$= -(h^2/128\pi^2)(2m)^{-1/2} \oint V'^2 (E-V)^{-5/2} dx.$$

The term in y_3 vanishes. This can be shown very easily because from Eq. (7)

$$y_3 = -d(y_2/2y_0)/dx, \tag{21}$$

and this integrates to zero around the closed cycle.

The term in y_4 can be reduced by integrating by parts. The result is:

$$(h/2\pi)^4 \oint y_4 dx = -h^4\pi^{-4}m^{-1}(2m)^{-1/2}2^{-16}\Big[49 \oint V'^4 (E-V)^{-1/2} dx \tag{22}$$
$$- 16 \oint V'V''(E-V)^{-7/2} dx\Big].$$

Collecting all of these expressions and neglecting y_5 and higher terms, we find for Eq. (16)

$$\oint (E-V)^{1/2} dx - (B/32) \oint V'^2 (E-V)^{-5/2} dx$$
$$- (B^2/2048) \oint [49V'^4 (E-V)^{-11/2} - 16V'V'''(E-V)^{-7/2}] dx \tag{23}$$
$$+ \cdots = (n + \tfrac{1}{2}) 2\pi B^{1/2}.$$

where $n = 0, 1, 2, 3 \cdots$. This is as far as Eq. (16) can be simplified without more knowledge of the function V.

I am indebted to Professor E. C. Kemble for suggestions and discussions of various points raised in this paper.

The Energy Levels of a Rotating Vibrator

By J. L. DUNHAM
Harvard University

(Received May 11, 1932)

The energy levels of a rotating vibrator are calculated in considerable detail by means of the Wentzel-Brillouin-Kramers method. The new terms determined are $\omega_e z$ and a set of correction terms which appear in the earlier members of the equation. These correction terms enter in such a way that ω_e is not exactly the coefficient of $(v+\frac{1}{2})$; B_e is not exactly the coefficient of $K(K+1)$, etc. However the differences are small and are detectable only in the case of light molecules. The correction terms are of the magnitude of B_e^2/ω_e^2. Formulas for the effect of the correction terms on isotope shifts are given, and for the calculation of the correction terms themselves. Also a method is given for obtaining actual potential functions from band spectrum data, based on Morse's potential function. Finally the numerical magnitude of the correction terms for several states of H_2 and for NaH is discussed.

INTRODUCTION

RECENT work on the measurement of isotope masses by means of band spectra[1,2,3] has led to the necessity of examining in more detail the theory of a rotating vibrator. The energy levels of this sytem were thoroughly investigated by Kratzer,[4] Born and Hückel,[5] Kemble[6] and Birge[7] on the basis of the Bohr theory, but no detailed quantum mechanical treatment of this system has been published. This seems to be at least partly because the potential function suggested by Morse[8] has energy levels which agree exactly with those predicted for it by the Bohr theory[9] (apart from the matter of half quantum numbers), and which fit the empirical energy levels remarkably well. Furthermore, the early work of Fues[10] indicated an almost complete agreement between the two theories for quite general potential functions, the difference between Fues' result and that of the Bohr theory being merely a constant term, spectroscopically undetectable. Calculation of the higher approximations, however, shows that this constant term is one of a set of terms which in general depend on the vibrational and rotational quantum numbers, adding small corrections to the familiar terms in the energy level formula. It happens that for Morse's potential function the corrections to the pure vibra-

[1] R. T. Birge, Phys. Rev. **37**, 841, 227, and 233 (1931).
[2] F. A. Jenkins, Phys. Rev. **39**, 549 (1932).
[3] Mecke and Wurm, Zeits. f. Physik **61**, 37 (1930).
[4] A. Kratzer: Zeits. f. Physik **3**, 289 (1920).
[5] M. Born and Hückel, Phys. Zeits. **24**, 1 (1923).
[6] E. C. Kemble, J. Opt. Soc. Am. **12**, 1 (1926).
[7] R. T. Birge, Nature **116**, 783 (1925) and Phys. Rev. **27**, 245 (1926). See also W. C. Pomeroy, Phys. Rev. **29**, 67 (1927).
[8] P. M. Morse, Phys. Rev. **34**, 57 (1929).
[9] P. M. Davidson and W. C. Price, Proc. Roy. Soc. **A130**, 105 (1931).
[10] E. Fues, Ann. d. Physik **80**, 367 (1926).

tion terms are exactly zero which leads us to expect they will be small in actual molecules. But the predictions of Morse's function for the corrections to the rotational terms are not zero, so we cannot expect these to be small.

The analysis shows that the coefficients of the various powers of $(v+\frac{1}{2})$ and $K(K+1)$ in the energy level formula are really a series in powers of the ratio B_e^2/ω_e^2. This ratio is, for most molecules, of the order of magnitude of 10^{-6} so that all of the terms beyond the first (given by the Bohr theory) are negligible. However, for hydrogen molecules and some of the hydrides this ratio is more nearly 10^{-3}, so that in these cases they cannot be neglected.

In this paper the energy levels of a rotating vibrator will be calculated in detail using a perfectly general type of potential function. To find the characteristic values of Schrödinger's equation we shall use the Wentzel-Brillouin-Kramers[11] method (hereafter called the W. B. K. method) because it solves our problem in a very simple fashion. The particular advantage of this method is that it uses the Bohr theory energy levels as its first approximation, correcting for higher quantum effects by its later approximations. Now according to the correspondence principle point of view, quantum effects become small not only for large quantum numbers, but also for large masses, and the nuclei of molecules have large masses compared to electronic masses. We would therefore expect the Bohr energy levels to be good approximations in this case. The W. B. K. method can make use of this fact by starting with the Bohr levels and calculating any further terms as small corrections. The details of the W. B. K. method necessary for application to this problem have been developed in the preceding paper and we shall apply them here to the solution of the rotating-vibrator, and then discuss applications to a few actual molecular states.

Calculation of the Energy Levels

Our first problem is to find the energy levels of a rotating vibrator. To do this we calculate the characteristic values of Schrödinger's equation for this system, which is:

$$\frac{d^2\psi}{d\xi^2}+\frac{8\pi^2 m r_e^2}{h^2}\left[E-V-\frac{h^2K(K+1)}{8\pi^2 r_e^2 m(1+\xi)^2}\right]\psi=0. \tag{1}$$

Here $\xi=(r-r_e)/r_e$, r_e being the equilibrium nuclear separation; m is the reduced nuclear mass; V the potential function with a minimum at r_e; and the last term in the bracket, which we shall call V_r, is due to the centrifugal force of rotation.

It would be convenient to use a potential function based on that of Morse, because this gives a very good approximation to actual energy levels. However, it is difficult to include the effect of rotation in Morse's potential function. In the end the simplest procedure is to use a power series expansion of

[11] G. Wentzel, Zeits. f. Physik **38,** 518 (1926); L. Brillouin, Comptes Rendus **183,** 24 (1926); H. A. Kramers, Zeits. f. Physik **39,** 828 (1926). For a good short account see A. Sommerfeld: Ergänzungsband, p. 158.

V around the point $\xi=0$, as V_r has a particularly simple expansion about this point. Having found the energy levels in terms of this sort of expansion, it is not difficult then to rewrite the formulas in terms of any simple expression for the potential function by expanding the latter in a power series about $\xi=0$ and equating coefficients. We shall therefore use

$$V = hca_0\xi^2(1 + a_1\xi + a_2\xi^2 + a_3\xi^3 + \cdots) \tag{2}$$

where $a_0=\omega_e^2/4B_e$; ω_e is the classical frequency of small oscillations expressed in cm^{-1} and $B_e=h/(8\pi^2 mr_e^2 c)$.

We shall first calculate the energy levels neglecting rotation (i.e., for the case $K=0$). The effect of rotation can then be found by rewriting the whole effective potential function in the form of Eq. (2) and comparing coefficients.

In the preceding paper I showed that the energy levels of a potential function with a single minimum could be found by evaluating a generalized phase integral (Eq. (23) of that paper). It will be convenient to express all quantities involving energy in this equation in terms of wave numbers. This involves replacing E by hcF and V by hcU. Eq. (23) then becomes

$$\oint (F-U)^{1/2}d\xi - (B_e/32)\oint U'^2(F-U)^{-5/2}d\xi + \cdots = 2\pi B_e^{1/2}(v+\tfrac{1}{2}). \tag{3}$$

The first integral on the left has been evaluated many times.[4,5,6] However, the method necessary to evaluate the second integral is also applicable to the first, and handles it in a particularly simple fashion, so we shall use it here.

The first step is to transform to the independent variable U. The integral becomes

$$\oint (F-U)^{1/2}d\xi = \oint (F-U)^{1/2}(U')^{-1}dU. \tag{4}$$

Here the integral is taken in the U plane twice around the two points $U=0$ and $U=F$ (the origin of energy being so chosen that $U=0$ for $\xi=0$). The cut in the ξ plane between the two turning points goes over into a cut in the U plane between the origin and the point $U=F$.

The integral can be evaluated if we know U' as a function of U, so we expand U'

$$U' = A_1U^{1/2} + A_2U + A_3U^{3/2} + A_4U^2 + \cdots, \tag{5}$$

from which we can calculate $(U')^{-1}$ in a series of the form

$$(U')^{-1} = A_1^{-1}U^{-1/2}[1 + B_1U^{1/2} + B_2U + B_3U^{3/2} + \cdots]. \tag{6}$$

We can therefore write the integral as:

$$\oint (F-U)^{1/2}d\xi = \oint iA_1^{-1}[1 - F/2U - F^2/8U^2 + \cdots][1 + B_1U^{1/2} + B_2U + \cdots]dU. \tag{7}$$

There is now a cut in the U plane extending from the point $U=0$ to ∞, introduced by the expansion Eq. (5). Consequently when the integration is performed all of the terms in $U^{n/2}$ for which n is odd will vanish because the integrand will have opposite signs on the two circuits around the point $U=0$. Of the remaining terms only those in U^{-1} will have a residue. The integration yields:

$$\oint (F-U)^{1/2}d\xi = (2\pi/A_1)[F + B_2F^2/4 + B_4F^3/8 + 5B_6F^4/64 + \cdots]. \quad (8)$$

The second integral in Eq. (3) can be evaluated similarly. As before we transform to U as independent variable. On substituting the expansion Eq. (5) for U' and expanding the denominator, we have

$$\oint U'(F-U)^{-5/2}dU = 4\pi[A_3 + 5A_5F/2 + 35A_7F^2/8 + 105A_9F^3/16 + \cdots]. \quad (9)$$

We have now evaluated the integrals of Eq. (3) in terms of the coefficients A_n of Eq. (5), and it remains to find these A_n's in terms of the a_n's of Eq. (2). If we expand $U^{n/2}$ and U' as power series in ξ and substitute all of these in Eq. (5), we can equate coefficients of like powers of ξ on both sides of the equation and obtain enough relations to determine the coefficients A_n.

The results of this procedure are:

$$\begin{aligned}
&A_1 = 2a_0^{1/2};\ A_2 = 2a_1;\ A_3 = a_0^{-1/2}(3a_2 - 7a_1^2/4)\\
&A_4 = a_0^{-1}(4a_3 - 6a_1a_2 + 5a_1^3/2)\\
&A_5 = a_0^{-3/2}(5a_4 - 19a_1a_3/2 - 17a_2^2/4 + 105a_1^2a_2/8 - 273a_1^4/64)\\
&A_6 = a_0^{-2}(6a_5 - 14a_1a_4 - 12a_2a_3 + 22a_1^2a_3 + 20a_1a_2^2 - 30a_1^3a_2 + 8a_1^5)\\
&A_7 = a_0^{-5/2}(7a_6 - 39a_1a_5/2 - 33a_2a_4/2 - 31a_3^2/4 + 279a_1^2a_4/8 + 75a_2^3/8\\
&\quad + 243a_1a_2a_3/4 - 825a_1^3a_3/16 - 2277a_1^2a_2^2/32 + 9009a_1^4a_2/128\\
&\quad - 8151a_1^6/512).\\
&\quad \cdots\cdots\cdots\cdots\cdots\cdots\cdots\cdots
\end{aligned} \quad (10)$$

We are now ready to go back to Eq. (3) and substitute the results we have obtained for the integrals. We shall at first express these in terms of the A_n's and B_n's for simplicity, using the a_n's only at the end.

Substituting Eqs. (8) and (9) in Eq. (3) we have

$$\begin{aligned}
&(2\pi/A_1)[F + B_2F^2/4 + B_4F^3/8 + 5B_6F^4/64 + \cdots]\\
&\quad - (2\pi B_e/16)[A_3 + 5A_5F/2 + 35A_7F^2/8 + \cdots] = 2\pi B_e^{1/2}(v+\tfrac{1}{2}).
\end{aligned} \quad (11)$$

By the inversion of this series we find F as a power series in $(v+\frac{1}{2})$. The result is:

$$\begin{aligned}
F = {}& B_eA_1A_3/16 + A_1B_e^{1/2}(v+\tfrac{1}{2}) + (B_e^{3/2}A_1^2/32)(5A_5 - B_2A_3)(v+\tfrac{1}{2})\\
&- (B_eB_2A_1^2/4)(v+\tfrac{1}{2})^2 + (B_e^2A_1^3/128)(35A_7 - 15B_2A_5 + 3A_3B_2^2\\
&- 3A_3B_4)(v+\tfrac{1}{2})^2 + (B_e^{3/2}A_1^3/8)(B_2^2 - B_4)(v+\tfrac{1}{2})^2\\
&+ (B_e^2A_1^4/64)(10B_2B_4 - 5B_2^3 - 5B_6)(v+\tfrac{1}{2})^4 + \cdots.
\end{aligned} \quad (12)$$

Substituting Eqs. (10) gives us the term value equation for an oscillator having Eq. (2) for a potential function up to and including terms in B_e^4/ω_e^4. (One term, not depending on $(v+\frac{1}{2})$, has been omitted.)

Before we carry out this substitution, however, it will be convenient to take account of rotation. In this case the effective potential function is $U+U_r=U_K$, which is of the form

$$U_K = a_0\xi^2(1 + a_1\xi + a_2\xi^2 + \cdots) + B_eK(K+1)(1 - 2\xi + 3\xi^2 - 4\xi^3 + \cdots). \quad (13)$$

We can introduce a new variable η such that $\xi=\eta+\epsilon$, ϵ being a constant, and choose ϵ so that the minimum of U_K falls at the point $\eta=0$. If we then express U_K as a power series in η of the same form as Eq. (2), and use the coefficients of this new series in Eq. (12) instead of the a_n's, we shall have the energy levels of a rotating vibrator.

The detail of determining these coefficients is rather tedious but quite straightforward, so we shall not reproduce it here. The energy level equation which one finds is most conveniently written in the following form

$$F_{vK} = \sum_{ij} Y_{ij}(v+\tfrac{1}{2})^i K^j(K+1)^j. \quad (14)$$

The first subscript under Y refers to the power of the vibrational quantum number, the second to that of the rotational quantum number.

The first fifteen Y_{ij}'s are found to be [12]

$$Y_{00} = (B_e/8)(3a_2 - 7a_1^2/4)$$

$$Y_{10} = \omega_e[1 + (B_e^2/4\omega_e^2)(25a_4 - 95a_1a_3/2 - 67a_2^2/4 + 459a_1^2a_2/8 - 1155a_1^4/64)]$$

$$Y_{20} = (B_e/2)[3(a_2 - 5a_1^2/4) + (B_e^2/2\omega_e^2)(245a_6 - 1365a_1a_5/2 - 885a_2a_4/2 - 1085a_3^2/4 + 8535a_1^2a_4/8 + 1707a_2^3/8 + 7335a_1a_2a_3/4 - 23865a_1^3a_3/16 - 62013a_1^2a_2^2/32 + 239985a_1^4a_2/128 - 209055a_1^6/512)]$$

$$Y_{30} = (B_e^2/2\omega_e)(10a_4 - 35a_1a_3 - 17a_2^2/2 + 225a_1^2a_2/4 - 705a_1^4/32)$$

$$Y_{40} = (5B_e^3/\omega_e^2)(7a_6/2 - 63a_1a_5/4 - 33a_2a_4/4 - 63a_3^2/8 + 543a_1^2a_4/16 + 75a_2^3/16 + 483a_1a_2a_3/8 - 1953a_1^3a_3/32 - 4989a_1^2a_2^2/64 + 23265a_1^4a_2/256 - 23151a_1^6/1024)$$

$$Y_{01} = B_e[1+(B_e^2/2\omega_e^2)(15+14a_1-9a_2+15a_3-23a_1a_2+21(a_1^2+a_1^3)/2)]$$

[12] Eq. (14) can be changed to a set of power series in $(K+1/2)^2$ instead of $K(K+1)$ by using the formulas

$$K^n(K+1)^n = [(K+\tfrac{1}{2})^2 - \tfrac{1}{4}]^n$$

This will affect only the second order terms (of the order of B_e^2/ω_e^2) in each of the Y's.

$$Y_{11} = (B_e^2/\omega_e)[6(1+a_1)+(B_e^2/\omega_e^2)(175+285a_1-335a_2/2+190a_3-225a_4/2$$
$$+ 175a_5 + 2295a_1^2/8 - 459a_1a_2 + 1425a_1a_3/4 - 795a_1a_4/2$$
$$+ 1005a_2^2/8 - 715a_2a_3/2 + 1155a_1^3/4 - 9639a_1^2a_2/16 + 5145a_1^2a_3/8$$
$$+ 4677a_1a_2^2/8 - 14259a_1^3a_2/16 + 31185(a_1^4 + a_1^5)/128)] \quad (15)$$

$$Y_{21} = (6B_e^3/\omega_e^2)(5 + 10a_1 - 3a_2 + 5a_3 - 13a_1a_2 + 15(a_1^2 + a_1^3)/2)$$

$$Y_{31} = (20B_e^4/\omega_e^3)(7 + 21a_1 - 17a_2/2 + 14a_3 - 9a_4/2 + 7a_5 + 225a_1^2/8$$
$$- 45a_1a_2 + 105a_1a_3/4 - 51a_1a_4/2 + 51a_2^2/8 - 45a_2a_3/2$$
$$+ 141a_1^3/4 - 945a_1^2a_2/16 + 435a_1^2a_3/8 + 411a_1a_2^2/8$$
$$- 1509a_1^3a_2/16 + 3807(a_1^4 + a_1^5)/128)$$

$$Y_{02} = -(4B_e^3/\omega_e^2)[1 + (B_e^2/2\omega_e^2)(163 + 199a_1 - 119a_2 + 90a_3 - 45a_4$$
$$- 207a_1a_2 + 205a_1a_3/2 - 333a_1^2a_2/2 + 693a_1^2/4 + 46a_2^2$$
$$+ 126(a_1^3 + a_1^4/2))]$$

$$Y_{12} = -(12B_e^4/\omega_e^3)(19/2 + 9a_1 + 9a_1^2/2 - 4a_2)$$

$$Y_{22} = -(24B_e^5/\omega_e^4)(65 + 125a_1 - 61a_2 + 30a_3 - 15a_4 + 495a_1^2/4 - 117a_1a_2$$
$$+ 26a_2^2 + 95a_1a_3/2 - 207a_1^2a_2/2 + 90(a_1^3 + a_1^4/2))$$

$$Y_{03} = 16B_e^5(3 + a_1)/\omega_e^4$$

$$Y_{13} = (12B_e^6/\omega_e^5)(233 + 279a_1 + 189a_1^2 + 63a_1^3 - 88a_1a_2 - 120a_2 + 80a_3/3)$$

$$Y_{04} = -(64B_e^7/\omega_e^6)(13 + 9a_1 - a_2 + 9a_1^2/4).$$

The new quantities are Y_{40}, Y_{13} and the second terms [13] in $Y_{10}Y_{20}Y_{01}Y_{11}Y_{02}$.

The connection between the Y's and the ordinary band spectrum constants is as follows:

$Y_{10} \sim \omega_e$	$Y_{20} \sim -\omega_e x$	$Y_{30} \sim \omega_e y$
$Y_{01} \sim B_e$	$Y_{11} \sim -\alpha_e$	$Y_{21} \sim \gamma_e$
$Y_{02} \sim D_e$	$Y_{12} \sim \beta_e$	$Y_{40} \sim \omega_e z$
$Y_{03} \sim F_e$	$Y_{04} \sim H_e$	

Throughout this paper the Y_{lj}'s will be used to denote the coefficients in Eq. (14), and the old coefficients will retain their mechanical significance. Thus B_e will be used only for $h/8\pi^2 I_e c$ and not for the coefficient of $K(K+1)$ in the energy level equation, etc.

Discussion of the Energy Level Formula

The most important point about Eq. (15) is that the Y's are not exactly equal to the coefficients given by the Bohr theory. For example, Y_{10}, which is the coefficient of $(v+\frac{1}{2})$, is not equal to ω_e, but differs from it by terms in B_e^2/ω_e^2. Similarly Y_{01} differs from B_e by small terms. In fact each of the Y's

[13] The second term in Y_{00} has been omitted because it is not important. It has the same form as Y_{40} or the second term in Y_{20}.

is a power series in B_e^2/ω_e^2. Now for many molecules this ratio is of the order of magnitude of 10^{-6} so that the first term of the power series is adequate for all practical purposes. But for some molecules, notably H_2, B_e^2/ω_e^2 is more nearly 10^{-3}, and higher terms in several of the Y's must be taken into consideration. This correction arises from the presence of the second term on the left hand side of Eq. (3), and one can see from the fact that m appears in the denominator of this term that the corrections will be small for heavy systems and large for light ones. It is for this reason that these terms will be most easily detectable in H_2.

Unfortunately the detection of the effect of these higher terms in actual spectra will be complicated by the fact that the nuclear potential function is defined only in so far as the nuclear and electronic wave functions are separable. This is ordinarily true to terms in B_e^2/ω_e^2, which means that this coupling will introduce terms of nearly the same size as the new terms which we have been discussing. In cases where the interaction is very large, such as l-uncoupling or when there are perturbations, the coupling effects will be much more important than the effects discussed here. This state of affairs can be detected by using the fact that for a simple rotator Y_{02} (D_e) is determined by the other Y's. The values of Y_{l0} and Y_{l1} determine all of the a_n's. Consequently Y_{02} can be found in terms of these Y's. If this theoretical value of Y_{02} does not agree with the observed value, the system is not a simple rotating vibrator, and we can expect that there is appreciable interaction. It is therefore important to find Y_{02} as accurately as possible from the data, as it is necessary to show that coupling effects are small before one can determine the size of the correction terms.

One of the chief uses of a detailed derivation of the energy level equation is to find how the terms depend on the nuclear mass. By definition we know that B_e is proportional to m^{-1} and that ω_e is proportional to $m^{-1/2}$, so we can find the mass dependence of the Y's if we assume that two isotopic molecules have identical potential functions.

The Bohr theory leads to the result suggested by Kemble[14] that

$$(Y_{lj}{}^i/Y_{lj}) = (m/m^i)^{(l+2j)/2} \tag{16}$$

the superscript i referring to one of the isotopes, but this equation takes account of only the first terms in the expressions for the Y's. The presence of the new correction terms will alter the mass dependence of the Y's, as they are now of the form

$$Y_{lj} = f_{lj}(B_e, \omega_e)\ [\alpha_{lj} - (B_e^2/\omega_e^2)\,\beta_{lj} + \cdots] \tag{17}$$

where $f_{lj}(B_e, \omega_e)$ contains that part of the first term in Y_{lj} which depends on m, whereas α_{lj} and β_{lj} do not depend on m. Since B_e^2/ω_e^2 is small, Eq. (16) now becomes

$$(Y_{lj}{}^i/Y_{lj}) = (m/m^i)^{l/2+j}[1 + (\beta_{lj}B_e^2/\alpha_{lj}\omega_e^2)((m - m^i)/m^i)] \tag{18}$$

[14] R. S. Mulliken, Phys. Rev. **25**, 126 (1925).

This gives us a simple way of finding the correction to the isotope effect due to the presence of the new correction terms in the energy level formula.

We want to be able to find the coefficients β (in Eq. (17)) from the experimental data. This is simplified by the fact that these correction terms are small enough so that we can use a method of successive approximations. If we regard the Y's as being given experimentally, and if we neglect the correction terms, a set of approximate a_n's can be calculated from the Y_{l0}'s and the Y_{l1}'s. These a_n's can then be used to calculate the correction terms with sufficient accuracy for most purposes. Carrying out this procedure algebraically we find the following equations for the corrections which are designated by β_{lj}.

$$\begin{aligned}
\beta_{01} &= Y_{10}^2Y_{21}/4Y_{01}^3 + 16a_1Y_{20}/3Y_{01} - 8a_1 - 6a_1^2 + 4a_1^3 \\
\beta_{10} &= 5Y_{10}Y_{30}/4Y_{01}^2 + a_1Y_{10}^2Y_{21}/3Y_{01}^3 - 10a_1 - 20a_1^2 - 15a_1^3/2 \\
&\quad - 5a_1^4/2 + Y_{20}(4a_1 + 16a_1^2/3)/Y_{01} + Y_{20}^2/2Y_{01}^2 \\
\beta_{02} &= 73/2 + 37a_1 + 67a_1^2/2 + 33a_1^3 - 6a_1^4 - 9Y_{10}Y_{30}/2Y_{01}^2 \\
&\quad + Y_{10}^2Y_{21}(3 - 11a_1/6)/2Y_{01}^3 - Y_{20}(130/3 + 4a_1 + 74a_1^2/3)/2Y_{01} \\
&\quad + 31Y_{20}^2/9Y_{01}^2 \\
a_1 &= (Y_{11}Y_{10}/6Y_{01}^2) - 1
\end{aligned} \tag{19}$$

The other β's (β_{20}, β_{11}, and others not given in Eqs. (15)) are more complicated but can be calculated in the same fashion. Eqs. (19) are not as simple as the expressions for the corresponding β's in Eqs. (15). However to use Eqs. (19), it is not necessary to calculate all of the a_n's involved first.

In view of the importance of Morse's[8] potential function for vibrational analysis we shall discuss briefly its relation to the formulas which we have used.

The most striking property of Morse's potential function is the simplicity of the energy level equation to which it leads. It is interesting to see how this simplicity arises in the method we have used for calculating energy levels. Morse's potential function can be written

$$U = D(1 - e^{-a\xi})^2. \tag{20}$$

From this it is easy to show that

$$U' = 2a(DU)^{1/2} - 2aU. \tag{21}$$

Comparing with Eq. (5) we see that for this case

$$A_1 = 2aD^{1/2}, \quad A_2 = -2a \tag{22}$$

and that all the other A's are zero. Now all of the Y_{l0}'s, except Y_{10} and Y_{20}, involve A_n's with $n \geqq 3$ so that they vanish, and the same is true of all of the terms beyond the first in Y_{10} and Y_{20}. A similar but not so far reaching simplification can be found in the case of Kratzer's potential function. This accounts in detail for the fact that the Bohr theory with half quantum numbers gives Morse's energy levels exactly.[9]

Because of its simplicity and because it represents actual molecular energy levels so well, it would be convenient to have a relatively simple potential function based on that of Morse. One could then determine a potential curve from band frequencies more easily than at present. The most satisfactory way to do this seems to be to write the potential function in the following form. (The a used here is equal to Morse's a multiplied by r_e.)

$$U = D[(1 - e^{-a\xi})^2 + P_4(1 - e^{-a\xi})^4 + P_5(1 - e^{-a\xi})^5 + \cdots]. \quad (23)$$

This can be expanded about the point $\xi = 0$ in a power series and the a_n's so determined can be substituted in Eqs. (15) and then the P's determined in terms of the Y's. Morse determined a from the relation $a\ {}^2B_e = -\omega_e x$. We shall use

$$a = 1 - (Y_{10}Y_{11}/6Y_{01}^2). \quad (24)$$

Then the P_n's can be expressed as follows:

$$P_4 = (2/3)[1 + Y_{20}/Y_{01}a^2]$$
$$P_5 = [Y_{10}^2Y_{21}/6Y_{01}^3 - 5 + 10a - 23a^2/4 + 7a^3/6 - 3P_4a^2(a-1)]/5a^3 \quad (25)$$
$$P_6 = Y_{10}Y_{30}/5a^4Y_{01}^2 + P_4/5 - 17P_4^2/20 - P_5.$$

Now since the first term in Eq. (23) is a very good representation of actual potential functions we would expect the P_n's to be quite small and Eq. (23) should converge rapidly.

In calculating Eqs. (25) the new correction terms were *not* used. For obtaining graphical potential functions they are not of enough importance. It should also be mentioned that although the P_n's make corrections to the heat of dissociation predicted by Morse's potential function, it is not to be supposed that these corrections are very reliable. It has been repeatedly shown that the extrapolation of energy levels to dissociation can be used only when most of the energy levels are actually known.

Discussion of Actual Data

We turn now to the calculation of the correction terms for some actual molecular states. These terms are most important in the case of the H_2 molecule. The upper states are known to show a good deal of l-uncoupling,[15] as can be seen easily from the difference between the observed and calculated values of $Y_{02}(D_e)$. The normal state of the molecule should be quite free from such coupling effects, but unfortunately the vibrational analysis has not been carried through with enough precision to be able to tell definitely whether or not this is the case.[16]

Nevertheless it is possible to see how large the correction terms will be for

[15] W. Weizel, Zeits. f. Physik **55**, 483 (1929) and **56**, 727 (1929); G. H. Dieke, Zeits. f. Physik **55**, 447 (1929).

[16] Birge and Jeppeson (Nature **125**, 463 (1930)) have found evidence for a "perturbation" of this lowest level, but there is not yet enough data on the constants of this state to determine the nature of the perturbation.

several states of this molecule, and they will give us some idea of what to expect.

For the normal state Hyman[17] has found the following values for the Y's

$$\begin{aligned} Y_{10} &= 4371 \qquad Y_{11} = 2.794 \\ Y_{01} &= 60.59 \qquad Y_{21} = 0.0105 \\ Y_{20} &= 113.5. \end{aligned} \tag{26}$$

From these β_{01} can be calculated and turns out to be

$$\beta_{01} = -1.37.$$

Also

$$B_e^2/\omega_e^2 = 1/5200.$$

So we conclude that Y_{01} differs from B_e by one part in 3790. In a careful analysis this would be detectable.

Similarly, using data from the analyses of Richardson and Davidson,[18] we find that for the $2^1\Sigma$ state

$$\begin{aligned} Y_{01} &= B_e(1 - 1/778) \\ Y_{10} &= \omega_e(1 - 1/9240) \\ Y_{02} &= D_e(1 - 1/213). \end{aligned} \tag{27}$$

Although in Y_{10} the correction is very small, it is obviously not negligible in either of the other two.

The behavior of the corrections for this state is of some interest as it seems to be typical. The correction to Y_{10} is very small. If Morse's potential function were correct it would be zero, and the fact that it is small shows that Morse's function is a good approximation. Now Morse's function is known to be a better fit for most molecules than for H_2,[9] so we would expect β_{10} to be even smaller for other molecules than it is here.

The correction to Y_{02} is quite large. This appears to be a typical behavior as can be seen from the fact that the value of β_{02} predicted by Morse's potential function varies between 10 and 500 for moderate values of a. This is considerably larger than the other β's we have been discussing.

In the $2^3\Sigma$ state[18] we find that the corrections are quite small. β_{02} is the largest, being equal to 5.2 so that

$$Y_{02} = D_e(1 - 1/1165).$$

The other two are negligible.

The corrections to Y_{20} and Y_{11} demand a knowledge of Y_{40} and of Y_{31}, but as these coefficients have not been determined for the states of H_2 it is not possible to find the corresponding corrections.

[17] H. H. Hyman, Phys. Rev. **36,** 187 (1930).
[18] O. W. Richardson and P. M. Davidson, Proc. Roy. Soc. **A125,** 23 (1929).

An interesting case arises in the alkali hydrides.[19] They are the only known bands for which Y_{20} is positive. We might therefore expect the correction terms to be abnormally large. Weizel[20] has tried to explain the strange behavior of these bands as due to l-uncoupling, but there also appears to be an abnormality in the pure vibration states, and it is therefore of interest to see how the corrections turn out in this case.

The best data available appear to be on NaH.[19] The value of B_e^2/ω_e^2 is 0.0000310 which is materially smaller than for the states of H_2. In this respect LiH would be the most suitable substance for finding large effects. The corrections are

$$\begin{aligned} Y_{01} &= B_e(1 - 1/2280) \\ Y_{10} &= \omega_e(1 - 1/3920) \\ Y_{02} &= D_e(1 - 1/886). \end{aligned} \tag{28}$$

In terms of β_{ij}'s one finds

$$\beta_{01} = -14.15 \qquad \beta_{10} = -8.23 \qquad \beta_{02} = -36.4.$$

These β's are, on the whole, larger than those for H_2 which indicates a slightly anomalous behavior of the potential function. The relatively small value of B_e^2/ω_e^2 prevents these large values of β from making large corrections to the Y's.

For molecules heavier than hydrides, the values of B_e^2/ω_e^2 are so small that unless the β's are abnormally large, the corrections will be undetectable.

A large part of this paper was prepared while I was a National Research Fellow at the University of Chicago. I wish to take this opportunity to express my appreciation of the grant of a Fellowship and of the generous way in which the facilities of the Ryerson Laboratory were placed at my disposal.

[19] LiH, G. Nakamura, Zeits. f. Physik **59**, 218 (1930); NaH, T. Hori, Zeits. f. Physik **62**, 352 (1930); KH, G. M. Almy and C. D. Hause, Phys. Rev. **39**, 178 (1932).

[20] W. Weizel, Zeits. f. Physik **60**, 599 (1930).

Rotational Analysis of Some CO_2 Emission Bands. Part I

By R. F. Schmid
Ryerson Physical Laboratory, University of Chicago

By using the light of a hollow cathode discharge and that of a Back box with direct current, the red degraded CO_2 bands at λλ3247, 3254, 3370, 3377, 3503, 3511, 3534, 3545, 3674 and 3839A have been photographed in the third order of a 21 foot Rowland grating and analyzed. The bands are composed of *P* and *R* branches and on first inspection they show no alternately missing lines. The lines of the bands at λλ3254, 3377, 3511, 3534, and 3839A show staggering, while the lines of the other bands do not (in the limit of observational accuracy). The single structure of the bands indicates that the molecule is linear in both initial and final states. The distance between the carbon and an oxygen atom computed from the rotational constants is almost the same as computed from the CO and CO^+ bands. The above enumerated bands show no Zeeman effect of the observable lines. Other bands which are found to show more complicated structure and Zeeman effect will be the subject of further investigations.

Experimental

As already reported,[1] the emission spectrum of CO_2 can be obtained in suitable intensity by pumping tank CO_2 quickly through a Back box, using a direct current discharge, the magnet pole-pieces serving as cathodes and a piece of tungsten between them as the anode. Besides the strong CO_2 bands, the plates show the entire, but weaker CO^+ spectrum, the third positive CO bands and rather strong angstrom bands. To suppress the CO and CO^+ bands the CO_2 pressure was kept about 4–6 cm Hg and the gas-streaming was made as fast as possible (the use of a *Hypervac* pump brought some success in that direction). The CO_2 consumption was about 5–6 kg per day exposure. In starting with low gas pressure and low current and gradually increasing both and by using magnetic field strengths over 12,000 gauss, the discharge could be kept on one of the magnet pole-pieces with a maximal current of 700–800 milliamperes. In this way the luminosity was enough to give strong third order pictures with the 21 foot grating in 50 hours exposure-time.

As already mentioned[1] some of the CO_2 bands show magnetic effects, and because the discharge in the Back box could not be concentrated on the one pole-piece front in suitable intensity without magnetic fields, it seemed necessary to find another source, which would give a strong CO_2 spectrum without any magnetic field. The steel hollow-cathode in the arrangement sketched in Fig. 1 was fastened in the center of a three liter bulb, the neck of which was cooled. A steel anode was placed 5 cm away from the cathode. This arrangement gave very satisfactory results in respect to CO_2 luminosity and relative weakness of CO and CO^+ bands. Of course, the spectrum contained some iron lines also, but no other metal could be used because of the high CO_2 pressure. Graphite, aluminum, tin, etc., burned away in a short time.

[1] R. F. Schmid, Phys. Rev. **39**, 589 (1932).

Some considerations (see below) showed it desirable to determine the effective emission temperature of the source used, which could be done by studying the rotational intensity distribution of certain well-known bands

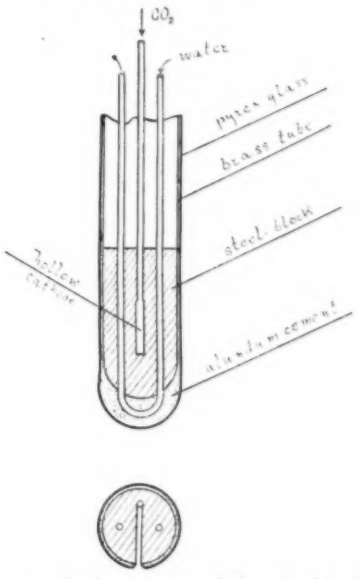

Fig. 1. Steel hollow cathode water-cooled and with direct gas-inlet in the hollow part itself.

present in the spectra. The λ 4835A, 0→1 angstrom band, having clear background and only a few overlappings, was especially suitable for that purpose and showed the maximal intensity in its P branch at $K''_{max}=15$ in the Q branch at $K''_{max}=14$ and in the R branch at $K''_{max}=13$. By using the formulas:[2]

$$P \text{ branch} \qquad kT = B'(K_{max}'' - 1)(2K_{max}'' - 1)$$

$$Q \text{ branch} \qquad kT = B'\tfrac{1}{2}(2K_{max}'' + 1)^2$$

$$R \text{ branch} \qquad kT = B'(K_{max}'' + 2)(2K_{max}'' + 3)$$

(where k is the Boltzmann factor and $B'=1.94$ cm^{-1}), it was found, in very good agreement for all the three branches: $kT=800$ cm^{-1}, that is $T=870$°C.

Besides that, having pictures on which (due to leaks) the λ3914A (0→0) and λ4278 (0→1) N_2^+ bands were also present, in which bands the maximum seemed to be between $K''_{max}=12$ for the stronger half R branch and $K''_{max}=13$ for the weaker odd numbered set, we have, by using the formula[3]

$$kT = B'(K_{max}'' + 1)(2K_{max}'' + 3)$$

with $B'=2.07$ cm^{-1} the value $kT=845$ cm^{-1} slightly higher than the above given one for CO, in agreement with what seems to be usual for ionized molecules.[4]

[2] F. London and H. Hönl, Zeits. f. Physik **33,** 803 (1925).
[3] R. S. Mulliken, Phys. Rev. **30,** 138 and 785 (1927).
[4] L. S. Ornstein, Zeits. f. Physik **49,** 315 (1928).

Results

The most recent report on the CO_2 emission spectrum—on the basis of low-dispersion photographs, however—was given by Smyth.[5] Comparing the pictures given by him in his Fig. 2, parts *a* and *b*, with the present plates, some differences were noticed, which are due probably to differences in methods of excitation.

(1) Smyth's electron beam discharge seems to be cooler than the present one, which gives better developed bands and is more suitable for rotational analysis purposes, while his pictures are more useful for a vibrational analysis.

(2) According to Smyth: . . . "from λ2900 to λ3500 the bands occur in five well-defined groups . . . from 3500 to 4000 is a terrific tangle." In the present pictures however, the bands from λ3500 to λ4000, as well as those from λ2900 to λ3500 fall into well-defined groups, four in number (at λλ3503, 3661, 3839 and 3905) in the former region.

(3) The electron beam method picture shows very strong bands at 3853, 3871 and 3961A. The present pictures show the two first mentioned bands much less intense and in the place of the third (about 3961A) they show practically nothing. Also the groups at 4108A and longer wave-lengths are weaker on the present plates.

Concerning the rotational fine structure, the present high-dispersion plates show that the strongest bands of the part of the spectrum which falls into groups, namely the bands λλ3247, 3254, 3370, 3377, 3503, 3511, 3534, 3545, 3674, and 3839A, all have the same simple structure, except that some show staggering and others do not (see below); they can be analyzed into *P* and *R* branches; *Q* branches could not be detected. The simple band structure indicates that the molecule is linear in both upper and lower energy states. The absence of a *Q* branch may be explained by assuming only such transitions, in which the orbital-angular momentum quantum number (in diatomic molecules Λ) does not change: $\Sigma \rightarrow \Sigma$, $\Pi \rightarrow \Pi$, etc. transitions.

Comparing pictures taken with and without magnetic fields, we find that the lines of the above-enumerated bands show no Zeeman effect. Other bands: λλ2880∼2900A and λ3661A, which differ from the above-mentioned bands in having more complicated structure also without fields, show up to the highest rotational states shiftings, broadenings, and in some places also splittings and polarizations in the magnetic field.

Calculations on the basis of the Zeeman effect energy level formula suitable for a diatomic molecule[6]

$$\Delta\nu = \Delta\nu_{\text{normal}} \cdot [M/K(K+1)]\Lambda^2$$

with $M = -K, -(K-1) \ldots (K-1)\ K$ show that, assuming a $^1\Pi \rightarrow {}^1\Pi$ transition ($\Lambda = 1$), we would get for 30,000 gauss field strength for the line $P(5)$ an overall width of the patterns $\Delta\nu = 0.16$ cm^{-1}, where, however, the intense components cover a width only of 0.06 cm^{-1}; for $P(9)$ we get an overall width

[5] H. D. Smyth, Phys. Rev. **38,** 2 000 (1931) and **39,** 380 (1932).

[6] J. S. Millis, Phys. Rev. **38,** 1148 (1931).

$\Delta\nu = 0.04$ cm^{-1}. In the case of a $^1\Delta \rightarrow {}^1\Delta$ transition ($\Lambda = 2$), we would get four times larger widths.

Now on the present plates the lines with the lowest rotational quantum number that can be observed are usually P lines from $P(7)$ or $P(9)$ up and R lines from $R(17)$ or $R(19)$ up. Only in two bands, λ3370 and λ3503A, where the overlappings with neighboring strong R lines are fewer, can we observe (without field) P lines from $P(3)$ or $P(4)$ up. The widths of the lines were found to be about 0.04 cm^{-1} and we may suppose that a broadening of the same magnitude in a magnetic field probably would be detected. However, the only observable effect of the magnetic field seems to be to cause a more

TABLE I. $\lambda = 3503A$.

P		R		P		R		P	
M	ν(cm^{-1})	M	ν(cm^{-1})	M	ν(cm^{-1})	M	ν(cm^{-1})	M	ν(cm^{-1})
2	28,530.47?	18	28,534.92	23	28,498.12	39	28,511.12	44	28,438.77
3	29.58	19	34.37	24	96.02	40	9.24	45	35.30
4	28.54	20	33.84	25	93.78	41	7.56	46	31.71
5	27.55	21	33.00	26	91.50	42	5.44	47	28.11
6	26.39	22	32.49	27	89.10	43	3.54	48	24.37
7	25.22	23	31.78	28	86.65	44	1.53	49	20.51
8	23.99	24	30.94	29	84.10	45	499.37	50	16.82
9	22.72	25	30.05	30	81.50	46	97.14	51	13.05
10	21.40	26	29.09	31	78.83	47	94.85	52	08.78
11	19.96	27	28.07	32	76.12	48	92.57	53	05.06
12	18.52	28	26.96	33	73.31	49	90.18	54	01.27
13	17.03	29	25.87	34	70.56	50	87.88	55	396.88
14	15.43	30	24.67	35	67.59	51	85.35	56	92.73
15	13.77	31	23.43	36	64.65	52	82.69	57	88.39
16	12.01	32	22.09	37	61.66	53	80.18	58	84.15
17	10.28	33	20.73	38	58.72	54	77.47	59	79.79
18	08.42	34	19.32	39	55.43	55	74.80	60	74.86
19	06.47	35	17.81	40	52.14	56	72.03	61	70.80
20	04.71	36	16.24	41	48.90			62	66.29
21	02.49	37	14.64	42	45.64			63	61.65
22	00.41	38	12.87	43	42.29			64	56.87

TABLE II. $\lambda = 3370A$.

P		R		P		R		P	
M	ν(cm^{-1})	M	ν(cm^{-1})	M	ν(cm^{-1})	M	ν(cm^{-1})	M	ν(cm^{-1})
3	29,656.18?	17	29,661.57	21	29,628.58	35	29,642.77	39	29,580.40
4	55.17	18	61.01	22	26.47	36	41.19	40	77.11
5	54.18	19	60.58	23	24.26	37	39.36	41	73.72
6	52.99	20	59.86	24	22.01	38	37.69	42	70.21
7	51.83	21	59.18	25	19.62	39	35.85	43	66.90
8	50.56	22	58.44	26	17.28	40	33.89	44	63.29
9	49.26	23	57.60	27	14.80	41	31.85	45	59.74
10	47.88	24	56.74	28	12.27	42	29.92	46	55.90
11	46.43	25	55.78	29	09.69	43	27.86		
12	44.95	26	54.80	30	07.08	44	25.61		
13	43.40	27	53.69	31	04.38	45	23.49		
14	41.78	28	52.50	32	01.50	46	21.11		
15	40.21	29	51.33	33	598.79	47	18.85		
16	38.32	30	50.06	34	95.90	48	16.30		
17	36.49	31	48.75	35	92.94	49	13.37		
18	34.61	32	47.34	36	89.82	50	11.34		
19	32.68	33	45.91	37	86.73	51	9.60		
20	30.69	34	44.41	38	83.45	52	7.11		

rapid decrease of intensity in the P branch in the direction of lower rotational quantum numbers. This may probably be attributed to an unresolved Zeeman splitting increasing in that direction. With field (25,400 gauss) the first observable P lines are about $P(8)$ or $P(9)$ in the above two bands. The widths of all the *observable* lines with field is the same (within observational accuracy) as without field.

TABLE III. $\lambda = 3247A$.

P		R	P		R	P	
M	$\nu(cm^{-1})$	M	M	$\nu(cm^{-1})$	M	M	$\nu(cm^{-1})$
	30,781.60	21	20	30,752.93	41	40	30,698.18
	80.59	22	21	50.76	42	41	94.74
	79.79	23	22	48.64	43	42	91.07
	78.83	24	23	46.36	44	43	87.64
	77.80	25	24	44.14	45	44	84.11
	76.67	26	25	41.72	46	45	80.37
	75.58	27	26	39.27	47	46	76.67
	74.39	28	27	36.73	48	47	72.61
	73.17	29	28	34.20	49	48	68.88
9	71.81	30	29	31.58	50	49	65.02
10	70.38	31	30	28.83	51	50	60.91
11	68.95	32	31	26.01	52	51	56.67
12	67.41	33	32	23.19	53	52	52.49
13	65.84	34	33	20.25	54	53	48.81
14	64.24	35	34	17.36	55	54	44.82
15	62.49	36	35	14.19	56	55	40.17
16	60.72	37	36	11.29	57	56	36.29
17	58.91	38	37	07.95	58	57	31.87
18	56.96	39	38	04.78	59	58	27.47
19	54.93	40	39	01.44			

TABLE IV. $\lambda = 3511A$.

P		R		P		R	
M	$\nu(cm^{-1})$	M	$\nu(cm^{-1})$	M	$\nu(cm^{-1})$	M	$\nu(cm^{-1})$
13	28,453.14	17	28,471.54	28	28,422.85	32	28,458.72
14	51.24	18	71.16	29	20.51	33	57.63
15	49.85	19	70.62	30	17.84	34	56.09
16	47.93	20	69.97	31	15.19	35	54.81
17	46.32	21	69.68	32	12.55	36	53.14
18	44.60	22	68.86	33	09.95	37	51.72
19	42.60	23	68.23	34	07.08	38	49.85
20	40.55	24	67.36	35	04.35	39	48.30
21	38.71	25	66.46	36	01.27	40	46.32
22	36.51	26	65.58	37	398.55	41	44.60
23	34.45	27	64.65	38	95.09	42	42.60
24	32.17	28	63.44	39	92.27		
25	30.01	29	62.35	40	89.08		
26	27.67	30	61.33	41	85.96		
27	25.62	31	60.12				

Considering these facts, we may conclude, that a $^1\Delta \rightarrow {}^1\Delta$ transition seems to be improbable, while the possibility of a $^1\Pi \rightarrow {}^1\Pi$ transition, and of course of a $^1\Sigma \rightarrow {}^1\Sigma$ transition (which should show no Zeeman effect) remain.

The bands beyond 3845A appear to be not much more complicated than the above-enumerated ten bands and also have no observable Zeeman effect, but there is so much overlapping that a third order picture does not permit their analysis into branches.

The present paper deals with the analysis of the ten bands enumerated above. Tables I to X contain the measurements of the bands. The accuracy

TABLE V. $\lambda = 3377A$.

P		R		P		R	
M	$\nu(cm^{-1})$	M	$\nu(cm^{-1})$	M	$\nu(cm^{-1})$	M	$\nu(cm^{-1})$
8	29,585.78	17	29,596.93	33	29,534.39	42	29,566.26
9	84.51	18	96.37	34	31.35	43	64.41
10	83.27	19	95.90	35	28.52	44	62.11
11	81.91	20	95.22	36	25.44	45	60.10
12	80.40	21	94.75	37	22.50	46	57.61
13	78.67	22	93.86	38	19.32	47	55.62
14	76.71	23	93.03	39	16.16	48	52.89
15	75.24	24	92.26	40	12.82	49	50.90
16	73.47	25	91.33	41	09.72	50	48.43
17	71.70	26	90.33	42	06.14	51	45.83
18	69.77	27	89.43	43	02.89	52	42.87
19	67.89	28	88.10	44	499.25	53	40.46
20	65.87	29	87.01	45	95.69	54	37.22
21	63.95	30	85.78	46	91.99	55	35.04
22	61.64	31	84.70	47	88.50	56	31.87
23	59.74	32	83.45	48	84.52	57	29.01
24	57.09	33	81.91	49	80.90	58	25.87
25	54.98	34	80.40	50	76.92	59	23.06
26	52.89	35	79.06	51	73.12	60	19.62
27	50.31	36	77.11	52	68.96		
28	47.74	37	75.70	53	64.97		
29	45.22	38	73.72	54	60.83		
30	42.43	39	72.09	55	56.78		
31	39.89	40	70.21	56	52.22		
32	37.09	41	68.38	57	48.19		

TABLE VI. $\lambda = 3254A$.

P		R		P		R	
M	$\nu(cm^{-1})$	M	$\nu(cm^{-1})$	M	$\nu(cm^{-1})$	M	$\nu(cm^{-1})$
6	30,708.77	17	30,717.36	29	30,665.02	40	30,689.08
7	07.59	18	16.75	30	62.28	41	87.12
8	06.41	19	16.17	31	59.69	42	84.76
9	04.78	20	15.63	32	56.67	43	82.97
10	03.68	21	14.93	33	53.96	44	80.37
11	02.15	22	14.19	34	50.86	45	78.36
12	00.60	23	13.31	35	48.10	46	75.78
13	699.20	24	12.26	36	44.82	47	73.63
14	97.51	25	11.29	37	41.64	48	70.95
15	95.91	26	10.17	38	38.39	49	68.13
16	93.88	27	09.27	39	35.33	50	65.57
17	92.14	28	07.95	40	31.87	51	63.37
18	90.19	29	06.84	41	28.61	52	60.28
19	88.36	30	05.38	42	24.82	53	57.82
20	86.07	31	04.25	43	21.47	54	54.61
21	84.11	32	02.64	44	18.08	55	51.96
22	82.01	33	01.44	45	14.31	56	48.81
23	79.86	34	699.62	46	10.30	57	45.82
24	77.44	35	98.18	47	06.90	58	42.56
25	75.13	36	96.30	48	02.72	59	39.74
26	72.61	37	94.70	49	598.99	60	36.29
27	70.26	38	92.68	50	94.84	61	33.40
28	67.60	39	91.07				

of the pure measurement is of the same order as that of the iron lines in that region serving as normals, i.e., a few thousandths of an angstrom unit or in

TABLE VII. $\lambda = 3534A$.

P		R		P		R	
M	$\nu(cm^{-1})$	M	$\nu(cm^{-1})$	M	$\nu(cm^{-1})$	M	$\nu(cm^{-1})$
9	28,275.43	17	28,288.23	25	28,247.12	33	28,273.99
10	73.99	18	87.75	26	44.69	34	72.76
11	72.76	19	87.13	27	42.41	35	71.34
12	71.34	20	86.62	28	39.69	36	69.47
13	69.79	21	86.00	29	37.45	37	68.37
14	68.37	22	85.45	30	34.64	38	66.28
15	66.74	23	84.80	31	32.39	39	64.88
16	64.88	24	84.00	32	29.68	40	62.86
17	63.27	25	83.12	33	27.19	41	61.18
18	61.18	26	82.13	34	23.99	42	59.02
19	59.55	27	81.21	35	21.49	43	57.43
20	57.43	28	80.12	36	18.28	44	54.97
21	55.65	29	79.06	37	15.54	45	53.43
22	53.43	30	77.79	38	12.28	46	50.71
23	51.49	31	76.74	39	09.42		
24	49.23	32	75.43	40	06.03		

TABLE VIII. $\lambda = 3545A$.

R		P		R		P	
$\nu(cm^{-1})$	M	M	$\nu(cm^{-1})$	M	M	$\nu(cm^{-1}$
28,195.81	17	9	28,182.91	32	23	28,158.68
95.33	18	10	81.67	33	24	56,53
94.88	19	11	80.19	34	25	54.22
94.24	20	12	78.69	35	26	51.87
93.70	21	13	77.23	36	27	49.72
92.87	22	14	75.67	37	28	47.10
92.26	23	15	74.04	38	29	44.77
91.43	24	16	72.28	39	30	42.09
90.60	25	17	70.45	40	31	39.65
89.75	26	18	68.83		32	36.84
88.71	27	19	66.84		33	34.26
87.65	28	20	64.84		34	31.38
86.67	29	21	62.88		35	28.58
85.53	30	22	60.81		36	25.62
84.24	31					

TABLE IX. $\lambda = 3674A$.

R		P		R		P	
$\nu(cm^{-1})$	M	M	$\nu(cm^{-1})$	M	M	$\nu(cm^{-1})$
27,205.77	18		27,195.54	31	20	27,175.44
05.38	19		94.38	32	21	73.53
04.82	20	9	93.24	33	22	71.57
04.32	21	10	92.22	34	23	69.46
03.69	22	11	91.48	35	24	67.36
03.04	23	12	89.44	36	25	65.20
02.28	24	13	88.00	37	26	62.76
01.60	25	14	86.48	38	27	60.56
00.64	26	15	83.94	39	28	58.16
199.82	27	16	82.26	40	29	55.94
98.83	28	17	80.76		30	53.66
97.74	29	18	79.18		31	50.87
96.71	30	19	77.17		32	48.15

TABLE X. $\lambda = 3839A$.

P				*R*			
M	back	Δ	forth	*M*	back	Δ	forth
5			26,030.72	16	26,039.70		
		1.13				0.29	
6	26,029.59			17			26,039.41
		0.89				0.35	
7			028.70	18	039.06		
		1.27				0.46	
8	027.43			19			038.60
		1.22				0.39	
9			026.21	20	038.21		
		1.33				0.53	
10	024.88			21			037.68
		1.30				0.60	
11			023.58	22	037.08		
		1.44				0.57	
12	022.14			23			036.51
		1.45				0.71	
13			020.68	24	035.80		
		1.47				0.69	
14	019.21			25			035.11
		1.56				0.85	
15			017.65	26	034.26		
		1.63				0.77	
16	016.02			27			033.49
		1.66				1.01	
17			014.36	28	032.48		
		1.78				0.93	
18	012.58			29			031.55
		1.77				1.07	
19			010.81	30	030.48		
		1.88				1.02	
20	008.93			31			029.46
		1.88				1.24	
21			007.05	32	028.22		
		2.05				1.01	
22	005.00			33			027.21
		1.92				1.50	
23			003.08	34	025.71		
		2.14				1.09	
24	000.94			35			024.62
		2.07				1.58	
25			25,998.87	36	023.04		
		2.04				1.24	
26	25,996.83			37			021.80
		2.38				1.74	
27			994.45	38	020.06		
		2.36				1.23	
28	992.09			39			018.83
		2.25				1.79	
29			989.84	40	017.04		
		2.60				1.44	
30	987.24			41			015.60
		2.33				1.98	
31			984.91	42	013.62		
		2.75				1.49	
32	982.16			43			012.13
		2.33				2.11	
33			979.83	44	010.02		
		2.83				1.53	
34	977.00			45			008.49
		2.53				2.21	
35			974.47	46	006.18		
		2.97				1.62	

TABLE X. (Continued)
$\lambda = 3839A$

P				R			
M	back	Δ	forth	M	back	Δ	forth
36	25,971.50			47			26,004.56
		2.65				2.47	
37			25,968.85	48	26,002.09		
		3.15				1.72	
38	965.70			49			000.37
		2.67				2.54	
39			963.03	50	25,997.83		
		3.09				1.82	
40	959.94			51			25,996.01
		2.87				2.72	
41			957.07	52	993.29		
		3.22				1.85	
42	953.85			53			991.44
						2.90	
				54	988.54		
						1.97	
				55			986.57
						3.02	
				56	983.55		

wave numbers $\pm 0.03 \sim 0.04$ cm^{-1}. Unfortunately, however, the overlappings are very frequent in these bands and this—together with the extraordinary closeness of the lines—causes some errors which, especially in the combination differences, in the worst cases give deviations up to ± 0.5 cm^{-1} which, however, are not systematic.

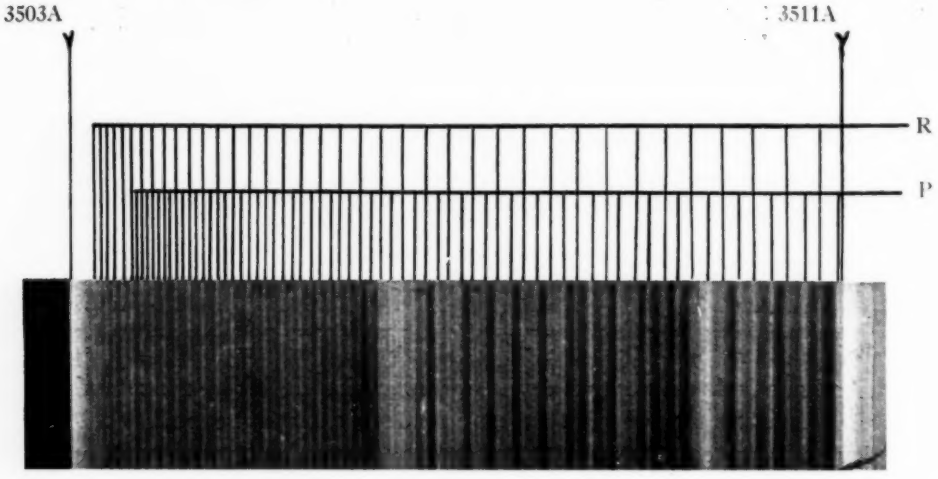

Fig. 2. Non-staggering CO_2 band at λ3503A.

Five of the measured bands, those at λλ3254, 3377, 3511, 3534 and 3839A show staggering, i.e., the lines of the branches are slightly displaced alternately toward lower and toward higher frequencies; the five others, in the limit of the observational accuracy do not. The staggering increases with the rotational quantum number. This phenomenon, together with the fact that

in the same or nearly the same place on the plates we have always P and R lines differing in rotational quantum number by 22–25 units, gives the impression that the P lines form a smooth series, while the R lines stagger back and forth between them. The measurements show, however, that the successive differences between adjacent P lines also alternate. To illustrate this fact, in Table X, for the band at λ3839A—which shows the staggering most prominently—these successive differences are listed in addition to the wave numbers. The rotational numbering of the lines listed in Table I–X should be taken as arbitrary. Some considerations (see below) show, however, that the true rotational numbering probably does not differ from that here given by more than a few units at most.

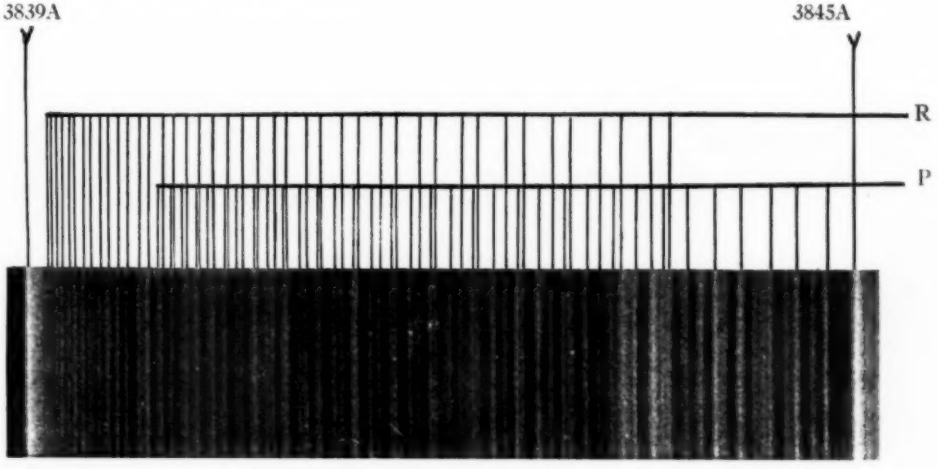

Fig. 3. Staggering CO_2 band at λ3839A.

A striking feature of the investigated bands may be mentioned now. This is: if we calculate differences between P and R lines, such as $R(M-2)-P(M)$ $R(M-1)-P(M)$, and so forth, we find that all the ten bands give almost the same sets of numbers. To illustrate this fact, in Table XI are listed the differences called $R(M)-P(M)$ for all bands. These differences are linear functions of M. At the bottom we find the values B, the constant coefficient (divided by four) of the in M linear sets. These, and B values calculated in other similar tables for several other difference sets, agree for all the ten bands within 0.004 cm^{-1}. This fact formed the common basis for the M numbering in all ten bands.

Since the time of their discovery, most of the CO_2 bands in the region here investigated have been believed to be members of v' progressions. The evidence for this opinion is that the wave numbers of the heads of most bands can be interpreted by the formula

$$\nu_{\text{head}} = \nu_a + 1136.85v' - 1.85v'^2 \qquad (1)$$

where v' is a vibrational quantum number. The different progressions have for ν_a different values (see Smyth[5] especially). The fact that the red degraded,

TABLE XI.

Supposed $R(M)$–$P(M)$ combinations for all bands

λ	3247	3254 stagg.	3370	3377 stagg.	3503	3511 stagg.	3534 stagg.	3545	3674	3839 stagg.
M										
15										
16										23.68
17		25.22	25.08	25.23		25.22	25.17	25.36		25.05
18		26.56	26.40	26.60	26.50	26.56	26.57	26.50	26.59	26.48
19		27.81	27.90	28.01	27.90	28.02	27.58	28.04	28.21	27.79
20		29.56	29.17	29.35	29.13	29.42	29.19	29.40	29.38	29.28
21	30.84	30.82	30.60	30.80	30.51	30.97	30.25	30.82	30.79	30.63
22	31.95	32.18	31.97	32.22	32.08	32.35	31.82	32.06	32.12	32.08
23	33.43	33.45	33.34	33.29	33.66	33.78	33.31	33.58	33.58	33.43
24	34.69	34.82	34.73	35.17	34.92	35.19	34.77	34.90	34.92	34.86
25	36.08	36.16	36.16	36.35	36.27	36.45	36.00	36.38	36.40	36.24
26	37.40	37.56	37.52	37.44	37.59	37.91	37.44	37.88	37.88	37.43
27	38.85	39.01	38.89	39.12	38.97	39.02	38.80	38.99	39.26	39.04
28	40.19	40.35	40.23	40.44	40.31	40.59	40.43	40.55	40.67	40.39
29	41.59	41.82	41.64	41.79	41.77	41.84	41.61	41.90	41.80	41.71
30	42.98	43.10	42.98	43.35	43.17	43.49	43.15	43.44	43.05	43.24
31	44.37	44.56	44.37	44.81	44.60	44.93	44.35	44.59	44.67	44.55
32	45.76	45.97	45.84	46.36	45.97	46.17	45.75	46.07	46.23	46.06
33	47.16	47.48	47.12	47.52	47.42	47.68	46.80	47.41		47.38
34	48.48	48.76	48.51	49.05	48.76	49.01	48.77	48.81		48.71
35	50.05	50.08	49.83	50.54	50.22	50.46	49.85	50.11		50.15
36	51.20	51.48	51.37	51.67	51.59	51.87	51.19	51.61		51.54
37	52.77	53.10	52.63	53.20	52.98	53.17	52.83			52.95
38	54.13	54.29	54.24	54.40	54.15	54.76	54.00			54.36
39	55.52	55.74	55.45	55.93	55.69	56.03	55.46			55.80
40	56.75	57.21	56.78	57.39	57.10	57.24	56.83			57.10
41	58.19	58.51	58.13	58.66	58.66	58.64				58.53
42	59.69	59.94	59.71	60.12	59.80					59.77
43	61.00	61.50	60.96	61.52	61.25					
44	62.25	62.59	62.32	62.86	62.76					
45	63.77	64.05	63.75	64.41	64.07					
46	65.05	65.48	65.21	65.62	65.43					
47	66.66	66.73		67.12	66.74					
48	67.85	68.23		68.37	68.20					
49	69.18	69.14		70.00	69.67					
50	70.67	70.73		71.51	71.06					
51		72.54		72.71						
52		73.65		73.91						
53		75.02		75.49						
54		76.43		76.39						
55		77.94		78.26						
56		79.53		79.65						
B	0.3467	0.3473	0.3464	0.3485	0.3482	0.3495	0.3468	0.3493	0.3497	0.3484

simple-structured CO_2 bands, and their lines themselves also, can be fitted in sets with almost the same constants, from the vibrational as well as from the rotational viewpoint, is one of the most prominent features of these bands, especially considering that a completely rigorous analysis has not yet been possible.

Among the ten bands here investigated there are three staggering and three non-staggering bands which form successive members of two v'progressions:

λλ3503, 3370, 3247A . . . non-staggering

λλ3511, 3377, 3254A . . . staggering.

To get the rotational numbering it therefore seemed suitable to look for identical sets of final state combination differences. The results of computations of this kind are given in Tables XII and XIII for the staggering and non-staggering sets, respectively.

In Table XII, best agreement is found in the set marked $R(M-2)-P(M)$. If we call this set $R(J-1)-P(J+1)$ and calculate the rotational constants as usual with the formula:

$$\Delta_2 T''(J) = R(J-1) - P(J+1) = 4B''(J+\tfrac{1}{2}) \qquad (2)$$

we get the surprising result, that the J values are (within limits of a few hundredths, which may be attributed to experimental error) half integers. The two neighboring sets $R(M-1)-P(M)$ and $R(M-3)-P(M)$, however, give whole numbers for J. It will be seen that the sets $R(M-1)-R(M+1)$ give almost as good agreements as $R(M-2)-R(M)$, while other sets give gradually increasing deviations which soon pass outside the range of possible experimental errors. Hence the correct combination set is probably not far different from $R(M-2)-P(M)$. If integral J values are assumed to be necessary, it is probably $R(M-1)-P(M)$. In any case, however, since the the calculated B'' values do not vary much from one set to another, the B'' value obtained from, say, $R(M-1)-P(M)$ is probably not far from correct. It also follows that the B' values are not very different from (slightly less than) the B'' values. For instance if $R(M-1)-P(M)$ gives $4B''(J+1/2)$, then $R(M+1)-P(M)=4B'(J+1/2)$. If we assume this we find that the B' values occur in succession as

$$B'_{3511} > B'_{3377} > B'_{3254}$$

in harmony with the vibrational numbering[5]

$$v'_{3511} < v'_{3377} < v'_{3254},$$

if we assume the formula well known for diatomic molecules:

$$B_v = B_0 - \alpha(v+\tfrac{1}{2})$$

with positive α, as is plausible for v' progressions with formula (1). The values for α seem to be very small, of the order of magnitude of 0.001 cm^{-1}. To this may be attributed the difficulty in deciding which combination sets are the correct ones. The alternate occurrence of whole and half J numbers for various possible combinations is marked in the right-hand corner of each combination in Tables XII and XIII.

Concerning Table XIII it should be mentioned that the data in the $\lambda 3247A$ band are in all probability not so accurate as those for the two others, because this band is composed of coincident P and R branches (at least for the eye), which among other things, results in a lower accuracy. Namely, the coinciding P and R lines have rotational quantum numbers differing by about 22 units, so that the coinciding components have not at all the same intensity and they contribute to the resulting line in unequal proportion and so a systematic shifting of the measured resulting line, i.e., of its center

TABLE XII. *Possible combinations in the staggering progressions.*

	$R(M-3)-P(M)$: whole					$R(M-2)-P(M)$: half					$R(M-1)-P(M)$: whole					$R(M)-P(M)$: half					$R(M+1)-P(M)$: whole				
M	3511		3377		3254	3511		3377		3254	3511		3377		3754	3511		3377		3254	3511		3377		3254
16																					23.61		23.46		23.48
17																25.22		25.23		25.22	24.84		24.67		24.61
18											26.94		27.16		27.17	26.56		26.60		26.56	26.02		26.13		25.98
19						28.94		29.04		29.00	28.56		28.48		28.39	28.02		28.01		27.81	27.37		27.33		27.27
20	30.99		31.06		31.29	30.61		30.50		30.68	30.07		30.03		30.10	29.42		29.35		29.56	29.13		28.88		28.86
21	32.45		32.42		32.64	31.91		31.95		32.06	31.26		31.27		31.52	30.97		30.80		30.82	30.15		29.91		30.08
22	34.11		34.26		34.16	33.46		33.58		33.62	33.17		33.11		32.92	32.35		32.22		32.18	31.72		31.39		31.30
23	35.52		35.48		35.77	35.23		35.01		35.07	34.41		34.12		34.33	33.78		33.29		33.45	32.91		32.42		32.40
24	37.51		37.66		37.49	36.69		36.77		36.75	36.06		35.94		35.87	35.19		35.17		34.82	34.29		34.24		33.85
25	38.85		38.88		39.06	38.22		38.05		38.18	37.35		37.28		37.13	36.45		36.35		36.16	35.57		35.35		35.04
26	40.56		40.14		40.70	39.69		39.37		39.65	38.79		38.44		38.68	37.91		37.44		37.56	36.98		36.54		36.66
27	41.74		41.95		42.00	40.84		41.02		41.03	39.96		40.02		39.89	39.02		39.12		39.01	37.82		37.79		37.69
28	43.61		43.59		43.69	42.73		42.59		42.57	41.80		41.69		41.67	40.59		40.44		40.35	39.50		39.27		39.24
29	45.07		45.11		45.15	44.14		44.21		44.75	42.93		42.88		42.93	41.84		41.79		41.82	40.82		40.56		40.36
30	46.81		47.00		46.99	45.60		45.67		45.67	44.51		44.58		44.56	43.49		43.35		43.10	42.28		42.27		41.97
31	48.25		48.21		48.26	47.16		47.12		47.15	46.14		45.89		45.69	44.93		44.81		44.56	43.53		43.56		42.95
32	49.80		49.92		50.17	48.78		48.69		48.71	47.57		47.61		47.58	46.17		46.36		45.97	45.08		44.82		44.77
33	51.38		51.39		51.42	50.17		50.31		50.29	48.77		49.06		48.68	47.68		47.52		47.48	46.14		46.01		45.66
34	53.04		53.35		53.39	51.64		52.10		51.78	50.55		50.56		50.58	49.01		49.05		48.76	47.73		47.71		47.32
35	54.37		54.93		54.54	53.28		53.39		53.34	51.74		51.88		51.52	50.46		50.54		50.08	48.79		48.59		48.20
36	56.36		56.47		56.62	54.82		54.96		54.80	53.54		53.62		53.36	51.87		51.67		51.48	50.45		50.26		49.88
37	57.54		57.90		57.98	56.26		56.56		56.54	54.59		54.61		54.66	53.17		53.20		53.10	51.30		51.22		51.04
38	59.72		59.74		59.79	58.05		57.79		57.91	56.63		56.38		56.31	54.76		54.40		54.29	53.21		52.77		52.68
39	60.87		60.95		60.97	59.45		59.54		59.41	57.58		57.56		57.35	56.03		55.93		55.74	54.05		54.05		53.75
40	62.64		62.88		62.83	60.77		60.90		60.81	59.22		59.27		59.20	57.24		57.39		57.21	55.52		55.56		55.25
41	63.89		64.00		64.07	62.44		62.37		62.46	60.36		60.49		60.47	58.64		58.66		58.51	56.64		56.54		56.15
42			65.95		66.25			64.07		64.26			62.24		62.30			60.12		59.94			58.27		58.15
43			67.32		67.61			65.49		65.65			63.37		63.29			61.52		61.50			59.22		58.90
44			69.13		69.04			67.01		66.68			65.16		64.89			62.86		62.29			60.85		60.28
45			70.57		70.45			68.72		68.66			66.42		66.06			64.41		64.05			61.92		61.47
46			72.42		72.67			70.12		70.07			68.11		68.06			65.62		65.48			63.63		63.33
47			73.61		73.47			71.60		71.46			69.11		68.88			67.12		66.73			64.39		64.05
48			75.58		75.64			73.09		73.06			71.10		70.91			68.37		68.23			66.38		65.41
49			76.71		76.79			74.72		74.64			71.99		71.96			70.00		69.14			67.53		66.58
50			78.70		78.79			75.97		76.11			73.98		73.29			71.51		70.73			68.91		68.53
51			79.77		80.12			77.78		77.30			74.31		74.74			72.71		72.54			69.75		69.45
52			81.94		81.50			79.47		78.94			76.87		76.74			73.91		73.65			71.50		71.19
53			83.46		82.77			80.86		80.57			77.90		77.48			75.49		75.02			72.25		71.81
54			85.00		85.19			82.04		82.10			79.63		79.64			76.39		76.43			74.21		73.78
55			86.09		86.26			83.68		83.80			80.44		80.59			78.26		77.94			75.09		74.79
56			88.24		88.54			85.00		85.33			82.82		82.68			79.65		79.53			76.79		76.54
57			89.03					86.85					83.68					80.82					77.68		
		average difference		average difference			average difference		average difference			average difference		average difference			average difference		average difference			average difference		average difference	
		-0.11		-0.06			-0.02		-0.01			$+0.02$		$+0.08$			$+0.08$		$+0.19$			$+0.16$		$+0.22$	
B even	0.3942		0.3974		0.3986	0.3801		0.3800		0.3799	0.3768		0.3764		0.3758	0.3498		0.3485		0.3472	0.3464		0.3449		0.3431
B odd	0.3927		0.3960		0.3958	0.3798		0.3802		0.3800	0.3749		0.3742		0.3733	0.3493		0.3486		0.3474	0.3443		0.3430		0.3410
possible combinations			Δ_2T''					Δ_2T''					Δ_2T'					Δ_2T'					Δ_2T'		
															Δ_2T''										

Note to this table. The explanation of B_{even} and B_{odd} is given in the text together with the explanation of the same signs in Table XIV.

TABLE VIII. *Possible combinations in the non-staggering progression.*

M	$R(M-3)-P(M)$: whole 3503	3370	3247	$R(M-2)-P(M)$: half 3503	3370	3247	$R(M-1)-P(M)$: whole 3503	3370	3247	$R(M)-P(M)$: half 3503	3370	3247	$R(M+1)-P(M)$: whole 3503	3370	3247
16														23.25	
17											25.08		24.64	24.52	
18								26.96		26.50	26.40		25.95	25.97	
19					28.89		28.45	28.33		27.90	27.90		27.37	27.18	
20		30.88		30.21	30.32		29.66	29.89		29.13	29.17		28.29	28.49	28.67
21	32.43	32.43		31.88	32.00		31.35	31.28		30.51	30.60	30.84	30.00	29.86	29.83
22	33.96	34.11		33.43	33.39		32.59	32.71	32.96	32.08	31.97	31.95	31.37	31.13	31.15
23	35.72	35.60		34.88	34.92	35.24	34.37	34.18	34.23	33.66	33.34	33.43	32.82	32.48	32.47
24	36.98	37.17	37.46	36.47	36.43	36.45	35.76	35.59	35.65	34.92	34.73	34.69	34.03	33.77	33.66
25	38.71	38.82	38.87	38.00	37.98	38.07	37.16	37.12	37.11	36.27	36.16	36.08	35.31	35.18	34.95
26	40.28	40.32	40.52	39.44	39.46	39.56	38.55	38.50	38.53	37.59	37.52	37.40	36.57	36.41	36.31
27	41.84	41.94	42.10	40.95	40.98	41.07	39.99	40.00	39.94	38.97	38.89	38.85	37.86	37.70	37.66
28	43.40	43.51	43.60	42.44	42.53	42.47	41.42	41.42	41.38	40.31	40.23	40.19	39.22	39.06	38.97
29	44.99	45.11	45.09	43.97	44.00	44.00	42.86	42.81	42.81	41.77	41.64	41.59	40.57	40.37	40.23
30	46.57	46.61	46.75	45.46	45.42	45.56	44.37	44.25	44.34	43.17	42.98	42.98	41.93	41.67	41.55
31	48.13	48.12	48.38	47.04	46.95	47.16	45.84	45.68	45.80	44.60	44.37	44.37	43.26	42.96	42.94
32	49.75	49.83	49.98	48.55	48.56	48.62	47.31	47.25	47.19	45.97	45.84	45.76	44.61	44.41	44.22
33	51.36	51.27	51.56	50.12	49.96	50.13	48.78	48.55	48.70	47.42	47.12	47.16	46.01	45.62	45.59
34	52.87	52.85	53.02	51.53	51.44	51.59	50.17	50.01	50.05	48.76	48.51	48.48	47.25	46.87	46.88
35	54.50	54.40	54.76	53.14	52.97	53.22	51.73	51.47	51.65	50.22	49.83	50.05	48.65	48.25	48.30
36	56.08	56.09	56.12	54.67	54.59	54.55	53.16	52.95	52.95	51.59	51.37	51.20	49.99	49.54	49.43
37	57.66	57.68	57.89	56.15	56.04	56.29	54.58	54.46	54.54	52.98	52.63	52.77	51.21	50.96	50.96
38	59.09	59.32	59.46	57.52	57.74	57.71	55.92	55.91	55.94	54.15	54.24	54.13	52.40	52.40	52.18
39	60.81	60.79	61.05	59.21	58.96	59.28	57.44	57.29	57.47	55.69	55.45	55.52	53.81	53.49	53.49
40	62.50	62.25	62.54	60.73	60.58	60.73	58.98	58.74	58.78	57.10	56.78	56.75	55.42	54.74	54.75
41	63.97	63.97	64.17	62.22	62.13	62.22	60.34	60.17	60.19	58.66	58.13	58.19	56.54	56.20	56.02
42	65.48	65.64	65.89	63.60	63.68	63.86	61.92	61.64	61.86	59.80	59.71	59.69	57.90	57.65	57.57
43	66.95	66.99	67.29	65.27	64.95	65.29	63.15	63.02	63.12	61.25	60.96	61.00	59.24	58.71	58.72
44	68.79	68.56	68.82	66.67	66.63	66.65	64.77	64.57	64.53	62.76	62.32	62.25	60.60	60.20	60.03
45	70.14	70.18	70.39	68.24	68.12	68.27	66.23	65.87	66.99	64.07	63.75	63.77	61.84	61.37	61.35
46	71.83	71.96	71.97	69.82	69.71	69.69	67.66	67.59	67.47	65.43	65.21	65.05	63.14	62.95	62.60
47	73.42		73.75	71.26		71.53	69.03		69.11	66.74		66.66	64.46		64.12
48	75.00		75.26	72.77		72.84	70.48		70.39	68.20		67.85	65.81		65.32
49	76.63		76.70	74.34		74.25	72.06		71.71	69.67		69.18	67.37		66.56
50	78.03		78.36	75.75		7 .82	73.36		73.29	71.06		70.67	68.53		67.92
B	0.391	0.391	0.393	0.379	0.379	0.380	0.362	0.360	0.362	0.348	0.346	0.346	0.332	0.328	0.328

average difference -0.03 (3503 → 3370); average difference -0.19 (3370 → 3247)

average difference $+0.04$ (3503 → 3370); average difference -0.12 (3370 → 3247)

average difference $+0.12$ (3503 → 3370); average difference -0.07 (3370 → 3247)

average difference $+0.19$ (3503 → 3370); average difference -0.003 (3370 → 3247)

average difference $+0.26$ (3503 → 3370); average difference $+0.06$ (3370 → 3247)

possible combinations

$\Delta_2 T''$ $\Delta_2 T'$

$\Delta_2 T''$ $\Delta_2 T'$

$\Delta_2 T''$ $\Delta_2 T'$

of gravity, may occur. Hence, less weight should be given to agreements involving the combination sets of this band.

In this table we may say that the supposed common final state may be interpreted by one of the left-hand columns. Anyway, we find that the numbering calculated on the basis of formula (2) does not differ from our arbitrary numbering by more than one or two (or by a half or one and a half) units .This is true for both progressions, and in view of Table XI, probably for all the bands. The B values for both initial and final states then probably lie within the interval of: $0.395 \sim 0.345$ cm^{-1}.

On the basis of these values, assuming the rotational axis perpendicular to the line through the three atoms of CO_2 and going through the carbon atom and assuming the effective mass for that axis:

$$\mu = 2M_{\text{oxygen}} = 53.12 \cdot 10^{-24}\text{g},$$

we can roughly calculate the distance between the carbon and one of oxygen atoms. We get in this way: r equal to about $1.25 \sim 1.15 \cdot 10^{-8}$ cm, that is, almost the same as, or slightly larger than, in the CO and CO^+ molecules.

In making the above computations concerning the numbering and rotational constants we have not mentioned the theoretical requirement that, because of the symmetry of the CO_2 molecule and the zero nuclear spin of the oxygen atoms, alternate rotational levels and band lines should be missing. As for the staggering bands, a very simple assumption (see below) may explain both staggering and missing lines. But considering only the non-staggering bands, the question might arise whether these bands could not be explained by supposing that they have alternately missing lines, so that the rotational constants would really have values roughly half as large and the rotational quantum numbers of the lines, values roughly twice as large as stated above. In making this assumption, we would encounter difficulties not only in the fact that in this case the nuclear separations would become improbably large, but also in interpreting the rotational intensity distribution of the bands. It was shown before that the intensity distribution of the angstrom bands present in the spectrum gives a value for $kT = 800$ cm^{-1} and assuming the formula

$$kT = B'(K_{\max}'' + 1)(2K_{\max}'' + 3)$$

for the R branches of the CO_2 bands, we would get with supposed B' values about $0.360 \sim 0.350$ (middle and left-hand columns in Table XIII) a value for $K''_{\max}$ about $31 \sim 32$; with B values half as large we get $K''_{\max}$ about $43 \sim 45$. The $R(43)$ or $R(45)$ line would of course be identical with our former lines $R(21) \sim R(23)$. Now the intensity distribution of the bands at λ3503A and λ3370A on several plates was registered with a Moll microphotometer and the curves show, although distorted by the close lying lines and some overlappings also, their maxima undoubtedly within the interval of $M = 30$ to 33. This confirms the assumption that alternate lines are not missing in the bands without staggering.

In surveying all the combinations given in Tables XII and XIII it seemed

of interest to determine whether the two progressions have or have not an exactly common level. Every conceivable kind of combination between the lines of the different bands in the different progressions was tried, but every set obtained showed—to be sure small but systematic deviations from the others.

A simple explanation of the staggering together with the theoretical requirement of missing levels can be given as follows: In analogy to diatomic molecules, we assume that the rotational levels of CO_2 form a set (in the first approximation) with the well-known formula

$$T(J) = BJ(J+1) \text{ or } T(K) = BK(K+1)$$

and in further analogy with diatomic molecules, we assume a splitting of the levels, something like the Λ-type doubling. Now, due to the zero nuclear spins

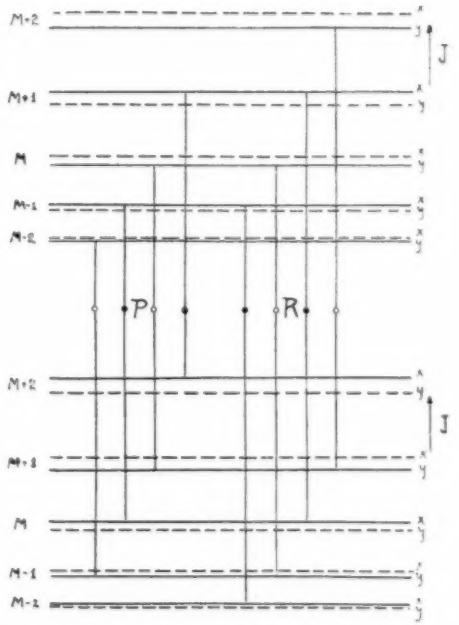

Fig. 4. Possible energy diagram and explanation of the staggering in some CO_2 bands. The rotational levels have doublings in analogy to the Λ-type doublings of a diatomic molecule. Because of the zero nuclear spin of the oxygen atoms, every second level is missing (broken lines). *P* and *R* branches appear to be divided into two alternating sets marked with full and empty circles. To get term-differences, we have to combine full circle *R* lines with full circle *P* lines and empty circle *R* lines with empty circle *P* lines.

of the oxygen atoms, every other level, alternately the upper and lower one of the sublevels of a Λ-like doublet, as in He_2, should be missing. The energy-level diagram could be drawn then somewhat as in Fig. 4 (where the Λ-like doublings are greatly exaggerated).[7] The *P* and *R* lines would then appear to be divided into the two sets, marked with full and empty circles (transitions

[7] See Figs. 17 and 32 for structure of bands like this given by R. S. Mulliken, Rev. Mod. Phys. **3**, 89 (1931).

only between x sublevels and transitions only between y sublevels). To get the x level combinations, we have to combine full circle P and R lines, to get y level combinations, we have to combine empty circle lines. But the question which half of the P and of the R branches represent the empty and which the full circle lines, and therefore which set of P lines should be combined with which set of R lines, remains at first unanswered.

The magnitude of the staggering is different in the different bands. In the band at λ3839A it is the largest, in the progresssion λλ3511, 3377 and 3254A it is less and in the band λ3534 it is only just observable. This suggests that perhaps the non-staggering bands have staggering also, only its magnitude is less than enough to become observable.

The λ3839A band shows the most striking staggering, so it may serve as an example for the following considerations. In Table X the lines of the bands are fitted in two columns, marked "forth" and "back," where the "forth" means a deviation in the direction of higher frequencies, that is, since the band is red-degraded, toward the head, and "back" in the opposite direction. The arbitrary numbering was chosen in such a way that even numbers belong to "back" staggered, odd numbers to "forth" staggered lines in both branches. (This was done also in the other staggering bands, and this served as a second basis, besides that explained by discussing Table XI (see above), for the common M numbering in the different bands.)

Table XIV contains a number of possible combinations in the λ3839 band; combinations in which the M value of the P line is even or odd are listed respectively in the left and right subcolumns of each combination set. Before each combination value is given the value J which is calculated, assuming the formula

$$\textit{combination}\ (R - P) = 4B(J + \tfrac{1}{2})$$

and the average constant differences in each column of two adjacent combination values are listed as "$8B$" at the bottom of the table. The approximate nature of the J values obtained is given at the top of each column under "whole" or "half." (In the bands without staggering, similar tables give almost exactly integers and half integers: cf., data in Tables XII, XIII.) Below these their deviations from the nearest whole and half numbers are also listed. The sum of the deviations for the two halves of each combination set seems to be zero in the "whole" sets. The deviations themselves seem to be two or three times as large in the "whole" combinations as in the "half" ones. The difference $8B_{\text{even}} - 8B_{\text{odd}}$ seems to be about four times as large in the "whole" sets as in the "half" sets, and also differs in sign.

The quantity $8B_{\text{even}} - 8B_{\text{odd}}$ in the other staggering bands also was found to be positive in the "whole" sets in all cases and negative in the "half" sets in most cases. Its magnitude (an approximate measure of the staggering) seems to be about $+0.016$ cm^{-1} in the "whole" sets. The calculated J values are equal to whole and half numbers within the lower observational accuracy—due to frequent overlappings in these bands, and do not permit a real calculation of their deviations from the next whole or half number.

TABLE XIV. *Possible combinations in λ3839A, strongly staggering band.*

	$R(M-2)-P(M)$:half				$R(M-1)-P(M)$:whole				$R(M)-P(M)$:half				$R(M+1)-P(M)$:whole				$R(M+2)-P(M)$:half				
	J	$R-P$	J	$R-P$	J	$R-P$	J	$R-P$	J	$R-P$	J	$R-P$	J	$R-P$	J	$R-P$	J	$R-P$	J	$R-P$	
	0.53		0.43		0.84		0.16		0.54		0.43		0.82		0.17		0.55		0.43		Average of the decimal part of apparent J.
	−0.03		+0.07		+0.16		−0.16		−0.04		+0.07		+0.18		−0.17		−0.05		+0.07		Deviation of apparent J from integers on half integers.
M																					
14																	15.54	20.49			
15															16.14	22.05			16.46	21.76	
16									16.53	23.68			16.85	23.39			17.54	23.04			
17							17.10	25.34			17.44	25.05			18.14	24.70			18.39	24.24	
18	17.52	27.12			17.87	26.83			18.54	26.48			18.80	26.02			19.57	25.63			
19			18.45	28.60			19.12	28.25			19.41	27.79			20.18	27.40			20.44	26.87	
20	19.52	30.13			19.81	29.67			20.55	29.28			20.83	28.75			21.54	28.15			
21			20.40	31.55			21.14	31.16			21.44	30.63			22.16	30.03			22.46	29.46	
22	21.57	33.21			21.87	32.68			22.57	32.08			22.88	31.51			23.61	30.80			
23			22.42	34.60			23.11	34.00			23.45	33.43			24.19	32.72			24.46	32.03	
24	23.52	36.14			23.85	35.57			24.57	34.86			24.85	34.17			25.59	33.32			
25			24.44	37.64			25.14	36.93			25.46	36.24			26.21	35.39			26.48	34.62	
26	25.40	38.97			25.71	38.28			26.41	37.43			26.70	36.66			27.41	35.65			
27			26.44	40.66			27.14	39.81			27.46	39.04			28.20	38.03			28.41	37.10	
28	27.53	42.17			27.84	41.40			28.54	40.39			28.78	39.46			29.56	38.39			
29			28.42	43.65			29.61	42.64			29.38	41.71			30.17	40.64			30.38	39.62	
30	29.57	45.24			29.83	44.31			30.59	43.24			30.82	42.22			31.58	40.98			
31			30.40	46.64			31.14	45.57			31.41	44.55			32.18	43.31			32.46	42.30	
32	31.61	48.32			31.88	47.30			32.62	46.06			32.92	45.05			33.60	43.55			
33			32.38	49.63			33.10	48.39			33.44	47.38			34.12	45.88			34.40	44.79	
34	33.54	51.22			33.87	50.21			34.52	48.71			34.83	47.62			35.54	46.04			
35			34.44	52.74			35.08	51.24			35.42	50.15			36.15	48.57			36.38	47.33	
36	35.53	54.21			35.86	53.12			36.56	51.54			36.82	50.30			37.52	48.56			
37			36.45	55.77			37.13	54.19			37.43	52.95			38.14	51.21			38.45	49.98	
38	37.61	57.34			37.90	56.10			38.59	54.36			38.92	53.13			39.69	51.34			
39			38.44	58.77			39.10	57.03			39.47	55.80			40.26	54.01			40.47	52.57	
40	39.45	60.12			39.81	58.89			40.56	57.10			40.79	55.66			41.53	53.68			
41			40.42	61.76			41.14	59.97			41.43	58.53			42.17	56.55			42.41	55.06	
42	41.49	63.19			41.77	61.75			42.48	59.77			42.74	58.28			43.48	56.17			
$8B$	3.0094		3.0186		2.9215		2.8802		2.7815		2.7921		2.6958		2.6504		2.5546		2.5665		
$8B_{even}-8B_{odd}$	−0.0092				+0.0413				−0.0106				+0.0454				−0.0119				

The levels of Λ-type doubling in a diatomic molecule can be interpreted by the formula[8]

$$\phi_i(J) = \kappa_i + \epsilon_i J + \delta_i J(J+1) + \cdots$$

where i refers to either x or y sublevels. We may try to use this formula for the present case.

Combining two sublevels differing by two units in J, but of the same kind (that is, two x, or two y levels) we get

$$\phi_i(J+1) + \phi_i(J-1) = 2\epsilon_i + 4\delta_i(J + \tfrac{1}{2}).$$

The difference between B_{even} and B_{odd} should then represent the difference between δ_x and δ_y, while the deviations of the apparent J's from whole numbers correspond to ϵ_x and ϵ_y, of which according to the observational data one is positive, the other negative. Both the "whole" and the "half" combinations in the band at λ3839A show effective B and J values which are consistent with this scheme, and there seems to be no way of deciding between them on this basis, nor of deciding which of the "whole" or of the "half" combinations is most likely to be correct, except roughly by assuming the intensity distribution to be analogous to that in the bands which belong to progressions.

In a separate paper Professor R. S. Mulliken expects to discuss some further points in connections with the theoretical interpretation of the CO_2 bands.

The writer wishes to express his thankfulness to Professor Robert S. Mulliken for his unceasing advice in analyzing the bands and to Professor George S. Monk for his kind assistance in experimental troubles, especially for the excellent temperature control of the grating-room.

[8] R. S. Mulliken, Rev. Mod. Phys. **3**, 89 (1931).

Electronic Structures of Polyatomic Molecules and Valence. II. Quantum Theory of the Double Bond

By ROBERT S. MULLIKEN
Ryerson Physical Laboratory, University of Chicago

(Received August 4, 1932)

The electronic structure of CH_2 in its probable normal and first excited states is described in terms of molecular orbitals. The formation of C_2H_4 from two (excited) CH_2 radicals is discussed, and it is shown, with the help of the Slater-Pauling overlapping criterion, to be theoretically obvious, in agreement with experiment, that for the normal state of C_2H_4 the energy is surely considerably lower if the two CH_2 are arranged symmetrically in one plane than if their planes make an angle of 90° (Figs. 1, 2). Similar statements apply to the derivatives of C_2H_4. The C=N and N=N double bonds can be treated similarly. The C=C and O=O double bonds are compared. The $(BH_2)=(BH_2)$ bond in B_2H_6 probably resembles the O=O more than the C=C bond. For certain predicted excited states of C_2H_4 and its derivatives, which are probably the upper states of ultraviolet absorption bands of these compounds, it is shown that the energy should be higher for the plane form than for the perp. form (one CR′R″ plane rotated through 90°). Hence the plane form should tend to go over spontaneously by rotation into the perp. form (90°) and on to the other plane form (180°) after absorption of suitable ultraviolet light. In this way the observed transformations of *cis* into *trans* isomers or vice versa by ultraviolet light may be explained.

INTRODUCTION

SEVERAL attempts have been made to explain quantum-mechanically the well-known double bond of organic chemistry.[1] Hückel formulated the double bond, e.g., in C_2H_4, as consisting of two electron-pairs $[\sigma]^2[\pi]^2$, where $[\sigma]$ has approximate rotational symmetry around the C-C axis, $[\pi]$ an angular distribution approximately proportional to $\sin\phi$ ($\phi=0$ in the common plane of all the nuclei). The stability of the double bond toward rotation is connected with properties of the $[\pi]_{\sin\phi}$ orbital, but Hückel's discussion of this stability is unsatisfactory.

Slater[2] and Pauling[3] give a different explanation using their tetrahedral atomic orbitals (s, p hybrids), as follows: Each CH_2 has two such orbitals which have formed electron-pair bonds with H atoms, and two which are unpaired. In C_2H_4, the two unpaired CH_2 orbitals form two electron-pairs which determine a plane perpendicular to that in which all the atoms lie, and cause this arrangement to be stable toward rotation.

Although the Slater-Pauling method generally gives a good approximation and a valid explanation of valence angles, the approximation appears to

[1] Cf. R. S. Mulliken, Phys. Rev. **41**, 49 and especially 55–61 (1932) for a summary and references.

[2] J. C. Slater, Phys. Rev. **37**, 481 (1931).

[3] L. Pauling, Jour. Am. Chem. Soc. **53**, 1367 (1931).

be relatively crude in the case of C_2H_4 and of double bonds in general, essentially because of the assumption of s-p hybridization. As will now be shown, it seems possible by means of a different approximation, resembling Hückel's but going farther, to obtain a more detailed correspondence with existing empirical, especially chemical, knowledge of the behavior of double-bonded molecules.

Electronic Structure of CH_2

It is useful to consider the formation of C_2H_4 from 2 CH_2 for two cases: (*a*) all the atoms lie in one plane ("plane C_2H_4"); (*b*) the planes of the two CH_2 make an angle of 90° ("perpendicular C_2H_4"). For this purpose, it is convenient to describe the molecular electronic structures in terms of molecular orbitals[1] of CH_2 and of C_2H_4. The possible types of molecular orbitals and their symmetry properties depend on the symmetry of the nuclear arrangement. They can be conveniently determined by group theory methods, or in simple cases by inspection. The exact meanings of the term symbols used here for electronic states, e.g., $^1\Gamma_1$, will be explained in a later detailed paper; it should be noted that the meaning of a given symbol may differ according to the nuclear arrangement.

That CH_2 should be triangular, with an angle of perhaps about 110° between the two C-H directions, can be seen most easily by using the Pauling-Slater methods, assuming either pure p valence (predicted angle somewhat over 90°) or tetrahedral bonds (predicted angle slightly larger than the tetrahedral angle), or an intermediate condition. In the following, a z axis will be chosen bisecting the apex angle of CH_2, an x axis perpendicular to the CH_2 plane. [In forming p bonds, Slater and Pauling would use y' and z' axes making angles of 45° with the y and z axes used here.] The probable normal state and the probable lowest excited state of CH_2 can then be described in terms of molecular orbitals as:

$$1s^2[s]^2[y]^2[z]^2,\ ^1\Gamma_1;\ 1s^2[s]^2[y]^2[z][x],\ ^3\Gamma_3. \qquad (1)$$

The symbols $[s]$, $[x]$, $[y]$, $[z]$ stand for orbitals which may be approximately built up as linear combinations respectively of $2s$, $2p_x$, $2p_y$, $2p_z$ of carbon[2,3] and $1s$ of hydrogen; $[s]$ consists mostly of $2s$, some $1s$, and a little $2p_z$; $[x]$ of $2p_x$ only; $[y]$ of $2p_y$ and $1s$; $[z]$ of $2p_z$, some $1s$, and a little $2s$. The C-H binding is taken care of by the $[y]$, $[s]$, and $[z]$ orbitals, especially by the $[y]$.

Formation of C_2H_4 from CH_2

The Slater-Pauling criterion of maximum overlapping, which can be applied to formation of pairs of molecular orbitals as well as to formation of electron-pair bonds,[1] can now be used to show that the most stable form of C_2H_4 should be a plane configuration built out of two CH_2 radicals each in the state . . . $[z][x]$, $^3\Gamma_3$ in such a way that the z axes of the two radicals coincide and form what may be called the z axis of C_2H_4. [Although best thought of as built out of two $^3\Gamma_3$, normal C_2H_4 should dissociate adiabatically into two $^1\Gamma_1$ unexcited CH_2 radicals.] With this arrangement, the two $[z]$

orbitals of the two CH_2 overlap strongly to form Hückel's $[\sigma]$ bond, the two $[x]$ orbitals somewhat less strongly to form his $[\pi]$ bond. The resulting (C-C)-bonding orbitals of C_2H_4 are approximately *const.* $\{[z]_A+[z]_B\}$ and *const.* $\{[x]_A+[x]_B\}$, or more briefly, $[z+z]$ and $[x+x]$, where A and B refer to the two CH_2 radicals. The (C-H) bonding orbitals $[s]$ and $[y]$ of the two CH_2 radicals are not very much disturbed by the formation of C_2H_4, and take little part in the (C-C)-bonding, so that one may describe C_2H_4 in its normal state approximately as:

$$1s^2 1s^2[s]^2[s]^2[y]^2[y]^2[z+z]^2[x+x]^2,\ {}^1\Gamma_{1g}. \tag{2}$$

The $[z]$ orbitals, in forming $[z+z]$, withdraw largely from their previous (C-H)-bonding function, their share being taken over by the $[s]$ orbitals; in the process, there is probably a somewhat increased hybridization of $[s]$ and $[z]$ which facilitates the alterations in their bonding roles: for $\alpha[s]+\beta[z]$ and $\beta[s]-\alpha[z]$ are respectively better adapted to C-H and to (C-C)-bonding than are pure $[s]$ and $[z]$.

The interaction between $[y]_A^2$ and $[y]_B^2$, likewise that between $[s]_A^2$ and $[s]_B^2$, should be a repulsive one. Instead of $[y]^2[y]^2$ one *might* write $[y+y]^2[y-y]^2$, where $[y+y]$, which means *const.* $\{[y]_A+[y]_B\}$, is (C-C)-bonding, while $[y-y]$ is (C-C)-antibonding. Probably, however, the (C-C)-nonbonding formulation $[y]^2[y]^2$ represents a better approximation here. The difference between the C=C double bond in C_2H_4 and the O=O double bond in O_2 lies chiefly in this last fact. This can be seen on comparing (2) with the following formulations (3) and (4), and noting that $(\pi+\pi)$ and $(\pi-\pi)$ of O_2 (usually called $\pi 2p$ and $\pi^* 2p$) are two-foldly degenerate orbitals, respectively of the types $\{(x+x)$ and $(y+y)\}$ and $\{(x-x)$ and $(y-y)\}$,—or $\{(x+x)\pm i(y+y)\}$, and $\{(x-x)+i(y-y)\}$,—where x and y stand for $2p_x$ and $2p_y$ of the O atom.

$$C_2H_4\text{: } 1s^2 1s^2[s]^2[s]^2[y+y]^2[y-y]^2[z+z]^2[x+x]^2,\ {}^1\Gamma_{1g} \tag{3}$$

$$O_2\text{: } 1s^2 1s^2 s^2 s^2(z+z)^2(\pi+\pi)^4(\pi-\pi)^2,\ {}^3\Sigma^-_g. \tag{4}$$

Here $[y+y]^2[x+x]^2$ of C_2H_4 corresponds to $(\pi+\pi)^4$ of O_2, $[y-y]^2$ to $(\pi-\pi)^2$; but because of the degeneracy involved in $(\pi-\pi)$, which means that $(y-y)$ and $(x-x)$ of O_2 have equal energy unlike $[y-y]$ and $[x-x]$ of C_2H_4, the lowest state of O_2 is a paramagnetic triplet state with one electron in $(x-x)$, one in $(y-y)$, while that of C_2H_4 is a diamagnetic singlet state.

Besides the ${}^1\Gamma_{1g}$ normal state of C_2H_4, the union of two CH_2 each in the state . . . $[z][x]$, ${}^3\Gamma_3$ should give an unstable quintet state and an excited, possibly also unstable (cf. Fig. 1), triplet state of C_2H_4. This and a corresponding singlet state should probably be the lowest excited triplet and singlet state of C_2H_4. They are (cf. (2)):

$$1s^2 1s^2[s]^2[s]^2[y]^2[y]^2[z+z]^2[x+x][x-x],\ {}^3\Gamma_{4u},\ {}^1\Gamma_{4u}. \tag{5}$$

These states should have a very considerably larger equilibrium C-C distance than the normal state. Absorption of suitable ultraviolet frequencies by normal C_2H_4 should take it readily to the ${}^1\Gamma_{4u}$ state, since it can be shown that

the transition is in agreement with selection rules appropriate to the case; absorption bands leading to the $^3\Gamma_{4u}$ state should be very weak because of the change in multiplicity. If Fig. 1 is correct, the absorption to the $^3\Gamma_{4u}$ state should consist mostly of a weak continuum causing dissociation into two CH_2.

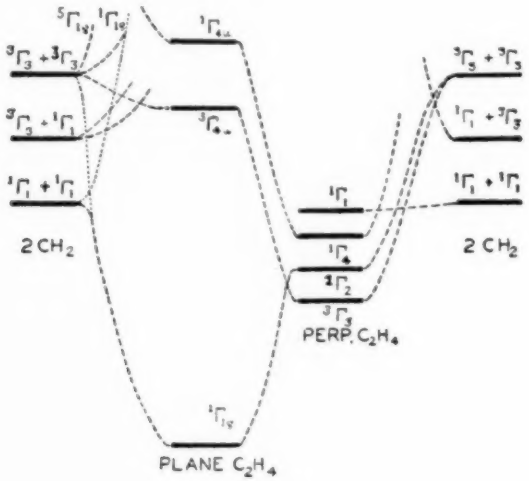

Fig. 1. Probable lowest energy levels of plane C_2H_4 and of perp. C_2H_4 (plane of one CH_2 at 90° to that of the other) and of 2 CH_2, and their adiabatic correlations as given by group theory. (The correlations with 2 CH_2 should not be considered absolutely certain, since the theory has not been carefully checked.) The spacings of the levels are of no more than qualitative significance, and the correct order of some of them may even be the reverse of that shown. It is not impossible that the energy of the $^3\Gamma_{4u}$ state of plane C_2H_4 may be higher than that of 2 $CH_2(^3\Gamma_3)$ so that the state is an unstable repulsive one. The state $^1\Gamma_{4u}$, however, is almost certainly stable. It should be noted that while C_2H_4 in its normal state may be thought of (dotted lines in the figure) as derived from, or to a considerable degree as consisting of, two excited CH_2 radicals both in the state $\cdots [z][x]$, $^3\Gamma_3$ (cf. (2) in the text), normal plane C_2H_4 would probably dissociate adiabatically into two unexcited $^1\Gamma_1$ CH_2 radicals (dashes in the figure). Various states of 2 CH_2 with only slightly higher energy than those shown could be added to the diagram, e.g., $^1\Gamma_1+^1\Gamma_3$, $^1\Gamma_3+^3\Gamma_3$, and $^1\Gamma_3+^1\Gamma_3$, but are not important for our purposes. The equilibrium separation of the two C atoms (r_e) is smallest for the normal state of plane C_2H_4, intermediate in value for the states of perp. C_2H_4, and relatively large for the Γ_{4u} excited states of plane C_2H_4. Diagrams similar to Fig. 1 would apply to *derivatives* of C_2H_4, e.g. R′R″C=CR″R‴, although the group theory designations of the electronic states would be different; also, there would be *two* plane forms (*cis* and *trans*) with slightly different energy levels. Further, the dissociation product correlations would be rather different, and some predissociation of the state corresponding to $^1\Gamma_{4u}$ of C_2H_4 seems likely. Perhaps this explains the more structureless character[8] reported for the absorption bands of C_2H_4 derivatives than for C_2H_4 itself.

It is instructive to consider what would be expected if two CH_2 each in the state $\ldots [z][x]$, $^3\Gamma_3$ were brought together with their planes at right angles. The orbitals $[z]$ would overlap nearly as strongly as before and their electrons would give a strong bond $[z+z]^2$, but the two $[x]$ orbitals would overlap very little, and give practically zero energy of bonding, as one sees clearly on examining carefully the appropriate interaction integrals, which

can conveniently be set up according to the methods of Slater.[4] Hence instead of getting a singlet state $[x+x]^2$ and a triplet state $[x+x][x-x]$ of widely different energy (cf. (2) and (5)), the singlet and triplet should be nearly equal in energy, and both probably fairly stable. There must of course also be an unstable quintet. Examination of the integrals indicates that the triplet state should be slightly below the singlet, but this is not certain. It will be noticed that with perp. C_2H_4 (the two CH_2 planes perpendicular), the x axis of one CH_2 is parallel to the y axis of the other, and vice versa. As can be shown conveniently by group theory, this leads to a degeneracy somewhat resembling the π degeneracy in O_2. One may write for perp. C_2H_4:

$$1s^2 1s^2 [s]^2 [s]^2 [\pi]_y^4 [z+z]^2 [\pi]_x^2, \ {}^3\Gamma_3, \ {}^1\Gamma_2, \ {}^1\Gamma_4, \ {}^1\Gamma_1. \tag{6}$$

It can be shown that the incomplete group $[\pi]_x^2$ yields four electron states ${}^3\Gamma_3$, ${}^1\Gamma_2$, ${}^1\Gamma_4$, ${}^1\Gamma_1$, of which ${}^3\Gamma_3$ and ${}^1\Gamma_2$ are the triplet and singlet state obtained by bringing together two CH_2 . . . $[z][x]$, ${}^3\Gamma_3$, with their planes at right angles. The states ${}^1\Gamma_4$ and ${}^1\Gamma_1$ probably lie a volt or so above the two lowest states ${}^3\Gamma_3$ and ${}^1\Gamma_2$ of perp. C_2H_4; their structure is as if derived from CH_2^+ plus CH_2^-.[5]

For the ${}^3\Gamma_3$ and ${}^1\Gamma_2$ (but not for the ${}^1\Gamma_4$ and ${}^1\Gamma_1$) one might write instead of (6):

$$1s^2 1s^2 [s]^2 [s]^2 [y]^2 [y]^2 [z+z]^2 [x][x], \ {}^3\Gamma_3, \ {}^1\Gamma_2. \tag{7}$$

This gives expression to the fact that the $[\pi]_y$ and $[\pi]_x$ orbitals of perp. C_2H_4 in (6), in the case of ${}^3\Gamma_3$ and ${}^1\Gamma_2$, really describe essentially the same state of affairs as if one had the original $[y]$ and $[x]$ orbitals of CH_2 unshared, only the $[z]$ orbitals of CH_2 forming a bond.[6]

Comparing plane C_2H_4 with perp. C_2H_4, it can be shown by group theory that (unless possibly other excited states of unexpectedly low energy intervene), the normal state ${}^1\Gamma_{1g}$ of plane C_2H_4 must go over, on rotation of the CH_2 planes, into the low state ${}^1\Gamma_2$ of perp. C_2H_4, and the two excited states ${}^3\Gamma_{4u}$ and ${}^1\Gamma_{4u}$ of plane C_2H_4 into the low states ${}^3\Gamma_3$ and ${}^1\Gamma_4$ of perp. C_2H_4. It is now of interest to consider the relative positions of the various energy levels

[4] J. C. Slater, Phys. Rev. **38**, 1109 (1931).

[5] The preceding results may appear less unfamiliar if it is remarked that ${}^3\Gamma_3$ of the present $[\pi]_x^2$ corresponds to ${}^3\Sigma_g^-$ of π^2 of a diatomic molecule, ${}^1\Gamma_2$ and ${}^1\Gamma_4$ correspond to ${}^1\Delta_g$ of π^2, and ${}^1\Gamma_1$ corresponds to ${}^1\Sigma_g^+$ of π^2. In fact if the H nuclei in perp. C_2H_4 could be united with the C nuclei to form O_2, the four above-mentioned states of $\cdots [\pi]_y^4 [\pi]_x^2$ of perp. C_2H_4 would go over into the three states of $\cdots \pi^4 \pi^{*2}$ of O_2, i.e., of $\cdots (\pi+\pi)^4 (\pi-\pi)^2$ of (4).

[6] In (6), $[\pi]_y^4$ is a degenerate group formed from $[y]_A^2$ and $[y]_B^2$, where the designation $[y]$ is based on a separate choice of axes for the two CH_2 radicals A and B. If a choice of x and y axes consistent for the *whole* perp. C_2H_4 *molecule* were used, one would have to speak of, say, $[y]_A^2$ and $[x]_B^2$ instead of $[y]_A^2$ and $[y]_B^2$. It is this peculiarity which causes these two types to belong to a single degenerate type, here called $[\pi]_y$, of perp. C_2H_4, regardless of whether or not they interact appreciably. Similarly the orbitals which, when expressed in terms of the x, y axes of the separate CH_2's, are called $[x]_A$ and $[x]_B$ of 2 CH_2, become $[x]_A$ and $[y]_B$ in terms of x and y axes consistent for the whole molecule. In C_2H_4 both, somewhat modified by the interaction of the two CH_2 of course, then belong to the degenerate type here called $[\pi]_x$.

of plane and perp. C_2H_4. Roughly, the energy differences depend only on that part of the energy of formation of C_2H_4 which is furnished by the interaction of the two $[x]$ electrons of the two CH_2. In perp. C_2H_4 this is approximately 0 volts ($^1\Gamma_4$ is perhaps about 1 volt higher). In plane C_2H_4 in its normal state it is the energy of the $[x+x]^2$ bond, say about -2.5 volts. In excited C_2H_4 with $[x+x][x-x]$ we may expect the anti-bonding action of $[x-x]$ to exceed considerably[7] the bonding action of $[x+x]$, giving a net result of say perhaps $+3$ volts. These estimates are plotted in Fig. 1, which shows qualitatively how we may expect the energies of the various states to change on going from plane C_2H_4 to perp. C_2H_4, also the probable correlations of the various states with those of CH_2+CH_2.

Other Double-Bonded Compounds

From Fig. 1 it will be seen that the normal state of plane C_2H_4 should be stable with respect to a relative rotation of the planes of the two CH_2's, but that the excited states $^3\Gamma_{4u}$ and $^1\Gamma_{4u}$ shown in Fig. 1 might be expected to rotate spontaneously into the corresponding states $^3\Gamma_3$ and $^1\Gamma_4$ of perp. C_2H_4. By applying methods similar to the above to ethylene derivatives, such as for example $R_1R_2C=CR_1R_3$, it is easily shown that they should show qualitatively the same behavior as $H_2C=CH_2$ itself, and should have energy level diagrams similar to Fig. 1. Experimentally, their lowest excited energy levels are apparently nearer the normal level than in C_2H_4, since the ultraviolet absorption bands of the derivatives begin at longer wave-lengths than those of C_2H_4 itself, the shift increasing with the complexity of the molecule.[8]

Application of the quantum theory to C=N and N=N double bonds along the lines used for the C=C bond indicate that they also have the structure $[z+z]^2[x+x]^2$ characteristic of the C=C bond (cf. (2)). But the bond in B_2H_6 is probably more like that in O_2, giving a paramagnetic normal state, and has probably almost no stability toward a relative rotation of the two BH_2 groups. Details will be given in later papers.

It is well known that derivates of ethylene, e.g., $R_1R_2C=CR_1R_3$, exist in two forms called *cis* and *trans*, where in the *cis* form the two R_1's are on the

[7] The difference between $[x+x]^2$, $^1\Gamma_{1g}$ and $\cdots[x+x][x-x]$, $^1\Gamma_{4u}$ of plane C_2H_4 is analogous to that between $\cdots(\pi+\pi)^1(\pi-\pi)^2$, $^3\Sigma^-_g$ and $(\pi+\pi)^3(\pi-\pi)^3$, $^3\Sigma^-_u$ of O_2, unless possibly the electron configuration assigned in the latter case is wrong. In this O_2 case the energy difference is 6.1 volts from $v=0$ of $^3\Sigma_g^-$ to $v=0$ of $^3\Sigma_u^-$. Another example of the dominant effect of antibonding electrons is the case of H_2, where the energy of $(1s_A+1s_B)^2$, $^1\Sigma^+_g$ is -4.4 volts compared with H+H, while for the same internuclear distance the energy of $(1s_A+1s_B)(1s_A-1s_B)$, $^3\Sigma^+_u$ is about $+5$ volts.

[8] Cf. J. Stark and collaborators, Jahrbuch der Rad. und Elek. **10**, 10–188 (1913); and data in Int. Crit. Tables, Vol. 5. It seems likely that the "first band" of Stark corresponds in each case to a transition to the state analogous to the $^1\Gamma_{4u}$ of C_2H_4. (In the case of C_2H_4 itself, Stark's "second band" near $\lambda 2000$ is probably really the "first band.") The transition to the state analogous to $^3\Gamma_{4u}$ of C_2H_4 is perhaps represented by weak absorption at longer wave-lengths, not carefully investigated by Stark. It is perhaps best not to venture an interpretation of Stark's second band at shorter wave-lengths, except to suggest that *possibly* it may belong to the same transition as the first band,—but more probably not. In regard to the structures of the "first bands," cf. remark at end of the Fig. 1 caption.

same side of the z axis (C-C axis), in the *trans* form on opposite sides.[9] Usually both forms are stable at low temperatures, but the higher-energy form (usually *cis*) can usually be transformed into the lower-energy form (*trans*) by heating. The "energy of activation" for this process is evidently the energy difference between the normal state of the plane form ($^1\Gamma_{1g}$ for C_2H_4 in Fig. 1) and the lowest state of the perp. form ($^3\Gamma_3$ of perp. C_2H_4 in Fig. 1). Experimentally, there is evidence that this energy of activation is lower in the ethylene derivatives than is indicated by Fig. 1 for ethylene itself.[9]

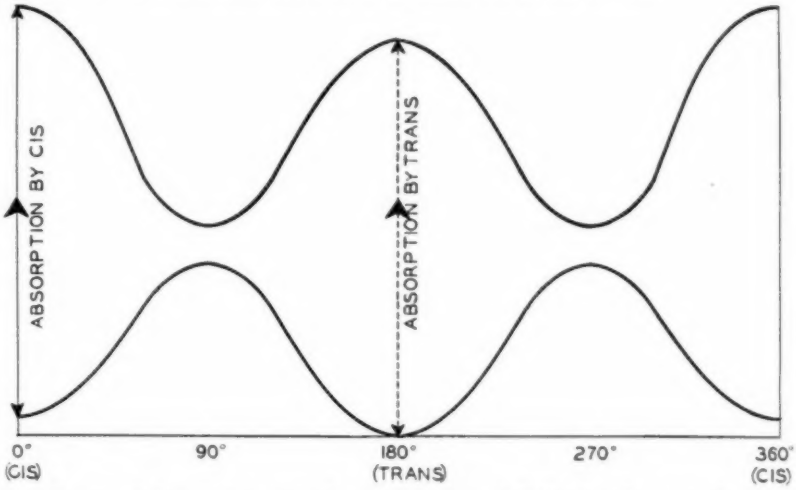

Fig. 2. Curves of electronic energy for a derivative of C_2H_4, for the normal state (lower curve) and (upper curve) for an excited state analogous to $^1\Gamma_{4u}$ of C_2H_4 in Fig. 1. The curves are of no more than qualitative significance. The *cis* form would probably usually correspond to 0°, the *trans* form to 180°, in a figure of the type of Fig. 2. The process of absorption of ultraviolet light by either form is indicated by vertical arrows. After such absorption, the molecule performs rotational vibrations about, or rotations through, the energy maxima at 0° and 180°. If light is emitted, or the energy is lost in a collision, when the angle of rotation away from the original angular position exceeds 90°, the molecule has been transformed from *cis* into *trans*, or vice versa.

Interpretation of Photochemical Experiments

Experimentally it is well known that the absorption of ultraviolet light can convert *cis* into *trans* forms and vice versa.[10] Probably the absorption carries the molecule to the singlet level analogous to $^1\Gamma_{4u}$ of C_2H_4 (Fig. 1), where it is unstable with respect to rotation into the perp. form.[11] [Olson[12] has pre-

[9] Cf. E. Hückel, Zeits. f. Physik **60,** 423 (1930) for a review of the experimental evidence on the behavior and nature of double-bonded compounds. This includes definite evidence for a plane arrangement of the six atoms nearest to the double bond.

[10] R. Stoermer and collaborators. Ann. d. Chemie **342,** 1 (1905); Chem. Ber. **42,** 4865 (1909); **44,** 637 (1911) and later articles.[9]

[11] Most absorbed frequencies would give rise to strong vibrations as well as to relative rotation of the CH_2 groups, but this has no necessary primary effect on the *cis-trans* transformation discussed here, except for absorbed frequencies causing direct dissociation or predissociation of $R_1R_2C_2R_1R_2$ into CR_1R_2 and CR_1R_2. Experimentally, the ultraviolet frequencies which cause the *cis-trans* change usually do not produce much decomposition.

[12] A. R. Olson, Faraday Soc. Trans. **27,** 69 (1931).

viously discussed the possible transformation of the *cis* into the *trans* isomer or vice versa by relative rotations of the CR′R″ groups as a result of ultraviolet absorption, but did not consider the simple mechanism which the present theory indicates.] The momentum of the rotation should, however, carry the molecule past the perp. form (90° rotation) into the form (*trans* or *cis*, as the case may be) opposite to that (*cis* or *trans*) in which it started (180° rotation): cf. Fig. 2. If the molecule is undisturbed, many rotations or rotational vibrations should take place, until eventually the energy is lost by a collision or by radiation, or sometimes perhaps by predissociation. For any individual molecule which has absorbed suitable light, the chances should then be nearly equal of returning to the original form or of ending in the isomeric form. Experiments of Warburg,[13] however, on the isomeric acids fumaric (*trans* form, higher energy) and maleic (*cis* form) of formula $(H \cdot C \cdot COOH)_2$ show only from 3 to 12 percent conversion of either isomer into the other per light quantum absorbed. Quite possibly this discrepancy can be attributed to disturbing factors, e.g., perhaps interference by collisions before completion of a single rotation or rotational vibration, since the experiments were made in water solution.

Prolonged exposure of ethylene derivatives to ultraviolet light tends to set up a photochemical equilibrium. Apparently this equilibrium is usually such that the lower-energy isomer is changed rather completely into the higher-energy isomer.[10] In the case of maleic and fumaric acid, equilibrium exists when there is about 75 percent of maleic acid;[13] the equilibrium ratio, however, apparently depends on the absorbed wave-lengths. Such results can be readily understood in terms of the present theory. They depend somewhat on the relative heights of the *cis* and *trans* maxima of the excited-state curve in Fig. 2, but probably more, or more directly at least, on differences in the absorption coefficients of the two isomers, which cause one to be transformed more rapidly than the other.

In conclusion, it may be remarked that the correctness of the preceding interpretation of the excited levels of ethylene and its derivatives, and of the effect of ultraviolet light on them, has not been proved. For the interpretation depends in part on estimates of the relative positions of energy levels which may conceivably be wrong to a sufficient extent to upset it. The interpretation should, however, be capable of experimental testing, and might also be the subject of theoretical calculations.

[13] E. Warburg, Sitzungsber. der Preuss. Akad. der Wiss., No. 50, p. 964 (1919).

Production of Infrared Spectra with Electric Fields

By E. U. CONDON
Palmer Physical Laboratory, Princeton University

(Received July 26, 1932)

A substance in a strong electric field acquires a new infrared spectrum owing to changes in the selection rules. The spectrum is governed by matrix components of the molecular polarizability and hence has the same intensity rules as the Raman effect.

IT IS well known from experience and from the theory of the Stark effect in atomic spectra that electric fields break down selection rules which apply to the atom when not in an electric field. It is natural therefore to suppose such effects might occur in molecular spectra with the consequence that nonpolar molecules like H_2 which have no infrared absorption would become absorbing when placed in a strong electric field. This question is given consideration in the following paper.

For a molecule the matter can be simply considered in terms of two properties: the molecular polarizability and the electric moment. The former is a tensor α_{ij} whose components have fixed values relative to a coordinate system fixed in the molecule. These values are functions of the coordinates fixing the nuclear configuration of the molecule. The electric moment is a vector M_i whose components are likewise most naturally taken in a coordinate fixed in the molecule and which are also functions of the nuclear coordinates of the molecule. The ordinary infrared spectrum of the molecule is determined by the matrix components of the electric moment M_σ referred to axes fixed in space. Suppose *1*, *2*, *3* are the unit vectors along which the axes $i=1, 2, 3$ are taken and that the orientation of these relative to an $(i\ j\ k)$ system fixed in space is specified by Eulerian angles θ, ϕ, ψ, then, if M_σ specifies a component of M in the new system

$$M_\sigma = a_{\sigma i} M_i \tag{1}$$

(using summation convention on double indices). Since the $a_{\sigma i}$ are functions of Euler's angles and the M_i are functions of the internal nuclear coordinates these electric moment components are functions of the vibration and rotation coordinates of the nuclear motion.

To find the infrared spectrum we have to calculate the matrix of the M_σ relative to the stationary states of the motion in the usual way. Letting j, m, λ be the quantum numbers of the rotational motion and writing n shortly for the ensemble of the vibrational motion's quantum numbers we have, for the eigenfunction of the molecule's nuclear state,

$$\psi(n, j, m, \lambda) = F_{\theta\phi\psi}(j, m, \lambda) G_q(n, j, m, \lambda) \tag{2}$$

where F and G are functions of the coordinates indicated as subscripts. F will be the rotator eigenfunctions of the unsymmetrical top in general but may be in special cases the simpler ones for the symmetrical top or even, for straight-line molecules, for the simple rotator. We neglect complicated cases of coupling of rotation and vibration motions. Because of the form of (1) and (2) the matrix components become

$$(n, j, m, \lambda \mid M_\sigma \mid n'j'm'\lambda') = \int \overline{F}(jm\lambda) a_{\sigma i} F(j'm'\lambda') \cdot \int \overline{G}(njm\lambda) M_i G(n'j'm'\lambda') \quad (3)$$

The first factor is simply the matrix components of the direction cosines which transform from the rotating to the fixed coordinate system and so can be calculated once and for all for the various simple cases, like the simple rotator and the symmetrical top. The probabilities for transitions by emission or absorption of light are given in the usual way by the squared absolute magnitudes of the matrix components in (3). This is the ordinary infrared spectrum.

Now let us consider the behavior of a molecule with regard to radiation when it is in a constant electric field of components, E_σ. It now has an induced electric moment which we call P_σ to distinguish from M_σ, the permanent electric moment. We shall have

$$P_\sigma = \alpha_{\sigma\tau} E_\tau \quad (4)$$

where $\alpha_{\sigma\tau}$ represents the components of α in the fixed coordinate system. By the tensor transformation law we have

$$\alpha_{\sigma\tau} = a_{\sigma i} a_{\tau j} \alpha_{ij}. \quad (5)$$

The new radiative transitions which the molecule may undergo while in the electric field are given by the matrix components of P_σ just as those in the absence of the field are given by the matrix of M_σ. Of course the ordinary infrared spectrum due to M_σ will be present perhaps with very small shifts due to a small Stark effect shift of the levels. The levels in the field are altered by the amount appropriate to the energy of an induced dipole in the field, i.e., by $-\frac{1}{2} P_\sigma E_\sigma$. The level with quantum numbers (n, j, m, λ) is therefore altered by the appropriate diagonal matrix element of this quantity, $(njm\lambda \mid -\frac{1}{2} P_\sigma E_\sigma \mid njm\lambda)$. We are not as much interested in such small shifts as we are in the new transition possibilities.

The matrix components of P_σ are evidently

$$(njm\lambda \mid P_\sigma \mid n'j'm'\lambda') = \int \overline{F}(jm\lambda) a_{\sigma i} a_{\tau j} F(j'm'\lambda') \cdot \int \overline{G}(njm\lambda) \alpha_i G(n'j'm'\lambda') \cdot E_\tau \quad (6)$$

The important point is that the selection rules for radiation associated with P_σ will be quite different from those for that due to M_σ for they depend on quite different characteristics of the molecule. As far as rotation is concerned however we can see immediately what the selection rules are for this induced

spectrum in terms of those for the ordinary spectrum, because of the form of the part of (6) that depends on the $a_{\sigma i}$. By the rules of matrix multiplication,

$$(jm\lambda \mid a_{\sigma i}a_{\tau i} \mid j'm'j') = (jm\lambda \mid a_{\sigma i} \mid j''m''\lambda'')(j''m''\lambda'' \mid a_{\tau j} \mid j'm'\lambda'),$$

which expresses the rotational factors of the new spectrum's matrix components in terms of those of the usual spectrum.

So far as rotation levels are concerned the transitions of $(jm\lambda) \rightarrow (j'm'\lambda')$ occurring in the induced spectrum will be those which are related by the property of each combining in the ordinary way with some third state (j'', m'', λ''). For the simple rotator this leads to the rule $\Delta j = \pm 2, 0$ in view of the $\Delta j = \pm 1$ of the usual spectrum. This is the selection rule of the Raman effect.

This last remark has a more deep-lying significance than an accidental coincidence, for on looking back over the work we see that the ideas involved are exactly those of Placzek's theory of the Raman effect. He calculates[1] the matrix components of the electric polarizability to get at the intensities and selection rules of the Raman effect. There the induced moment is due to the electric vector of the light wave, here it is due to the steady applied electric field. The induced spectrum we are describing is therefore what might be called the limit of the Raman effect as the frequency of the exciting light tends to zero. It has the same selection rules as the Raman effect.

When the Raman effect was first discovered it was assumed that it would be simply the usual infrared spectrum moved up into the visible part of the spectrum by combination with the frequency of the scattered light. This erroneous view was soon corrected by the facts and by a closer examination of the consequences of the Kramers-Heisenberg theory. This paper however points out how we can do the converse of the original view, namely put the Raman spectrum down into the infrared simply by letting the exciting light frequency tend to zero, it thus becoming an electrostatic field.

The connection with the Raman effect seems also to give a possibility of estimating the possibility of obtaining the induced spectrum in the laboratory. The integrated absorption coefficient over line width $\int \alpha d\nu$ is connected with the number of molecules in unit volume in the lowest state N_1 and the spontaneous transition probability A_{21} by the relation[2]

$$\int \alpha d\nu = N_1(c^2/8\pi\nu)A_{21}.$$

Using the relation of A_{21} to electric moment matrix components we have

$$\int \alpha d\nu = N_1(8\pi^3/3h^2)(h\nu/c) \mid P \mid^2$$

[1] Placzek, Zeits. f. Physik **70**, 84 (1931). Actually Placzek omits consideration of the rotational motion of the molecule. The writer worked out the above formulation including rotation last spring and would have calculated it through in detail but for the fact that W. V. Houston reported this problem at the Pullman meeting of the American Physical Society. His calculations are to be published soon according to what I have learned from his associate Mr. C. M. Lewis who is also a visitor at Massachusetts Institute of Technology this summer.

[2] Tolman, Phys. Rev. **23**, 693 (1924).

where P is written shortly for the matrix component in question. It is known that easily observable absorption is obtained say in HCl with $P \sim 10^{-19}$ and $N_1 \sim 10^{19}$ that is with a product of the order $N_1 P^2 \sim 10^{19}$. The polarizability of molecules is of the order 10^{-24} cm^3 and so if we use a liquid or a solid to make $N_1 \sim 10^{22}$ cm^{-3} and a field of 30,000 volts,cm $= 10^2$ e.s.u., we can obtain a product $N_1 P^2 \sim 10^{-22}$ which is still but 10^{-3} of that in HCl. Nevertheless, by use of long tube lengths it might be possible to observe the induced absorption.

One could use a long absorption cell with long condenser plates, applying the field with a high-potential transformer. The alternations of the potential would make no difference since their only effect would be to impress the alternation frequency on the spectrum which would be negligible in spectroscopic units.

The Impacts of Fast Electrons and Magnetic Neutrons

By J. F. CARLSON AND J. R. OPPENHEIMER
University of California, Berkeley, California

(Received July 18, 1932)

In this paper we consider the behavior of electrons with energy very large compared to their proper energy in their passage through matter, and further treat the impacts suffered by a certain type of hypothetical elementary neutral particle whose existence was tentatively suggested by Pauli. In the introduction we outline the problem and the methods to be employed, and give a summary of the formulae which embody our results. In Section I we develop the method suggested by Møller for the relativistic treatment of impacts; in (a) we apply it to the impacts of two free electrons; in (b) we show how it is to be applied to those impacts of a fast electron in which little energy is transferred to the secondary; in (c) we develop the theory of the magnetic neutron, and apply Møller's method to the treatment of its impacts. In II we give the detailed calculation of the energy transfers from a fast electron to the electrons of the matter through which it is passing, and compute the range and ionizing power of the primary electron. In III we apply the theory of the neutron to compute the number and nature of its impacts.

INTRODUCTION

RECENT experiments on the cosmic rays and on the penetrating radiation produced in the artificial disintegration of beryllium have raised again the question of the behavior of particles of very high energy in their passage through matter. Both these radiations have been shown to be extremely penetrating; and cloud chamber photographs have shown that both are accompanied by electrons of velocity very close to that of light; in the case of the cosmic rays the presence of electrons of energy over 10^9 volts has been established. The range of such particles, the number and nature of the secondary particles produced in their passage through matter can be computed theoretically. It has seemed to us desirable for a better understanding of the nature and properties of these radiations to have a more complete theoretical answer to these questions than is available. We shall, in this paper, be concerned with the behavior of two types of particle; chiefly we wish to study the electron of high energy; energy large, that is, compared with the proper energy mc^2. But we shall also study the impacts of a certain type of neutron, a hypothetical elementary neutral particle carrying a magnetic moment. This particle necessarily has a spin and presumably satisfies the exclusion principle; its existence was tentatively proposed by Pauli,[1] on the ground that by its introduction certain difficulties in the theory of nuclei could be resolved, and on the further ground that such a particle could be described by a wave function which satisfies all the requirements of quantum mechanics and rela-

[1] Professor Pauli presented the considerations which led him to the introduction and definition of the magnetic neutron at a seminar on theoretical physics in Ann Arbor in the summer of 1931.

tivity. These requirements, for instance, show that an elementary particle can have a magnetic but not an electric dipole moment; they do not suffice to fix the magnitude of the moment nor of the mass of the particle. Pauli supposed that such neutrons might form a third element in the building of nuclei, in addition to the electrons and protons; in this way one could understand the anomalous spin and statistics of certain nuclei, and the apparent failure of the conservation of energy in beta-particle disintegration. Pauli accordingly supposed that the mass of the neutron was not much greater than that of the electron, and that its magnetic moment was small compared to the Bohr magneton. One may, however, assume that the neutron has a mass very close to that of the proton, and that such neutrons are substituted for pairs of electrons and protons in certain nuclei, instead of being added to them; such neutrons would help explain the anomalous spin and statistics of nuclei, although they would throw no light on the beta-ray disintegrations. The experimental evidence on the penetrating beryllium radiation suggests that neutrons of nearly protonic mass do exist; and since our calculations may be carried through without specifying the mass or magnetic moment of the neutron, we shall consider the most general particle which satisfies the wave equation proposed by Pauli. It is important to observe that there may very well be other types of neutral particles, which are not elementary, and to which our calculations do not apply; and for clarity we shall call the particle which satisfies Pauli's wave equation a magnetic neutron. Certain of our results, such as the relatively great penetration of the particle, relatively rare impacts, and large mean energy loss per impact, characterize the behavior of any neutral particle.

The collisions and range of beta-particles have been often studied theoretically; and even the case in which the primary velocity of the beta-particle is very close to that of light has been studied by Bohr[2] in his classical theory of range. But Bohr used a classical model for the atom and the beta-particle, and a classical method for treating their interaction; and Bohr's treatment of the close impacts involving large energy losses is even classically not free from ambiguity. A very complete quantum theoretical calculation has been made by Bethe[3] for the case that the electron has a velocity not comparable with that of light; and our first problem in this paper is to make this calculation relativistically, so that it may be applied to electrons of energy very large compared to their proper energy.

At first sight the semi-classical method used by Gaunt[4] would appear appropriate for our purpose. Gaunt's method is semi-classical in that, in the quantum mechanical expression for the probability of excitation (ionization) of an atom, the matrix component of the interaction energy between primary and atomic electrons is in part replaced by a Fourier component, replaced, that is, by the matrix component for the transition of the atomic electron of the Fourier component of the potential of the primary electron. For transi-

[2] N. Bohr, Phil. Mag. **30,** 58 (1915).
[3] H. Bethe, Ann. d. Physik **6,** 325 (1930).
[4] J. A. Gaunt, Proc. Cam. Phil. Soc. **23,** 732 (1928).

tions in which the primary electron has a small change of momentum, small energy loss and small deflection, this method constitutes a valid application of the correspondence principle. And this method is readily extended to high velocity primaries, since we have now only to take, in place of the electrostatic potential, the Fourier component of the retarded four-vector potentials of the primary as a perturbation which induces transitions of the atomic electrons. The method is, however, not very elegant, even for the computation of the probability of small energy losses, because it gives an incorrect and very large probability of transitions involving small energy losses but large deflections, transitions to the study of which it may not legitimately be applied. We shall, therefore, not use this method; but in §II we shall give an outline of it, because it gives an illuminating insight into our formulae, and makes clear in a simple way the reason for the increase in ionization power with increasing energy of the primary. Quite recently Møller[5] has given a beautiful method of treating the relativistic impact of two electrons. This method is based upon a refinement of the correspondence principle; it neglects higher powers of the interaction energy between the electrons, and the effect of radiative forces; but within these limits it is strict and unambiguous, and enables one to take account, not only of the relativistic variation of mass with the velocity of the electrons, but of the retardation of the forces between them, of the spin forces, of interchange and the exclusion principle. The method is applicable not only to the impacts between two free electrons, but to the impacts of a free and an atomic electron in which small energies are transferred; it is further applicable to the impact of a neutron with an electron or proton; and it is this method which we shall use. In doing this we may take advantage of the fact that for energy losses very large compared to the ionization energy of the atomic electron we may treat both electrons as free; whereas for small energy losses we may neglect relativistic effects for the atomic electron, and, as it turns out, interchange. For extranuclear electrons there is a region of energy loss large compared to the binding energy and small compared to the proper energy where the two calculations merge and agree. For the neutron the probability of small energy losses is small, and the binding of an atomic electron can be largely neglected.

In §I then we shall give an outline of Møller's method, and its application to the three calculations; intimate collisions with an electron, collisions with a bound electron involving small energy loss, and collisions of a neutron. We shall have to discuss here the limitations imposed upon the method by the neglect of higher powers of the interaction energy and of radiative forces. These points cannot be fully settled without an adequate quantum electrodynamics, since they involve questions whose classical analogue is the theory of the structure of the electron. But we shall see that our method gives an upper limit to the range and a lower limit to the ionizing power; and we shall see further that the neglect we have made is small of the order of the fine structure constant. We shall have to carry the details of the calculation of the

[5] C. Møller, Zeits. f. Physik **70**, 786 (1931). Further L. Rosenfeld, ibid. **73**, 253 (1931).

impact of two free electrons rather further than was done by Møller, and shall obtain a formula for the differential probability of a given energy loss, a formula which may be applied to the impact of an electron with an atomic electron for all energy losses large compared to the binding energy.

In §II we shall treat impacts involving small energy losses, and compute the range and the number of primary ions for a beta-particle. In §III we shall carry through the calculations of the impacts of a magnetic neutron, and apply them for a few typical values of the constants characterizing the particle.

We shall give here a summary of certain of our results. Let the energy of the primary electron be

$$E = \epsilon mc^2 \tag{I}$$

and the binding energy of the second electron be I, and the energy lost by the primary be E'. We have to consider only collisions in which

$$E' \leqq \tfrac{1}{2}[(\epsilon - 1)mc^2 - I] \tag{II}$$

since one particle has always at least half the initial energy (see 1.32). The following formulae hold for large ϵ.

1.

The differential cross section for an energy loss $E' \gg I$ is

$$\sigma dE' = \frac{2\pi e^4}{mc^3} \frac{dE'}{E'^2} \cdot \frac{E^4 + E'^4 + (E - E')^4}{2E^2(E - E')^2} . \tag{III}$$

The angle γ between the trajectories of the two electrons after such an impact is given by

$$\gamma^2 = (2mc^2/E')(1 - E'/E) .$$

2.

If the cross section for ionization of the atomic electron by a primary electron of velocity v be

$$\sigma_{\text{ion}} = k_1(2\pi e^4/mv^2I) \ln mv^2/k_2I \tag{IVa}$$

then the cross section for ionization by the fast electron of energy ϵmi^2 is

$$\sigma_{\text{ion}} = k_1(2\pi e^4/mc^2I)\{\ln (mc^2/k_2I) + 2 \ln \epsilon\} . \tag{IVb}$$

When the atomic electron was initially bound in the normal state of a hydrogen-like atom,

$$k_1 = 0.29; \; k_2 = 0.024. \tag{IVc}$$

3.

If the mean energy loss to the atomic electron for a primary of velocity v is

$$\delta E = (4\pi e^4/mv^2) \ln mv^2/k_3I \tag{Va}$$

then for a primary of large energy

$$\delta E = (4\pi e^4/mc^2)\{\ln mc^2/k_3I + (3/2) \ln \epsilon + 0.22\} . \tag{Vb}$$

For an electron in the normal state of a hydrogen-like atom

$$k_3 = 1.1. \tag{Vc}$$

4.

When a magnetic neutron hits a charged particle, the mean energy loss per impact is of the same order as the maximum energy loss permitted by the conservation laws. If the mass of the neutron be M, its magnetic moment μ, its velocity small compared to that of light and its energy E, and if the charge and mass of the secondary be respectively e, and $m=\lambda M$, then the mean energy loss of the neutron is

$$\delta E = (7\pi^3 e^2\mu^2/6h^2c^2)E \tag{VIa}$$

for $\lambda=1$

and

$$\delta E = (2\pi^3 e^2\mu^2/h^2c^2)\lambda E \tag{VIb}$$

for $\lambda \ll 1$. Further details and other cases of impacts of the magnetic neutron are treated in §III.

NOTE: After the completion of this work, a very interesting paper[6] of Heisenberg has come to hand. Heisenberg is concerned with the problem of the nature of cosmic rays; and he derives theoretical formulae for the range of high speed particles with which to compare the experimental findings. Heisenberg's formula for the range of a fast electron differs only very slightly from that which we have found (Vb); we do not believe that the application of our formulae would lead to sensibly different conclusions. Note added in proof: An outline of a derivation of a formula for the energy loss of a fast electron, by a method also based on Møller's and altogether similar to that used by us in II, has been given in a recent paper of Bethe (Zeits. f. Physik, **76,** 283 (1932)).

I. RELATIVISTIC THEORY OF IMPACTS

The method which Møller proposed for the relativistic treatment of impacts is a generalization of two familiar elementary methods; the nonrelativistic collision theory of the quantum mechanics, and the theory of the transitions induced in a quantum mechanical system by a known electromagnetic field. According to the nonrelativistic quantum mechanics, we can write down the interaction energy V of the two particles which are colliding as a function of the coordinates (and in some cases momenta) of the particles; for two electrons this energy is just the electrostatic interaction energy. We can further specify the stationary states of the non-interacting particles by certain quantum numbers r, ρ, e.g., the components of momenta of the two particles. In the matrix scheme in which these quantum numbers are diagonal there will be a matrix $V_{rs}{}^{\rho\sigma}$ which corresponds to the interaction energy. Then with neglect of higher powers of the interaction energy, and with suitable normalization, the transition probability for a transition in which the one particle changes its state from $s\to r$ and the other from $\sigma\to\rho$ will be given by

$$P_{rs}{}^{\rho\sigma} = (4\pi^2/h)\left| V_{rs}{}^{\rho\sigma}\right|^2 \delta(E_r + E_\rho - E_s - E_\sigma). \tag{1.1}$$

[6] W. Heisenberg, Ann. d. Physik [5,] **13,** 430 (1932).

(The energy of a particle in state r is written E_r; and $\delta(x)$ is the delta function.) Further, when we know the wave functions for the particles in their non-interacting stationary states

$$\begin{aligned} \psi_s &= u_s e^{(-2\pi i/h)\cdot E_s t} \\ \psi_\sigma &= u_\sigma e^{(-2\pi i/h)\cdot E_\sigma t} \end{aligned} \tag{1.2}$$

we can compute the matrix $V_{rs}^{\rho\sigma}$:

$$V_{rs}^{\rho\sigma} = \int\int d\boldsymbol{r} d\boldsymbol{r}' \bar{u}\bar{u}_\rho' V u_s u_\sigma'. \tag{1.3}$$

(Integral over configuration space $\boldsymbol{r}$, $\boldsymbol{r}'$ of two particles.) Now when we are dealing with particles whose velocity is close to that of light, we must of course use relativisitic wave functions to characterize their stationary states; there is no difficulty in doing this. For the electron we must use solutions of Dirac's wave equation; for the neutron we may use solutions of the wave equation given by Pauli. But the function V no longer exists, since one cannot, when the retardation of the forces is taken into account, express the interaction energy as a function of the coordinates and momenta alone. What then, in the relativistic theory, should replace the matrix element $V_{rs}^{\rho\sigma}$?

We can answer this question if we consider first the perturbation induced in a quantum mechanical system by a given electromagnetic field. Let the four-vector potential of the field be $\phi_\mu(x, y, z, t)$; $\mu = 1 \cdots 4$, and the charge and current density vector of the system be

$$J^\mu = \psi j^\mu \psi. \tag{1.4}$$

Then

$$V = -1/c\phi_\mu j^\mu \tag{1.5}$$

is the operator representing the interaction energy of field and system. We resolve this operator in a Fourier integral

$$V = \int V_\nu e^{-2\pi i\nu t} d\nu; \; V_\nu = (-1/cj^\mu) \int e^{2\pi i\nu t} \phi_\mu dt. \tag{1.6}$$

To V_ν there now corresponds a matrix in the scheme of the stationary states without field

$$V_\nu^{\rho\sigma} = \int u_\rho V_\nu \mu_\sigma d\boldsymbol{r}. \tag{1.7}$$

Here, again neglecting higher powers of the interaction energy, we find for the transition probability

$$4\pi^2/h \left| V_\nu^{\rho\sigma} \right|^2 \delta(E_\rho - E_\sigma - h\nu). \tag{1.8}$$

Now when the field ϕ_μ is produced by a particle of known trajectory, a trajectory uninfluenced by the reaction of the system upon it, we express the potentials in terms of the retarded charge and current density J'^μ of this particle:

$$\phi^{\mu}(\mathbf{r}, t) = (1/c) \int d\mathbf{r}' \frac{[J'^{\mu}]}{r} t - r/c;\ r = |\mathbf{r} - \mathbf{r}'| . \tag{1.9}$$

Then

$$V_{\nu} = (-1/c^2) \int d\mathbf{r}' \left[j_{\mu} \int J'^{\mu} e^{2\pi i \nu t} dt \right] (e^2/r)^{\pi i \nu r/c} \tag{1.10}$$

and the transition probability $\sigma \rightarrow \rho$ is given by

$$(4\pi^2/h) \left| V_{\nu}^{\rho\sigma} \right|^2 \delta(E_{\rho} - E_{\sigma} - h\nu)$$

with

$$V_{\nu}^{\rho\sigma} = (-1/c^2) \int\int d\mathbf{r} d\mathbf{r}' \tilde{u}_{\rho} \left[j_{\mu} \int J'^{\mu} e^{2\pi i \nu t} dt \right] \frac{e^{2\pi i \nu r/c}}{r} u_{\sigma}. \tag{1.11}$$

This at once suggests that, when the trajectory of the particle is influenced by the reaction of the system, so that the state of the particle also changes as a result of the interaction, we replace the Fourier component of the retarded potentials of the particle by the matrix component corresponding to the transition in question. Thus if again

$$J'^{\mu} = \tilde{\psi} j'^{\mu} \psi$$
$$\psi_{\tau} = u_{\tau} e^{(-2\pi i/h) E_{\tau} t}$$

are the wave functions for the stationary states of the particle, we have to replace $\int J'^{\mu} e^{2\mu i \nu t} dt$ by $\tilde{u}_{\tau} j'^{\mu} u_{s}$ with $E_s - E_r = h\nu$.
This gives

$$\begin{aligned} P_{rs}^{\rho\sigma} &= (4\pi^2/h) \left| V_{rs}^{\rho\sigma} \right|^2 \delta(E_{\tau} + E_{\rho} - E_{s} - E_{\sigma}) \\ V_{rs}^{\rho\sigma} &= (-1/c^2) \int\int d\mathbf{r} d\mathbf{r}' \tilde{u}_{r} \tilde{u}_{\rho}' j_{\mu} j'^{\mu} e^{(2\pi i/hc)(E_s - E_r)r} u_{s} u_{\sigma}'/r. \end{aligned} \tag{1.12}$$

This reduces to (1.3) when retardation may be neglected and the velocity of the particles is small compared to that of light; it reduces to (1.11) when the reaction of the system on the particle may be neglected.

This is the formula proposed by Møller.[5] Although the derivation of the formula distinguishes between the system and the particle, the result which we obtain for $V_{rs}^{\rho\sigma}$ when we reverse the roles of the two

$$(-1/c^2) \int\int d\mathbf{r} d\mathbf{r}' \tilde{u}_{\rho} \tilde{u}_{r}' j^{\mu} j_{\mu}' e^{2\pi i/hc(E_{\sigma} - E_{\rho})r} u_{s}' u_{\sigma}/r.$$

gives the same transition probability, and the same matrix to represent the interaction energy.

We are thus led to consider the interaction energy represented by the matrix (1.12), $V_{rs}^{\rho\sigma}$. One might at first suppose that by the use of this expression for the energy, and the higher approximations of the method of variation of constants by which the transition probabilities may be computed, one

could obtain a strict expression for these transition probabilities. This is not so, however, because in the derivation of (1.12) the reaction of each particle to its own field had been neglected; this reaction should be taken into account in any strict theory, and its omission makes the higher approximations —involving higher powers of the charge or moment of the particles, invalid. Thus (1.12) gives no account of collisions between the particles in which radiation is emitted; but we know that such transitions will in fact occur. Their relative frequency, frequency relative to the transitions in which no radiation is emitted, is known to be of the order

$$\alpha(\bar{v}/c)^2 \tag{1.13}$$

where α is the fine structure constant, and $\bar{v}$ the mean velocity of the charges. This probability can thus be neglected when one of the particles moves with a velocity small compared to light; even when this is not so, radiative processes are presumably relatively rare because of the smallness of α. We shall see that in our theory of the impact of a high velocity electron upon matter the impacts in which very little energy is lost are the only ones of importance. But in these impacts the secondary electron has very low velocities, so that we know that radiative processes cannot be important in these impacts. For this reason the results we obtain with neglect of radiative forces furnish a lower limit to the ionizing power and energy loss of the fast electron. On the other hand the formulae derived from (1.12) for impacts in which large energies are transferred may be seriously in error; this error is at least of the order α.

When the two colliding particles are electrons, (1.12) must be modified to take account of interchange and the exclusion principle. When the interaction energy matrix corresponds to an operator in configuration space, it is known that this may be done by writing for the interaction energy

$$\tfrac{1}{2}\sum_{r,s\ \rho,\sigma} V_{rs}^{\rho\sigma} a_\rho^+ a_r^+ a_s a_\sigma \tag{1.14}$$

and by treating the a's as dynamical variables which satisfy

$$a_\rho^+ a_\sigma + a_\sigma a_\rho^+ = \delta_{\rho\sigma}; \qquad \begin{matrix} a_\rho a_\sigma + a_\sigma a_\rho = 0 \\ a_\rho^+ a_\sigma^+ + a_\sigma^+ a_\rho^+ = 0. \end{matrix} \tag{1.15}$$

The order of the a's has been so chosen that the interaction of each particle with its own field has been eliminated. Now although $V_{rs}^{\rho\sigma}$ corresponds to no operator in configuration space, and there is no wave equation in the configuration space of the two particles with which to compare our results, we still take (1.14) to represent the interaction energy. Since each a_r^+ corresponds to a transition in which a particle enters the state r, and each a_r to one in which a particle leaves the state r, there are now four terms in this sum which give rise to a transition in which the two particles go from the states s and σ to r and ρ. Because of the symmetry of $V_{rs}^{\rho\sigma}$, these four terms are equal in pairs; for the transition probability we find, in place of (1.12)

$$P_{rs}^{\rho\sigma} = (4\pi^2/h)\left| V_{rs}^{\rho\sigma} - V_{rs}^{\rho\sigma}\right|^2 \delta(E_r + E_s - E_\rho - E_\sigma). \tag{1.16}$$

In dealing with the impacts of a fast electron on an atom, it is easy to see that when the energy transferred to the atomic electron is small the interchange terms in (1.16) are negligible; for such impacts we may use (1.12) in place of (1.16).

We have now to apply these formulae to the three cases: (a) Impacts of two free electrons. (b) Impacts of a fast electron with an atomic electron, in which little energy is given to the secondary. (c) Impacts of a neutron with an electron or proton.

(a) High velocity impacts of free electrons

To apply (1.16) to the impacts of two free electrons we have to write down explicitly the wave functions for the stationary states of the free electrons and the expressions for the matrix components of the charge and current vector. The states of each electron we may specify by giving the components of momentum

$$\boldsymbol{p}^{(1)} = (p_x^{(1)}, p_y^{(1)}, p_z^{(1)}); \; \boldsymbol{p}^{(2)} = (p_x^{(2)}, p_y^{(2)}, p_z^{(2)})$$

and the component of spin $\sigma^{(1)}$, $\sigma^{(2)}$ of each electron in the z direction. (We exclude states of negative energy; and to the approximation here considered this causes no ambiguity.) For each of the electrons we take the wave functions to be solutions of the equations

$$[(h/2\pi i)(\partial/\partial t) + (hc/2\pi i)(\alpha \text{ grad}) - \alpha_0 mc^2]\psi = 0 \tag{1.17}$$

in which for each electron we take the α's in the familiar form

$$\alpha_x = \begin{pmatrix} 0 & 0 & 0 & 1 \\ 0 & 0 & 1 & 0 \\ 0 & 1 & 0 & 0 \\ 1 & 0 & 0 & 0 \end{pmatrix}; \quad \alpha_y = \begin{pmatrix} 0 & 0 & 0 & -i \\ 0 & 0 & i & 0 \\ 0 & -i & 0 & 0 \\ i & 0 & 0 & 0 \end{pmatrix};$$

$$\alpha_z = \begin{pmatrix} 0 & 0 & 1 & 0 \\ 0 & 0 & 0 & -1 \\ 1 & 0 & 0 & 0 \\ 0 & -1 & 0 & 0 \end{pmatrix}; \quad \alpha_0 = \begin{pmatrix} 1 & 0 & 0 & 0 \\ 0 & 1 & 0 & 0 \\ 0 & 0 & -1 & 0 \\ 0 & 0 & 0 & -1 \end{pmatrix}. \tag{1.18}$$

The solutions of these equations we write in the form

$$\psi_{p\sigma}{}^j = a_{p\sigma}{}^j e^{(2\pi i/h)[(\boldsymbol{p}\cdot\boldsymbol{r})-Et]} \tag{1.19}$$

with

$$E = c(m^2c^2 + p^2)^{1/2}$$

and with the $a_{p\sigma}{}^j$ functions of $(\boldsymbol{p}, \sigma)$. For an electron initially at rest we take for the a^j:

$$\begin{array}{ll} \sigma = +1 & \sigma = -1 \\ a_1 = a_2 = a_4 = 0; \; a_3 = 1; & a_1 = a_2 = a_3 = 0; \; a_4 = 1. \end{array} \tag{1.20}$$

These states will be characterized by an index (0). Thus

$$\boldsymbol{p}^{(0)} = 0,\ E^{(0)} = mc^2;\ \sigma^{(0)} = \pm 1;\ \text{etc.}$$

This wave function represents a uniform electron density of one electron per unit volume. For an electron moving in the z direction we take

$$\begin{array}{ll} \sigma = +1 & \sigma = -1 \\ a_2 = a_4 = 0 & a_1 = a_3 = 0 \\ a_1 = -Np_z/g & a_2 = Np_z/g \\ a_3 = N & a_4 = N \end{array} \tag{1.21}$$

where

$$g = mc + E/c$$

and

$$N^2 = 2g\,(E^2 - m^2c^4)^{1/2}.$$

These states will be characterized by a superscript (i). This wave function is normalized to represent a stream of unit flux, so that the transition probabilities computed from it will give directly the cross section for scattering.

We may without loss of generality suppose that after impact both electrons are moving in the xz plane, since, as we shall see, momentum is conserved in the impact. For such an electron we take

$$\begin{array}{ll} \sigma = +1 & \sigma = -1 \\ a_1 = -Np_z/g & a_1 = -Np_x/g \\ a_2 = -Np_x/g & a_2 = Np_z/g \\ a_3 = N & a_3 = 0 \\ a_4 = 0 & a_4 = N \end{array} \tag{1.22}$$

where

$$g = mc + E/c$$

and

$$N^2 = -gc/2Eh^3.$$

These states will be characterized by superscripts (1) and (2). This wave function is normalized to $dp_x\,dp_y\,dp_z = d\boldsymbol{p}$. We shall need the Jacobian

$$J^{(1)} = \partial(p_x^{(1)}, p_y^{(1)}, p_z^{(1)})/\partial(E^{(1)} + E^{(2)}, \vartheta^{(1)}, \phi^{(1)})$$

where, by the conservation of momentum,

$$E^{(2)}(p^{(2)}) = E^{(2)}(p^{(i)} - p^{(1)}). \tag{1.23}$$

We find

$$j^{(1)} = \frac{2mp^{(1)}E^{(1)}E^{(2)} \sin \vartheta^{(1)}}{mc^2(1 + \cos^2 \vartheta^{(1)}) + E \sin^2 \vartheta^{(1)}}$$

Note: There is at this point in Møller's paper an error, in that Møller uses in place of j^1

$$j^{(1)} = \partial(p_x^{(1)}, p_y^{(1)}, p_z^{(1)})/\sigma(E^{(1)}, \vartheta^{(1)}, \phi^{(1)}).$$

Now $J^1 \neq J^{(1)}$, because by the conservation laws $E^{(2)}$ depends on $p^{(1)}$. It is $J^{(1)}$ that we must use to take out the $\delta(E^{(0)}+E^{(i)})-(E^{(1)}+E^{(2)})$ in (1.16). We are indebted to Dr. Heisenberg for tellung us that Møller had found an error at this point in his paper.

Further the charge density is given by

$$e\sum_{j=1}^{4}\tilde{\psi}^j\psi^j \tag{1.24}$$

and the current density by

$$ec\sum_{j,k}\tilde{\psi}^j\alpha jk\psi^k. \tag{1.25}$$

If we put these expressions in (1.16), we find for the transition probability from the intial states [(1.20) and (1.21)] of the two electrons to states

$$\boldsymbol{p}^{(1)}, \sigma^{(1)}, \boldsymbol{p}^{(2)}\sigma^{(2)}$$

such that

$$E^{(1)} + E^{(2)} = E^{(0)} + E^{(i)}$$

the expression

$$4h^3e^4J^{(1)} \left| A \right|^2 \left| \int d\boldsymbol{r}e^{2\pi i/h([\boldsymbol{p}^{(i)}-\boldsymbol{p}^{(1)}-\boldsymbol{p}^{(2)}]\cdot\boldsymbol{r})} \right|^2 d\boldsymbol{p}^{(2)}d\vartheta^{(1)}d\phi^{(1)} \tag{1.26}$$

$$A = \frac{A_{1,i}{}^0A_{2,0}{}^0 - (\boldsymbol{A}_{1,i}\cdot\boldsymbol{A}_{2,0})}{\left|\boldsymbol{p}^{(i)}-\boldsymbol{p}^{(1)}\right|^2 - (1/c^2)(E^{(i)}-E^{(1)})^2} - \frac{A_{1,0}{}^0A_{2,i}{}^0 - (\boldsymbol{A}_{1,0}\cdot\boldsymbol{A}_{2,i})}{\left|\boldsymbol{p}^{(i)}-\boldsymbol{p}^{(2)}\right|^2 - (1/c^2)(E^{(i)}-E^{(2)})^2}. \tag{1.27}$$

Here

$$A_{1,0}{}^0 = \sum_{j=1}^{4}\bar{a}^j(p^{(1)}, \sigma^{(1)})a^j(p^{(0)}, \sigma^{(0)}).$$

$$\boldsymbol{A}_{1,0} = \sum_{j,k=1}^{4}\bar{a}^j(p^{(1)}, \sigma^{(1)})\alpha jka^k(p^{(0)}, \sigma^{(0)}).$$

Now

$$Q = \lim_{V\to\infty}\left|\int_V d\boldsymbol{r}e^{(2\pi i/h)([\boldsymbol{p}^{(i)}-\boldsymbol{p}^{(1)}-\boldsymbol{p}^{(2)}]\cdot\boldsymbol{r})}\right|^2 \to V\delta(\boldsymbol{p}^{(i)} - \boldsymbol{p}^{(1)} - \boldsymbol{p}^{(2)}). \tag{1.28}$$

Thus momentum as well as energy are conserved, and we may set

$$\boldsymbol{p}^{(2)} = \boldsymbol{p}^{(i)} - \boldsymbol{p}^{(1)}. \tag{1.29}$$

Further if we divide (1.27) by V we get the cross section for impact with a single electron at rest. In (1.27) we have to consider all the possible orientations of spin of the two electrons in initial and final states: to take one fourth the sum of (1.27) over the sixteen combinations of values of $\sigma^{(i)}$, $\sigma^{(0)}$, $\sigma^{(1)}$, $\sigma^{(2)}$. The resulting cross section can be expressed as a function of ϵ and ϑ, the angle of deflection of one of the electrons; it is independent of the azimuth of deflection of this electron; and all the components of momentum are determined by the conservation laws when ϑ and ϕ are given for one electron. Before carrying out this reduction we may make a few observations on the geometry of the impact.

According to the conservation laws, if the two electrons after impact have direction of motion making the angles ϑ_1, ϑ_2 with the z axis,

$$p^{(1)} \sin \vartheta_1 = p^{(2)} \sin \vartheta_2. \tag{1.30}$$

Further, the energy of a particle coming off at an angle ϑ is

$$E' = mc^2 \frac{2\epsilon - (\epsilon - 1)\beta^2}{2 + (\epsilon - 1)\beta^2}; \quad \begin{matrix} \alpha = \cos \vartheta; \\ \beta = \sin \vartheta; \end{matrix} \tag{1.31}$$

and the absolute value of its momentum is $mc[2\alpha(\epsilon^2-1)^{1/2}]/[2+(\epsilon-1)\beta^2]$. Thus the particle with the smaller energy always comes off at a larger angle; when the energy is shared equally the two particles come off at the same angle ϑ_m such that

$$\sin^2 \vartheta_m = 2/(\epsilon + 3). \tag{1.32}$$

In general the angle γ between the particles is

$$tg\gamma = [2 + (\epsilon - 1)\beta^2]/[(\epsilon - 1)\alpha\beta] \tag{1.33}$$

which reduces to

$$\gamma^2 = (2mc^2/E')(1 - E'/E) \tag{1.34}$$

for large ϵ. [Here E' is the smaller of the two energies $E^{(1)}$, $E^{(2)}$.] In no impact do both electrons come off at an angle larger than ϑ_m; and since (0. 7) gives the probability that an electron come off at an angle ϑ, and the other at the corresponding angle determined by (1.30), we have only to consider impacts in which $\vartheta \leqq \vartheta_m$; impacts in which $\vartheta > \vartheta_m$ will be the same impacts as those for which $\vartheta < \vartheta_m$, but in which the angle ϑ refers to the slower and not the faster of the two electrons.

We should note that by (1.34) the angle between the electrons grows smaller as the both the primary energy and the energy transferred grow large compared to the proper energy. This point is of some importance in connection with the interpretation of cloud chamber experiments, since it leads us to expect that very high energy secondary electrons produced by elastic impact with high energy primaries will come off nearly parallel to the direction of the primary.

We shall let then ϑ be the angle which the faster of the two secondary electrons, for which we use (1), makes with the primary direction. Further we

shall write $\alpha=\cos\vartheta$, $\beta=\sin\vartheta$, $q=(\epsilon-1)\beta^2$. Then the conservation laws give us the relations

$$\begin{aligned}
p_x^{(1)} &= -p_x^{(2)} = [(\epsilon^2-1)^{1/2}2\alpha\beta/(2+q)]mc\\
p_z^{(i)} &= (\epsilon^2-1)^{1/2}mc\\
p_z^{(1)} &= [2\alpha^2(\epsilon^2-1)^{1/2}/(2+q)]mc\\
p_z^{(2)} &= [(\epsilon^2-1)^{1/2}(\epsilon+1)\beta^2/(2+q)]mc\\
|\boldsymbol{p}^{(i)}-\boldsymbol{p}^{(1)}|^2-(1/c^2)(E^{(i)}-E^{(1)})^2 &= [2(\epsilon^2-1)\beta^2/(2+q)]m^2c^2\\
|\boldsymbol{p}^{(i)}-\boldsymbol{p}^{(2)}|^2-(1/c^2)(E^{(i)}-E^{(2)})^2 &= [4(\epsilon-1)\alpha^2/(2+q)]m^2c^2\\
g^{(0)} &= 2mc \qquad g^{(2)} = [(4+(\epsilon+3)q)/(2+q)]mc\\
g^{(i)} &= (\epsilon+1)mc \qquad p^{(1)} = [2\alpha(\epsilon^2-1)^{1/2}/(2+q)]mc \qquad (1.35)\\
g^{(1)} &= [2(\epsilon+1)/(2+q)]mc \qquad E^{(1)} = [(2\epsilon-q)/(2+q)]mc^2.
\end{aligned}$$

Thus we get for the differential cross section,

$$\sigma d\alpha = \frac{\pi e^4}{m^2c^4}\cdot\frac{(\epsilon+1)^2\alpha}{2(\epsilon-1)^2}\cdot\frac{4+(\epsilon+3)q}{(2+q)^2}\cdot d\alpha \sum_{\sigma^{(0)},\sigma^{(1)},\sigma^{i},\sigma^{(2)}}^{\pm}\left|\frac{L(\sigma)}{(\epsilon+1)\beta^2}-\frac{M(\sigma)}{2\alpha^2}\right|^2 \qquad (1.36)$$

Here each of the $L(\sigma)$, $M(\sigma)$ refers to a different one of the sixteen possible orientations of electron spin; $L(\sigma)$ is the direct term, $M(\sigma)$ the interchange term. The L and M can be tabulated as a function of ϵ and ϑ. We write

$$y=(\epsilon-1)/(\epsilon+1);\quad S^{-1}=4+(\epsilon-1)(\epsilon+3)\beta^2;$$

$\sigma^{(0)}$	$\sigma^{(i)}$	$\sigma^{(1)}$	$\sigma^{(2)}$	$L(\sigma)$	$M(\sigma)$
+	+	+	+		
−	−	−	−	$1+y\alpha^2-(1+\alpha^2)(\epsilon^2-1)\beta^2S$	$1-y\alpha^2+(\epsilon^2-1)\beta^4S$
−	+	−	+	$1+y\alpha^2+(\epsilon-1)[4\alpha^2\beta^2$	
+	−	+	−	$-(1+\alpha^2)(\epsilon+1)\beta^2]S$	$-2y\alpha^2[1+3\alpha^2+\epsilon\beta^2]S$
−	+	+	+		
+	−	−	−	$\mp 2\alpha\beta(\epsilon-1)(2+q)S$	$\pm 2\alpha\beta y[2(\epsilon+2)\alpha^2+(\epsilon+1)^2\beta^2)S$
+	+	+	−		
−	−	−	+	$\pm 2\alpha\beta(\epsilon-1)(1+\alpha^2)S$	$\mp 2\alpha\beta qS$
−	−	+	−		
+	+	−	+	$\mp 4\alpha^3\beta yS$	$\pm 2\alpha\beta y[2\alpha^2+(\epsilon+1)\beta^2]S$
+	−	+	+		
−	+	−	−	$\mp 4y\alpha\beta(1+\epsilon\beta^2)S$	$\pm 2y\alpha\beta[4\alpha^2+(\epsilon+1^2)\beta^2]S$
+	+	−	−		
−	−	+	+	$2\alpha^2qS$	$2\alpha^2qS$
−	+	−	+		
+	−	+	−	$-2q(1+\epsilon\beta^2)S$	$1-y\alpha^2+q[4\alpha^2+(\epsilon+1)\beta^2]S$

(1.37)

For large ϵ the last six contribute nothing to the cross section; the first four are important for energy losses not large compared to the proper energy; the next four are important for all energy losses comparable with the proper

energy; the next two are important only for energy losses comparable with the primary energy. From (1.35) the energy transferred is

$$E' = mc^2(\epsilon + 1)q/2 + q. \tag{1.38}$$

We must consider only impacts for which

$$\theta \leqq \theta_m, \; E' \leqq \tfrac{1}{2}(\epsilon - 1) \cdot mc^2. \tag{1.39}$$

For these the differential cross section is given by

$$\sigma dE' = \frac{2\pi e^4}{mc^2} \frac{dE'}{E'^2} \cdot \frac{E^4 + E'^4 + (E - E')^4}{2E^2(E - E')^2}. \tag{1.40}$$

This concludes our study of the impacts in which large energies are transferred. Certain further calculation by this method, primarily for the case of smaller ϵ, were given[5] by Møller; and there, too, the connection between certain results of this calculation with earlier attempts at the calculation of impacts were given. One point we may mention here: when ϵ is not large, we may use Rutherford's formula to give us the differential cross section for energy loss,—or rather the nonrelativistic quantum mechanically extension of Rutherford's formula which takes account of interchange and the exclusion principle. This gives, for $E' \ll E$,

$$\sigma dE' \cong 2\pi e^4 dE'/EE'^2. \tag{1.41}$$

This agrees with our result for energy losses small compared to the proper energy; but for larger energy transfers it gives too large a cross section. When higher powers of the interaction energy are not neglected, terms of the order of the fine structure constant must be added to (1.40). In the case of the nonrelativistic calculation (1.41) these are only of importance when E' is of the same order as E; and presumably, although not certainly, these terms will not be of importance for large ϵ except in this case $E' \sim E$.

(b) Small energy transfers to bound electrons

We have now to consider the case that a primary electron of very large energy gives to a secondary which was originally bound in an atom an energy not comparable to its proper energy. The states for the primary electron are still given by (1.21) and (1.22); but certain simplifications are introduced even here by the fact that the energy of the primary changes very little. For practically all such impacts involve a very small deflection for the primary; and in their treatment it is legitimate to neglect quantities which are small when the primary momentum changes by a relatively very small amount. With this understanding we see that only the matrix components of the charge and current of the primary in which the spin of the primary does not change are important, and that these are independent of the original orientation of the primary spin, which we may thus take parallel to z. (Case $\sigma = +1$). Further the components of current, and thus of vector potential, in the xy plane, are negligible. We have to consider only the scalar potential and the z component of the vector potential of the primary.

There are two further simplifications. In the first place interchange is negligible (interchange terms are important in general only when the energy transferred in of the order of the primary energy); we may thus use (1.12) in place of (1.16). In the second place the secondary electron never gets a velocity comparable with that of light, so that for it we may use nonrelativistic wave functions and expressions for charge and current density; and we may neglect the spin of this electron. On the other hand we may not use wave functions which neglect the binding of the atomic electron, and must replace for it (1.19) and (1.21). Let the initial energy and wave function of the electron be

$$E^{(0)} = -I;\ \psi_0 = e^{(2\pi i/h)It}u_0. \tag{1.42}$$

After the impact the atomic electron may be excited or ionized. Let the corresponding energies and wave functions be

$$\begin{aligned} E_{nl};\ \psi_{nl} &= e^{(-2\pi i/h)E_{nl}t}u_{nl}; \\ E,\ \psi_{El} &= e^{(-2\pi i/h)Et}u_{El}; \end{aligned} \tag{1.43}$$

where l stands for the two other quantum numbers in addition to the energy, necessary in the most general case to specify the state of the electron. Further let the continuous wave functions for energies above the ionizing potential be normalized in the energy scale.

The expressions for the charge and current density are then simply

$$\begin{aligned} \rho &= e\bar{\psi}\psi \\ J &= (e/2m)\left[(h/2\pi i)(\bar{\psi}\ \mathrm{grad}\ \psi - \psi\ \mathrm{grad}\ \bar{\psi})\right. \\ &\quad \left. - (2e/c)\bar{\psi}\boldsymbol{A}\psi\right] \sim (eh/2\pi im)\bar{\psi}\ \mathrm{grad}\ \psi. \end{aligned} \tag{1.44}$$

The terms in the vector potential $\boldsymbol{A}$ are of higher order in the interaction energy and may be dropped.

If as before we let the primary electron be deflected in the plane, and call the angles of deflection again ϑ, ϕ, we get from (1.12) for the probability of excitation to a state n, l:

$$\sigma_{nl} = \frac{4\pi^2e^4}{h^4c}\int\int d\vartheta d\phi J^{(1)}\left|V_{p^{(1)}nl}\right|^2 \qquad r = |\boldsymbol{r}_1 - \boldsymbol{r}_2|$$

$$\begin{aligned} V_{p^{(1)}nl} = \int\int d\boldsymbol{r}_1 d\boldsymbol{r}_2 \bar{u}_{nl}(\boldsymbol{r}_2)\exp\{2\pi i/h[(\boldsymbol{p}^{(i)} - \boldsymbol{p}^{(1)})\cdot\boldsymbol{r}_1) \\ - (1/c)(E^{(i)} - E^{(1)})r\}\left[1 - h/2\pi imc(\partial/\partial z_2)/r\right]u_0(\boldsymbol{r}_2) \end{aligned} \tag{1.45}$$

and for the probability of ionization to a state of energy in the range dE

$$\sigma_E dE = \frac{4\pi^2e^4}{h^4c}dE\int\int d\vartheta d\phi J^{(1)}\sum_a\left|V_{p^{(1)}El}\right|^2.$$

To get the total probability of excitation or ionization these expressions must be summed over n, l; to get the energy loss per impact they must be multiplied by

$$E' = E_{nl} + I,\quad E' = E + I \tag{1.47}$$

and summed over l, summed and integrated over n and E. In the next section we shall evaluate these expressions as far as possible when we leave the atomic wave functions arbitrary; and we shall evaluate them in detail for the case that the wave functions are those of a hydrogen like atom. From them we shall find, for the differential cross section for an energy loss E' large compared to the ionizing energy I,

$$\sigma dE' = 2\pi e^4 dE'/mc^2 E'^2$$

in agreement with (1.40); but for smaller energy losses we shall obtain results which differ very markedly from those given by (1.40).

(c) Theory of magnetic neutron

For the impacts of a neutron with a free electron we have again to use (1.12). Here the wave function for the electron before impact is given by (1.29); that after impact by (1.22); and the charge and current density of the electron by (1.24–5). We have only to find the matrix components of the charge and current density of the neutron.

The wave equation proposed by Pauli[1] for the magnetic neutron is simply related to the Dirac equation for the electron. In the absence of a field this latter may be written

$$[\gamma^\mu p_\mu - imc]\phi = 0;\ p_4 = (-h/2\pi i)(\partial/\partial t);\ p_0 = (h/2\pi i)(\partial/\partial x_l);\quad l = 1, 2, 3 \tag{1.48}$$

where the γ^μ satisfy

$$\gamma^\mu\gamma^\nu + \gamma^\nu\gamma^\mu = 2\delta_{\mu\nu}. \tag{1.49}$$

In the absence of a field this equation is to hold for the magnetic neutron, except that the neutron's mass M must be substituted for that of the electron. In the presence of a field new terms are to be added to the wave equation:

$$[\gamma^\mu p_\mu - iMc + P]\phi = 0;\ P = k\sigma^{\mu\nu}F_{\mu\nu}. \tag{1.50}$$

Here $F_{\mu\nu}$ is the field tensor,

$$\sigma^{\mu\nu} = \gamma^\mu\gamma^\nu - \gamma^\nu\gamma^\mu$$

and κ is a constant which is related to the magnetic moment μ of the neutron:

$$\kappa = \mu/4c. \tag{1.51}$$

These terms are not altogether arbitrary. Thus $\sigma^{\mu\nu}$ must be an antisymmetric tensor; it may not involve the coordinates nor powers of the momenta higher than the first. Thus (1.50) turns out to be the only hermitian not identically vanishing possibility which involves the field strengths linearly. The fact that κ is real is required by the hermiticity of the term; otherwise one could not interpret the wave function of a particle which was conserved. The sign of the term is arbitrary, and determines whether the magnetic moment of the neutron is parallel or antiparallel to its spin.

From (1.50) one may deduce two conservations laws. One asserts that the divergence of the four vector

$$s^\mu = \phi^+\gamma^\mu\phi \tag{1.52}$$

vanishes, and gives the conservation law for the neutron density. The other

$$\partial J^\mu/\partial x^\mu = 0; J^\mu = (-\mu/2)(\partial/\partial)x^\nu(\phi^+\sigma^{\mu\nu}\phi) \tag{1.53}$$

gives, as we shall show, the conservation of the charge and current vector. The two four vectors-particle density and flux, charge and current density, do not, as in the case of the electron, differ merely by a constant factor.

The first justification for calling μ the magnetic moment of the neutron we obtain if we reduce (1.50) for the case of velocities small compared to that of light. We find then that the neutron is described by a two-component wave function which satisfies

$$[(h/2\pi i)(\partial/\partial t) - h^2/8\pi^2 M\Delta + \mu(\boldsymbol{H}\cdot\sigma)]\phi = 0. \tag{1.54}$$

Here the σ's are the Pauli spin matrices

$$\sigma_x = \begin{pmatrix} 0 & 1 \\ 1 & 0 \end{pmatrix}; \quad \sigma_y = \begin{pmatrix} 0 & -i \\ i & 0 \end{pmatrix}; \quad \sigma_z = \begin{pmatrix} 1 & 0 \\ 0 & -1 \end{pmatrix} \tag{1.55}$$

and $\boldsymbol{H}$ the magnetic field. This is just what we should expect for the wave equation of a neutral particle carrying a spin and a magnetic moment μ.

A further justification for calling μ the magnetic moment of the neutron we can obtain by showing that

$$J^\mu = (-\mu/2)(\partial/\partial x^\nu)(\phi^+\sigma^{\mu\nu}\phi) \tag{1.56}$$

does correspond to the charge and current vector. For if we calculate the potentials and field strengths of a wave packet moving with low velocity by using (1.53) for the charge and current vector, we get just the field we should expect for the neutron of magnetic moment. Here as in the case of the electron the components of momentum do not completely specify the state; we need also to specify the orientation of the spin; and by doing this we determine the orientation of the field-producing magnetic moment.

We can verify that (1.53) is right in the following way. The wave equation (1.50) and its adjoint equation may be obtained by variation of ϕ^+ and ϕ in the Lagrangian.

$$L = \int dV\phi^+[\gamma^\mu p_\mu - iMc + \kappa\sigma^{\mu\nu}F_{\mu\nu}]\phi. \tag{1.57}$$

If we add to (1.54) the Lagrangian of the empty electromagnetic field,

$$(1/16\pi)\int dV F^{\mu\nu}F_{\mu\nu} \tag{1.58}$$

and in this vary, precisely as in the familiar case of the electron, the potentials, we get in place of Maxwell's equations for the empty field

$$\partial F^{\mu\nu}/\partial x^\nu = 4\pi J^\mu \tag{1.59}$$

with J^μ given by (1.53). Thus, as far as the field produced by the neutron is concerned, J^μ given by (1.53) acts like the charge and current density. It is a four vector, and its divergence vanishes.

It is convenient to rewrite the Eqs. (1.50) in the form corresponding to (1.17). Thus for the free neutron (no field), we get

$$[(h/2\pi i)(\partial/\partial t) + (hc/2\pi i)(\mathfrak{a}\cdot\text{grad}) - \alpha_0 Mc^2]\psi = 0 \tag{1.60}$$

where the α's are given by (1.18), if we take

$$\gamma^4 = \alpha_0;\ \gamma^l = i\alpha_0\alpha_l;\ \phi = i\alpha_0\psi. \tag{1.61}$$

The density current four vector then becomes

$$\tilde{\psi}\psi,\ c\tilde{\psi}\alpha\psi. \tag{1.62}$$

The neutron density is, as it must be, essentially non-negative. The terms corresponding to P in (1.50) then become

$$-i\alpha_0\kappa\sigma^{\mu\nu}F_{\mu\nu} \tag{1.63}$$

and the charge and current vector is given by

$$J^\mu = -\mu\partial/\partial x^\nu(\tilde{\psi}\tau^{\mu\nu}\psi). \tag{1.64}$$

Here the four row matrices $\psi^{\mu\nu}$ are given in terms of the Pauli spin matrices (1.55) by

$$\begin{aligned}
\tau^{\mu\mu} &= 0 \\
\tau^{l4} &= -\tau^{4l} = \begin{pmatrix} 0 & is_l \\ -is_l & 0 \end{pmatrix} \\
\tau^{kl} &= -\tau^{lk} = \begin{pmatrix} -s_m & 0 \\ 0 & s_m \end{pmatrix}.
\end{aligned} \tag{1.65}$$

Here (k, l, m) are a cyclic permutation of (1, 2, 3). This expression must be used in (1.12) to compute cross sections for impacts. For the states of the free neutron we may again use the wave functions (1.20) and (1.21). In place of (1.27) we find

$$16\pi^2 he^2\mu^2 J^{(1)} \left| B \right|^2 Q d\boldsymbol{p}^{(2)} a\vartheta^{(1)} d\phi^{(1)} \tag{1.66}$$

where Q is given by (1.28) and where now

$$B = \frac{A_{2,0}{}^0 T_{1,i}{}^4 + (\boldsymbol{A}_{2,0}\boldsymbol{T}_{1,i})}{\left| \boldsymbol{p}^{(i)} - \boldsymbol{p}^{(1)} \right|^2 - 1/c^2(E^{(i)} - E^{(0)})^2}. \tag{1.67}$$

Here the A's are given by (1.27) and the T's are defined

$$\begin{aligned}
T_{1,i}{}^\nu &= \sum_{j,k} a^r(p^{(1)}, \sigma^{(1)}) T_{jk}{}^{\mu\nu} a^k(p^{(1)}\sigma^{(1)}) \Delta p_{1,i}{}^\nu \\
\Delta\boldsymbol{p}_{1,i} &= \boldsymbol{p}^{(1)} - \boldsymbol{p}^{(1)}; \\
\Delta p_{1,i}{}^4 &= -(1/c)(E^{(i)} - E^{(1)}).
\end{aligned} \tag{1.68}$$

As before $Q \rightarrow V\delta(\boldsymbol{p}^{(i)} - \boldsymbol{p}^{(1)} - \boldsymbol{p}^{(2)})$.
We can write the cross section for a particular set of spin orientations

$$16\pi^2 he^2\mu^2 J^{(1)} \left| B(\sigma) \right|^2 d\vartheta^{(1)} d\phi^{(1)}. \tag{1.69}$$

As before we must take, to find the differential cross section, one fourth the sum of these expressions over all sixteen orientations of initial and final spins:

$$\sigma d\vartheta d\phi = 4\pi^2 h e^2 \mu^2 J^{(1)} \sum^{\pm}_{\sigma^{(i)},\sigma^{(1)}\ \sigma^{(0)},\sigma^{(2)}} \left| B(\sigma) \right|^2 d\delta d\phi. \tag{1.70}$$

The quantities T occurring here may be tabulated in terms of the initial and and final momenta and energy of the neutron. If for brevity we write

$$\begin{aligned} &p_z^{(i)} = r; \quad p_z^{(1)} = r'; \quad p_x^{(1)} = p'; \\ &g^{(i)} = g; \quad g^{(1)} = g'; \qquad \Delta r = r - r'; \ \Delta g = g - g'; \end{aligned} \tag{1.71}$$

then we find for the T's the following values:

$\sigma^{(i)}$	$\sigma^{(1)}$	T_z	T_y
$+$	$+$	$i\Delta r(rp'/gg')+i\Delta g p'/g'$	$\mp p'(1-rr'/gg')\pm\Delta r p'/gg'\pm\Delta g p'/g$
$+$	$-$	$\pm\Delta r(rp'/gg'\pm i\Delta g((r/g)+r'/g')$	$(\pm rp'^2/gg')+\Delta r(1+rr'/gg')$ $+\Delta g((r/g)+r'/g')$
$-$	$+$		
$\sigma^{(i)}$	$\sigma^{(1)}$	T_x	T^4
$+$	$+$	$(-ip'^2 r/gg')-i\Delta g((r/g)-r'/g')$	$(-ip'^2/g')+i\Delta r((r/g)-r'/g')$
$-$	$-$		
$+$	$-$	$\pm ip'(1+rr'/gg')\pm i\Delta g p'/g'$	$\pm ip'(r/g)+r'/g')\mp i\Delta r p'/g'$
$-$	$+$		

(1.72)

It is not possible, without knowing the mass of the neutron, to reduce these expressions further. We shall, therefore, postpone until §III the discussion of these formulae. There, too, we shall make such elementary investigations of the effect of the binding of the electron as are necessary to our purpose.

Before proceeding to the further application of this method of Møller, we wish again to emphasize the approximate character of the method. We have throughout neglected two things: the reaction of the particles to their own field, and all radiative processes; and higher order terms in the interaction of the two particles. In the case of the electron, both these neglects mean the omission of terms of the order of the fine structure constant, terms which are genuinely small unless both particles involved are moving with velocities comparable to light. Just what effect these terms could have on the things in which we are most interested—range and ionizing power of the primary, energy distribution of the secondaries—we shall discuss when we have our results before us. But the formula (1.40), which is derived with neglect of these terms, is subject to grave doubt, since we have no assurance that terms of the form $\epsilon\alpha$ will not appear, and no physical assurance that in the intimate collision of two electrons this approximate method can be legitimately employed. It seems at present by far the soundest method available, and perhaps experiment can show in what measure it is inadequate. The further study of impacts involving neutrons, a study which should not neglect

higher powers of the interaction energy, presents even in the nonrelativistic case serious analytic complications; and we have not thought it advisable to attempt these without some more certain information about the characteristic constants, in particular the moment, of this hypothetical particle.

II. Ionizing Power and Range of Fast Electrons

We must now consider in detail the small energy losses suffered by a fast electron in its impacts with an atom. Just as in the nonrelativistic theory, if we neglect the binding of the atomic electron we find an infinite probability for small energy losses; and just as in the nonrelativistic treatment the proper consideration of the binding gives us a finite probability of energy loss and a finite range.

Before using our formula (1.46) to study these impacts we may outline briefly the semiclassical method of treating this same problem. This method, it will be remembered, is valid only for such impacts as involve small energy loss and small deflection of the primary; in this method we treat the primary particle classically, neglect the reaction of the atom upon it, and use the field calculated for this undeflected trajectory as a perturbation causing transition of the atomic electron. If we choose our coordinates so that the particle passes along the z-axis, and goes through the origin at $t=0$, then the field of the particle is given by the potentials

$$\begin{aligned} A_x = A_y = 0;\ A_z &= (e v \epsilon/c)\left[x^2 + y^2 + \epsilon^2(z - vt)^2\right]^{-1/2}; \\ \phi &= e\epsilon\left[x^2 + y^2 + \epsilon^2(z - vt)^2\right]^{-1/2}; \end{aligned} \tag{2.1}$$

where v is the velocity of the particle and

$$1/\epsilon = (1 - v^2/c^2)^{1/2}.$$

The probability of a transition of the atomic electron in which its energy changes by E' is determined by the Fourier component of this field of frequency $\nu' = E'/h$. We therefore analyze the potentials by a Fourier integral:

$$\begin{aligned} A_z &= (4e/c)\int_0^\infty K_0(2\pi\nu p/\epsilon v)\cos 2\pi\nu(t - z/v)d\nu \\ \phi &= (4e/v)\int_0^\infty K_0(2\pi\nu p/\epsilon v)\cos 2\pi\nu(t - z/v)d\nu \end{aligned} \tag{2.2}$$

where K_0 is the Hankel function:

$$K_0(\xi) = \int_0^\infty \frac{\cos\lambda d\lambda}{(\lambda^2 + \xi^2)^{1/2}};\ \text{and}\ p = (x^2 + y^2)^{1/2}.$$

The perturbation energy for the atomic electron is given by

$$V = e\phi - (1/c)A_z j_z \tag{2.3}$$

where j is the current operator which, to a sufficient approximation, is given by (1.44): $j_z = (he/2\pi mi)\partial/\partial z$. Thus the transition probability for an atomic

transition $n \rightarrow n'$ in which the energy of the atom changes by $E' = E_{n'} - E_n = h\nu'$ is just

$$P_{nn'} = (4\pi^2/h^2) \left| \int \tilde{u}_{n'}(2e^2/v) K_0(2\pi\nu' p/\epsilon v) e^{2\pi i \nu' z/v} [1 - (h\nu/2\pi imc^2)\partial/\partial z] u_n d\boldsymbol{r} \right|^2 \quad (2.4)$$

where the u's are the wave amplitudes for the atomic electron. The nonrelativistic expression is[5]

$$P_{nn'} = \frac{4\pi^2}{h^2} \left| \int \tilde{u}_{n'} \frac{2e^2}{v} K_0\left(\frac{2\pi\nu' p}{v}\right) e^{2\pi i \nu' z/v} u_n d\boldsymbol{r} \right|^2. \quad (2.5)$$

Now for distant collisions, to which alone this method may be legitimately applied, we may expand the potentials about the position of the nucleus of the atom, which we take to be on the y axis at a distance from the track, and consider only the first two terms of the expansion, i.e., the dipole moment of the atom. If we let the y-component of the displacement of the electron from the center of the atom be ζ then we find

$$P_{nn'}(p) = (16\pi^2 e^4/h^2 v^2) \left| \zeta_{nn'} \right|^2 [K'(2\pi\nu' p/v\epsilon)]^2 \quad (2.6)$$

where $K'(\xi) = \partial K_0(\xi)/\partial\xi$ and $\zeta_{nn'} = \int \tilde{u}_{n'} \zeta u_n d\boldsymbol{r}$. The nonrelativistic formula is[5]

$$P_{nn'}(p) = (16\pi^2 e^4/h^2 v^2) \left| \zeta_{nn'} \right|^2 [K'(2\pi\nu' p/v)]^2. \quad (2.7)$$

Thus in this calculation the effect of retardation is to introduce p/ϵ in place of p in the argument of K'. Since K' is a rapidly decreasing function

$$\begin{aligned} K'(\xi) &\sim 1/\xi \text{ for } \xi \rightarrow 0, \\ K'(\xi) &\sim -(\pi/2\xi)^{1/2} e^{-\xi} \text{ for } (\xi) \rightarrow \infty, \end{aligned} \quad (2.8)$$

this means that for a given transition and a given position of the atom the probability of a given energy loss is increased by considering retardation; energy losses occur at greater and greater distances from the track as the velocity of the primary approaches more and more closely that of light. We are, therefore, led to expect a greater number of low velocity secondaries than we should find from an extrapolation of the nonrelativistic formula; and this is just what we shall find. It is an immediate consequence of the flattening out of the field of the electron in the equatorial plane.

As the position of the atom approaches the track, $p \rightarrow 0$, and the total number of transitions becomes infinite. For these intimate collisions the expansion of the potentials about p and the assumption that the track is undeflected are both illegitimate. There are a number of ways in which, for small energy losses, we might try to modify the calculation of these close impacts, in such a way that the integral over p converges and gives a finite result. Perhaps the simplest is to stop the integration at a point $\bar{p}$ where, according to (2.6), the probability of inelastic impact is unity. This point turns out to be, for a hydrogen-like electron, of the order of the Compton wave-length divided by the effective nuclear charge z:

$$\bar{p} = 1.4h/2\pi mcz \sim h/2\pi mcz. \quad (2.9)$$

This procedure gives for the mean energy loss due to small energy transfer, small compared to the proper energy,

$$\delta E = (4\pi e^4/mc^2) \ln (mc^2\epsilon/W) \tag{2.10}$$

where W is of the order of the ionizing potential I, and for a hydrogen like atom is $W=3.0\ I$. This result is in remarkable agreement with that which we shall obtain by our strict calculations with the help of (1.46); and it is of some interest to inquire into the ground for this. The answer is very simple. We shall see that in our strict calculations (2.6) is right for distant impacts, impacts, that is, in which the deflection of the primary is negligible. For angles of deflection ϑ which are much smaller than

$$\bar{\vartheta} = (2mI)^{1/2}/mc\epsilon \tag{2.11}$$

we get just this result (2.6), if we connect ϑ and the parameter p by the dynamical relation $p\vartheta \sim e^2/mc^2\epsilon$. For larger ϑ i.e., smaller p, the transition probability for transitions involving small energy loss decreases rapidly, instead of becoming infinite as it does by (2.6). Thus it is approximately right to break off the integral over p at a point

$$\bar{p} \sim (e^2/mc^2\epsilon\bar{\vartheta}) \sim (h/2\pi mcz)$$

and this is what, in these preliminary calculations, we have done.

We must now turn to the strict calculation. We shall here be dealing only with small energy losses, and since our expressions converge very rapidly as the angle of deflection ϑ increases, we have only to evaluate them for small ϑ. As before, we shall assume throughout that ϵ is a large number, and neglect higher powers of $1/\epsilon$. We need to know the change of momentum of the primary in terms of the energy lost E' and the angle of deflection ϑ. Thus, with these approximations,

$$\begin{gathered} p_z^{(i)} - p_z^{(1)} = E'/c;\ p_x^{(1)} = E\vartheta/c; \\ \left| \boldsymbol{p}^{(i)} - \boldsymbol{p}^{(1)} \right|^2 = (1/c^2)(E'^2 + E^2\vartheta^2). \end{gathered} \tag{2.12}$$

Further

$$\left| \boldsymbol{p}^{(i)} - \boldsymbol{p}^{(1)} \right|^2 - (1/c^2)(E^i - E^{(1)})^2 \leq (1/c^2)((E'^2/\epsilon^2) + E^2\delta^2) \tag{2.13}$$

and

$$J^{(1)} = \frac{\partial(p_x^{(1)}, p_y^{(1)}, p_z^{(1)})}{\partial(E, \vartheta, \phi)} = \frac{p^{(1)}E^{(1)}}{c^2} \sin\vartheta \sim m^2\epsilon^2 c \sin\vartheta . \tag{2.14}$$

We start with the formulae (1.45), (1.46):

$$\begin{aligned} V_{p^{(1)}nl} = \int d\boldsymbol{r}_1 d\boldsymbol{r}_2 \bar{u}_{nl}(r_2) \exp\{(2\pi i/h)[(&[\boldsymbol{p}^{(i)} - \boldsymbol{p}^{(1)}]\cdot\boldsymbol{r}_1) \\ &- 1/c(E^{(i)} - E^{(1)})r]\}[(1 - (h/2\pi imc)\partial/\partial z)u_0(r_2)]/r. \end{aligned}$$

In all cases the matrix integral may be written as the product of two integrals if we replace throughout

$$\boldsymbol{r}_1 = \boldsymbol{r}_2 + \boldsymbol{r}_{12}.$$

Thus

$$V_{p^{(1)}nl} = \rho_{12}(p^{(1)})\rho_2(n, l, p^{(1)}) \tag{2.15}$$

where

$$\rho_{12}(p^{(1)}) = \int (d\boldsymbol{r}/r) \exp\{(2\pi i/h)[([\boldsymbol{p}^{(i)} - \boldsymbol{p}^{(1)}]\cdot\boldsymbol{r}) - (1/c)(E^{(i)} - E^{(1)})r]\} \tag{2.16}$$

and

$$\rho_2(n, l, p^{(1)}) = \int d\boldsymbol{r}\tilde{u}_{nl} \exp\left\{\frac{2\pi i}{h}([\boldsymbol{p}^{(i)} - \boldsymbol{p}^{(1)}]\cdot\boldsymbol{r})\right\}[1 - (h/2\pi imc)\partial/\partial z]u_0. \tag{2.17}$$

The former integral may be evaluated at once, and gives just, by (2.14)

$$\rho_{12}(p^{(1)}) = (h^2c^2/\pi)1/((E'^2/\epsilon^2) + E^2\vartheta^2). \tag{2.18}$$

The second integral may be considerably simplified, for it may be replaced by

$$\rho_2 = \int d\boldsymbol{r}\tilde{u}_{nl}e^{-i\gamma z}u_0; \text{ with } \gamma = 2\pi mc\epsilon \sin\vartheta/h. \tag{2.19}$$

We may see this in the following way. We may expand

$$\exp\{(2\pi i/h)([\boldsymbol{p}^{(i)} - \boldsymbol{p}^{(1)}]\cdot\boldsymbol{r})\}$$

in powers of ϑ:

$$e^{(2\pi i/hc)\cdot E'z}\left\{1 - \frac{2\pi i}{hc}E\vartheta_z - \frac{2\pi^2}{h^2c^2}E^2\vartheta^2\cdots\right\}. \tag{2.20}$$

In all terms but the first the factor

$$e^{(2\pi i/hc)E'z}[1 - (h/2\pi imc)(\partial/\partial z)] \tag{2.21}$$

gives a correction of the order, by (2.12), E'/mc^2 which is small of the order $(v/c)^2$ for the atomic electron, and negligible. If we neglect (2.21) in the first term the integral vanishes; and we have to show that here, too, this neglect is justified. But now the integral

$$\int d\boldsymbol{r}\tilde{u}_{nl}e^{(2\pi i/hc)E'z}[1 - (h/2\pi imc)\partial/\partial z]u_0 \tag{2.22}$$

is just the matrix component of a perturbation produced by a field of potential

$$A_x = A_y = 0;\ A_z = -e^{(2\pi i/hc)E'(z-ct)};\ \phi = e^{(2\pi i/h)E'(z-ct)}. \tag{2.23}$$

These potentials may be derived for the scalar

$$\Lambda = -h/2\pi ie^{(2\pi i/hc)E'(z-ct)} \tag{2.24}$$

by differentiation $\boldsymbol{A} = \text{grad}\,\Lambda;\ \phi = -\partial\Lambda/\partial t$. They thus correspond to no field;

and the corresponding matrix element vanishes. (This may be verified by direct calculation as far as the dipole moment of the atom is concerned.)

The transition probability is thus given by

$$\sigma_{nl} = (e^4h^2c^2/\pi)\int d\gamma^2 \mid \rho_2(n, l, \gamma) \mid^2 [1/(\gamma^2 + \eta^2)^2] \tag{2.25}$$

with $\eta = 2\pi E'/hc\epsilon$ and $\rho_2(n,l,\gamma) = \int d\boldsymbol{\tau}\, \tilde{u}_{n\epsilon} e^{-i\gamma x} u_0$. This expression may, of course, be evaluated when we know the u's. We shall not need this evaluation to calculate the energy loss of the primary; but we do need it to compute the probability of ionization; and it is instructive to have the explicit expressions. We shall consider the very simplest case of an electron bound in the normal state of a hydrogen-like atom, with an effective nuclear charge z; we shall calculate σ for transitions to the continuum. We need to introduce the length

$$1/b = h^2/4\pi^2 mze^2 \tag{2.26}$$

and the quantum number

$$n = 1/bk = 2\pi e^2 z/hv;\ k = 2\pi mv/h;\ v = (2E/m)^{1/2} = [(2/m)(E' - I)]^{1/2}; \tag{2.27}$$

which measures the energy of the secondary electron. If we now use parabolic coordinates with the pole along the x axis, and use the well-known wave functions for the hydrogen-like atom in such coordinates, we can evaluate not only ρ_2, but the sum (integral) of $|\rho_2|^2$ over all states l of the same energy. We thus find

$$\sum_l \mid \rho_2(n, l, \gamma) \mid^2 = \frac{z^{10}\pi^2 mb^6}{h^2} \frac{\exp\left[-2ntg^{-1}2kb/(b^2 + \gamma^2 - k^2)\right]}{1 - e^{-2\pi n}} \frac{\gamma^2[\gamma^2 + (b^2 + k^2/3]}{\{[b^2 + (\gamma - k)^2][b^2 + (\gamma + k)^2]\}^3}. \tag{2.28}$$

For very small energy losses

$$E' \sim I \tag{2.29}$$

the integrand $G(\gamma)$ of the expression for the transition probability decreases with increasing γ, and becomes very large for $\gamma \to 0$. For small γ $G(\gamma) \sim \gamma^2/(\gamma^2+\eta^2)^2$ whereas for larger $\gamma \gg b$; $G(\gamma) \sim \gamma^{-12}$. Thus the transition probability begins to fall off more rapidly with increasing angle of deflection when the angle grows of the order

$$\bar{\vartheta} = hb/2\pi mc\epsilon. \tag{2.30}$$

This is the result quoted before (2.11) in connection with the semi-classical calculation. In this earlier calculation we neglected higher powers of γ higher moments of the atomic electron—and thus replaced $e^{-i\gamma x}$ by $1 - i\gamma x$. And this reduced expression becomes wrong when $\gamma \sim b, \vartheta \sim \bar{\vartheta}$.

For energy losses large compared to the ionizing potential the value of G for $\gamma \to 0$ grows very small, and the integral over γ comes entirely from the

region $\gamma^2 \sim k^2$; with neglect of higher powers of I/E' the integral may then be evaluated, and gives just

$$\sigma dE' = 2\pi e^4 dE'/mc^2 E'^2. \tag{1.40a}$$

This agrees with our result (1.40) for the energy loss to a free electron for $E' \ll mc^2$.

We may use (2.28) to compute the cross section for ionization. For (1.40) gives a negligible contribution for high energy losses, and we do not need here to supplement it with the result (1.40). We so find, carrying out approximately the quadratures over γ and E for the cross section for ionization

$$\sigma_{\text{ion}} = 0.29(2\pi e^4/mc^2 I) \ln (mc^2\epsilon^2/0.024I). \tag{2.31}$$

The nonrelativistic result is, for this case of a hydrogen like[3] atom

$$\sigma_{\text{ion}} = 0.29(2\pi e^4/mv^2 I) \ln (mv^2/0.024I) \tag{2.32}$$

where v is the velocity of the primary. The two differ by $(1.2\pi e^4/mc^2)\ln\epsilon$ for $v \to c$. The constant 1.2 is here computed only for the simple atom which we have considered; it depends upon the f-values for the atomic electron, and no universal closed formula can be given for it. We may get a somewhat more general result by comparing our formula with the nonrelativistic one. For (2.25) differs from the corresponding nonrelativistic formula in three points: (1) In the nonrelativistic formula c is to be replaced throughout by v. (2) In the nonrelativistic formula the quantity η in the denominator of (2.25) is to be replaced by $\eta' = 2\pi E'/hv$. (3) The upper limits of integration for γ and E' are greater in our formula. This third difference is not essential in computing the probability of ionization, since high energy loss impacts contribute relatively little to this probability. Now the nonrelativistic formula may always be written[3]

$$\sigma_{\text{ion}} = k_1(2\pi e^4/mv^2) \ln (mv^2/k_2 I). \tag{2.33}$$

By (1) this becomes

$$k_1(2\pi e^4/mc^2 I) \ln (mc^2/k_2 I), \tag{2.34}$$

and (2) may be taken into account in the following way. For the range $0 \leqq \gamma \leqq \eta'$, γ/b is small, and we may write

$$\int d\boldsymbol{r} \tilde{u}_{nl} e^{-i\gamma x} u_0 \sim -i\gamma x_{nl,0},\ x_{nl,0} = \int \tilde{u}_{nl} x u_0 d\boldsymbol{r}.$$

Thus the term to be added to the nonrelativistic cross section is

$$\frac{16\pi^3 e^4}{h^2 c^2} \int_0^\infty dE \sum_l |\, x_{El,0}\,|^2 \ln \frac{\eta'^2}{\eta^2}. \tag{2.35}$$

But the nonrelativistic cross section (2.34) itself may with $v = c$ be written

$$\frac{16\pi^3 e^4}{h^2 c^2} \int_0^\infty dE \sum_l |\, x_{El,0}\,|^2 \cdot \ln \frac{mc^2}{k^2 I}$$

i.e., $k_1 = (8\pi^2 mI/h^2) \cdot \int_0^\infty dE \sum_l |x_{El0}|^2$. Thus our result is

$$\sigma_{\text{ion}} = k_1(2\pi e^4/mc^2 I) \ln mc^2\epsilon^2/k_2 I. \tag{2.36}$$

This shows that the number of ions produced by a fast electron increases as its velocity approaches that of light. The ionizing power passes through a minimum for $\epsilon \sim 3$; the increase is very slow; if we use the value of k_2 given by (2.31) for a hydrogen-like atom; and if for air we take I to be about fifty volts, then the number of ions is double the minimum value for electrons of $\epsilon \sim 10^3$, or energy of the order of 10^9 volts.

To compute the mean energy loss, and thus the range, of the fast electron, we might again use the hydrogen-like atomic model, and supplement (2.28) with the corresponding expression for the probability of excitation. But here, too, it is simpler to compare our expression (2.25) with the corresponding non-relativistic one. It is simpler still to use the sum theorem of Bethe[3]

$$(8\pi^2 m/h^2\gamma^2) \sum_{nl} (E_n - E_0) \left| \int d\mathbf{r} \tilde{u}_{nl} e^{-i\gamma z} u_0 \right|^2 = 1 \tag{2.37}$$

directly. If we apply this directly, we get for the mean energy loss

$$\delta E' = \frac{2\pi e^4}{mc^2} \int_0 \frac{d\gamma^2}{\gamma^2 + \tilde{\eta}^2} \tag{2.38}$$

where $\tilde{\eta} = (2\pi/hc\epsilon) W$, and $W = k_3 I$ is an appropriately chosen mean value of the energy transferred per impact; and where the integration over γ is to be taken up to the maximum value permitted by the conservation laws. We have here, however, to consider that the method used in the derivation of(2.25) is not applicable for large energy losses and large values of γ, since it leads to (1.40a) in place of the correct (1.40). It is easy to correct for this, because of the fact that when

$$E' \gg I \tag{2.39}$$

we may use the calculations of §I for free electrons. Since when (2.39) is satisfied the conservation laws are fulfilled, we know that in the range $I \ll E' \ll mc^2$ we may set

$$E' = h^2\gamma^2/8\pi^2 m. \tag{2.40}$$

Thus if we integrate (2.38) up to a γ value corresponding to an energy loss $\overline{E}$:

$$I \ll \overline{E} \ll mc^2; \ \bar{\gamma}^2 = 8\pi^2 m\overline{E}/h^2 \tag{2.41}$$

we get

$$\delta E' = (2\pi e^4/mc^2) \ln 8\pi^2 m\overline{E}/h^2\bar{\eta}^2. \tag{2.42}$$

And we may add to this the mean energy loss given by (1.40) for impacts involving an energy transfer $E' \geqq \overline{E} \gg I$. This gives for large ϵ

$$\delta E'' = \int_{\overline{E}}^{E_m} E' dE' \frac{E^4 + (E - E')^4 + E'^4}{2E^2(E - E')^2 E'^2} \sim \frac{2\pi e^4}{mc^2} \left[\ln \frac{mc^2}{\overline{E}} + \ln \epsilon + 9/8 - 2\ln 2 \right] \tag{2.43}$$

Thus for the total energy loss

$$\delta E = \delta E' + \delta E''$$
$$= \frac{2\pi e^4}{mc^2}\left[2 \ln \frac{mc^2}{W} + 3 \ln \epsilon + 0.43\right] \tag{2.44}$$

which is our result for the mean energy loss.

The direct calculation with the model of a hydrogen-like atom gives (2.44) with the constant

$$k_3 = 1\big| \cdot \big|1; W = 1.1I. \tag{2.45}$$

This result gives just *half* the energy loss we should expect from Bohr's classical formula;[2] it gives twice the range. When ϵ is large we get for the range R of the particle in a gas containing N electrons per cc

$$R^{-1} = (4\pi e^4 N/m^2c^4\epsilon)[\ln mc^2/W + (3/2) \ln \epsilon] \tag{2.46}$$

where now W is a properly taken average energy of the order of the mean ionization potential. As ϵ grows large compared with mc^2/W this approaches

$$R^{-1} \rightarrow (6\pi e^4 N)/(m^2c^4) \ln \epsilon/\epsilon. \tag{2.47}$$

Note: We get an upper limit for the range if we set

$$\partial E'' = 0,$$

since this means that no large energy losses occur, and since we know that the neglects of our theory (radiative forces) can have no sensible effect upon the small energy losses. With $\delta E^{11} = 0$ we get asymptotically

$$R^{-1} \rightarrow 4\pi e^4 N/m^2c^4 \ln \epsilon/\epsilon,$$

which is four times the distance traveled according to the Klein-Nishina formula, by a gamma-ray before its first Compton encounter. This range (2.47) is just one-sixth the distance which (according to the Klein-Nishina formula) a quantum of energy (ϵmc^2) travels, on the average, before its first Compton encounter. Thus even for the greatest energies a gamma-ray is, according to theoretical results at present available, more penetrating than an electron of the same energy. It should be remarked that in the application of these formulae nuclear electrons may not, presumably, be neglected; they should be included in counting the total number (N) of electrons per cc. But unless ϵ is very large, the contribution of these electrons to the stopping power will be smaller than that of the extranuclear electrons, since the binding energy of the former must be of the order of a few million volts. It seems at present impossible to extend our calculations to the case of electrons bound in nuclei, because of our ignorance of the nature of that binding. But insofar as wave mechanics is applicable to such particles, (2.46) should give a reliable estimate of their effect on a fast electron.

III. Impacts of the Magnetic Neutron

We want now to study in a little more detail the expression which we have derived for the impact of a magnetic neutron with a free electron. The cross section for such encounters is given in (1.67) and the somewhat complicated quantities occurring in this expression are given in (1.69). We shall consider first and chiefly the case that the neutron has a velocity small compared with that of light; in this case it will be unable to give the electron a very high velocity, and we may greatly simplify (1.67) by neglecting higher powers of v/c for both particles. The complicated summation of the square of the numerators of (1.67) then reduces to

$$N = 2\left| T_{++}^{4} \right|^2 + 2\left| T_{+-}^{4} \right|^2 \tag{3.1}$$

and we find from (1.72)

$$N = (1/2M^2c^3)\{p'^4 + p'^2(4r^2 - 8r\Delta r + 2(\Delta r)^2] + (\Delta r)^4\}. \tag{3.2}$$

Further the denomination of (1.67) becomes

$$\left| \boldsymbol{p}^{(i)} - \boldsymbol{p}^{(1)} \right|^2 = (\Delta r)^2 + p'^2. \tag{3.3}$$

If we introduce for the ratio of the mass m of the secondary to that of the neutron

$$\lambda = m/M \tag{3.4}$$

and the further abbreviations

$$\alpha = \cos\vartheta, \beta = \sin\vartheta, g = [\alpha + (\lambda^2 - \beta^2)^{1/2}]/(1 + \lambda), \tag{3.5}$$

we find

$$\sigma d\alpha = \frac{2\pi^3 e^2\mu^2}{h^2c^2} g d\alpha \frac{\{g^4\beta^4 + g^2\beta^2[4 - 8(1 - g\alpha) + 2(1 - g\alpha)^2] + (1 - g\alpha)^4\}}{(1 - 2g\alpha + g^2)^2}. \tag{3.6}$$

The energy transferred is

$$E' = (E/\lambda)(1 - 2g\alpha + g^2). \tag{3.7}$$

Several points are at once clear. Since for $\alpha \to 1$, $g \to 1$ the cross section behaves for small angles like

$$\sigma d\alpha \sim d\alpha/(1 - \alpha) \sim d\beta^2/\beta^2 \tag{3.8}$$

whereas in the case of the Coulomb field it behaved like

$$d\alpha/(1\alpha)^2 \sim d\beta^2/\beta^4. \tag{3.9}$$

The mean energy transferred may be computed without considering the binding of the secondary, since $\delta E = \int \sigma E' d\alpha$ converges. Further, the cross section is independent of the velocity or energy of the neutron, and the mean energy loss is directly proportional to the initial energy; finally the cross section is proportional to the square of the magnetic moment of the neutron.

We shall reduce (3.6) for the case that the neutron has a mass equal to that of the secondary, $\lambda = 1$, or much smaller, $\lambda \gg 1$ or much larger $\lambda \ll 1$.

$\lambda = 1$. Here $g = \alpha$,

$$\sigma d\alpha = \frac{2\pi^3 e^2 \mu^2 \alpha}{h^2 c^2 \beta^4} \{\alpha^4\beta^4 + 2\alpha^2\beta^2(2 - 4\beta^2 - \beta^4) + \beta^8\}. \tag{3.10}$$

The quadrature over the angle of deflection gives for the energy loss

$$\delta E = \int \sigma E' d\alpha = (7/96)\sigma_0 E \tag{3.11}$$

where $\sigma_0 = 16\pi^3 e^2 \mu^2 / h^2 c^2$. This cross section σ_0 may be written

$$\sigma_0 = \pi c^4 n^2 / m^2 c^4, \text{ with } n = \mu/\mu_B;\ \mu = eh/4\pi mc \cdot n \tag{3.12}$$

where n is the magnetic moment of the neutron measured in Bohr magnetons. This quantity n is presumably quite small, so that σ_0 is very small indeed. The expression for the total number of impacts

$$\sigma = \int \sigma d\alpha \tag{3.13}$$

does not converge in the small angles. The preponderance of small energy losses is not nearly so marked here as for the impacts of an electron; and it is easy to show, by repeating the familiar nonrelativistic calculations for the impact of a particle with a bound electron, that the total number of impacts in which an energy of the order of a few times the binding energy or less in transferred is finite and independent of the primary energy and corresponds to a cross section of the order of σ_0. The total cross section thus turns out to be

$$\sigma = \int \sigma d\alpha \sim \sigma_0 \{\tfrac{1}{4} \ln (E/W) - 7/16\} \tag{3.14}$$

where W is of the order of the ionizing energy. The mean energy transferred per impact is thus

$$\delta E/\sigma \sim (E/24) \ln E/W. \tag{3.15}$$

Such a magnetic neutron, quite apart from the great infrequency of its impacts, a factor $In^2/4mc^2$ smaller cross section than an electron—will never produce ion tracks in a cloud chamber, since it tends to lose an appreciable fraction of its energy, and suffer an appreciable deflection at every impact.

$\lambda \gg 1$. For this case we find

$$\sigma \sim (\sigma_0/4) \ln 2E/\lambda W \tag{3.16}$$

$$\delta E = (19/96)\sigma_0 E/\lambda \tag{3.17}$$

and for $\lambda \ll 1$:

$$\sigma = (\sigma_0/4) \ln E\lambda/W \tag{3.18}$$

$$\delta E = \sigma_0 E\lambda/8. \tag{3.19}$$

In both these cases impacts are relatively rare; in both, the mean energy loss is necessarily smaller than for equal masses; only for a heavy neutron are impacts without large deflection possible. If such a neutron as this had a large magnetic moment, large compared to the Bohr magneton, it could produce recognizable cloud chamber tracks; but values of n large enough to give this seem *a priori* extremely improbable.

The formulae we have given apply equally—especially to the impacts of a magnetic neutron with a proton or nucleus. They do not account very well for the phenomena observed in the penetrating radiation from Be bombarded with alpha-particles. In the first place, such a magnetic neutron would have more impacts with highly charged nuclei than with protons, whereas the observations show that this is not so; in the second place the number of impacts would depend so little on the energy of the neutron, so that it would be hard to account for the observed inhomogeneous absorption of the radiation. Finally the distance between impacts would be enormous; with $n=10^{-3}$ and $\lambda=1$, a neutron of 5.10^6 volts would travel $\sim$100 km before ejecting a visible proton from paraffin.

One might suppose that in the general case of velocities not small compared to that of light, different and more satisfactory results might be obtained. We have investigated this case only for $\lambda=1$, in which case the conservation laws give simple algebraic relations between angle of deflection and final momenta and energy. For this case the total cross section increases with ϵ, where again $E=\epsilon Mc^2$ is the initial energy of the neutron, and is of the order.

$$\sigma_0\epsilon^2. \tag{3.20}$$

In this case $\epsilon\gg1$, the preponderance of small deflections and relatively small energy losses is still less marked than in the case of low velocity magnetic neutrons. When

$$\epsilon > \ln E/W$$

the electron tends to lose a large part of its energy in each encounter it makes. Such a neutron could not produce cloud chamber tracks; and since it is certain on energetic grounds that the radiation from beryllium does not consist of such neutrons, we have not thought it desirable to give further details in the evaluation of (1.67).

We believe that these computations show that there is no experimental evidence for the existence of a particle like the magnetic neutron.

Photoelectric and Thermionic Emission from Composite Surfaces

By WAYNE B. NOTTINGHAM*
Massachusetts Institute of Technology

(Received August 6, 1932)

Classical methods when applied to photoelectric and thermionic emission from composite surfaces often lead to inconsistent results. A study of the thermionic emission, with a new thyratron circuit for heating tungsten and thoriated tungsten filaments, reveals that many points can be explained if we take into consideration the complex form of the potential barrier produced by an atom layer of electropositive metal when deposited on an "electronegative" base. From an experimental knowledge of the transmission coefficient of the barrier as a function of electron energy and the use of the Wentzel approximation for the transmission coefficient $D(v)=\exp-(4\pi/h)\int_{x_1}^{x_2}(2mH)^{1/2}dx$), it is possible to calculate the shape of the barrier which turns out to be practically parabolic and about 4.3×10^{-8} cm in width one electron-volt below the top of the hill. Since the width and perhaps the height of the barrier seem to depend upon the temperature, it becomes clear that the Richardson-Dushman equation $I=AT^2\exp(-b_0/T)$ is applicable only as an empirical representation of the data obtained with composite surfaces as emitters. This surface model explains very naturally the fact that the electrons emitted from a composite have an apparently Maxwellian distribution of velocities corresponding to a temperature fifty percent higher than that of the filament as reported by Koller and Rothe. It also gives a qualitative explanation of the observed dependence of the photoelectric long wavelength limit on the applied potential for thin films of sodium on nickel using very low fields.

INTRODUCTION

A COMPOSITE surface may be formed by depositing a thin layer of "electropositive" metal on a more "electronegative" one. Many investigators have found such surfaces to be more active thermionic and photoelectric emitters of electrons than either of the metallic constituents when taken in bulk. The thermionic current from a composite surface has been observed to depend on the temperature according to the Richardson equation $I=AT^2\exp(-e\phi_0/kT)$ but differences between values of the work function ϕ_0 for different surfaces are not in satisfactory agreement with measurements of the contact difference in potential.[1]

The thermionic current varies with the accelerating field according to the Schottky mirror image theory[2] only for high fields.[3] At low fields the current falls much more rapidly than might be expected. Electrons emitted from a

* Fellow at the Bartol Research Foundation, Swarthmore, Pennsylvania, while carrying on the experimental work reported in this paper.

[1] I. Langmuir and K. H. Kingdon, Phys. Rev. **34**, 129 (1929).

[2] K. T. Compton and I. Langmuir, Rev. Mod. Phys. **2**, 123 (1930). See part B (5) for complete discussion.

[3] J. Becker and D. Mueller, Phys. Rev. **31**, 431 (1928); N. B. Reynolds, Phys. Rev. **35**, 158 (1930).

clean tungsten surface have been found to have a Maxwellian distribution of velocities[4] with a temperature equal to that of the filament but according to the results of Koller[5] and Rothe,[6] the apparent temperature of the electrons emitted from a composite surface is at least fifty percent higher than that of the emitting surface.

The above difficulties serve to illustrate the nature of some of the broader aspects of the problem at hand. We see that the observed results follow more or less according to the theories which have been well able to describe the thermionic emission from clean surfaces, but in almost every case there is a definite difference between observation and theory which is much larger than the experimental error. It is the object of the first part of this paper to describe as concisely as possible a series of experiments on the thermionic emission from thoriated filaments and the photoelectric emission from films of sodium deposited on nickel. In the latter part of this paper an attempt will be made to coordinate these new, and many of the old, results into a theory.

The experimental work upon which this paper depends was carried on at the Bartol Research Foundation with the liberal support of the Franklin Institute of Philadelphia between January, 1929, and August, 1931.

The Experimental Problem

From his studies of *photoelectric emission*, Dr. Ives[7] reported that as a thin film of sodium is deposited on a platinum surface, "the long wave limit of the emission first moves toward the red as the film increases in thickness and then, after the maximum of the photoelectric sensitiveness is passed, moves back toward the violet." Later, Ives and Olpin[8] reported that in the cases of lithium, sodium, potassium, rubidium and caesium this maximum "excursion" of the long wave limit was "found to coincide with the first line of the principal series, i.e., the resonance potential." Stimulated by these researches an attempt was made to investigate the energy distribution of the emitted electrons and test the linearity of photoelectric response of these surfaces to light of a wave-length very near that of the threshold. What was thought to be a nonlinearity in the response[9] and reported as such was later found[10] to be due to a nonlinearity in the amplifier system used to measure the extremely small currents. These studies also yielded results which were interpreted as a departure from Einstein's photoelectric equation.[11] The experimental data, which are now being published in detail for the first time, can apparently be explained on the wave-mechanical theory of electron transmission through a potential barrier.

[4] L. H. Germer, Phys. Rev. **25,** 795 (1925).
[5] L. R. Koller, Phys. Rev. **25,** 671 (1925).
[6] H. Rothe, Zeits. f. Physik **37,** 414 (1926).
[7] H. E. Ives, Astrophys. J. **60,** 209 (1924).
[8] Ives and Olpin, Phys. Rev. **33,** 281 (1929); **34,** 117 (1929).
[9] W. B. Nottingham, Phys. Rev. **33,** 633 (1929).
[10] W. B. Nottingham, Phys. Rev. **35,** 669 (1930).
[11] W. B. Nottingham, Phys. Rev. **33,** 1081 (1929).

In the field of *thermionic emission*, Reynolds[12] reported work which might be considered as an extension of that of Becker and Mueller[13] on the variation of the thermionic emission from a thoriated tungsten filament as a function of the electric field. The fact that the results reported by Reynolds could be interpreted qualitatively with the same "surface models" as those used in the interpretation of the photoelectric[14] emission data made it clear that a thorough investigation of the problem of the thermionic emission from a thoriated tungsten wire using small retarding and accelerating potentials on the collector, might greatly extend our understanding of the general problem of composite surface emitters. Two important difficulties of the experiment not satisfactorily disposed of by Reynolds were (1) the lack of uniformity of potential difference between the filament and the collector due to the filament heating current and (2) the adequate insulation of the collector. Preliminary work done by the author before these difficulties were overcome verified the general experimental results of Reynolds, but suggested new explanations.

With the help of wave mechanics, it is now possible to explain many of the observed facts of electron emission from composite surfaces by considering the transmission *through* the potential barrier produced by an atom layer of an electropositive element when deposited on a more electronegative base. These points will be discussed in detail later in this paper. Since practically all of the experimental work being reported in this paper was done before an application of the present theory[15] was made, it will not be difficult to discover points in the argument which can be disposed of by additional experiments. Although there are a number of such investigations under way already, it has been thought worth while to report in detail on the results obtained to date, partly to help other workers in the field and partly to invite criticism of the experiments and theories presented here.

Electric Circuits

a. Filament heating circuit

In order to heat the filament and yet have no drop in potential over it during measurement an intermittent heating system like that used so successfully by Germer[16] was employed. Instead of using a 500 cycle generator and tungar rectifiers as done by Germer, a thyratron "inverter" circuit was developed at the suggestion of Dr. A. W. Hull and patterned essentially after his circuit.[17] This is shown in Fig. 1.

With thyratron T_1 conducting 0.25 ampere the plate P_1 is only about 12 volts positive with respect to the filament and there is a difference in potential of 250 volts across the condenser C. When the oscillator voltage carries

[12] N. B. Reynolds, Phys. Rev. **35,** 158 (1930).
[13] J. Becker and D. Mueller, Phys. Rev. **31,** 431 (1928).
[14] W. B. Nottingham, Phys. Rev. **35,** 669 (1930).
[15] W. B. Nottingham, Phys. Rev. **38,** 1918 (1931).
[16] L. H. Germer, Phys. Rev. **25,** 795 (1925).
[17] A. W. Hull, Gen. Elec. Rev. **32,** 390 (1929).

the grid G_2 of thyratron T_2 *positive*, this tube suddenly becomes conducting and the quick drop of potential at P_2 causes that of P_1 to become very negative with respect to F_1. If the de-ionization time is shorter than the time required for the condenser C to charge up through the 1000 ohm resistance, then thyratron T_1 will remain nonconducting until the next half cycle of the oscillator at which time G_1 is made positive and the cycle of operation as described above is repeated. It is easy to see that the wave form of the current through T_1 will be qualitatively that of Fig. 2.

The part of the cycle during which the filament is heated is shown cross-hatched. The sharp peaks showing reverse current for an extremely short

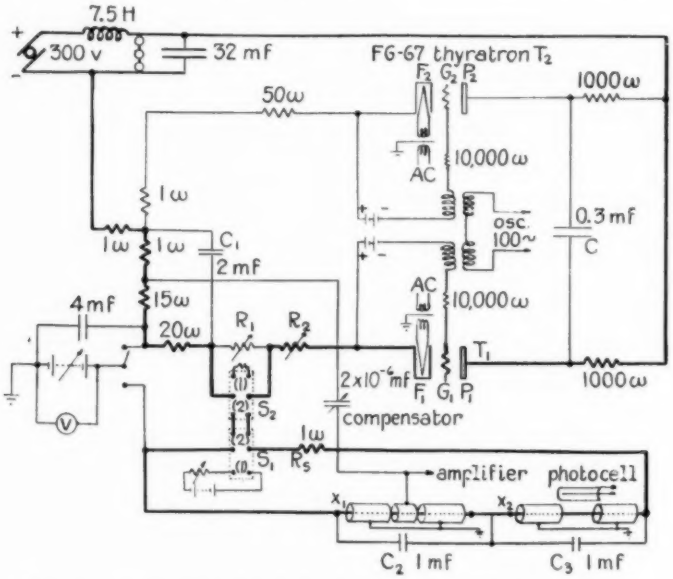

Fig. 1. Thyratron[18] inverter circuit for heating filament with pulsating current.

time were assumed to be there on indirect evidence only. The condensers C_1, C_2 and C_3 were introduced to eliminate the effect due to this reverse current. Now that a cathode-ray oscillograph which can follow such rapid

[18] Since the thyratron has not yet come into common use in physical research, it will perhaps be desirable to describe very briefly its operating characteristics.

The thyratron is a gas filled (mercury vapor) three-electrode tube containing a cathode, anode and grid. With positive potentials of a few hundred volts on the plate, a few volts negative grid potential prevents the electron current flow from cathode to anode. At a certain critical value of grid bias enough current flows, however, to start ionization in the gas. Within a few microseconds an arc is fully developed with the current limited only by the external circuit under normal conditions. After the formation of the arc the grid has no control over the flow of current. Thus in a circuit with a d.c. plate supply, provision must be made for stopping the flow of current through the thyratron after it has once been started by effectively cutting off the plate supply. It is for this reason that we have the plates of the two thyratrons of Fig. 1 connected together by the 0.3 mf condenser.

For detailed discussion see: A. W. Hull, reference 17; W. B. Nottingham, J. Frank. Inst. **211,** 271 (1931); W. B. Nottingham, J. Frank. Inst. **211,** 751 (1931).

changes in potential is available, the exact nature of this objectionable reverse peak is to be investigated.

The power was supplied by a 300 volt d. c. generator driven by a three-quarter hp, three phase synchronous motor. With the generator brushes in good condition the output voltage was steady to within about 0.1 percent for a considerable period of time.

An inductance and condenser were used as shown to eliminate the commutator ripple.

b. Adjustment of filament temperature

The Langmuir and Jones[19] temperature scale for pure tungsten was used. Approximate values of the temperature were calculated from measurements of the current flowing and the diameter of the filament. With this approximate temperature, the end loss correction was calculated[20] and the final temperature was determined from the Langmuir-Jones table for $V'(A')^{1/3}$ which involves measurement of the filament length, voltage drop, and current.

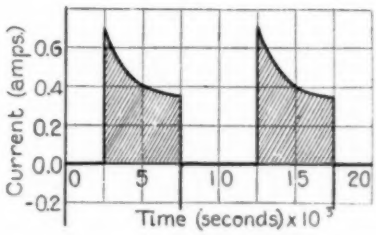

Fig. 2. Wave form of current through thyratron T_1.

The current was determined by measuring the drop in potential over a standardized one ohm resistance R_s using a Leeds and Northrup type K potentiometer. The voltage drop over the filament was accurately measured using a type K potentiometer with ten times the usual current flowing through the coils and slide wire. With this method, it was possible to measure accurately d.c. voltages as high as 16.1 volts. By throwing the switch S_1 to position (1) the filament under test X_1 and the auxiliary filament X_2 were heated by d.c. These two filaments were of approximately equal length and from the same stock. Under this condition the temperature of the test filament could be determined and the light emitted from the auxiliary filament accurately measured by a null method. With switches S_1 and S_2 both in position (2) filaments X_1 and X_2 could be heated with pulsating current. By adjusting R_1 and R_2 the temperature of X_2 was brought very accurately to that previously determined by observing the photoelectric current produced by the light emitted from X_2. It was then assumed that the temperature of the test filament was the same as that determined from the d.c. measurements. The frequency of the pulsating current was varied from 100 to 500 cycles per second with no change in the thermionic current observed. Prac-

[19] I. Langmuir and H. A. Jones, Gen. Elec. Rev. **30**, 310, 354, 408 (1927).
[20] Langmuir, McLane and Blodgett, Phys. Rev. **35**, 478 (1930).

tically all measurements were therefore carried out with the oscillator set to deliver 100 cycles.

c. Amplifier circuit for photoelectric current

The photoelectric current produced by the light from the auxiliary filament X_2 was measured with the circuit shown in Fig. 3.

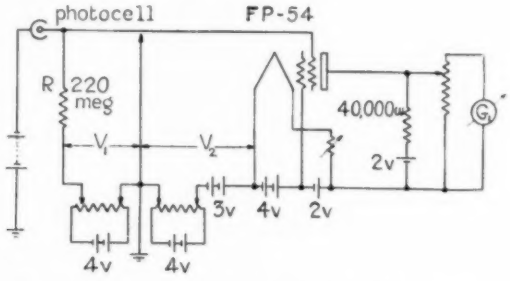

Fig. 3. Amplifier circuit for photoelectric current.

The underlying theory of the operation of this type of circuit has been discussed elsewhere.[21] The low voltage batteries used were 150 amp.-hr. storage batteries and were carefully maintained. Under these conditions the single tube amplifier circuit has been found to be more steady than the two tube circuit and much easier to maintain. With no light on the photoelectric cell and V_1 zero, potential V_2 was adjusted to make the current through the galvanometer G_1 zero.

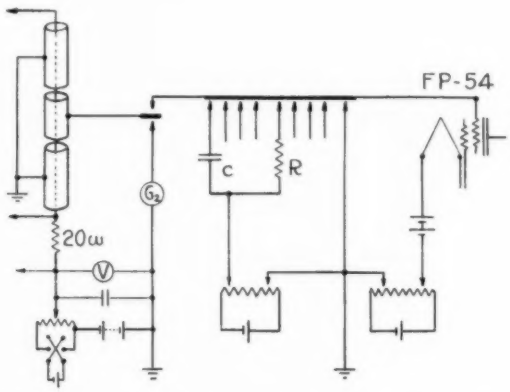

Fig. 4. Grid circuit of vacuum tube amplifier used to measure thermionic current.

When the filaments X_1 and X_2 were heated by direct current, the light from the auxiliary filament X_2 falling on the cell caused a current to flow through R. The potential V_1 was then adjusted to bring the galvanometer to zero. The pulsating current was adjusted to maintain the light emitted from X_2 constant as indicated by the galvanometer.

[21] W. B. Nottingham, J. Frank. Inst. **209**, 287 (1930); L. A. DuBridge, Phys. Rev. **37**, 392 (1931).

d. Amplifier circuit for thermionic current

The circuit for measuring the thermionic current was very similar to that of Fig. 3, except that a 2500-b type R galvanometer was used in place of a 2500-e instrument. Instead of a standard FP-54 vacuum tube, an early model of the same general design having a higher mutual conductance was used with a resulting maximum sensitivity of about 10.5 cm per millivolt applied to the grid. Certain special features incorporated in the grid circuit are shown in Fig. 4.

Condensers or resistances were used in the grid circuit to give a means of varying the sensitivity. The capacities of a specially selected set of fixed condensers ranged from 0.002 mf to 8.0 mf and the values of resistance ranged from 5000 megohms to zero. With the capacities it was possible to use the rate of deflection method of measurement for the current range of 10^{-13} to 5×10^{-8} amp after which the galvanometer G_2 could be used directly.

Experimental Tubes

a. Construction and preparation

The filaments, kindly furnished by the Research Laboratory of the General Electric Company, were of types known as "T," "E," and "C" wire. "T" and "E" were thoriated tungsten, the latter being free from carbon and the "C" wire was pure tungsten. The wire diameter was approximately 1.6 mils and the length of the filaments were about 10.8 cm. The collector was 1 cm in diameter and about 2.5 cm long. Cylinders of the same diameter and about 4 cm long were used to make the field uniform near the ends of the collector and also receive the emission from the cool ends of the filament.

The collector was supported on long "beads" held by "sealed-in" tungsten connections maintained at the collector potential. A special lead was brought out for the collector to give high insulation from the other leads coming through the press. All the metal parts were made of "baked out" nickel or tungsten. A rather elaborate outgassing schedule was carried out with oven baking at temperatures up to 400°C and heating of the collectors with the induction furnace as well as extensive heating of the filament.

b. Activation of the filament

Langmuir and Rogers[22] found that tungsten wire containing about one percent of thorium oxide could be made, by a proper heat treatment, a much more efficient emitter of electrons than pure tungsten at filament temperatures of less than 2000°K. The details of this process are given in full by Langmuir[23] and also by Dushman.[24] At a filament temperature of 2700°K to 2900°K some of the thorium oxide decomposes leaving a small amount of thorium between the tungsten crystals and near enough to the surface so that the thorium can diffuse, at the activation temperature, to the surface and form a layer of thorium atoms. The filament temperature must be 1800°K

[22] I. Langmuir and W. Rogers, Phys. Rev. **4**, 544 (1914).
[23] I. Langmuir, Phys. Rev. **22**, 357 (1923).
[24] S. Dushman, Rev. Mod. Phys. **2**, 381 (1930).

or greater for this "activation" to take place at a reasonably rapid rate. After a long time of activation the equilibrium surface condition is governed by the rate of diffusion and the rate of evaporation.

Fig. 5 shows a typical set of curves[25] representing the first activation carried out in steps at $T_a = 1920°K$.

The accumulated time is plotted along the abscissa while the thermionic current observed at a test temperature of $T_t = 1230°K$ and a collector potential of +20.0 volts is plotted as the ordinate. The maximum found after 90 minutes' acitvation is undoubtedly related to the maxima found by Becker[26] in his studies of the thermionic emission from a caesium covered tungsten filament. In Becker's work the surface coverage corresponding to the maximum emission was thought to correspond to a monatomic layer of caesium

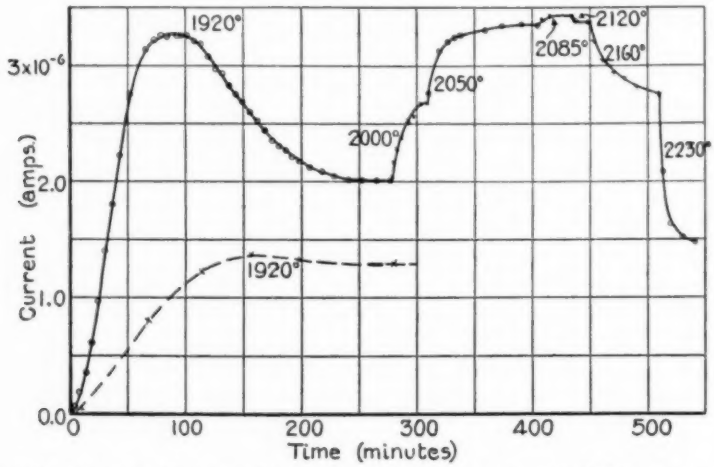

Fig. 5. Activation of a thoriated filament with test temperature 1230°K (T wire). Solid curves applied accelerating potential 20 volts; dashed curve potential 2.0 volts.

atoms on the tungsten and by analogy it is thought that the maximum in Fig. 5 corresponds to a monatomic layer of thorium atoms on tungsten. With $T_a = 1920°K$ the equilibrium condition was practically reached after 280 minutes of activation. By raising the activation temperature to 2000°K this equilibrium was disturbed immediately and a sharp *rise* in the curve was observed. At about 2100°K the *equilibrium* condition corresponds very closely to that of the maximum observed at 90 minutes. Activation at still higher temperatures, leaves the surface only partly covered. At low fields the maximum practically disappears. The significance of this observation will be discussed later.

The main features of the activation curve shown in Fig. 5 are thus easily understood. There are, however, many details concerning the activation process which may be of importance in the explanation of results obtained with more complicated composite surfaces. For example, after a filament has been

[25] W. B. Nottingham, Phys. Rev. **35**, 1128 (1930).
[26] J. A. Becker, Phys. Rev. **28**, 341 (1926).

fully activated, the emission has been observed to *increase* two to six fold in the cource of time even though the filament is maintained at liquid air temperature between observations. This effect is undoubtedly brought about by the adsorption of some gas. A detailed examination of this effect is being undertaken.

Measurement of Thermionic Current

a. Velocity distributions

The experimental difficulties associated with the measurement of the thermionic emission from composite surfaces have long been recognized. For example, work function measurements involving a change in temperature of

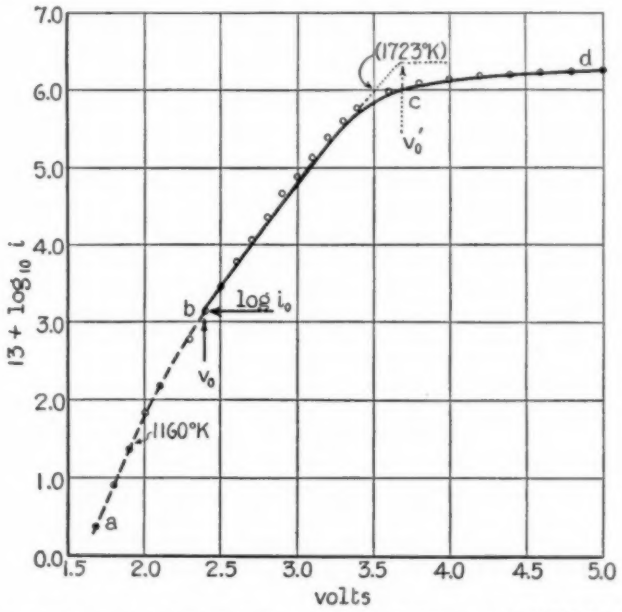

Fig. 6. Thermionic current from a fully activated filament at 1160°K (pulsating filament current used). Range *ab* calculated by Schottky equation. Range *bcd* identical to that observed with tungsten filament at 1723°K.

the emitter are often invalidated because the surface conditions may change with the temperature. Some of these changes are slow enough to be observed; others may be rapid and escape observation. Surface conditions also change with an alteration in the current drawn from the filament and may thus be subject to variation with applied field and temperature. Changes at the surface of the collector as indicated by a shift in contact potential have also been observed.[27] In order to minimize these difficulties a definite procedure of measurement was adopted. Before beginning a set of measurements, maxima of accelerating potential (usually less than 10 volts) and temperature (about 1200°K) were decided upon. During the run these standard conditions were maintained except during the time required for each reading, i.e., after

[27] W. B. Nottingham, Phys. Rev. **39**, 183 (1932).

making a reading standard conditions were reproduced before taking the next. In Fig. 6 a typical curve is given showing the thermionic current received by the collector as a function of the applied potential difference between the collector and the filament.

The points enclosed in circles are the observed points. The curves drawn through the points are of theoretical significance. The dashed curve from *a* to *b* is the theoretical curve, computed from the classical equation developed by Schottky,[28] for the current received against a retarding potential by a cylindrical collector from a filament of small diameter supported along the axis of the cylinder, with the distribution of velocities assumed to be Maxwellian and the temperature that of the filament. Over the part of the range covered, there is a very close agreement between the observed points and the theoretical curve.

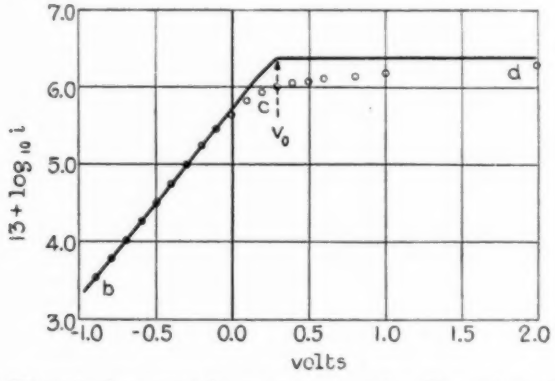

Fig. 7. Thermionic current from a pure tungsten filament at 1723°K. (Pulsating filament current used.)

There is, however, no sign of saturation at the point *b* as one would expect from classical theory and on the basis of Germer's experience with pure tungsten filaments. It is only natural to suggest that the observed results are distorted by space charge effects which would invalidate a calculation using the Schottky theory. In order to test this point measurements were made on a filament of "*E*" wire in the *completely deactivated* state and also on a pure tungsten "*C*" wire. These filaments were heated to such a temperature that the saturation current was exactly equal to that observed on the activated filament with about 6 volts applied potential. The results of one of these tests are shown in Fig. 7.

In the case of the clean tungsten filament, the Schottky curve and the observed points agree almost perfectly up to within about 0.2 volt of the theoretical saturation point. At lower temperatures the agreement is even closer. These results are in very close agreement with those of Germer which showed that space charge effects could be neglected in the case of pure tungsten filaments up to about 1830°K. Since space charge phenomena are controlled

[28] Walter Schottky, Ann. d. Physik **44**, 1011 (1914). Germer's table in Phys. Rev. **25**, 795 (1925) was used for all of these computations.

primarily by the current density and the electric field near the surface of the filament, the fact that the space charge can be neglected in the case of the pure tungsten indicates that it can also be neglected in the case of an activated thoriated filament for temperatures less than 1200°K.

A comparison was made between the observed curves for clean tungsten at 1723°K and thoriated tungsten at 1160°K and it was found that the curves were almost identical over the range *b c d* of Figs 6 and 7. The range *bc* in the case of pure tungsten indicates that the velocity distribution of the electrons is Maxwellian with a temperature of 1723°K. *But the similar range bc for the thoriated filament is also characteristic of* 1723°K, *although the temperature of the filament was only* 1160°K. This is a fundamentally important result, and it will be shown that the new theories of transmission through potential barriers can give just this result, i.e., given a potential barrier of the required dimensions, the distribution of electron velocities of those electrons which are transmitted through the barrier can be described as Maxwellian with a temperature 45 to 50 percent *higher* than that of the filament.

Measurements of the velocity distribution of the electrons from thoriated filaments operated at 987°K, 1045°K and 1103°K showed the same agreement between observed points and the Schottky curve for the range of applied potential negative to that designated as "v_0," while over the range of potential positive to "v_0" the distribution was quite accurately the same as that of a pure tungsten filament operated at temperature high enough to give the same saturation current at about 6 volts applied potential. With the filament in a particular state of activation all of the values of "v_0" for the various temperatures were the same within about ± 0.1 volt and the ratio of these temperatures was extraordinarily constant, as indicated by Table I.

TABLE I.

Thoriated fil. temp.	Case 1		Case 2	
	Tungsten	Ratio	Tungsten	Ratio
987	1458	1.48	1490	1.51
1045	1540	1.47	1570	1.50
1103	1620	1.47	1650	1.50
1160	1685	1.45	1723	1.48

It will be noticed that these results check well with the estimations made by Koller[5] and Rothe[6] that the electron temperature as indicated by the apparent velocity distribution is 50 percent higher than that of the filament, although their work applied to the oxide-coated filament. The theory to be proposed here would presumably be approximately applicable also to this more complicated type of surface.

These experiments have therefore suggested the existence of two groups of emitted electrons, the one with higher speeds classically characteristic of the filament temperature and the other (comprising nearly 99.9 percent of the saturation emission) being apparently characteristic of a 50 percent higher temperature. The discovery of the former group is due to the experimental extension of the velocity distribution curve through a larger range of

values than is usually done. The latter group, which has heretofore been treated classically is, on the present theory, a group which could not escape classically but is allowed to escape by wave mechanics according to a probability factor which depends jointly on the "potential barrier" created by the adsorbed electropositive layer and on the applied potential.

b. Work-function measurements

Really accurate determinations of the thermionic constants ϕ_0 and A of the Richardson equation $I = A\ T^2 \exp -e\phi_0/kT$, are exceptionally difficult when the range of permissible temperature variation is small. Data which were obtained show definitely that both of the constants depend very decidedly on the exact state of the surface. No two activation and filament aging curves have been observed which are exactly alike and therefore no two values of ϕ_0 and A are the same although attempts have been made to control activation conditions accurately. Studies now under way will no doubt throw new light on this question.

With an applied accelerating potential of 6.0 volts, the observed values of ϕ_0 ranged from 2.38 to 2.83 electron-volts while the value of A ranged from 0.56 to 10.2 amp. per cm^2 per deg.^{2}.

One of the best determinations gave $\phi_0 = 2.64$ and $A = 3.2$ which compare very satisfactorily with those of Dushman and Ewald[29] of $\phi_0 = 2.63$ and $A = 3.0$. Measurements with applied potentials of 2.0 and 2.4 volts, corresponding to values of v_0 as defined above for various conditions of activation, gave ϕ_0 between 3.1 and 3.5 electron-volts and A between 10 and 60 amp. per cm^2 per deg.^{2}.

The results reported[30] for solid thorium are $\phi_0 = 3.35$ v with $A = 60$. This suggests that the effective work function of a composite surface measured at a very low potential such as v_0 changes from that of the base metal to that of the surface metal as the film thickness increases to that of a single layer or greater. Thus we have a qualitative explanation of the fact that the activation curve of Fig. 5 taken at a very low field shows no maximum. The analogous result has been found photoelectrically.

Photoelectric Experiments

Although considerable work was done on the problem, photoelectric emission from composite surfaces, very little of it is of permanent value since the problem must be reinvestigated in the light of the recent theories of photoelectric effect such as that of Fowler.[31] The results reported here are therefore preliminary and show simply some of the more easily observed facts.

A sketch of one of the experimental tubes is shown in Fig. 8.

[29] S. Dushman and J. W. Ewald, Phys. Rev. **29**, 857 (1927).

[30] Dushman, Rev. Mod. Phys. **3**, 394 (1931). (Calculation based on data of C. Zwikker, Proc. Amst. Acad. Sci. **29**, 792 (1926). W. Espe gives $\phi_0 = 3.39$ v and $A = 70$ in Zeits. f. tech. Physik **10**, 489 (1929).

[31] R. H. Fowler, Phys. Rev. **38**, 45 (1931).

The collector c_1, c_2, c_3 was made in three parts and the circuit arranged so that only the current collected on c_2 was measured. The emitter was a nickel cylinder 8 mm in diameter and about 6 cm long mounted on a movable support. By means of the iron weight sealed into a glass envelope, this electrode could be moved to positions I, II or III. During the baking and exhaust it

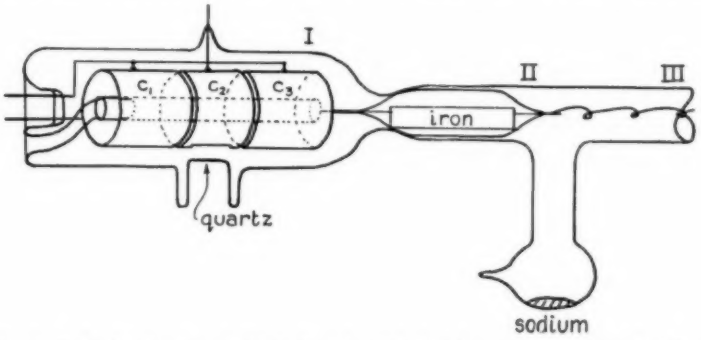

Fig 8. Tube for study of photoelectric emission from a thin film of sodium on nickel.

was in position III. In position II sodium could be deposited on the surface by evaporation from the side tube. While in position I, the electrode was supported concentric with the collecting cylinders by a glass tube sealed in the end as shown. A slit in collector c_2 permitted the light to fall on the emitter after having entered the tube through the quartz window.

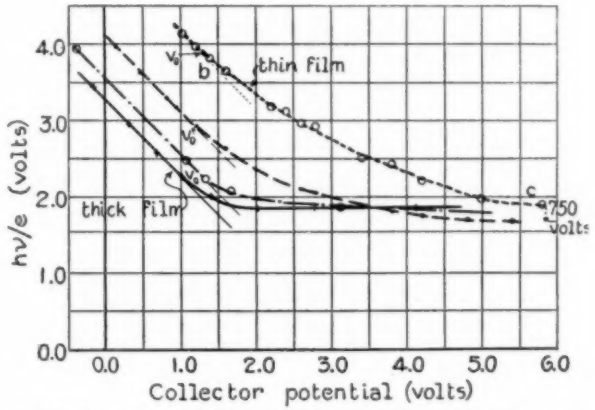

Fig. 9. Minimum-frequency limit as a function of applied potential.

The primary object of the study was to observe the dependence of the effective photoelectric long wave limit on film thickness and applied potential. The range of applied potential varied from a few volts retarding to about 700 volts accelerating. The most interesting results were obtained at low potentials and are shown in Fig. 9.

Over the range of applied potentials greater than 3 volts, the current was measured as a function of the wave-length holding the potential constant. The curve covering a range of current from 10^{-13} to 10^{-14} amp. was then extra-

polated into the axis to give the long wave limit. Over the range of small positive and negative potentials, the current was measured as a function of applied potential while the light frequency was constant. The extrapolation of these curves thus gave additional points for the limiting frequency at which an emission of the order of 10^{-14} amp. would take place under the particular conditions of illumination and applied potential. This limiting frequency expressed in equivalent electron volts is plotted as the ordinate while the applied potential is shown on the abscissa.

According to this method of plotting, points at the left of each curve which fall on straight lines with a slope of (-1) correspond to the range of applied potential over which the Einstein photoelectric equation is applicable. The fact that the points do not break away from this line and quickly approach a nearly horizontal line at some definite value of applied potential is a characteristic phenomenon of composite surfaces. The experimental facts of particular interest are (1) the frequency ν_0 at which the departure from the Einstein line takes place decreases progressively as the thickness of the film increases, presumably starting at that for nickel and finally reaching that for solid sodium; (2) with an accelerating potential of five volts or more the minimum-frequency "limit" undoubtedly decreases as the film thickness increases going through a "maximum excursion" and then returning to that of sodium in bulk. This fact was demonstrated by Ives[8] some years ago but it is interesting to note that the extent of this "excursion" is considerably greater than that of the resonance lines of sodium.

Analysis of Data According to Classical Methods

a. Theory*

If we assume that the curves of Fig. 9 give us a measure of the *effective* photoelectric work function ϕ_e as a function of the applied potential, we can deduce the "force-distance" curve against which the electrons must be working. In the absence of an applied field we have for the work of escape:

$$e\phi_0 = e\int_0^\infty F(s)ds \tag{1}$$

where $F(s)$ is the electric intensity against which the electron is working and s is distance measured from the surface of the metal. If we have an applied field the force against which an electron works in order to escape is increased or decreased. The decrease in work which the electron must do in order to escape with the help of an accelerating field is

$$\Delta\phi_e = \int_0^{s_c} V\phi(s)ds + \int_{s_c}^\infty F(s)ds. \tag{2}$$

Here s_c is the critical distance which the electron must go in order to escape V is the difference in potential between the electrodes and $\phi(s)$ depends on

* The theory presented here has undoubtedly been worked out by others. A less general discussion is given by Hughes and DuBridge, *Photoelectric Phenomena* p. 210.

the geometry of the electrodes. The critical distance is of course given by the condition

$$V\phi(s_c) = F(s_c). \tag{3}$$

If we make a small variation in V we obtain

$$\Delta\phi_e + (d(\Delta\phi_e)/dV)\delta V = \int_0^{s_c+(ds_c/dV)\delta V} (V+\delta V)\phi(s)ds + \int_{s_c+(ds_c/dV)\delta V}^{\infty} F(s)ds. \tag{4}$$

After subtracting Eq. (2) from Eq. (4) it follows that

$$d(\phi_e)/dV = \int_0^{s_c} \phi(s)ds \tag{5}$$

since $d(\Delta\phi_e)/dV = d(\phi_e)/dV$.

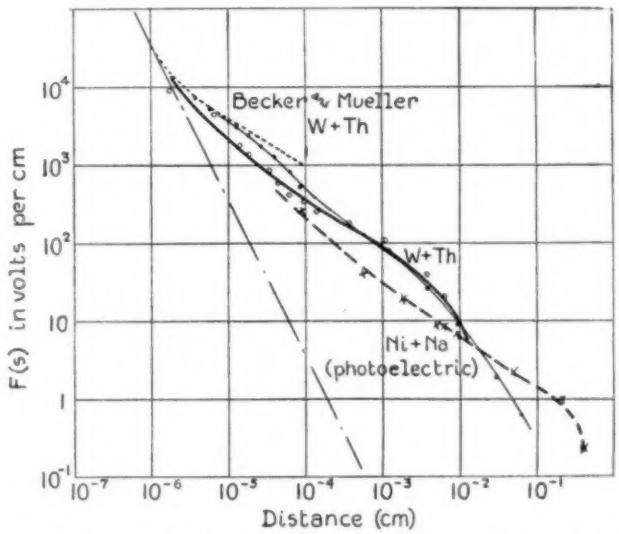

Fig. 10. Computed force functions for various composite surfaces. Solid lines thoriated tungsten; dotted line Becker-Mueller data thoriated tungsten; dashed line sodium on nickel observed photoelectrically. Dot-dash line given by mirror image theory.

The left-hand side of Eq. (5) comes from the slope of such curves as those of Fig. 9. If $\phi(s)$ can be integrated s_1 can be determined as a function of V and using Eq. (3), $F(s)$ can be deduced. For infinite cylinders we obtain

$$s_c = r[(R/r)^{d\phi_e/dV} - 1] \tag{6}$$

where R = radius of outer and r = radius of inner cylinder.

Thermionic data can also be analyzed in this way if we assume that all current changes with applied potential are due to an alteration in the work function. Differentiating the Richardson equation we obtain

$$d(\log i)/dV = -(e/kt)(d\phi_e/dV). \tag{7}$$

In this way $d\phi_e/dV$ as a function of V can be obtained from observed data and Eqs. (6) and (3) can be used to determine the "force function" $F(s)$.

b. Experimental test of classical method

The results of the experimental test of this method of analysis are best illustrated by the curves of Fig. 10.

It is interesting to note that the general trend of the curves is remarkably uniform. It is not difficult to show that data taken at different temperatures, such as that summarized in Table I above, will give the same force function if the temperature ratios of columns three and five are constant.

There are at least two serious objections to this method of analysis which are (1) forces as great as 5.0 to 10.0 volts per cm at distances as great as 10^{-2} cm from the surface are certainly impossible, and (2) determinations of the thermionic constant A made with applied potentials between 2.6 and 6.0 volts have not been found to be constant as is required if the entire change in thermionic current with field is the result of a change in the effective work function.

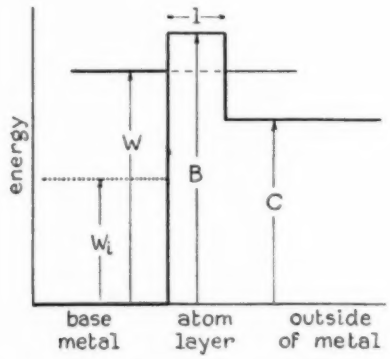

Fig. 11. Hypothetical potential barrier of Fowler and Nordheim. W_i is the highest electron energy assuming a Fermi-Dirac distribution in the base metal at 0°K. Electrons with energy $B > W > C$ must pass *through* a barrier of width l in order to escape.

Transmission through Potential Barrier Explains Results at Low Fields

a. Theory and application to thermionic data

Although the theories of Fowler[32] and Nordheim[33] and the approximate solution to the wave equation used by Wentzel[34] and others have been known for some years, no applications of these results to the voltage-current thermionic curves were made until last year.[15] It is clear that a hypothetical potential barrier of the Fowler-Nordheim type, shown in Fig. 11, will give results qualitatively like those shown in Fig. 6.

Upon heating, the electrons in a metal acquire energies greater than W_i. Those with energy greater than B can escape and the probability of escape upon approach to the boundary should be independent of the energy. The distribution of velocities of these electrons will of course follow the classical

[32] R. H. Fowler, Proc. Roy. Soc. **A122,** 36 (1929).
[33] L. Nordheim, Phys. Zeits. **30,** 177 (1929). Further bibliography here.
[34] Wentzel, Zeits. f. Physik **38,** 518 (1926).

laws and therefore be practically Maxwellian as is indicated by the observed curve *ab* of Fig. 6. For electrons of energy $W<B$ the probability transmission is distinctly less than that for $W>B$ and is furthermore a function of the energy W. Since the transmission coefficient decreases as W decreases the group of electrons with energy $B>W>C$ received by a collector will certainly not have a Maxwellian distribution at the temperature of the filament and if they have anything like a Maxwellian distribution at all it will certainly correspond to a temperature considerably higher than that of the filament since the transmission coefficient decreases with decreasing W thus favoring the high velocity electrons.

With a barrier of this type in mind, we see that the electron emission received with the collector at the potential v_0 (Fig. 6) corresponds to all of the electrons with energies greater than B.

From the fact that the velocity distribution of these electrons is Maxwellian at the temperature of the filament, we can calculate the number of electrons with energy greater than W which approach the barrier from within the metal and can therefore calculate the transmission coefficient as a function of W which must be obtained in order to produce the observed current-voltage curve. This was done using the Nordheim equation. For this B and C of Fig. 11 were held constant and three values of l were determined for three arbitrary values of W. The smooth curve drawn through the points looked very much like a parabola and the width at 1.0 electron-volt below the top of the "hill" was 4.5×10^{-8} cm. This result suggested that the barrier might be assumed to be parabolic and the Wentzel equation used.

The current-voltage characteristic of Fig. 6 can be idealized as shown in Fig. 12. The line *abb'* is given by the equation

$$\log_\epsilon i = \log_\epsilon i_0 + (e/kT_1)(v - v_0)/300 \tag{8}$$

while the line $c'c$ is given by

$$\log_\epsilon i = \log_\epsilon i_2 + (e/kT_2)(v - v_0)/300. \tag{9}$$

We know that the complete curve must be given by

$$i = i_0 \frac{e}{300kT_1} \int_{-\infty}^{v} \epsilon^{e(v-v_0)/300kT_1} D(v)dv \tag{10}$$

where $D(v)$ is the transmission coefficient. Our experiments show that we may take

$$D(v) = 1 \text{ for } (v - v_0) < 0 \tag{11}$$

and

$$D(v) = \epsilon^{e(v-v_0)(1/T_2-1/T_1)/300k} \text{ for } v - v_0 > 0, \tag{12}$$

for then Eq. (10) reduces to

$$i = i_0\epsilon^{e(v-v_0)/300kT_1} \text{ for } (v - v_0) < 0 \tag{13}$$

and

$$i = i_0[1 + T_2/T_1(\epsilon^{e(v-v_0)/300kT_2} - 1)] \text{ for } v - v_0 > 0. \tag{14}$$

For values of $(v-v_0)>0.3$ volt, this equation reduces to Eq. (9) with $i_2 = i_0 T_2/T_1$. The complete curve given by Eqs. (13) and (14) is shown by the solid line of Fig. 12.

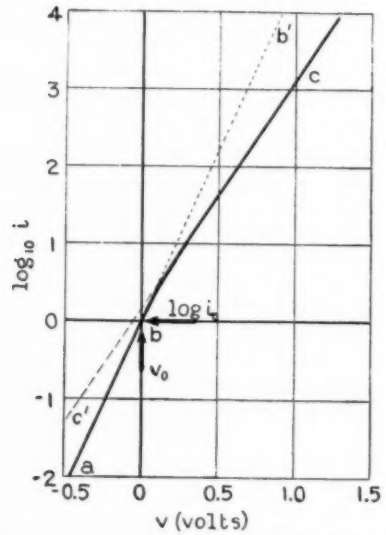

Fig. 12. Idealized current-voltage characteristic; equivalent to observed curve Fig. 6.

The Wentzel approximation gives the transmission coefficient for a barrier like that of Fig. 13 as

$$D(v) = \epsilon^{-(4\pi/h)\int_{x_1}^{x_2}(2mH)^{1/2}dx}. \tag{15}$$

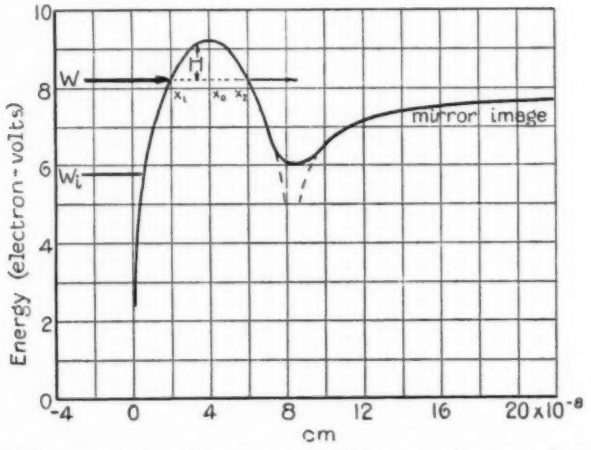

Fig. 13. Potential barrier calculated from observed data on thoriated filament $T=1160°K$.

Let us assume that the potential curve is a parabola above the line at W and is given by

$$H = [e(v - v_0)/300] - C^2(x - x_0)^2 \tag{16}$$

where C is a constant and x_0 is the value of x at the maximum. Remembering that $H=0$ at x_1 and x_2 Eq. (15) reduces for this case to

$$D(v) = \epsilon^{[-2\pi^2(v-v_0)e(2m)^{1/2}/300hC]}. \tag{17}$$

Equating the empirical Eq. (12) and the theoretical Eq. (17) we can solve for C to get

$$C = [2\pi^2 k(2m)^{1/2}/h]T_1T_2/(T_2 - T_1) \tag{18}$$

$$= 17.54 \times 10^{-3}T_1T_2/(T_2 - T_1). \tag{19}$$

The width of the barrier at any point is thus given as a function of v by

$$(x_2 - x_1) = 1.438 \times 10^{-4}[(T_2 - T_1)/T_1T_2](v - v_0)^{1/2}. \tag{20}$$

Putting in $T_1=1160$ and $T_2=1723$ we obtain $(x_2-x_1)=4.05\times10^{-8}$ cm with $(v-v_0)=1.0$ volt which is a reasonably good check on the result obtained using the Nordheim formula which gave 4.5×10^{-8} for the same data.

Using Eq. (20) we can calculate the appropriate barrier widths at one volt under the hill to fit the data summarized by Table I. The results are given in Table II.

TABLE II.

T_1	Barrier width $(v-v_0)=1$ volt Case I.	Case II.
987	4.77×10^{-8} cm	4.92×10^{-8} cm
1045	4.39	4.6
1103	4.15	4.33
1160	3.87	4.05

According to these data the effective width of the barrier seems to be *decreasing* with *increasing* temperature. This may be due to the inaccuracy of determining the appropriate value of T_2 although it is possibly a real effect since the transmission coefficient is probably determined more by the minimum distance of approach of the thorium atom to the tungsten surface rather than by its average position. If this result is true, it is evident that the use of the equation $I=AT^2\exp(-b_0/T)$ to determine the thermionic work function for composite surfaces cannot be of much theoretical significance since the observed current must depend on some "effective" work function which must be a complicated time average and also a function of the temperature. The area over which the emission actually takes place would also be decreased with the result that the surface area of the filament could not be used as is usually done to calculate a value of A.

This method of analysis thus provides a possible explanation for that part of the current-voltage characteristic which has been most troublesome for the classical theory, namely, that of the low voltage range. It also shows how the apparent velocity distribution of the electrons can very well be described as Maxwellian with a temperature 50 percent higher than that of the emitting surface as first pointed out by Koller.[5]

b. Application to photoelectric data

It is evident that a surface model similar to that of Fig. 13 is in qualitative agreement with the results shown by Fig. 9 in which we have the observed minimum-frequency limit shown as a function of the applied field. We see that if the collector potential is adjusted to turn back all electrons transmitted through the barrier, as the potential is varied, then the measured results can be expected to follow the Einstein equation and we will obtain a linear relation between potential and the minimum-frequency limit. Since the minimum-frequency limit as measured depends on the reception of a current of about 10^{-14} amp. at the collector over the range of small positive potentials, the apparent minimum-frequency limit will decrease less rapidly than before, thus accounting for the range *bc* of the curve shown in Fig. 9. With moderate accelerating fields the minimum-frequency limit is set primarily by the height of the plateau (Fig. 13) above the highest occupied energy level in the metal W_i. It is at once clear that photoelectric and thermionic studies should be carried out on the same filament under well controlled conditions for results so obtained are complimentary in many respects and would almost certainly give us the necessary information out of which a detailed picture of composite surface phenomena could be constructed.

It is with the greatest pleasure that I acknowledge my obligation to the members of the staff at the Franklin Institute, the Bartol Research Foundation and the director, Dr. W. F. G. Swann. To Dr. Karl T. Compton, I am greatly indebted for his continued interest and his many helpful suggestions.

A Relation between the Electric and Diamagnetic Susceptibilities of Monatomic Gases

By J. P. VINTI
Massachusetts Institute of Technology

(Received August 6, 1932)

A relation is derived by quantum-mechanical perturbation theory, using a center of gravity argument and the Kuhn-Reiche sum rule, between the polarizability and diamagnetic susceptibility of monatomic gases. On comparison with a similar paper by Kirkwood, who uses a variational method, a criterion is derived for the validity of a perturbed wave function of the form $\psi_0(1+\lambda v)$, where ψ_0 is the unperturbed wave function of the normal state and v the perturbing potential energy of a uniform electric field. It is also pointed out that inclusion of an electronic interaction term σ neglected by Kirkwood removes a difficulty appearing in his paper.

ACCORDING to dispersion theory,[1] if a uniform electric field vibrating sinusoidally with frequency ν is applied to an N-electron atom in the ground state 0, the polarizability (induced electric moment per unit field) is given by the equation:

$$\alpha = \frac{2e^2}{h} \sum_{n \neq 0} \frac{\nu_{n0} |z_{0n}|^2}{\nu_{n0}^2 - \nu^2}$$

where the direction of the electric field is taken as the z-axis, $z = \sum_{\mu=1}^{N} z_\mu$ (where z_μ refers to the μth electron),

$$\nu_{n0} = (W_n - W_0)/h\,, \quad z_{0n} = \int \bar{\psi}_0 z \psi_n d\tau\,,$$

(matrix elements referred to unperturbed wave functions), and the summation is extended over all the excited states n, continous included. For a static field ($\nu = 0$), this becomes:

$$\alpha = 2e^2 \sum_{n \neq 0} \frac{|z_{0n}|^2}{W_n - W_0}\,. \tag{1}$$

Let us denote this summation by $\sum'$, and abbreviate $W_n - W_0$ to W_{n0}. In order to evaluate this sum, it is necessary to find a suitable center of gravity of the term system W_{n0}. We may define the proper average $\tilde{W}_{n0}$ by the equation

$$\tilde{W}_{n0} \sum' = \sum_{n \neq 0} |z_{0n}|^2,$$

but by the rule for a matrix product,

$$\sum_{n \neq 0} |z_{0n}|^2 = (z^2)_{00} - |z_{00}|^2.$$

[1] J. H. Van Vleck, *Theory of Electric and Magnetic Susceptibilities*, p. 362, Eq. (31) (Oxford 1932).

Thus

$$\tilde{W}_{n0} \sum' = (z^2)_{00} - |z_{00}|^2.$$

We may define another average W_{n0}^* by the equation

$$W_{n0}^* \sum_{n \neq 0} |z_{0n}|^2 = \sum_n W_{n0} |z_{0n}|^2,$$

which by the Kuhn-Reiche sum rule equals $(h^2/8\pi^2 m)N$. Since ez_{00} denotes the electric moment averaged with respect to the wave function of the normal state unperturbed by the electric field, it must vanish, since experimentally no atoms have permanent dipole moments. One can also show[2] this by writing z_{00} as $\int |\psi_0|^2 z d\tau$ and applying the transformation $z_\mu' = -z_\mu$, whereupon $\psi_0(z) = \pm\psi_0(z')$, from which $z_{00} = -z_{00}$ and therefore vanishes. Thus

$$\sum_{n \neq 0} |z_{0n}|^2 = \sum_n |z_{0n}|^2 = (z^2)_{00},$$

so that

$$W_{n0}^* = (h^2/8\pi^2 n)N/(z^2)_{00}.$$

If we now take as an approximation $\tilde{W}_{n0} = W_{n0}^*$, we find:

$$\sum' = (8\pi^2 m/h^2)[(z^2)_{00}]^2/N. \tag{2}$$

Now

$$(z^2)_{00} = \sum_i \sum_j (z_i z_j)_{00} = \sum_{i=1}^N (z_i^2)_{00} + \sum_{i \neq j} \sum (z_i z_j)_{00}$$

and

$$(z_i^2)_{00} = (x_i^2)_{00} = (y_i^2)_{00},$$

since these are averages with respect to the unperturbed wave function, in which the z direction is not favored; thus

$$(z_i^2)_{00} = \tfrac{1}{3}(x_i^2 + y_i^2 + z_i^2)_{00} = \tfrac{1}{3}(r_i^2)_{00}.$$

Similarly

$$(z_i z_j)_{00} = \tfrac{1}{3}(\vec{R}_i \cdot \vec{R}_j)_{00},$$

so that

$$(z^2)_{00} = \tfrac{1}{3} \sum_i (r_i^2)_{00} + \tfrac{1}{3} \sum_{i \neq j} \sum (\vec{R}_i \cdot \vec{R}_j)_{00}. \tag{3}$$

Let us denote

$$\sum_{i \neq j} \sum (\vec{R}_i \cdot \vec{R}_j)_{00}$$

by σ, and recall that for a monatomic gas, the molal diamagnetic susceptibility[3] is given by

$$\chi = -\frac{e^2 L}{6mc^2} \sum_{i=1}^N (r_i^2)_{00}, \tag{4}$$

[2] J. H. Van Vleck, reference 1, p. 202.
[3] J. H. Van Vleck, reference 1, p. 206, Eq. (2).

where L is Avogadro's number. Then, using Eqs. (1), (2), (3), and (4),

$$\alpha = \frac{16\pi^2 e^2 m}{9h^2 N}\left(\frac{6mc^2}{e^2 L}|\chi| + \sigma\right)^2. \tag{5}$$

We have here an approximate relation between the polarizability and the diamagnetic susceptibility of a monatomic gas, which can be tested only for the inert gases, since almost all others have strong paramagnetic susceptibilities which greatly outweigh the diamagnetic part. Since electrons repel each other, the average angle between two of the radius vectors R_i and R_j in an atom is expected to be greater than $\pi/2$, thus making σ a negative number. Actual calculation for helium using a wave function due to Hylleraas which gives the energy correct to one part in 3000, gave for σ the value $-0.146\ a_0^2$, so that σ is small compared to $(6mc^2/e^2L)|\chi| = \sum_i (r_i^2)_{00} = +2.34\ a_0^2$ for helium. For neon σ was calculated by means of Slater's theory of complex spectra, using hydrogenic radial functions (with screening) for $1s$, $2s$, $2p$, giving a value of the order $-1.5\ a_0^2$; this is also small compared to $\sum_i (r_i^2)_{00} = 8.31\ a_0^2$ for neon.

We can rewrite (5) in the form:

$$|\chi| = (e^2 a_0^{1/2}/4mc^2)(N\alpha)^{1/2} - (e^2 L/6mc^2)\sigma. \tag{6}$$

We can now test this equation by calculating $|\chi|$ from the observed polarizability, and comparing with the observed $|\chi|$. We get the Table I.

TABLE I. *In this table K is the volume susceptibility reduced to 20° C and 1 atmos. $= K_{20} = (\rho_{20}/M)\chi$, where ρ is the density and M the atomic weight.*

	N	$10^{24}\alpha$ (obs.)	$10^6\lvert K\rvert$ (calc.)	$10^6\lvert K\rvert$ (obs.)
He	2	0.205	0.000088	0.000078
A	10	0.390	0.00031	0.00028

The law (6), with σ placed equal to zero, has been derived by Kirkwood,[4] using a method quite different formally from ours, so that it is of interest to show the equivalence of his assumptions to ours. Letting ψ_0 be the wave function of the normal state and $v = -eF\sum_1^N z_\mu$ the perturbing potential energy due to a uniform electric field of strength F, he writes an approximate wave function for the perturbed atom in the form $\psi_0(1+\lambda v)$, where λ is a parameter which he determines by minimizing the energy $\int \bar{\psi} H \psi d\tau$. Using the fact that v_{00} vanishes, the energy turns out after variation to be W_0 plus a second order term $-(\frac{1}{2})\alpha F^2$, where $\alpha = (8\pi^2 m/h^2)[(z^2)_{00}]^2/N$. He thus gets a formula for the polarizability which checks with ours except for the fact that he arbitrarily neglects [5]σ. If one makes use of the theorem that such a variational method applied to the lowest state of an atom must always give an

[4] J. G. Kirkwood, Phys. Zeits. **33**, 57 (1932).

[5] Kirkwood does not take his z-axis parallel to the field, but one can verify that on doing so, his method does lead directly to our Eq. (5). He places $\sigma = 0$ by writing $\Theta_z = \sum_{i=1}^N (x_i^2)_{00}$ instead of $\Theta_z = \sum_i \sum_k (x_i x_k)_{00}$.

energy higher than the true energy, one sees that the calculated $|K|$ should be larger than the true $|K|$ in all cases. Kirkwood finds $|K|$ (calc.) for neon and argon less than $|K|$ (obs.), contrary to expectation; this is to be explained by his neglect of the interaction term σ.

Now the perturbed wave function which leads to the formula (1) for polarizability is that deducible from first-order perturbation theory:

$$\psi = \psi_0 + \sum_{j\neq 0}(v_{j0}/W_{0j})\psi_j. \tag{7}$$

If we make the assumption that

$$\sum_{j\neq 0}(v_{j0}/W_{0j})\psi_j = \lambda_a v\psi_0 \tag{8}$$

(where λ_a is the adjusted value of λ), our wave function checks with Kirkwood's and will thus give the same second order energy and the same polarizability. Eq. (8), however, on multiplication by $\bar{\psi}_0 v$ and integration over the electron coördinates leads (using Kirkwood's $\lambda_a = -(8\pi^2 m/h^2)(v^2)_{00}/(e^2F^2N)$), to

$$\sum_{j\neq 0}\frac{v_{j0}v_{0j}}{W_{0j}} = \lambda_a(v^2)_{00} = -\frac{8\pi^2 m[(v^2)_{00}]^2}{h^2c^2F^2N}.$$

Using $v = -eFz$, this becomes

$$\sum_{j\neq 0}|z_{0j}|^2/W_{j0} = (8\pi^2 m/h^2N)[(z^2)_{00}]^2,$$

or, using the Kuhn-Reiche sum rule,

$$\sum_{j\neq 0}\frac{|z_{0j}|^2}{W_{j0}} = \frac{[(z^2)_{00}]^2}{\sum_j W_{j0}|z_{0j}|^2}. \tag{9}$$

This, however, is just the assumption $\tilde{W}_{n0} = W_{n0}^*$ of our method. Thus the assumption (8) that leads to Kirkwood's treatment also leads to our assumption as to averages. Eq. (9) can be written:

$$\frac{\sum_{j\neq 0}|z_{0j}|^2/W_{j0}}{\sum_j|z_{0j}|^2} = \frac{\sum_j|z_{0j}|^2}{\sum_j W_{j0}|z_{0j}|^2}. \tag{10}$$

That is, the average (formed with respect to the squared matrix elements) of the reciprocal of W_{j0} must equal the reciprocal of the average of W_{j0}, in order that $\psi = \psi_0(1+\lambda v)$. The accuracy of fulfilment of this relation thus constitutes a criterion for the accuracy of a perturbed wave function of the form $\psi_0(1+\lambda v)$. Eq. (10) is seen to work well when $|z_{01}|^2 \gg |z_{02}|^2$ etc., with the $|z_{0j}|^2$ falling off rapidly. It is thus expected to work well in the case of the alkali vapors, since the first absorption line is very strong compared to the succeeding ones; unfortunately, however, these vapors are paramagnetic, so

that comparison with experiment is impossible. For the alkaline earth vapors (ground state $^1S_0$), there is no paramagnetism, but also no susceptibility measurements. Since they have no permanent magnetic moment, however, the Zeeman effect would be a measure of the magnetic polarizability. One should thus be able to use the law (6) to predict qualitatively second order Zeeman effect of the normal state from refractive index data or vice versa.

The author takes this opportunity to acknowledge his gratitude to Professors J. C. Slater and P. M. Morse, who have read the manuscript and taken a helpful interest in the paper.

Variation of the Principal Magnetic Susceptibilities of Certain Paramagnetic Crystals with Temperature

By B. W. Bartlett
Bowdoin College and Columbia University

(Received July 19, 1932)

Curie and Weiss Constants for the Principal Susceptibilities of Certain Crystals. The Curie and Weiss constants, respectively C_m and Δ of the equation $\chi_m = C_m/(T+\Delta)$, over the temperature range 60° to −45°C have been determined for 5 crystals of the isomorphic monoclinic double sulphate series [M $R_2(SO_4)_2$ $6H_2O$] containing cobalt, nickel, or copper, and for cobalt sulphate heptahydrate. The measurements were made by Rabi's method of determining the principal magnetic susceptibilities of crystals, which was found applicable over this temperature range. The use of ethyl alcohol as a solvent for the auxiliary paramagnetic salt permitted the extension of the method to temperatures below the freezing point of water solutions, such as those used by Rabi, for crystals of volume susceptibilities less than 35×10^{-6}. The lower limit of the applicability of the method depends only on the availability of low freezing point solutions of sufficient susceptibility. In general the Curie constants for the principal susceptibilities of any given crystal were very nearly the same. The Weiss constant showed considerable variation, both between the different principal magnetic axes of the same crystal, and from one crystal to another. Both the Curie and Weiss constants decreased progressively as the metal ion was changed from cobalt to nickel to copper. The effect of change in the alkali ion from NH_4 to potassium was less pronounced, although there was a slight tendency for the Curie constant to increase and for the Weiss constant to become more positive. The accuracy claimed for the measurements is 1 percent. In general there was a small continuous change in the orientation of the principal magnetic axes in the plane of symmetry of the crystal with respect to the crystallographic axes as the temperature was varied.

Introduction

A NUMBER of investigators have made measurements by various methods of the principal magnetic susceptibilities of crystals. An interesting set of crystals is the isomorphic monoclinic double sulphate hexahydrate series, upon which very complete crystallographic and optical data have been obtained by Tutton.[1] The principal susceptibilities of several members of this series have been measured by Fincke[2] and by Jackson.[3] There is considerable disagreement between the results of these two investigators for the same members of the series. Using a quite different method, Rabi[4] has determined the principal susceptibilities of a large number of crystals of this series. His method has two intrinsic advantages over those of the other investigators;

[1] A. E. H. Tutton, Proc. Roy. Soc. London **A88,** 361 (1913); Phil. Trans. Roy. Soc. **A216,** 1 (1916).

[2] W. Fincke, Ann. d. Physik [4] **31,** 149 (1910).

[3] L. C. Jackson and H. Kamerhigh Onnes, Phil. Trans. Roy. Soc. **A224,** 1 (1923); Proc. Roy. Soc. **A104,** 671 (1923); L. C. Jackson, Phil. Trans. Roy. Soc. **A226,** 107 (1927).

[4] I. I. Rabi, Phys. Rev. [2] **29,** 174 (1927).

it requires no accurate knowledge of the fields and field gradients involved, and it permits a direct measurement of the orientation of the principal axes of susceptibility with respect to the crystallographic axes.

The present paper is concerned primarily with the effects of temperature upon the principal susceptibilities. It also serves, however, as a further check on the values already obtained at room temperatures. A comparison of existing results with those obtained during this research will be given later.

Jackson[3] has made measurements on two crystals of the double sulphate series over a considerable range of temperatures. Due to the disagreement between his values and those of Fincke and Rabi at room temperatures it was considered desirable to repeat these measurements over as wide a range as possible by Rabi's method, in addition to measurements on members of this series not previously investigated over a range of temperatures. The need for accurate data of this kind has been enhanced by recent advances in the quantum theory of susceptibilities.[5,6]

METHOD

In Rabi's method[4] of measuring the principal susceptibilities of crystals the crystal is suspended from a torsion head by a glass fibre so as to lie in the inhomogeneous part of the field of a Weiss magnet, in the position shown in Fig. 1. In this position it rests in a solution, the susceptibility of which may be varied at will by the addition of a strongly paramagnetic salt. In general the direction of the field and that of the resulting intensity of magnetization in the crystal will not coincide. In this case displacement of the crystal will result, no matter what the susceptibility of the solution, when the field is applied. If, however, the crystal is so oriented that either its axis of maximum or minimum susceptibility in the XY plane is parallel to the field, the directions of field and resulting intensity in the plane coincide. In this case if the susceptibility of the solution is the same as that of the crystal in the direction of the field, the resultant force on the crystal is zero and it suffers no displacement. For mathematical demonstration of this statement and those which follow the reader is referred to Rabi's paper. It should be noted that the foregoing statement applies to the axes of maximum and minimum susceptibility in the XY plane, these being 90° apart.

In the special case where the direction of one of the principal axes of susceptibility is known, the crystal may be suspended parallel to this direction, and then the other two principal axes will automatically lie in the XY plane. This is the case with monoclinic crystals, in which one principal axis coincides with the symmetry axis of the crystal. In this case the three principal susceptibilities and the orientation of the axes may be determined very simply and directly. The crystal is suspended parallel to its symmetry axis, the torsion head turned and the susceptibility of the solution varied until no displacement of the crystal occurs when the field is applied. The value of one of the

[5] J. H. Van Vleck, *Theory of Electric and Magnetic Susceptibilities*, Oxford University Press, New York, 1932.

[6] O. M. Jordahl, W. G. Penney, and R. Schlapp, Phys. Rev. [2] **40**, 637 (1932).

principal susceptibilities in the plane of symmetry is then directly equal to that of the solution, which may be measured very simply by the well-known Gouy method.[7] The crystal is then rotated through 90° and the susceptibility of the solution again varied until no displacement takes place, determining the other principal susceptibility in the symmetry plane. The crystal is next suspended perpendicular to the symmetry axis, rotated until this axis is parallel to the field, and the susceptibility of the solution is then varied as before until there is no displacement. The susceptibility of the solution is then equal to that of the third principal axis. In practise, displacement of the crystal along the X and Y axes of the magnet (Fig. 1) is observed independently. Motion along the Y axis is governed by the susceptibility of the solution, and along the X axis largely by the angular orientation of the crystal about the axis of suspension. The procedure is therefore simply to turn the

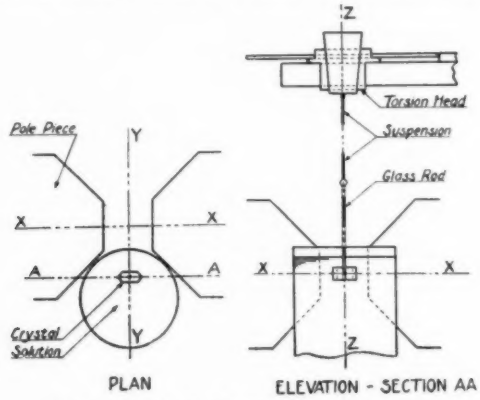

Fig. 1. Method of suspension of crystal.

crystal until there is no motion along the X axis when the field is applied, and then to vary the susceptibility of the solution until displacement in the Y direction is eliminated.

The angle which the maximum axis of principal susceptibility in the plane of symmetry of the crystal makes with one of the crystallographic axes, say the c axis, may be obtained directly as follows. The orientation of the c axis of the crystal is first determined with respect to the X axis of the magnet by reflecting a beam of light back on itself from a known face of the crystal along the Y axis of the magnet. The angle through which the crystal must be turned to obtain a balance with the solution with either its maximum or minimum principal axis parallel to X is then read from the torsion head. Since the angle which the c axis makes with X is determined from this reading and its previous orientation, the angle between the c axis and the principal axis is also given. It is assumed throughout that the glass fibre is stiff enough not to allow the crystal to twist with respect to the torsion head.

The sensitivity of the measurement of the orientation of the principal axes is high. Displacement of the crystal in the X direction for any given field

[7] E. C. Stoner, *Stoner, Magnetism and Atomic Structure*, E. P. Dutton, New York, p. 40 (1916).

strength is a function of the difference between maximum and minimum susceptibility in the XY plane. It is greater when the axis of minimum principal susceptibility is being balanced, and in the case of crystals for which the difference in principal susceptibilities is 10 percent or more it is considerable even if the crystal is away from balance by only one degree. Observation is simplified by the fact that the displacement along the X axis changes direction as the crystal is rotated from one side of the equilibrium position to the other.

This method of determining principal susceptibilities is independent of the shape of the crystal, provided it is not too large. It does not, therefore, require the grinding of crystal sections of definite shape and orientation with respect to the crystallographic axes. This discussion has been limited to the application of the method to monoclinic crystals. It is, however, perfectly general, although in the most general case a greater number of observations and somewhat more complicated calculations are required.

Experimental Procedure

The experimental procedure followed in this research was essentially the same as that described in Rabi's paper. Certain minor modifications were made necessary to permit measurements to be made satisfactorily over the temperature range. Two magnets were used, one for the comparison of the crystals with the solution, and one for the determination of the susceptibilities of the solutions by the Gouy method. While this arrangement facilitates the measurements under any conditions, it is essential with hot and cold solutions that the two measurements be made as nearly simultaneously as possible to prevent change in the solution, either by evaporation, condensation, or precipitation.

The crystals were suspended from a torsion head graduated in degrees by glass suspensions about 30 cm long and 5 mils in diameter. It was found that Rabi's method of attaching the crystals to the suspension with molten shellac was impracticable at the higher temperatures, as the shellac softened and the crystals dropped off. The same thing occurred at all temperatures when alcohol was used as a solvent, as might be expected. After considerable experimentation with other adhesives, it was finally found necessary to drill a properly oriented hole through each crystal, and suspend it upon a slightly tapered glass rod inserted through the hole and attached in turn to the suspension. The diameter of the hole thus drilled was in general less than 10 mils and the rods used had a maximum diameter of about this value. The holes were drilled by hand with a jeweler's drill, and after a little practise it was found easily possible to orient them within one or two degrees of the desired direction.

Motion of the crystals was observed by means of two microscopes focussed on the rods just as they came out of the solution. Both microscopes had scales in their eyepieces, and in particular that used for observing motion in the Y direction had sufficient magnification to detect displacement of 0.002 cm, which was less than the random motion of the crystals due to convection

currents in the solution. The solution was contained in a Dewar flask inserted in the angle of the pole pieces so as to permit the crystal to be suspended in a reasonably strong gradient. Temperatures were measured to half a degree by means of a standard thermometer graduated in tenths. This was sufficiently accurate for the balance of crystal and solution, the critical temperature measurement being that made when the solution was being measured by the Gouy method.

To ensure constancy of temperature during the measurement of the susceptibility of the solution the magnet used for this purpose had a jacketed brass tube inserted between its pole pieces. The jacket was connected to a coil run through a three gallon bath, and constant temperature was maintained by pumping water or alcohol through the system. For temperatures above the room the bath was water heated by an immersion heater, and for low temperatures it was alcohol or alcohol and water cooled with solid carbon

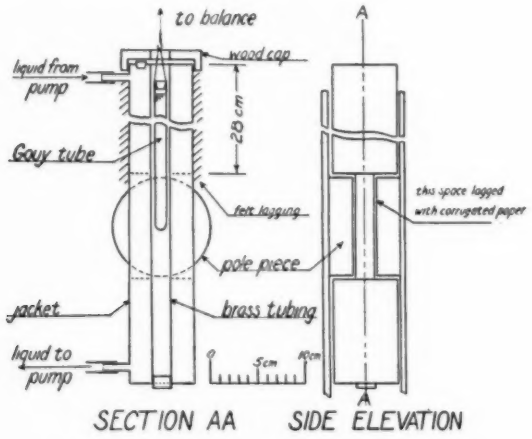

Fig. 2. Diagram of temperature control jacket.

dioxide. Fig. 2 shows diagrammatically the arrangement of the jacket. The whole investigation was carried on in a double walled constant temperature room to ensure constancy of temperature of the magnet throughout.

The Gouy tubes used were of Pyrex glass, approximately 30 cm long and 1 cm in diameter. They were suspended from a chainomatic balance, sensitivity 0.05 mg, located well out of the field, which had no detectable influence upon the balance or suspension. The Gouy tubes were calibrated with distilled water, -0.720×10^{-6} being taken as standard for the susceptibility of water.[8]

Temperatures of the solutions were measured by the insertion of a thermocouple into the tube containing the solution at the time of measurement. Constancy of temperature during the measurement was checked by means of another couple inserted through the walls of the jacket into the inside of the brass tube in which the Gouy tube was suspended. As there was a slight

[8] Int. Crit. Tables, Vol. **VI**, p. 356.

gradient in the Gouy tube, care was taken to measure the temperature at the point where the field gradient was a maximum.

For measurements at room temperatures and above water solutions were used, saturated with respect to the material of the crystal. Susceptibilities were varied by the use of manganous chloride, the amount of this salt in the solution being varied as necessary to balance the crystal. The maximum temperatures at which measurements could be made by this method were limited in general by the disturbance of the solution due to convection currents, although in the case of cobalt sulphate heptahydrate change in the chemical state set the limit. Obviously the lower limit to the method is the freezing point of the solution. In general with water solutions freezing started, or at least the solution became too thick for precise observations, in the neighborhood of $-25°C$. Accordingly search was made for satisfactory solvents of lower freezing point. Experimentation with alcohols, acetone, and other organic liquids of low freezing point resulted in the choice of ethyl alcohol as solvent and anhydrous manganous chloride as solute. This combination gave the largest volume susceptibility of those tried, about 35×10^{-6}, a value sufficiently high for all the crystals except those containing cobalt. For the latter the lower limit was therefore the freezing point of the water solutions. The use of the alcohol solution extended the range to $-45°C$ for the copper and nickel crystals, Below $-50°C$ the alcohol solutions became so viscous as to prevent further measurements.[9]

Crystals

The crystals measured were Co $(NH_4)_2(SO_4)_2 6H_2O$, Co $K_2(SO_4)_2 6H_2O$, Co SO_4 $7H_2O$, Ni $(NH_4)_2(SO_4)_2 6H_2O$, Cu $(NH_4)_2(SO_4)_2 6H_2O$, Cu $K_2(SO_4)_2$ $6H_2O$. Of these the hexahydrates are of the isomorphous monoclinic series so thoroughly investigated crystallographically by Tutton.[1] The two containing cobalt have been investigated magnetically by Jackson[3] over a considerable range of temperatures. Cobalt sulphate heptahydrate is also monoclinic, and has been investigated crystallographically by Marignac,[10] and magnetically by Fincke[2] at room temperatures. The mean susceptibilities of all these salts, in powdered form, except those containing copper have been measured over a wide range of temperatures by Jackson.[3]

Some of the crystals were grown by slow cooling and some by evaporation. Only materials of tested purity were used, and all the crystals selected for measurement had been recrystallized at least twice for further purification. Further check on the purity of the specimens was provided by using at least 6 different crystals for each set of measurements and rejecting any which varied by more than two percent from the mean value. It was found that

[9] Work is in progress at Columbia University on the susceptibilities of these and other crystals at liquid air temperatures. Paramagnetic and diamagnetic liquids offer no difficulties at these temperatures, since liquid oxygen is paramagnetic and liquid nitrogen is diamagnetic, and they are miscible in all proportions. For measurements at intermediate temperatures special liquids would have to be found.

[10] C. de Marignac, Mem. Soc. Phys. Genève **14,** 245 (1858); C. F. Rammelsberg, Hdb. d. Kr-Phys. Chem. **1,** 419 (1881).

great care was required in selecting crystals without flaws or cloudiness if consistent results were to be obtained. In this connection it is suggested that some of the disagreement in published results may have come from the use of imperfect crystals. The writer found that some crystals which were perfect in outward appearance gave out small amounts of saturated liquid when pierced by the drill, indicating imperfect crystallization within the core of the crystal. In general the crystals used were about 0.5 cm on an edge.

It was found necessary to wash the crystals very carefully after each measurement to prevent any manganous chloride drying out of the solution onto the crystal. If this was not done errors of five percent or more were introduced into the results. As a check on the care with which this was done each set of crystals was measured again at room temperature at the completion of the temperature run.

In addition to the measurements on the individual crystals a check on the general consistency of the results was obtained by making a run on powdered crystals by the Gouy method. The accuracy of such measurements was limited by the uniformity with which the powders could be packed into the tube. Also the measurement of temperature was not so accurate as with the solutions, as the temperature of the powder could not be read directly, but had to be determined from dummy tubes held at the same jacket temperatures for the same lengths of time. These measurements however serve as a check against any gross errors in the individual measurements.

Accuracy

The absolute accuracy of the method of the present investigation is definitely limited by the accuracy of the standard value for the susceptibility of water, which is probably about 0.5 percent. In the present work the sensitivity of the null balance of crystal against solution was of the order of 0.1 percent except in the case of the crystals containing copper, for which it was about $\frac{1}{4}$ percent. The sensitivity of the gravitational balance was 0.1 percent or better. The measurement of temperature had a precision of 0.2°, and allowing for temperature gradient in the tube was probably accurate to better than 0.5°. The couples used were calibrated against standard thermometers and against the freezing point of mercury. The field of the Gouy method magnet was checked for constancy by a meter with a precision of 0.1 percent. The magnet itself was in a constant temperature room, and its temperature did not vary by more than one or two degrees throughout the investigation. Heating of the magnet by the current used was highly improbable, as the currents were well below the capacity of the magnet, and were on only for comparatively short time intervals. Further check on this fact is afforded by the fact that the currents were remarkably constant, indicating no heating of the coils.

The insertion of the glass rod through the crystal introduces a systematic error approximately equal to the ratio of the volume of the rod in the solution to the volume of the crystal. From the geometrical dimensions involved this error was in all cases well under 0.5 percent.

Probably the most serious source of error, aside from impurities and irregularities in the crystals themselves, was that which might arise from change in the solution between the balancing of the crystal and the measurement of the susceptibility of the solution. To get the solution from the Dewar flask into the Gouy tube in general required from one to two minutes. To prevent precipitation from the solution the temperature of the bath and the

TABLE I. *Principal susceptibilities.* Axes 1 and 2 refer respectively to the maximum and minimum principal susceptibilities in the plane of symmetry of the crystal, axis 3 to the principal susceptibility perpendicular to this plane. Temperatures are given in degrees centigrade. K is the volume susceptibility, x the mass susceptibility, and x_m' the molecular susceptibility corrected for diamagnetism.

Crystal	T	$K\times10^6$			$x\times10^6$			$x_m'\times10^6$		
		1	2	3	1	2	3	1	2	3
$Co(NH_4)_2(SO_4)_2$-$6H_2O$	55.0	50.4	38.1	44.8	26.5	20.0	23.6	10660	8080	9500
	20.0	58.3	41.5	50.5	30.7	21.8	26.6	12300	8790	10690
	3.0			53.5			28.2			11320
	−3.5	64.1	44.4		33.7	23.4		13480	9430	
	−11.0			56.4			29.7			11900
	−20.0	69.3	46.8	58.9	36.4	24.6	31.0	14570	9900	12440
$CoK_2(SO_4)_26H_2O$	55.0	52.2	41.1	44.0	23.5	18.6	19.8	10460	8330	8840
	20.0	58.6	44.9	48.6	26.4	20.2	21.9	11720	9010	9750
	0.0	63.5	47.7		28.6	21.5		12690	9580	
	−5.0			51.7			23.3			10360
	−20.0	67.8	50.2	54.6	30.5	22.6	24.6	13500	10060	10930
$CoSO_47H_2O$	45.0			59.5			30.5			8700
	40.0	67.3	55.9		34.5	28.6		9830	8170	
	21.0	71.8	59.4	63.9	36.8	30.4	32.8	10470	8680	9350
	0.0	76.4	63.0	67.9	39.2	32.3	34.8	11150	9210	9910
	−15.0			71.6			36.7			10440
	−20.0	81.7	67.2		41.9	34.5		11920	9830	
$Ni(NH_4)_2(SO_4)_2$-$6H_2O$	51.0	18.75	18.23	18.47	9.74	9.47	9.59	4030	3920	3970
	21.0	20.62	20.12	20.02	10.72	10.48	10.40	4420	4320	4290
	−15.0	23.11	22.57	22.46	12.03	11.75	11.66	4930	4820	4790
	−42.0	25.65	25.20	25.28	13.37	13.10	13.15	5460	5350	5370
$Cu(NH_4)_2(SO_4)_2$-$6H_2O$	53.0	6.35	5.17	6.13	3.30	2.69	3.18	1500	1257	1452
	19.0	7.27	5.81	7.02	3.78	3.02	3.65	1692	1388	1640
	−5.0	7.97		7.65	4.14		3.97	1837		1768
	−9.0		6.49			3.37			1528	
	−45.0	9.55	7.53	9.26	4.96	3.91	4.81	2163	1743	2103
$CuK_2(SO_4)_26H_2O$	55.0	6.62	5.24	6.26	2.96	2.34	2.80	1490	1215	1420
	22.0	7.47	5.90	7.10	3.34	2.64	3.18	1658	1349	1587
	−15.0	8.51	6.78		3.81	3.04		1865	1523	
	−45.0	9.71	7.72	9.16	4.35	3.46	4.10	2105	1710	1998

Note: It may be wise to emphasize here that the actual experimental results obtained by the method of this paper are the volume susceptibilities.

solution had to be very closely the same. By working rapidly results could be checked to about $\frac{1}{4}$ percent at any temperature, although the precision of the check was better the closer the temperature of the solution was to that of the room. While in the Gouy tube the solutions were enclosed with a stopper to prevent evaporation or condensation. In calibrating the Gouy tubes correction for the susceptibility of air was necessary. From the foregoing, the

agreement of the writer with the results of Rabi, and the general consistency of the results, it appears reasonable that the values of susceptibility given in this paper are accurate to 1 percent, and that their relative accuracy is somewhat greater, probably of the order of 0.5 percent.

The measurements of the angle between the maximum axis of principal susceptibility and the crystallographic c axis are probably accurate to $1°$[4] and consistent to $\frac{1}{2}°$, except in the case of the nickel crystal, for which the sensitivity of angle measurement was very low with the fields available, about 2°.

Results

Table I gives the results of the measurements of the principal susceptibilities of the various crystals, including volume susceptibilities, mass susceptibilities, and molecular susceptibilities corrected for diamagnetism. Each value is the average of several individual crystals, in most cases six. The average deviation in no case exceeded 1 percent, and in all except a very few cases was less than $\frac{1}{2}$ percent. Table II gives the angle, θ, which the maximum axis of principal susceptibility in the symmetry plane makes with the c crystallographic axis. Fig. 3 shows the symmetry plane of the double sulphates, and Fig. 4 that of cobalt sulphate heptahydrate. Table III gives the Curie and Weiss constants for the crystals. Figs. 5, 6, and 7 show curves of the reciprocal of the molecular susceptibilities corrected for diamagnetism plotted against absolute temperature.

TABLE II. *Orientation of principal susceptibilities.* The numbers in this table are the values in degrees of the angle, θ, which the maximum axis of principal susceptibility in the plane of symmetry makes with the c crystallographic axis. θ is measured positive in the direction of the acute angle between the c and a crystallographic axes.

Crystal	Temperature in degrees centigrade									
	55	50	45	40	30	20	0	−10	−20	−45
$Co(NH_4)_2(SO_4)_26H_2O$	$-43\frac{1}{2}$					$-43\frac{1}{2}$			$-43\frac{1}{2}$	
$CoK_2(SO_4)_26H_2O$	−14					−13	$-12\frac{1}{2}$		$-11\frac{1}{2}$	
$CoSO_47H_2O$			*$-56\frac{1}{2}$			$-55\frac{1}{2}$	$-54\frac{1}{2}$		$-53\frac{1}{2}$	
$Ni(NH_4)_2(SO_4)_26H_2O$		−13				−17			−21	−23
$Cu(NH_4)_2(SO_4)_26H_2O$		−87	−84	−83	−81	−79		−76		$-72\frac{1}{2}$
$CuK_2(SO_4)_26H_2O$	$-101\frac{3}{4}$					$-102\frac{1}{2}$			−104	−105

* Above this point a large and variable change in angle indicated a change in the state of the crystal. This change was accompanied by a corresponding change in susceptibilities, and a distinct change in the appearance of the crystal, probably due to dehydration.

TABLE III. *Curie and Weiss constants.* In the following table the Δ's and the C_m's are those of the Weiss formula $x_m' = C_m/(T+\Delta)$, in which x_m' is the molecular susceptibility corrected for diamagnetism and T is the temperature in degrees Kelvin.

Crystal	Δ_1	Δ_2	Δ_3	C_{m1}	C_{m2}	C_{m3}
$Co(NH_4)_2(SO_4)_26H_2O$	−50	81	−10	2.9	3.3	3.0
$CoK_2(SO_4)_26H_2O$	5	88	67	3.5	3.5	3.4
$CoSO_47H_2O$	23	44	45	3.3	2.9	3.2
$Ni(NH_4)_2(SO_4)_26H_2O$	30	25	25	1.42	1.36	1.36
$Cu(NH_4)_2(SO_4)_26H_2O$	−9	24	−2	0.475	0.44	0.47
$CuK_2(SO_4)_26H_2O$	14	20	18	0.51	0.425	0.49

Correction for diamagnetism included that for water of crystallization, the alkali molecule, and the sulphate ion of the metal molecule, and totalled 180×10^{-6} for the double sulphates and 100×10^{-6} for cobalt sulphate hepta-

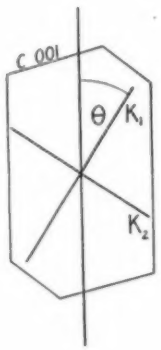

Fig. 3. Plane of symmetry of double sulphate crystals.

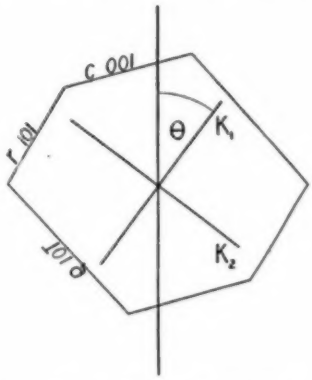

Fig. 4. Plane of symmetry of cobalt sulphate heptahydrate.

hydrate. The values used were those given in the International Critical Tables, vol. **IV**, page 365. In the case of crystals containing cobalt and nickel the diamagnetic correction is small compared with the total susceptibilities. In

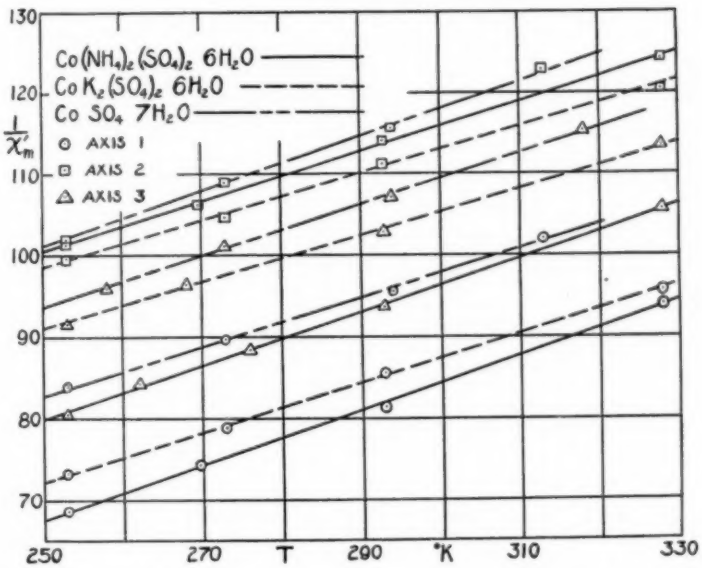

Fig. 5. Curves of $1/x_m'$ against temperature for crystals containing cobalt.

the case of the copper crystals, however, it becomes considerable, 15 percent in the extreme. This undoubtedly introduces some uncertainty into the values of the Curie and Weiss constants for these crystals, as the accuracy of the diamagnetic correction may be held in question. There is no certainty

that the linking of the components in the complex molecule does not alter the commonly accepted values of the ionic susceptibilities, and there is further no inherent reason that the diamagnetic correction is the same along

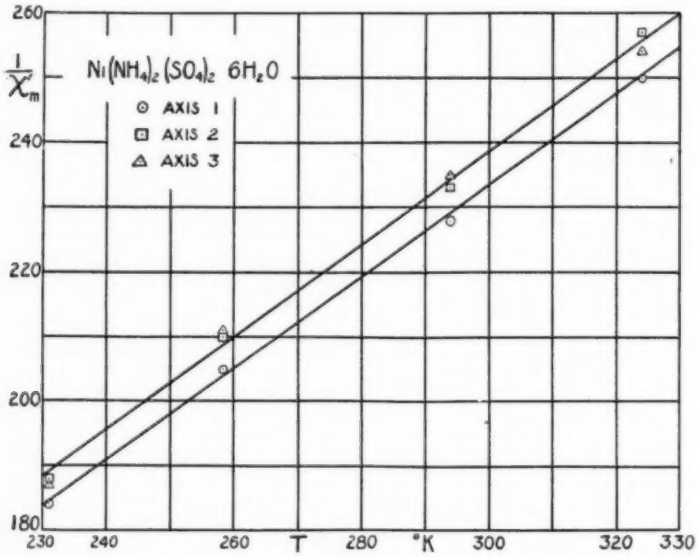

Fig. 6. Curves of $1/x_m'$ against temperature for nickel ammonium sulphate.

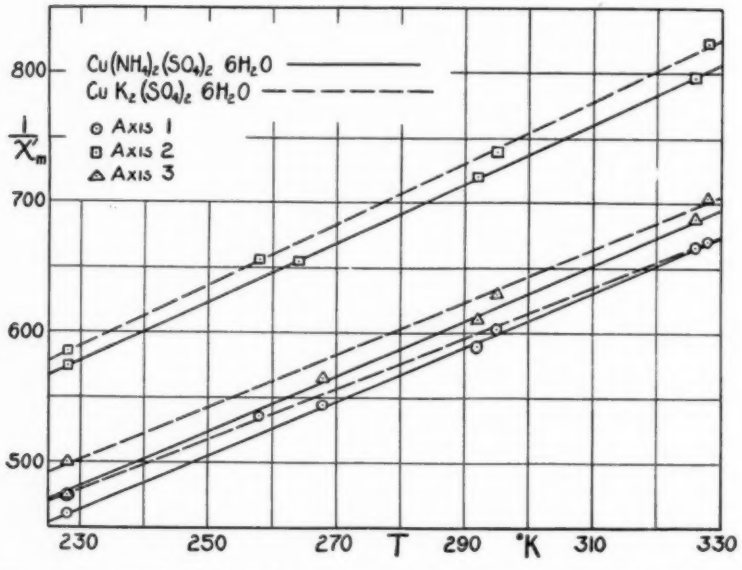

Fig. 7. Curves of $1/x_m'$ against temperature for crystals containing copper.

each axis, as has been assumed in making the correction for want of data on the subject.

The results of Table I have not been corrected for the volume expansion of the crystals with temperature. This will introduce some error into the

mass and molecular susceptibilities given in the table. Values for the coefficient of volume expansion of these crystals are not available, at least to the knowledge of the writer. Coefficients of volume expansion for crystals such as $MgSO_47H_2O$ and $CuSO_45H_2O$ as given in the International Critical Tables, vol. III, page 44, are, however, all less than 10^{-4} per °C. In the extreme case this would entail a correction of about 1 percent in the mass susceptibilities. The effect of this correction would be to increase the Curie constants slightly, and to make the Weiss constants all slightly more positive. Table IIIA gives values of these constants corrected for an assumed coefficient of volume expansion of 10^{-4} per °C. Additional evidence that this correction is small is furnished by the measurements on the powdered crystals. In this case mass susceptibilities are measured directly, so that if the effect is appreciable it should show up when the mass susceptibilities of the powders are compared

TABLE IIIA. *Curie and Weiss constants corrected for volume expansion.* The values in this table are the Curie and Weiss constants obtained after the mass susceptibilities were corrected for volume expansion, the coefficient of volume expansion being assumed as 10^{-4} per degree centigrade for all the crystals.

Crystal	Δ	Δ_2	Δ_3	C_{m1}	C_{m2}	C_{m3}
$Co(NH_4)_2(SO_4)_26H_2O$	−44	93	0	3.05	3.4	3.1
$CoK_2(SO_4)_26H_2O$	15	100	78	3.6	3.6	3.5
$CoSO_47H_2O$	31	55	56	3.4	3.0	3.3
$Ni(NH_4)_2(SO_4)_26H_2O$	40	35	35	1.47	1.40	1.40
$Cu(NH_4)_2(SO_4)_26H_2O$	−1	33	6	0.49	0.465	0.485
$CuK_2(SO_4)_26H_2O$	23	30	27	0.525	0.435	0.505

TABLE IV. *Susceptibilities of powdered crystals.* In this table x is the mass susceptibility, and x_m' the molecular susceptibility corrected for diamagnetism. C_m and Δ are the Curie and Weiss constants, respectively. Temperatures are in degrees centigrade.

Crystal Powder	T	$x\times10^6$	$x_m'\times10^6$
$Co(NH_4)_2(SO_4)_26H_2O$	56	23.2	9340
$C_m=3.2$	22	25.9	10400
$\Delta=14$	−7	28.8	11560
$CoK_2(SO_4)_26H_2O$	55	21.3	9490
$C_m=3.45$	19	23.8	10580
$\Delta=37$	−38	28.5	12600
$CoSO_47H_2O$	45	30.7	9030
$C_m=3.4$	19	34.3	9780
$\Delta=60$	−20	38.3	10880
$Ni(NH_4)_2(SO_4)_26H_2O$	52	9.60	3960
$C_m=1.38$	20	10.55	4350
$\Delta=27$	−40	13.08	5340
$Cu(NH_4)_2(SO_4)_26H_2O$	56	3.00	1380
$C_m=0.47$	20	3.42	1550
$\Delta=15$	−39	4.25	1890
$CuK_2(SO_4)_26H_2O$	56	2.68	1363
$C_m=0.46$	20	3.06	1538
$\Delta=13$	−40	3.86	1888

with the average mass susceptibilities of the crystals. In general there is no appreciable consistent difference of the sort which might be expected if the correction for volume expansion were of importance.

In Table IV are given the results of the measurements on the powdered crystals. These were not originally intended as precision measurements, and as has already been pointed out under the heading *Crystals*, they are probably somewhat less accurate than the results of Table I. The agreement between the powder measurements and the averages for the crystals is in general so good, however, as to warrant their inclusion as a check on the latter.

Discussion

Comparison of the results obtained at room temperatures by Fincke, Jackson, Rabi, and the writer is given in Table V. The agreement between the two latter is in general within the experimental error, except for the crystals containing copper, where there is a consistent difference of from 2 to 4

Table V. *Comparison of results.* This table contains a comparison of the results of different investigators at room temperatures reduced to the common temperature 27°C. The K's are the principal volume susceptibilities, and θ is the angle between K_1 and the c crystallographic axis.

Investigator	$K_1\times10^6$	$K_2\times10^6$	$K_3\times10^6$	θ
		$Co(NH_4)_2(SO_4)_26H_2O$		
Bartlett	56.8	40.6	49.3	−43
Fincke*	55.9	43.6	45.5	−27
Jackson	48.0	40.4	46.9	−31
Rabi	56.2	40.7	48.9	−44**
		$CoK_2(SO_4)_26H_2O$		
Bartlett	57.3	43.9	47.6	−13
Fincke*	66.6	49.6	77.2	−21
Jackson	61.1	49.6	53.6	−20
Rabi	57.6	44.6	48.6	−13**
		$CoSO_47H_2O$		
Bartlet	70.4	58.2	62.6	−55
Fincke*	70.9	64.0	68.5	−40
		$Ni(NH_4)_2(SO_4)_26H_2O$		
Bartlett	20.2	19.7	19.7	−17
Fincke*	19.6	15.8	18.0	−16
Rabi	20.2	19.9	20.0	−17**
		$Cu(NH_4)_2(SO_4)_26H_2O$		
Bartlett	7.08	5.65	6.83	−79
Rabi	6.80	5.40	6.62	−74
		$CuK_2(SO_4)_26H_2O$		
Bartlett	7.14	5.80	6.98	−102
Rabi	7.52	5.62	6.83	−99

* Fincke does not state the temperature at which his measurements were made.

** There is a misprint in the published values of θ in Rabi's paper. The values given for cobalt ammonium and cobalt potassium sulphate should be interchanged, as should those for nickel ammonium and nickel potassium.

percent. This difference may be partially explained by an indeterminate temperature correction, as Rabi's measurements were not primarily concerned with temperature, which accordingly was not determined with care. There remains a discrepancy in the value of K_1 for copper potassium sulphate which is not consistent with the other differences. Comparing the values of the copper group with those of the nickel and cobalt groups in Rabi's paper, it appears that the value given in this paper is more consistent than that given by Rabi. In general Fincke's and Jackson's results do not agree nearly so closely, either with each other or with Rabi.

Comparison of the Curie and Weiss constants found for the cobalt double sulphates by Jackson and by the writer shows qualitative agreement for the Weiss constants, and reasonably good quantitative agreement for the Curie constants, considering the accuracy of the determinations. For the Curie constants this is of the order of 3 percent, and for the Weiss constants not better than 5°. Jackson's value for the maximum principal susceptibility of cobalt ammonium sulphate is inconsistent with the relative values bound by the other three investigators of this salt. Agreement between the average values of the constants in this paper and those found by Jackson for the cobalt and nickel double sulphates in powdered form is qualitatively good. In the case of the curves in this paper for nickel ammonium sulphate, the writer has drawn them as straight lines. An equally good case might be made for drawing them with a slight downward curvature at the lower end. Further data at still lower temperatures are needed to indicate which is nearer the truth.

The effect of changing the alkali ion from ammonium to potassium seems to be to increase slightly the Curie constants, and to make the Weiss constants more positive. There appear to be definite, though small, differences in the Curie constants for different axes of the same crystal in some cases. A recent note by Jordahl, Penney, and Schlapp[6] states that this may be expected from theoretical considerations.

Thus far most of the work done on this problem has been done over a comparatively small range of temperatures near room temperature, or at very low temperatures. The first type is open to the objection that the range of temperature is scarcely sufficient to give high accuracy to the determination of the constants, while the second has the difficulty that at low temperatures the variation from the Weiss law makes computation of the constants somewhat uncertain. Thus in certain of Jackson's work no values of susceptibilities are available between room temperature and about 75°K, at which point deviation from the Weiss law is already taking place. A complete run upon a typical crystal like cobalt ammonium sulphate from room temperature or above down to the lowest temperatures obtainable, with points at frequent temperature intervals, seems needed as an adequate test of theory.

Any theoretical discussion of the magnetic behavior of these crystals must recognize that in the case of the copper group the diamagnetic correction is particularly important, a small uncertainty having a considerable effect on the constants. It is quite probable from results on diamagnetic crystals[4,11]

[11] W. Voigt and S. Kinoshita, Ann. d. Physik [4] **24,** 492 (1907).

that this correction should be different in different directions. At present it is practically impossible to obtain from susceptibility measurements an accurate knowledge of what the paramagnetic susceptibilities of this group really are. The thermal expansion is in all likelihood different along different axes, and consequently the force field acting on the paramagnetic ion will be changed in both magnitude and direction. That this may be the case is shown by the particular example of copper ammonium sulphate, where the ellipsoid of induction is rotated almost 15 degrees with respect to the crystallographic axes over a temperature range of 95 degrees. This type of datum may serve to give insight into the nature of these force fields and their dependence on temperature. An investigation of triclinic crystals, where there are no necessary fixed relations between crystal axes and ellipsoid of induction, might yield results of interest.

In conclusion the writer wishes to express his appreciation of the interest and advice of Professor I. I. Rabi, who suggested this problem to him, and his thanks to Professor N. C. Little for placing at his disposal the magnet used for measuring the susceptibilities of the solutions.

Supersonic Dispersion and Absorption in CO_2

By W. H. PIELEMEIER
Pennsylvania State College

(Received August 8, 1932)

Since supersonic velocity determinations in air near a crystal oscillator usually yield values in excess of the accepted value, $V_0 = 331.6$ m/sec., a similar effect with CO_2 was suspected. The velocity and the absorption coefficient were measured at frequencies beginning in the dispersion region, theoretically and experimentally investigated by Kneser, and extending beyond it to 2.09 megacycles. The author's velocity values are slightly less than Kneser's experimental values but they fit his theoretically determined dispersion curve equally well. At the lowest frequency tested (303 kilocycles) the absorption coefficient was found to exceed, by the greatest amount, its value computed from Lebedew's formula. This frequency is near the middle of the dispersion region where maximum absorption is expected. According to Pierce the absorption becomes excessive also when this frequency is approached from lower values. The results are presented in tabular and in graphical form. A sharp absorption maximum appears at 217 k.c.

IF THE satellite spacing is used to compute the velocity of high-frequency sound in air as outlined in a previous article[1] the value $V_0 = 331.6$ m/sec. is obtained. If, however, the major peak spacing for short resonance columns is used the value of V_0 is usually about 0.5 percent higher than this, the excess being due, apparently, to the much greater intensity. A similar effect was suspected in the case of CO_2. It was, therefore, considered desirable to check the velocity measurements of H. O. Kneser[2] and to extend the region which he investigated, if possible. It was also considered desirable to search the dispersion region determined theoretically[3] and experimentally by Kneser for excessive absorption.

The general method of investigation is the same as that used previously by the author[1] and by many other investigators. Some of the latest experimental investigations were reported by Barnes,[4] Hershberger,[5] Hopwood,[6] Richards[7] and Randall.[8]

APPARATUS

The apparatus is the same as that used in the previous investigation[1] with the addition of another thermometer mounted beside the sound path and a

[1] W. H. Pielemeier, Phys. Rev. **38,** 1236 (1931).
[2] H. O. Kneser, Ann. d. Physik [5] **11,** 777 (1931).
[3] H. O. Kneser, Ann. d. Physik [5] **11,** 761 (1931).
[4] G. F. Barnes, J. Acous. Soc. Am. **3,** 579 (1932).
[5] W. D. Hershberger, J. Acous. Soc. Am. **3,** 263 (1931); also, Physics **2,** 269 (1932).
[6] F. L. Hopwood, Nature **128,** 748 (1931).
[7] W. T. Richards, Proc. Nat. Acad. Sci. **17,** 611 (1931); also, G. B. Kistiakowsky and W. T. Richards, Jour. Am. Chem. Soc. **52,** 4661 (1930).
[8] C. R. Randall, Bureau of Standards Jour. of Research **8,** 79 (1932).

radiometer or pressure vane which could be interchanged with the moveable reflector. An orsat apparatus was used to analyze the gas after a run was completed.

Results

The results are presented in Table I and in Figs. 1 and 2. The ratio, $V^2(CO^2)/V^2(A)$, is plotted against log ν in Fig. 1. In this figure $V(CO_2)$ represents the velocity of sound in CO_2 reduced to 0°C, the relative humidity ranging from 24 to 30 percent and the purity of the CO_2 ranging from 91 to 95 percent. $V(A)$ represents the velocity in argon reduced to 0°C ($V(A) = 307.8$ m/sec.). This method of plotting is used in order to make a direct comparison with Kneser's[2] dispersion curve. The values of A, the absorption constant, are plotted against log ν in Fig. 2. These values were computed from pressure vane deflections and also from the height of the peaks which were used for the velocity determinations.

Table I.

Frequency, in kilocycles	$V(CO_2)$ in meters per sec.	Percent CO_2	Relative humidity, H, in percent	$V^2(CO_2)/V^2(A)$ in percent	c	$A = c\lambda^2 \times 10^{-3}$
303.8	262.5 to 265.1*	91 to 95	27 to 31	72.7 to 74.2	1.6	14.
409.6	264.3	94	—	73.7	1.7	8.1
645.8	265.1 to 267.0	91	24 to 30	74.2 to 75.3	1.7	3.2
1159.1	268.1 to 268.6	92 to 95	25 to 26	75.5 75.7	1.8	1.1
1224.	268.6 to 268.7	90	30	75.8 75.9	2.2	1.1
1403.	269.6 to 269.9	91 to 92	25 to 26	76.0 76.2	1.7	0.67
2089.	268.2	94	24	75.6	2.7	0.49

* The value from each of five runs was 263.6 (94 to 95 percent CO_2).

Discussion of Results

With a resonance column of cross section small in comparison with the wave-length the wave fronts in the component trains rapidly lose their flatness and their intensity decreases much more rapidly than it would on account of mere absorption. If the cross section is kept constant and the frequency is increased this effect *diminishes* but the actual absorption *increases* in general. (Neglecting absorption *bands*, the coefficient of absorption should be porportional to the square of the frequency.) If the deviation from flatness is not prevented nor taken into account in absorption measurements an apparent or false absorption minimum might be found. With velocity depending on intensity such a minimum would be accompanied by an apparent dispersion. In consideration of these statements the measurements of Pierce,[9] Barnes,[4] and Kneser[2] on the velocity of high-frequency sound in CO_2 were viewed with a possible doubt and the upper range covered by Kneser was remeasured and extended to $\nu = 2089$ k.c. The coefficient of absorption was also measured over this range. Sound beams of greater cross section were

[9] G. W. Pierce, Proc. Amer. Acad. **60**, 271 (1925).

used. The original intention was to use the satellites for the velocity determinations but they were so weak with CO_2 that this plan was rejected. Even with the lowest frequency ($\nu = 303.8$ k.c.) the satellites could be definitely located for only a few wave-lengths from the crystal surface. This fact and the constant space rate at which the logarithm of the peak height decreases

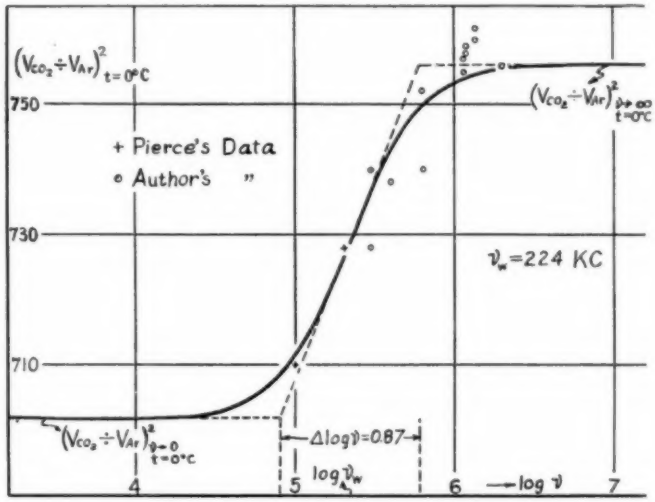

Fig. 1. Kneser's dispersion curve (ordinates $\times 10^{-3}$).

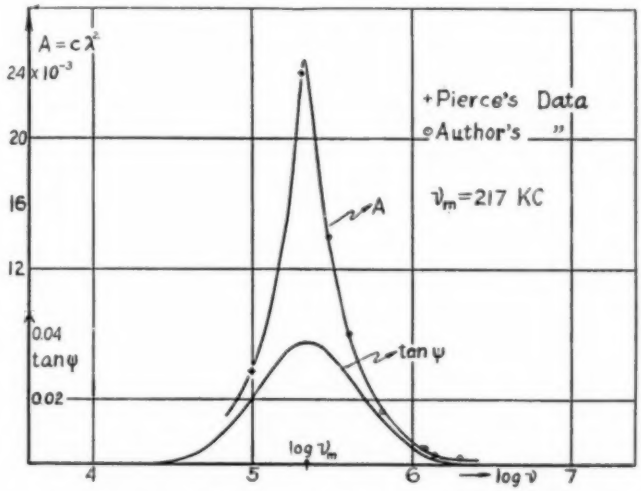

Fig. 2. Observed absorption curve and Kneser's tan ψ curve.

after the first few peaks, are good evidence that there is but one effective return trip of the emitted waves in CO_2.

Since the satellites observed with air at mirror positions such as to give resonance for low intensity (minimum velocity) waves could not be used with CO_2, the velocity values are probably slightly greater than the *limiting* velocity at the given frequency. The presence of some air (5 to 9 percent)

also has the effect of increasing the velocity. Probably the apparent drop in velocity between 1.4 and 2.09 megacycles is merely an approach to the limiting velocity for low intensity waves. (The intensity decreases through this range.)

A dispersion approximately as located by Kneser is quite evident in spite of the uncertainties listed above. Kneser's[2] observed maximum dispersion occurs at approximately 224 k.c. Pierce's[9] velocity curve ends near this point (205.6 k.c.). It is in good agreement with Kneser's[2] curve. The author's data agree reasonably well with the remainder of Kneser's curve (see Fig. 1).

A number of different symbols for the absorption coefficient are used in the publications on sound absorption. Lebedew and Neklapajew[10] use A/λ^2, Abello[11] uses k for one percent CO_2 and therefore 100 k for the pure gas, Herzfeld and Rice[12] use $4\pi k_2$ which they also express in terms of other constants including n^2 and τ, n being the frequency and τ a time measuring the rate of exchange between external and internal degrees of freedom. In Table I the symbol c is used for the absorption coefficient. ($I=I_0e^{-cx}$). We may then write

$$100k = 4\pi k_2 = n^2a = a/V^2 = c. \qquad (1)$$

From Eq. (1) $$a = A/\lambda^2n^2 = A/V^2.$$

If there were no internal degrees of freedom nor dissociation of the molecules or if the internal energy were at all times in equilibrium with the external energy A and a would have constant values for all frequencies. This, however, is not the case with CO_2. As may be seen from Table I, the greatest value of A observed by the author occurs with the lowest frequency (303.8 k.c.). Even this is above Kneser's[2] observed value for ν_w, the frequency for maximum dispersion, which is approximately 224 k.c. If that value of β is selected which yields 224 k.c. it is found to be 0.95 $(10)^{-6}$ and not 0.95 $(10)^{-5}$ sec. as he records it. This may be seen from Kneser's equation,

$$\nu_w = 224\,\text{k.c.} = 2.24(10)^5 = \frac{1}{2\pi}\,\frac{1}{\beta}\,\frac{C}{Ca} = \frac{1}{2\pi}\,\frac{1}{\beta}\,\frac{3.349}{2.5}.$$

Thus ν_m, the frequency for maximum value of ψ, has for its value 217 k.c. ψ represents the phase lag of the density behind the pressure. A *maximum* value of A is also expected at 217 k.c. Evidently A is approaching this maximum at the lower end of the observed frequency range. If the value of c at 303.8 k.c. is used to compute τ from the equation[12]

$$c = 4\pi k_2 = n^2a = n^2[3.16(10)^{-13} + 1.16(10)^{-4}\tau] \qquad (2)$$

we obtain $\tau=0.9\ (10)^{-7}$ sec.

This is not in agreement with Kneser's[2] *Abklingungszeit der inneren Energie* nor with β', the life of the vibration quanta; *Lebensdauer der Schwingungs-*

[10] N. Neklapajew, Ann. d. Physik **35**, 175 (1911).
[11] T. P. Abello, Phys. Rev. **31**, 1083 (1928).
[12] K. F. Herzfeld and F. O. Rice, Phys. Rev. **31**, 691 (1928).

quanten. $\beta' = (10 \pm 2)(10)^{-7}$ sec. The difference may be due to the values of c and n used in Eq. (2). With Abello's[11] exterpolated value for 100 k, τ becomes 0.66 $(10)^{-7}$ sec. This is for $n = 612$ k.c. which is farther above the peak frequency. Pierce[9] states that 4 mm of CO_2 at 205.6 k.c. are more than equivalent to 204 mm of air. Accordingly τ is 3 $(10)^{-7}$ sec. and $A = 24$ $(10)^{-3}$. If τ is computed from the first 2 mm of Pierce's[9] curve the result is 8 $(10)^{-7}$ sec. This frequency is just below that for the absorption peak. Probably τ for 217 k. c. would agree better with $\beta' = 10$ $(10)^{-7}$ sec. Peirce's[9] data for 100 k.c. gives 5.7 $(10)^{-3}$ as the value of A. This is definitely on the low-frequency side of the absorption maximum.

Small but very definite variations in the values of A for a given frequency were obtained by the author. These are probably due to the differences in the temperature and the humidity for the separate runs. This problem is being investigated and will be reported by H. H. Rogers.

Simultaneous measurements on velocity and absorption in other gases by a new method of detection[13] are being investigated by H. L. Yeagley and H. L. Saxton.

Hershberger[5] states two possible reasons for the multiple peaks which he observed. One is a frequency shift as the mirror approaches a resonance position. The other is the complexity in the motion of the crystal itself. The latter might well be the cause of those observed by the author. It is thought, however, that this complexity is *caused* by the slight deviation from simultaneity in arrival of the multiply reflected components of the stationary waves. Only the components of lowest intensity and minimum velocity arrive *together* if the length of the resonance column is adjusted for this minimum velocity.

[13] In a recent article by Grossmann (Ann. d. Physik [5] **13**, 681 (1932)) a somewhat similar method is outlined. Grossmann's ν_m is lower and his maximum value of A is much greater than the author's corresponding values. The value of τ computed from Grossmann's maximum A is much in excess of $10(10)^{-7}$ sec. Possibly his method of correcting for diffraction is not sufficient to prevent an apparent additional absorption at the lower frequencies. If so, it would explain the above deviations. Further measurements near the peak frequency and below it are being made.

LETTERS TO THE EDITOR

Prompt publication of brief reports of important discoveries in physics may be secured by addressing them to this department. Closing dates for this department are, for the first issue of the month, the twenty-eighth of the preceding month; for the second issue, the thirteenth of the month. The Board of Editors does not hold itself responsible for the opinions expressed by the correspondents.

The Angular Distribution of Elastically Scattered Electrons in Mercury Vapour

In a recent paper[1] in the Physical Review Tate and Palmer have reported results of an investigation of the angular scattering of electrons in mercury vapour, which confirm in general the results obtained by the writer about two years ago.[2] However, in the particular case of the scattering of 80-volt electrons between 5° and 60°, Tate and Palmer obtain a curve which does not fall off so steeply as the curve I obtained first in 1929 for 82-volt electrons.[3]

Tate and Palmer suggest in explanation of this disagreement that I "collected not only electrons scattered elastically but also a large number of inelastically scattered electrons" owing to the fact that I used an accelerating potential between the Faraday cylinder and its shield to prevent secondary electron emission from the Faraday cylinder.

This must surely be a mistake, for reference to my paper will show that, in the apparatus I used in 1929 to obtain the curve reproduced by Tate and Palmer, I had no means of applying such an accelerating potential. A retarding potential only was applied in the collecting system to prevent the collection of inelastically scattered electrons.

It is true that I obtained an almost identically similar curve with my new apparatus in which an accelerating potential was applied to prevent secondary emission, but the very fact that the curve was almost identical shows that no error was introduced by using this accelerating potential.

The reason why an accelerating potential may lead to the collection of inelastically scattered electrons is that part of the retarding potential may be rendered ineffective in stopping electrons which have lost energy, owing to penetration of the accelerating field into the retarding field. The extent of this penetration will obviously depend upon the size of the opening in the diaphragm separating the two fields, and the fraction of the retarding field neutralized by the accelerating field will depend upon the ratio of the size of this opening to the distance between the slits across which the retarding potential is placed. In my new apparatus this ratio is 2/5, whereas in the apparatus used by Tate and Palmer the ratio is about 5/3, i.e., the width of the slit is *greater* than the distance over which the retarding field extends. It is not surprising therefore that serious distortion of the retarding field was produced by the accelerating field in their apparatus, while in my apparatus the effect of the accelerating field was very small. There is thus no justification for the statement made by Tate and Palmer that "as Arnot's slit system is similar in dimensions to ours it would seem that his measurements are subject to this error."

A very slight interpenetration of the fields was observed in my work, but the small reduction in the retarding field so caused was always corrected by increasing the retarding field until only the elastically scattered electrons were received. This was effected by the following procedure. At each energy of the primary electron beam a velocity distribution curve of the scattered electrons was taken. From an examination of this curve the retarding potential could then be set so as to exclude all inelastically scattered electrons from the Faraday cylinder. In an investigation of this nature one naturally takes such precautions as these.

F. L. ARNOT

The University
St. Andrews
August 9, 1932.

[1] J. T. Tate and R. R. Palmer, Phys. Rev. **40**, 731 (1932).

[2] F. L. Arnot, Proc. Roy. Soc. **A130**, 655 (1931); **A133**, 615 (1931).

[3] F. L. Arnot, Proc. Roy. Soc. **A125**, 660 (1929).

Lower Limit for the Ground State of the Helium Atom

In a recent paper[1] I have derived an expression for a lower limit of the lowest energy level of a Schrödinger equation. In order to show how practical this expression was, it was evaluated for the case of helium with a hydrogen-like function. This turned out to involve an integral which I was not then able to evaluate, and what was thought to be a safe approximation of $(7/16)a^2$ was given. Through Mr. E. B. Wilson, Jr., however, I have obtained the exact value, which is $(2/3)a^2$. The result is that the lower limit is pushed so far down (9.4 *Rh*, experimental value 5.809 *Rh*) that this simple example is of no value. This does not vitiate the expression theoretically inasmuch as it approaches the true value from the bottom as rapidly as the upper limit does from the top, but practically its usefulness is strongly impaired since more exact functions, such as those given by Hylleraas,[2] are required in order to get a reasonably close lower limit; and for these functions the computations are much more involved. So far, the computations have been carried out only for the worst function of a group given by Hylleraas.

[1] D. H. Weinstein, Phys. Rev. **40**, 797 (1932).

[2] E. A. Hylleraas, Zeits. f. Physik **54**, 347 (1929).

I have found an expression for a lower limit which is an improvement over the one originally given. We have in the same notation as before,

$$I_2 - I_1^2 = \sum_{n=0}^{\infty} (w_n - I_1)^2 a_n^2$$
$$= (w_0 - I_1)^2 + \sum_{n=1}^{\infty} (w_n - w_0)(w_n + w_0 - 2I_1)a_n^2 .$$

If now $I_1 \leqq (w_1+w_0)/2$, Eq. (1a) will contain positive terms only. Hence, $I_2 - I_1^2 \geqq (w_0 - I_1)^2$. Now since $I_1 \geqq w_0$, $I_1 - (I_2 - I_1^2)^{1/2} \leqq w_0$. This new lower limit is virtually an absolute lower limit since the restriction (2) is nearly always satisfied, and a theoretical discussion of it can be easily made.

It is also worth noting that $I_2 \geqq I_1^2$ in general, as is obvious from Eq. (1).

If we use a hydrogen-like function we get $I_1 - (I_2 - I_1^2)^{1/2} = -7.6$ *Rh*, while the upper limit is -5.5 *Rh*. If we use the Hylleraas function $\xi = (1+c_1t^2)\exp(c_2s)$ we obtain -6.8 *Rh* for the lower limit and -5.75 *Rh* for the upper limit. It is seen that, as expected, improving the function also improves the lower limit, which, however, does not approach the experimental value so rapidly as the upper limit.

D. H. WEINSTEIN
California Institute of Technology,
August 16, 1932.

BOOK REVIEW

Elektrolyte. HANS FALKENHAGEN. Pp. 346+xvi, Figs. 104. S. Hirzel, Leipzig. Price 23. RM.

This is a comprehensive monograph on various aspects of the electrolyte problem from the point of view of the Debye-Hückel theory. The author has made valuable contributions to the subject of electrolytic conductance and is well qualified to present this subject. Purely thermodynamic properties are treated in extenso as well as important related subjects, such as the dielectric constants and viscosities of electrolytes.

The mathematical treatment naturally follows closely the notation and methods developed by the German school, but significant variations and advances introduced by others receive recognition. Both the expert and the investigator who approaches the subject for the first time will find the book a valuable source of information.

VICTOR K. LA MER
Columbia University

AUTHOR INDEX TO VOLUME 41

References with (A) are to abstracts of papers presented at meetings of the Physical Society and references with (L) are to Letters to the Editor.

Abbott, Frank R. (see Henderson, Jos. E.)—261(A)
Abramson, Harold A. and Hans Mueller. Surface charge of large particles in liquids—386(A)
Adams, W. S. and Theodore Dunham, Jr. Absorption bands in the infrared spectrum of Venus—264(A)
Allison, Samuel K. Reflecting and resolving power of calcite for x-rays—1; 688(L)
Almy, John E. Book reviews—259
Anderson, Carl D. Energies of cosmic-ray particles—405
Appleyard, E. T. S. Electronic structure of the a-X band system of N_2—254(L)
Arnot, F. L. Angular distribution of elastically scattered electrons in mercury vapour—838

Bacher, R. F. and E. U. Condon. Spin of the neutron—683(L)
Bainbridge, K. T. Isotopic weight and packing fraction of H^2—115(L)—396(A)
Banta, H. E. Some thermo- and galvanomagnetic properties of a bismuth crystal—239
Barker, E. F. Constants of the N_2O molecule—369(L)
——— (see Martin, P. E.)—291
Bartlett, B. W. Variation of the principal magnetic susceptibilities of certain paramagnetic crystals with temperature—818
Bartlett, James H., Jr. Structure of atomic nuclei—370(L)
Barton, Vola P. and Geo. A. Lindsay. Fine structure in the x-ray K absorption edge of calcium in compounds—391(A)
Batho, Harold F. Equilibrium between positive ions and neutral atoms in positive rays of the rare gases—686(L)
Bayley, P. L. (see Thorne, A. M.)—376(L)
Bayliss, Noel S. (see Gibson, G. E.)—388(A)
Beals, C. S. On the temperatures of Wolf-Rayet stars and novae—264(A)
Beams, J. W. Some evidence indicating a removal of positive ions from cold surfaces by electric fields—687(L)
——— **and John W. Flowers.** Initiation of electrical discharges in effectively ion free gases—394(A)
Bearden, J. A. Status of x-ray wave-lengths—399(A)
Beck, F. J. and L. W. McKeehan. Monocrystal Barkhausen effects in rotating fields—385(A)
Bennett, R. D., J. C. Stearns, and A. H. Compton. Diurnal variation of cosmic rays—119
Benz, Carl A. (see Poulter, Thos. C.)—366
Berkey, Donald K. Yield of fluorescent x-rays from the K shells of various elements—390(A)
Birch, Francis. Electrical resistance and the critical point of mercury—641
Bitter, Francis. Magnetism and plasticity—401(A)
——— Experiments on the nature of ferromagnetism—507
Bleakney, Walker. Search for isotopes of hydrogen and helium—32
Bond, W. N. Probable values of e, h, e/m and α.—Reply to R. T. Birge—368(L)
Bowen, I. S. Ionization of air by γ-rays as a function of pressure and collecting field—24
Bozorth, Richard M. and Joy F. Dillinger. Barkhausen effect. III. Nature of change of magnetization in elementary domains—345
Bradbury, Norris E. Photoelectric currents in gases between parallel plates as a function of the potential difference—262(A)
Brady, James J. Photoelectric properties of alkali metal films as a function of their thickness—613
Bramley, A. (see Swann, W. F. G.)—393(A)
Brasefield, Charles J. Ionization of helium, neon and argon under impact of their own positive ions—394(A)
Breit, G. (see Rosenthal, Jenny E.)—459
Brown, R. R. H. and J. J. Muir. Vapor pressure of sulphur at 50°C—111(L)
Bruce, C. W. Kerr electro-optical effect in carbon dioxide—394(A)
Buckley, Francis (see Poulter, Thos. C.)—364

Campbell, J. W. Book review—118
Carlson, J. F. and J. R. Oppenheimer. Impacts of fast electrons and magnetic neutrons—763
Clay, J. (see Zanstra, H.)—679(L)
Cole, Kenneth S. Theory of surface conductance at an electrolyte-solid interface—387(A)
——— Electric phase angle of cell membranes—387(A)

Compton, Arthur H. Variation of the cosmic rays with latitude—111(L)
——— Progress of cosmic-ray survey—681(L)
——— (see Bennett, R. D.)—119
——— **and John J. Hopfield.** Use of argon in the ionization method of measuring cosmic rays—539(L)
Condon, E. U. Production of infrared spectra with electric fields—759
——— (see Bacher, R. F.)—683(L)
Cooksey, D. and M. C. Henderson. Threshold counting voltage of the Geiger-Müller tube and some related phenomena—392(A)
Cork, J. M. Further experiments on x-ray reflections from quartz crystals oscillating piezoelectrically—391(A)
——— (see Witmer, R. B.)—391(A)
Coven, Allen W. Scattering of x-rays from solids—422
Cram, W. and J. G. Winans. Observations on the fluorescence spectra of cadmium vapor—388(A)
Cunningham, W. Peyton. Zeeman effect in the $^2\Pi$–$^2\Sigma$ CaH bands—389(A)
Curtis, H. J. Dielectric constant of liquid sulphur—386(A)
Curtiss, L. F. Rôle of gas adsorption in counting chambers—379(L)

Dahlstrom, R. K. (see Henderson, Jos. E.)—261(A)
Davis, H. M. (see Glockler, Geo.)—370(L)
Del Rosario, C. Very soft x-ray spectra of heavy elements—136
Dennison, David M. Vibrational levels of linear symmetrical triatomic molecules—304
——— **and G. E. Uhlenbeck.** Two-minima problem and the ammonia molecule—313
De Vore, H. B. (see Workman, E. J.)—262(A)
Dillinger, Joy F. (see Bozorth, Richard M.)—345
Du Mond, J. W. M. X-ray evidence for high electron momenta in atoms and in solid bodies—398(A)
Duncan, J. A. Absorption spectrum of sulfur dioxide—388(A)
Dunham, J. L. Wentzel-Brillouin-Kramers method of solving the wave equation—713
——— Energy levels of a rotating vibrator—721
Dunham, Theodore, Jr. (see Adams, W. S.)—264(A)

Eckart, Carl. Book review—382
Elbe, Guenther von. (see Lewis, Bernard)—678(L)
Epstein, Paul S. On the specific heats of ferromagnetic materials—262(A)
——— On ferromagnetism and related problems of the theory of electrons—91
Evjen, H. M. On the effect of a secondary structure upon the interference of x-rays—265

Flowers, John W. (see Beams, J. W.)—394(A)
Ford, O. Rex. Survey of the *K*-satellites—577
Foster, Ronald M. Mutual impedance of grounded wires above the surface of the earth—536
Froman, Darol K. Faraday effect with x-rays—693

Giacomini, Amedeo. Production of ultra-short electromagnetic waves—113(L)
Gibbs, R. C. (see Kruger, P. Gerald)—322
Gibson, G. E. and Noel S. Bayliss. Continuous absorption spectrum of chlorine—388(A)
Gingrich, Newell S. Dependence of the ionization produced by γ-rays upon pressure and temperature—679(L)
Glockler, George. Electron affinity of hydrogen—685(L)
——— **and H. M. Davis.** Raman effect of methyl acetylene—370(L)
Gray, J. A. Spectrum of scattered radiation—397(A)
Green, J. B. and R. A. Loring. Zeeman effect of Pb III—389(A)
Grew, K. E. Variation with temperature of the thermoelectric power of nickel and some copper-nickel alloys—356
Gropper, L. (see Uhlenbeck, G. E.)—79
Gunn, Ross. Diurnal variation of cosmic rays and terrestrial magnetism—683(L)

Hanawalt, J. D. Fine structure in x-ray absorption spectra—399(A)
Hardy, J. D. and G. B. B. M. Sutherland. Isotope separations in the infrared absorption spectrum of HCl and the possible existence of a chlorine isotope of Mass 39—471
Harrington, E. L. New type of vacuum or circulating pump—395(A)
Hartig, Henry E. Book review—380
Havens, Glenn G. Magnetic susceptibility of nitrogen dioxide—337
Henderson, Jos. E., R. K. Dahlstrom and Frank R. Abbott. Energy distribution of electrons in field current emission—261(A)
Henderson, M. C. Gamma-ray spectrometer—392(A)
——— (see Cooksey, D.)—392(A)
Higley, Elizabeth A. and Carolyn C. Thorsen. Mobilities of gaseous ions in mixtures of hydrogen and nitromethane and hydrogen and methyl cyanide—263(A)
Hill, E. L. Book review—117
Holmes, F. T. Raman effect in crystalline NH_4Cl—389(A)
Hopfield, John J. (see Compton, Arthur H.)—539(L)
Houston, William V. Theory of the Raman rotation spectra—263(A)

Hoyt, Archer. Errata: Shape of an x-ray line—110
Hubbard, J. C. Acoustic resonator interferometer: II. Ultrasonic velocity and absorption in gases—523
Hughes, A. L. and J. H. McMillen. Elastic and inelastic electron scattering in hydrogen—39
——— **J. H. McMillen and G. M. Webb.** Elastic electron scattering in helium—154

Jauncey, G. E. M. and P. S. Williams. Diffuse scattering of x-rays from sodium fluoride—127
Joffe, Joseph. Alternation of intensities in the sodium bands—388(A)
Johnson, Thomas H. Interpretation of cosmic-ray phenomena—393(A); 545
——— **and J. C. Street.** Variation of the cosmic-ray intensity with azimuth—690(L)

Kaplan, Joseph. Predissociation in nitrogen—114(L)
Kellogg, J. M. B. Reflection of thallium, lead and antimony atoms from sodium chloride crystals—635
Kelly, M. J. (see Prescott, C. H., Jr.)—395(A)
Kenty, Carl. Escape of imprisoned resonance radiation from a gas—390(A)
Kistiakowsky, G. B. and M. Nelles. Resonance fluorescence of benzene—595
Korff, S. A. Frequency of resonance radiation—538(L)
Kruger, P. Gerald and R. C. Wagner. Note on the hyperfine structure of beryllium lines—373(L)
——— **R. C. Gibbs and R. C. Williams.** Nuclear moment of barium as determined from the hyperfine structure of the Ba II lines—322
Kuhn, H. and O. Oldenberg. Evidence of space quantization of atoms upon impact—72
Kunz, Jakob. Distribution of electrons in the photoeffect by Roentgen rays, classically treated—263(A)
Kurie, F. N. D. New measurements of the ranges of alpha-particles from polonium, uranium I and uranium II with the Wilson chamber—392(A); 701
La Mer, Victor. Book review—840
Langer, R. M. Theorem on spectroscopic stability—390(A)
——— Book review—258

Lewis, Bernard and Guenther von Elbe. Experimental evidence for and determination of the predicted $^1\Delta$ level of the neutral oxygen molecule—678(L)
Lewis, Charlton M. Rotational Raman effect of gases—389(A)
Linder, Ernest G. Mass-spectrograph study of the ionization and dissociation by electron impact of benzene and carbon bisulfide—149
Lindsay, Geo. A. (see Barton, Vola P.)—391(A)
Loeb, Leonard B. Mobilities of sodium ions in helium measured in short time intervals—261(A)
Loring, R. A. (see Green, J. B.)—389(A)
Luyten, W. J. Book reviews—380; 381

March, H. W. Book review—259
Martin, Emmet V. Band spectrum of sulphur monoxide—167
Martin, P. E. and E. F. Barker. Infrared absorption spectrum of carbon dioxide—291
McKeehan, L. W. (see Beck, F. J.)—385(A)
McMillen, J. H. (see Hughes, A. L.)—39; 154
McPherson, A. I. Radiation from moving helium, neon and argon ions—686(L)
Meserve, Wilbur E. Some photovoltaic properties of $Cu:Cu_2O\,|Pb(NO_3)_2$ solution $|Cu:Cu_2O$ photocells—396(A)
Miller, Henry J. Study of getter action of phosphorous—394(A)
Mimno, Harry R. and P. H. Wang. New devices for recording Kennelly-Heaviside layer reflections—395(A)
Mouzon, J. Carlisle. Ionization of neon and argon by positive alkali ions of energies from 650 to 2000 volts—605
Mueller, Hans (see Abramson, Harold A.)—386(A)
Muir, J. J. (see Brown, R. R. H.)—111(L)
Muller, R. H. and A. Spector. Becquerel effect as a special case of the barrier-layer photoelectric cell—371(L)
Mulliken, Robert S. Electronic structures of polyatomic molecules and valence. II. General considerations—49
——— Electronic structures of polyatomic molecules and valence. III. Quantum theory of the double bond—751
Murphy, George M. and Harold C. Urey. On the relative abundances of the nitrogen and oxygen isotopes—141

Nathansen, J. B. Newton's rings in transparent metallic films—373(L)
Nelles, M. (see Kistiakowsky, G. B.)—595
Nottingham, Wayne B. Photoelectric and thermionic emission from composite surfaces—793

O'Brien, Brian and Vernon L. Parks. Photographic reciprocity and intermittency defects near the long wave-length limit of plate sensitivity—387(A)
Oldenberg, O. (see Kuhn, H.)—72
Olpin, A. R. Book review—116
Oppenheimer, J. R. (see Carlson, J. F.)—763

Parker, Allan E. Analysis of the (0,0) $^3\Pi \rightarrow {}^3\Sigma$ CN band at 9168A—274

Parks, Vernon L. (see O'Brien, Brian)—387(A)
Parratt, Lyman G. X-ray diffraction from calcite for wave-lengths 1.5 to 5A—561
——— Design of a double-crystal x-ray vacuum spectrometer—553
Pearce, J. A. Absolute magnitudes of the 05 to B2 stars determined from the interstellar lines—264(A)
Penney, William G. and Robert Schlapp. Influence of crystalline fields on the susceptibilities of salts of paramagnetic ions. I. The rare earths, especially Pr and Nd—194
Pielemeier, W. H. Supersonic dispersion and absorption in CO_2—833
Plesset, Milton S. Dirac electron in simple fields—278
Potapenko, G. Investigations in the field of the ultra-short electromagnetic waves. IV. On the dependence of the ultra-short electromagnetic waves upon the heating current and upon the amplitude of the oscillations—216
Poulter, Thos. C., Carter Ritchey and Carl A. Benz. Effect of pressure on the index of refraction of paraffin oil and glycerine—366
——— **and Francis Buckley.** Diamond windows for withstanding very high pressures—364
Prescott, C. H., Jr. and M. J. Kelly. Caesium-oxygen-silver photoelectric cell—395(A)

Rao, S. Ramachandra. Total secondary electron emission from metal faces—374(L)
Rashevsky, N. Some remarks on the physical constants of cells in connection with their size and shape—387(A)
Rayton, W. M. (see Wilkins, T. B.)—396(A)
Richardson, R. S. Investigation of the hydrocarbon bands in the solar spectrum—264(A)
Ritchey, Carter (See Poulter, Thos. C.)—366
Robertson, H. P. Book reviews—543
Rogers, Henry H. Relation of relative humidity to the absorption of supersonic waves in various mixtures of CO_2—369(L)
Rojansky, V. Book review—380
Rosen, N. (see Vallarta, M. S.)—708
Rosenthal, Jenny E. and G. Breit. Isotope shift in hyperfine structure—459
Roth, Herman. Elimination of one boundary condition for a sphere in radiative equilibrium by a layer in adiabatic equilibrium—327
Ruedy, J. E. Series and term values in the arc spectrum of tellurium—588

Sabine, Paul E. Book review—691
Sanders, Frederick H. Determination of the coefficient of ionization by collision using large plate distances and higher pressures—263(A)
——— Value of the Townsend coefficient for ionization by collision at large plate distances and near atmospheric pressure—667
Sanford, R. F. Further details ascribable to bands of the carbon isotope C_{13} in stars of spectral classes *R* and *N*—264(A)
Schlapp, Robert. (see Penney, William G.)—194
Schmid, R. F. Rotational analysis of some CO_2 emission bands—732
Serber, Robert. Theory of the Faraday effect in molecules—489
Silverman, S. Absorption spectrum of benzene in the region of 6.75μ—486
Sixtus, K. J. (see Tonks, Lewi)—539(L)
Slater, J. C. Note on molecular structure—255(L)
Smallwood, Hugh M. Infrared dispersion of carbon dioxide—164
Smith, P. T. Book review—382
Soroos, Adolf. Thermoelectric power of single crystal bismuth near the melting point—516
Spector, A. (see Muller, R. H.)—371(L)
Spencer, Roy C. Additional theory of plane gratings for x-rays—392(A)
Stearns, J. C. (see Bennett, R. D.)—119
Street, J. C. (see Johnson, Thomas H.)—690(L)
Sutherland, G. B. B. M. (see Hardy, J. D.)—471
Swann, W. F. G. Electrons as cosmic rays—540(L)
——— Bearing of the earth's internal magnetic permeability upon the self- and mutual inductance by coils wound on its surface—649
——— **and A. Bramley.** Generalization of wave mechanics suggested by higher order terms in the classical electrodynamic equation of motion, and its influence on β-particles ionization for velocities approaching that of light—393(A)

Thorne, A. M. and P. L. Bayley. Raman spectra of two liquid phases of nitrobenzene—376(L)
Thorsen, Carolyn C. (See Higley, Elizabeth A.)—263(A)
Tonks, Lewi and K. J. Sixtus. Strain and magnetic orientation—539(L)
Turner, Louis A. Optical dissociation of iodine and enhancement of predissociation by collisions—627

Uhlenbeck, G. E. and L. Gropper. Equation of state of a non-ideal Einstein-Bose or Fermi-Dirac gas—79
——— (see Dennison, David M.)—313
Urey, Harold C. (see Murphy, George M.)—141

Valasek, Joseph. Book review—381
Vallarta, M. S. and N. Rosen. Relativistic Thomas-Fermi atom—708
Vance, Bruce B. Spectra of Na II, III, and IV in the extreme ultraviolet—480

Van Vleck, J. H. Theory of the variations in paramagnetic anisotropy among different salts of the iron group—208; 385(A)
——— (see Whitelaw, N. G.)—389(A)
——— Book reviews—117; 381; 543
Vinti, J. P. Relation between the electric and diamagnetic susceptibilities of monatomic gases—813
——— Sum rules for atomic transition probabilities—432

Wagner, R. C. (see Kruger, P. Gerald)—373(L)
Walther, H. (see Wegel, R. L.)—402(A)
Wang, P. H. (see Mimno, Harry R.)—395(A)
Waterman, A. T. Form of potential barrier at the surfaces of conductors—395(A)
Watson, William W. New band system of barium hydride in the infrared—377(L)
——— Zeeman effect and perturbations in the CO angstrom and N_2^+ bands—378(L)
Webb, G. M. (see Hughes, A. L.)—154
Wegel, R. L. and H. Walther. Internal dissipational resistance to distortion in solids and its correlation with other physical properties—402(A)
Weinstein, D. H. Lower limit for the ground state of the helium atom—839(L)
Wheeler, Mary A. Magnetic susceptibilities of alpha- and beta-manganese—331
Whitelaw, N. G. and J. H. Van Vleck. Theory of quantum defect due to polarization, with application to multiplet anomalies in Al II—389(A)
Wilkins, T. B. and W. M. Rayton. Isotopes of uranium—396(A)
Williams, J. W. Dielectric constant and particle weight—386(A)
Williams, P. S. (see Jauncey, G. E. M.)—127
Williams, Robley C. Deposition of chromium on glass—255(L)
——— (see Kruger, P. Gerald)—322
Williams, S. R. Mechanical hardness influenced by magnetism—386(A)
———Does nickel show a positive elongation in the Joule magnetostrictive effect?—251
Winans, J. Gibson. Origin of the mercury bands at 2480A—388(A)
——— (see Cram, W.)—388(A)
Witmer, R. B. and J. M. Cork. X-ray wave-lengths by ruled grating—391(A)
Wolfe, Hugh C. Multiplet splitting and intensities of intercombination lines—Part I—443
Woo, Y. H. Scattering of x-rays by gases and crystals—21
Wood, Lawrence A. Hall effect with audiofrequency currents—231
Workman, E. J. Secondary effects in the ionization by hard gamma-rays—264(A)
——— **and H. B. De Vore.** Electroscope of high charge sensitivity—262(A)
Wulf, Oliver R. Theory of the ozone of the lower atmosphere and its relation to the general problem of atmospheric ozone—375(L)

Zanstra, H. and J. Clay. Remark on Erikson's measurements of the ionization by γ-rays at various pressures and potentials—679(L)
Zwicky, F. On the problem of the solid state—400(A)

ANALYTIC SUBJECT INDEX TO VOLUME 41

References marked (A) are to abstracts of papers presented at meetings of the Physical Society, those marked with (L) are to Letters to the Editor.

Acoustics

Humidity and absorption supersonic waves, H. H. Rogers—369(L)

Supersonic dispersion and absorption in CO_2, W. H. Pielemeier—833

Ultrasonic velocity and absorption, J. C. Hubbard—523

Affinity

Electron affinity of H, G. Glockler—685(L)

Alpha-particles (see also **Radioactivity**)

Ranges from Po, Ur I and Ur II, F. N. D. Kurie—701; 392(A)

Astrophysics

Sphere in radiative equilibrium, H. Roth—327

Atomic and molecular beams

Equilibrium between ions and neutral atoms, H. F. Batho—686(L)

Radiation from He, N and A, A. I. McPherson—686(L)

Reflection of Tl, Pb and Sb from NaCl crystals, J. M. B. Kellogg—635

Atomic structure (see also **Energy states of atoms; Spectra**)

Ground state of He, D. H. Weinstein—839(L)

High electron momenta in atoms, J. W. M. Du Mond—398(A)

Relativistic Thomas-Fermi atom, M. S. Vallarta, N. Rosen—708

Atmosphere

Theory of the ozone of the lower atmosphere and its relation to the general problem of atmospheric ozone, O. R. Wulf—375(L)

Atmospheric electricity (see also **Geophysics**)

Recording Kennelly-Heaviside layer reflections, H. R. Mimno, P. H. Wang—395(A)

Barkhausen effect (see **Magnetic properties**)

Biophysics

Electric phase angle of cell membranes, K. S. Cole—387(A)

Size and shape of cells, N. Rashevsky—387(A)

Book reviews

Bateman, H. Partial Differential Equations of Mathematical Physics—543

Brinkman, H. C. Zur Quantenmechanik der Multipolstrahlung—382

ten Bruggencate, P. Ergebnisse der Exacten Naturwissenschaften—380

Darwin, C. G. New Conceptions of Matter—259

Falkenhagen, Hans. Elektrolyte—840

Gans, Richard. Vector Analysis, with Applications to Physics—380

Gorter, C. J. Paramagnetische Eigenschaften von Salzen—117

Hanle, W. and K. Larché. Die Lichtausbeute bei Stossanregung—382

Hopf, Ludwig. Die Relativitätstheorie—543

Hughes, A. L. and L. A. DuBridge. Photoelectric Phenomena—116

International Research Council and the International Union of Pure and Applied Chemistry. Annual Tables of Constants and Numerical Data, Chemical, Physical, Biological and Technological—258

Jeffreys, Harold. Cartesian Tensors—117

Knudsen, Vern O. Architectural Acoustics—691

v. Laue, M. Die dynamische Theorie der Roentgenstrahlinterferenzen in neuer Form—381

Pease, F. G. Interferometer Methods in Astronomy—381

Pirani, N. Graphische Darstellung in Wissenschaft und Technik—380

Pohl, R. W. Einführung in die Mechanik und Akustik—118

Stuart, H. A. Kerr-Effekt, Lichtzerstreuung und Molekülbau—381

Tietjens, O. Hydro- und Aeromechanik nach Vorlesungen von L. Prandtl, Bd. II—259

Waerden, B. L. van der. Die gruppentheoretische Methode in der Quantenmechanik—543

Wiersma, E. E. Eenige Onderzoekingen over Paramagnetisme—117

Colloids

Dielectric constant, J. W. Williams—386(A)

Conductivity, electrical (see **Electrical conductivity; Discharge of electricity in gases**)

Constants, physical

Status of x-ray wave-lengths, J. A. Bearden—399(A)

Values of e, h, e/m and α, W. N. Bond—368(L)

Cosmic radiation

Absorption coefficients, interpretation of phenomena, T. H. Johnson—545; 393(A)

β-particle ionization for velocities approaching that of light, W. F. G. Swann, A. Bramley—393(A)

Dependence of ionization on pressure and temperature, N. S. Gingrich—679(L)

Diurnal variation, R. D. Bennett, J. C. Stearns, A. H. Compton—119

Diurnal variation and terrestrial magnetism, R. Gunn—683(L)

Electrons as cosmic rays, W. F. G. Swann—540(L)

Energies of particles; photographs, C. D. Anderson—405

γ-ray ionization at high pressure, H. Zanstra, J. Clay—679(L)

Impacts of fast electrons and neutrons, J. F. Carlson, J. R. Oppenheimer—763

Ionization as a function of pressure and collecting field, I. S. Bowen—24

Use of A for measuring rays, A. H. Compton, J. J. Hopfield—539(L)

Variation with azimuth, T. H. Johnson, J. C. Street—690(L)

Variation with latitude and altitude, A. H. Compton—111(L); 681(L)

Crystals and crystal structure

Reflection of x-ray from calcite; mosaic structure, S. K. Allison—1; 688(L)

Seconday structure and the interference of x-rays, H. M. Evjen—265

Secondary structures. Solid state, F. Zwicky—400(A)

Thermo- and galvanomagnetic properties of Bi, H. E. Banta—239

Thermoelectric power of near melting point. Crystals in liquid state, A. Soroos—516

X-ray diffraction from calcite, L. G. Parratt—561; S. K. Allison—688(L)

Dielectric constants

Of liquid S, H. J. Curtis—386(A)

And particle weight, J. W. Williams—386(A)

Dielectrics and dielectric properties

Electric and diamagnetic susceptibilities of monatomic gases, J. P. Vinti—813

Diffraction of molecules (see **Atomic and molecular beams**)

Discharge of electricity in gases

Townsend coefficient for ionization by collision, F. H. Sanders—667; 263(A)

Discharge of electricity in high vacua (see also **Thermionic emission; High voltage tubes and machines**)

Energy distribution, J. E. Henderson, R. K. Dahlstrom, F. R. Abbott—261(A)

Initiation of discharge, J. W. Beams, J. W. Flowers—394(A)

Positive ions from cold surfaces by electric fields, J. W. Beams—687(L)

Dissociation

Of benzene and carbon bisulfide, E. G. Linder—149

Of I_2 by light, L. A. Turner—627

Efficiency of ionization

By positive ions, J. C. Mouzon—605

Elasticity

Internal resistance; correlation with other physical properties, R. L. Wegel, H. Walther—402(A)

Magnetic hardening of metals, S. R. Williams—386(A)

Magnetism and plasticity, F. Bitter—401(A)

Strain and magnetic orientation, L. Tonks, K. J. Sixtus—539(L)

Electrical conductivity and resistance

Of Hg and its critical point, F. Birch—641

Electrical circuits

Inductance of coils wound on the earth, W. F. G. Swann—649

Mutual impedance of grounded wires, R. M. Foster—536

Electrolytes

Conductance at an electrolyte-solid interface, K. S. Cole—387(A)

Electromagnetic theory

Inductance of coils wound on the earth, W. F. G. Swann—649

Mutual impedance of grounded wires, R. M. Foster—536

Electromagnetic waves

Ultra-short waves, G. Potapenko—216

Electrons, scattering of
Angular distribution in Hg, F. L. Arnot—838(L)
In He; elastic, A. L. Hughes, J. H. McMillen, G. M. Webb—154
In H; elastic and inelastic, A. L. Hughes, J. H. McMillen—39

Electrons, secondary
Number from metal surfaces, S. R. Rao—374(L)

Electrons, thermionic (see **Thermionic emission**)

Electron tubes (see **Discharge of electricity in high vacua; Vacuum tubes**)

Electro-optical effects (see also **Photoelectric effect and properties**)
Kerr effect in CO_2, C. W. Bruce—394(A)

Energy states of atoms (see also **Atomic structure; Spectra, atomic**)
Ground state of He, D. H. Weinstein—839(L)

Errata
Shape of an x-ray line, A. Hoyt—110

Faraday effect (see also **Magneto-optical effects**)
Faraday effect with x-rays, D. K. Froman—693

Field currents (see also **Discharge of electricity in high vacua**)
Energy distribution, J. E. Henderson, R. K. Dahlstrom, F. R. Abbott—261(A)
Positive ions from cold surfaces by electric fields, J. W. Beams—687(L)

Fluorescence
Of benzene, G. B. Kistiakowsky, M. Nelles—595
Of Cd, W. Cram, J. G. Winans—388(A)
Space quantization of atoms upon impact, H. Kuhn, O. Oldenberg—72

Galvanomagnetic effects
In Bi crystal, H. E. Banta—239

Geophysics
Permeability of the earth, W. F. G. Swann—649

Getters
Getter action of P, H. J. Miller—394(A)

Hall effect
In Te with audiofrequency currents, L. A. Wood—231

High voltage tubes and machines
Removal of positive ions from cold surfaces by electric fields, J. W. Beams—687(L)

Hyperfine structure
Of Ba II lines, P. G. Kruger, R. C. Gibbs, R. C. Williams—322
Of Be, P. G. Kruger, R. C. Wagner—373(L)
Isotope shift, J. E. Rosenthal, G. Breit—459

Instruments (see **Methods and instruments**)

Intensities in spectra (see also **Spectra, etc.**)
And multiplet splitting, H. C. Wolfe—443

Interference phenomena
Newton's rings in metallic films, J. B. Nathanson—373(L)

Ionization by positive ions (see also **Ionization potentials**)
Of C_6H_6 and CS_2, E. G. Linder—149
β-particle ionization for velocities approaching that of light, W. F. G. Swann, A. Bramley—393(A)
Ionization of He, Ne and A under impact of their own positive ions, C. J. Brasefield—394(A)
Ne and A by alkali ions, J. C. Mouzon—605

Ionization by radiation (see also **Photo-ionization**)
Dependence of the ionization produced by γ-rays upon pressure and temperature, N. S. Gingrich—679(L)
Use of A in the ionization method of measuring cosmic rays, A. H. Compton, J. J. Hopfield—539(L)

Ionization potentials
Of C_6H_6 and CS_2, E. G. Linder—149
Of He, Ne and A by atoms and positive ions, C. J. Brasefield—394(A)

Ions, in gases
Townsend coefficient for ionization by collision, F. H. Sanders—263(A)

Ions, mobility (see also **Ions, in gases**)
In H_2 with nitromethane and methyl cyanide, E. A. Higley, C. C. Thorsen—263(A)
Of Na ions in He, L. B. Loeb—261(A)
Photoelectric currents in gases, N. E. Bradbury—262(A)

Isotopes
Existence of Cl^{39}; separations in the infrared absorption spectrum of HCl, J. D. Hardy, G. B. B. M. Sutherland—471
Of H and He, W. Bleakney—32
Relative abundances in N and O, G. M. Murphy, H. C. Urey—141

Isotopes continued
Theory of rotation spectra, W. V. Houston—263(A)
Of U, T. B. Wilkins, W. M. Rayton—396(A)
Weight of H^2, K. T. Bainbridge—115(L); 396(A)

Kerr effect (see **Electro-optical effects**)

Liquids
Surface charge of large particles, H. A. Abramson, Hans Mueller—386(A)

Magnetic properties
Barkhausen effects in rotating fields, F. J. Beck, L. W. McKeehan—385(A)
Of Bi crystal, thermo- and galvanomagnetic properties, H. E. Banta—239
Electric and diamagnetic susceptibilities of monatomic gases, J. P. Vinti—813
Ferromagnetism and theory of electrons, P. S. Epstein—91
Mechanical hardness influenced by magnetism, S. R. Williams—386(A)
Paramagnetic anisotropy in salts of the iron group, J. H. Van Vleck—208; 385(A)
Patterns showing irregularities of magnetization, F. Bitter—507
And plasticity, F. Bitter—401(A)
Specific heats of ferromagnetic materials, P. S. Epstein—262(A)
Strain and magnetic orientation, L. Tonks, K. J. Sixtus—539(L)
Susceptibilities of α- and β-Mn, M. A. Wheeler—331
Susceptibilities of salts of paramagnetic ions, W. G. Penney, R. Schlapp—194
Susceptibility of NO_2, G. G. Havens—337
And thermoelectric power of Ni and Cu-Ni alloys, K. E. Grew—356
Transverse Barkhausen effect. Domain theory, R. M. Bozorth, J. F. Dillinger—345
Variation of susceptibilities of crystals with temperature, B. W. Bartlett—818

Magneto-optical effects
Faraday effect in molecules, R. Serber—489
Faraday effect with x-rays, D. K. Froman— 693

Magnetostriction
Does nickel show a positive elongation, S. R. Williams—251

Mechanics, quantum—general
Dirac electron in simple fields, M. S. Plesset—278
Electric and diamagnetic susceptibilities of monatomic gases, J. P. Vinti—813
Equation of state of Einstein-Bose or Fermi-Dirac gas, G. E. Uhlenbeck, L. Gropper—79
Ferromagnetism and theory of electrons, P. S. Epstein—91
Impacts of fast electrons and neutrons, J. F. Carlson, J. R. Oppenheimer—763
Space quantization of atoms upon impact, H. Kuhn, O. Oldenberg—72
Transition probabilities, J. P. Vinti—432
Wentzel-Brillouin-Kramers method of solving wave equations, J. L. Dunham—713

Mechanics, quantum—molecular structure and spectra
Energy levels of rotating vibrator, J. L. Dunham—721
Two-minima problem, D. M. Dennison, G. E. Uhlenbeck—313

Mechanics, statistical
Equation of state Einstein-Bose or Fermi-Dirac gas, G. E. Uhlenbeck, L. Gropper—79

Methods and instruments
Cs-O-Ag photoelectric cell, C. H. Prescott, Jr., M. J. Kelly—395(A)
Deposition of Cr on glass, R. C. Williams—255(L)
Diamond windows for high pressures, T. C. Poulter, F. Buckley—364
Double-crystal x-ray vacuum spectrometer, L. G. Parratt—553
Electroscope of high-charge sensitivity, E. J. Workman, H. B. De Vore—262(A)
γ-ray spectrometer, M. C. Henderson—392(A)
Gas adsorption in counting chambers, L. F. Curtiss—379(L)
Getter action of P, H. J. Miller—394(A)
Recording Kennelly-Heaviside layer reflections, H. R. Mimno, P. H. Wang—395(A)
Refractometer for high pressures, T. C. Poulter, C. Ritchey, C. A. Benz—366
Threshold voltage of the Geiger-Müller tube, D. Cooksey, M. C. Henderson—392(A)
Vacuum or circulating pump, E. L. Harrington—396(A)

Mobility of ions (see **Ions, mobility**)

Molecular structure and constants (see also **Spectra, molecular; Raman spectra**)
Ammonia molecule; two-minima problem, D. M. Dennison, G. E. Uhlenbeck—313
$^1\Delta$ of O_2, B. Lewis, G. von Elbe—678(L)
Electron affinity of H, G. Glockler—685(L)

Molecular structure and constants continued
Of N_2O, E. F. Barker—369(L)
Of polyatomic molecules and valence, R. S. Mulliken—49; 751; J. C. Slater—255(L)
Vibrational levels of triatomic molecules, (CO_2), D. M. Dennison—304

Nuclear Spin (see also **Hyperfine structure**)
Of neutron, R. F. Bacher, E. U. Condon—683(L)

Nucleus
Moment of Ba from hfs, P. G. Kruger, R. C. Gibbs, R. C. Williams—322
Moment of Be, P. G. Kruger, R. C. Wagner—373(L)
Structure, J. H. Bartlett, Jr.—370(L)

Neutrons
In atomic nuclei, J. H. Bartlett, Jr.—370(L)
Magnetic neutrons, J. F. Carlson, J. R. Oppenheimer—763
Spin, R. F. Bacher, E. U. Condon—683(L)

Optical constants and properties (see also **Electro-optical effects**)
Effect of pressure on index of refraction, T. C. Poulter, C. Ritchey, C. A. Benz—366
Infrared dispersion of CO_2, H. M. Smallwood—164

Optical instruments (see also **Methods and instruments**)
Deposition of Cr on glass, R. C. Williams—255(L)

Oscillators (see also **Electrical circuits**)
Ultra-short electromagnetic waves, A. Giacomini—113(L)
Ultra-short electromagnetic waves, G. Potapenko—216

Packing fraction
Of H^2, K. T. Bainbridge—396(A)

Photoelectric effect and properties
Of alkali metal films as a function of thickness, J. J. Brady—613
Barrier-layer photoelectric cell and Becquerel effect, R. H. Muller, A. Spector—371(L)
Cs-O-Ag cell, C. H. Prescott, Jr., M. J. Kelly—395(A)
Cu:Cu_2O $Pb(NO_3)_2$ solution Cu:Cu_2O photocells, W. E. Meserve—396(A)
Distribution of electrons classically treated, J. Kunz—263(A)
Photoelectric currents in gases, N. E. Bradbury—262(A)
Properties of composite surfaces, W. B. Nottingham—793

Photography
Reciprocity and intermittency defects, B. O'Brian, V. L. Parks—387(A)

Photo-ionization (see also **cosmic radiation**)
Of A in cosmic-ray apparatus, A. H. Compton, J. J. Hopfield—539(L)
Of air by γ-rays, dependence on pressure and collecting field, I. S. Bowen—24
γ-ray ionization at high pressures, H. Zanstra, J. Clay—679(L)
By hard γ-rays, E. J. Workman—264(A)
Produced by γ-rays, pressure and temperature changes, N. S. Gingrich—679(L)

Photometry
Reciprocity and intermittency defects for long wave-length, B. O'Brian, V. L. Parks—387(A)

Piezoelectric effect
And x-ray reflection, J. M. Cork—391(A)

Potential barriers
Form at the surfaces of conductors, A. T. Waterman—395(A)

Predissociation
Of I_2 enhanced by collisions, L. A. Turner—627
In N, J. Kaplan—114(L)
In SO, E. V. Martin—167

Radiation
Sphere in radiative equilibrium, H. Roth—327

Radioactivity
Isotopes of U, T. B. Wilkins, W. M. Rayton—396(A)
Ranges of α-particles, F. N. D. Kurie—701; 392(A)

Raman spectra
In crystalline NH_4Cl, F. T. Holmes—389(A)
Of liquid phases of nitrobenzene, A. M. Thorne, P. L. Bayley—376(L)
Of methyl acetylene, G. Glockler, H. M. Davis—370(L)
Rotational effect of gases, C. M. Lewis—389(A)

Relativity
Applied to Thomas-Fermi atom, M. S. Vallarta, N. Rosen—708
Dirac electron in simple fields, M. S. Plesset—278

Resistance, electrical (see **Electrical conductivity and resistance**)

Resonance radiation
Escape from a gas, C. Kenty—390(A)
Frequency of resonance and exciting radiation, S. A. Korff—538(L)

Specific heat
a-X band of N_2, E. T. S. Appleyard—254(L)
Of Ba H, W. W. Watson—377(L)
Of ferromagnetic materials, P. S. Epstein—262(A)

Spectra, absorption
Of benzene. New H_2O lines, S. Silverman—486
Continuous of Cl, G. E. Gibson, N. S. Bayliss—388(A)
Infrared of CO_2, P. E. Martin, E. F. Barker—291
Isotope separations in spectrum of HCl, J. D. Hardy, G. B. B. M. Sutherland—471
Of N_2O, E. F. Barker—369(L)
Production of infrared with electric fields, E. U. Condon—759
Of O_4, O. R. Wulf—375(L)
Of SO_2, J. A. Duncan—388(A)

Spectra, atomic
Isotope shift in hfs, J. E. Rosenthal, G. Breit—459
Of Na II, III and IV in extreme ultraviolet, B. B. Vance—480
Ground state of He, D. H. Weinstein—839(L)
Quantum defect due to polarization, N. G. Whitelaw, J. H. Van Vleck—389(A)
Radiation from moving He, Ne and A atoms, A. I. McPherson—686(L)
Of Te I, J. E. Ruedy—588
Transition probabilities, J. P. Vinti—432

Spectra, general
Multiplet splitting and intensities, H. C. Wolfe—443
Production of infrared with electric fields, E. U. Condon—759
Spectroscopic stability, R. M. Langer—390(A)

Spectra, molecular (see also **Molecular structure and constants**)
CN band at 9168A, A. E. Parker—274
CO_2 emission bands rotational analysis, R. F. Schmid—732
Electronic structures of polyatomic molecules, R. S. Mulliken—49; J. C. Slater—255(L)
Energy levels of rotating vibrator, J. L. Dunham—721
Origin of Hg bands at 2480A, J. G. Winans—388(A)
Polyatomic molecules; double bonds, R. S. Mulliken—751
Of SO rotational and vibrational structure, E. V. Martin—167
Vibrational levels of triatomic molecules, (CO_2), D. M. Dennison—304

Spectra, Raman (see **Raman spectra**)

Statistical mechanics (see **Mechanics, statistical**)

Supersonics (see also **Acoustics**)
Relation of relative humidity to the absorption of supersonic waves in various mixtures of CO_2, H. H. Rogers—369(L)
Supersonic dispersion and absorption in CO_2, W. H. Pielemeier—833

Susceptibility, magnetic (see **Magnetic properties**)

Thermionic emission of electrons, emitting surfaces
And photoelectric emission from composite surfaces, W. B. Nottingham—793

Thermoelectric effects
Of Ni and Cu-Ni alloys, variation with temperature, K. E. Grew—356

Vacuum tubes
Ultra-short electromagnetic waves, G. Potapenko—216

Valence
Quantum theory of the double bond, R. S. Mulliken—751
Structures of polyatomic molecules, R. S. Mulliken—49; J. C. Slater—255(L)

Vapor pressure
Of S, R. R. H. Brown, J. J. Muir—111(L)

Viscosity
Dielectric constant variation with frequency, J. W. Williams—386(A)
Internal resistance; correlation with other physical properties, R. L. Wegel, H. Walther—402(A)

Wave mechanics (see **Mechanics, quantum, etc.**)

X-rays, absorption
Fine structure, J. D. Hanawalt—399(A)
Fine structure in Ca K edge, V. P. Barton, G. A. Lindsay—391(A)

X-rays, diffraction scattering, reflection and refraction

From calcite for wave-lengths 1.5 to 5A, L. G. Parratt—561; S. K. Allison—688(L)
From crystals oscillating piezoelectrically, J. M. Cork—391(A)
Diffuse scattering from NaF, G. E. M. Jauncey, P. S. Williams—127
Formula for scattering, Y. H. Woo—21
Reflecting and resolving power of calcite, S. K. Allison—1; 688(L)
Scattering from solids, A. W. Coven—422
Spectrum of scattered radiation, J. A. Gray—397(A)
Width of modified line, J. W. M. Du Mond—398(A)

X-rays, emission

Errata, shape of an x-ray line, A. Hoyt—110
Soft x-rays of heavy elements, C. Del Rosario—136
Survey of *K*-satellites, O. R. Ford—571
Yield of fluorescent x-rays, D. K. Berkey—390(A)

X-rays, polarization

Faraday effect with x-rays, D. K. Froman—693

X-ray spectra and spectroscopy, wave-length measurements

Additional theory of plane gratings, R. C. Spencer—392(A)
Crystal secondary structure and the interference of x-rays, H. M. Evjen—265
By ruled gratings, R. B. Witmer, J. M. Cork—391(A)
Status of wave-length measurements, J. A. Bearden—399(A)

X-ray tubes, apparatus

Double-crystal x-ray vacuum spectrometer, L. G. Parratt—553

Zeeman effect

In Ca *H* bands, W. P. Cunningham—389(A)
Of Pb III, J. B. Green, R. A. Loring—389(A)
And perturbations in CO and N_2^+, W. W. Watson—378(L)

CURRENT LITERATURE OF PHYSICS

Extracts from the Tables of Contents of Some of our Contemporaries

NATURE

VOL. 130, No. 3277 — AUGUST 20, 1932

Letters to the Editor:

Theory of Induced Polarities in Benzene. By **A. Lapworth and R. Robinson** 273
Diffraction of Gas Atoms. By **H. S. W. Massey and C. B. O. Mohr** 276
Velocity of Light. By **Roy J. Kennedy** 277

ZEITSCHRIFT FÜR PHYSIK

VOL. 77, 5 AND 6 — AUGUST 2, 1932

Kinetics of Crystallization Processes. By **Frhr. v. Göler und G. Sachs** 281
Experiment on the Recombination of Hydrogen Atoms on Metallic and Oxidized Nickel. By **L. S. Ornstein and A. A. Kruithof** 287
Stark Effect of Hydrogen Lines. By **Karl Sjögren** 290
Interaction of Two Electrons. By **H. Bethe and E. Fermi** 296
Inverse Stark Effect in the Second Members of the Principal Series of Rubidium and Caesium. By **Y. T. Yao** 307
Remark on the Radiation Disintegration Theory of Matter. By **H. Hönl** 317
Comment on the Theory of the Thermoelectric Effect. By **Wolfgang Kroll** 322
Least Current Strength in the Normal Cathode Fall and the Positive Space Column. By **A. Güntherschulze and Herbert Schnitger** 333
Sensitivity of the Zero Instrument in Bridge Circuits for the Measurement of Alternating Potentials. By **W. Spielhagen** 346
Drift Velocity of Electrons. By **M. Didlaukis** 352
Potential of Carrier Formation in Helium. By **Arnold Plümer** 356
Long Wave-Length Portion of the Visible Spectrum of the Night Sky. By **L. A. Sommer** 374
Reversal of Certain Radioactive Processes. By **H. Zanstra** 391
Remenance and Hysteresis of Magnetostriction in Nickel. By **F. Lichtenberger** 395
Theory of the Breadth of Coupling. By **V. Weisskopf** 398
Plastic Boundary Relations of Natural Rock Salt Subjected to Tension under Water. By **Luigi Piatti** 401
Quantitative Investigation of the Absorption Spectra of HBr and HI. By **Arun K. Data** 404
Quartz Double Monochromator and Vario-Illuminator with Mirrors in Place of Lenses for the Region from 0.2 to 3 mμ. By **Carl Leiss** 412
On A. Güntherschulze: Electrons, Protons and So-Called Electromagnetism. By **Emil Klein** 415
Remarks on the Work of R. Sewig: "Photoelectric Cells with Thin Film Alkali Cathodes." By **P. Selenyi** 420

PHYSIKALISCHE ZEITSCHRIFT

VOL. 33, No. 14 — JULY 15, 1932

Original Communications:

Extension of the Sum Rule for Alkalies with an Application to the Stark Effect. By **J. G. Kirkwood** 521
Free Rotation and the Dipole Moments of Formamide, Ethylene Chlorhydrine, Ethylene Glykol, Ethylene Diamine and Diethyl Succinate. By **C. T. Zahn** 525
Safety Devices for the Unattended Continuous Operation of High Vacuum Pumps. By **W. Pupp** 530

Phenomena Accompanying the Electro-optical Kerr Effect in High-Frequency Fields. By **H. Hoyer and L. Pungs** 531
Dispersion of the Electrical Conductivity of Aqueous Electrolytic Materials. By **M. E. Spaght** 534
The van der Waals Equation of State. I. By **K. Jablczynski** 536
Progress in Photography of Northern Lights. By **C. Störmer** 543
Determination of Electrometer Capacities. By **R. Rinkel** 544
Interpretation of the Curie-Weiss Law. By **C. J. Gorter** 546
Remarks on the Paper by G. Stetter. By **M. Laporte** 547

ANNALEN DER PHYSIK

VOL. 14, SERIES 5, NO. 2

Remark on Molecular Streaming. By **P. Clausing** 129
Remark on an Investigation of Streaming by Gaede. By **P. Clausing** 134
Thermal Conductivity, Wiedemann-Franz-Lorenz Number and Thermoforce of Mercury Crystals. By **Hermann Reddemann** 139
Electrical and Thermal Conductivity in Zinc and Cadmium Crystals. By **E. Goens and E. Grueneisen** 164
Agreement of the Regular with the Thermodynamic Temperature Scale below 0°. By **W. Heuse and J. Otto** 181
Gas Thermometric Determination of a Few Fixed Points below 0° with Tension and Resistance Thermometers. II. By **W. Heuse and J. Otto** 185
Electrical and Optical Behavior of Semi-Conductors. V. A Method for the Measurement of the Electrical Conductivity of Powders. By **A. Völkl** 193
Electrical and Optical Properties of Semi-Conductors. VI. Conductivity Measurements on Powders. By **P. Guillery** 216
Intensity Measurements on Raman Lines. By **Gerhard Ellenberger** 221

ANNALEN DER PHYSIK

VOL. 14, SERIES 5, NO. 3

Viscosity and Density in Flames. By **A. Becker and K. Vogt** 241
Ferromagnetism and Electrical Properties. V. The Thermomagnetic Effect in Longitudinal Magnetic Fields. Observations on Nickel and Iron. By **Heinz Broili** 259
Influence of Gases on Barkhausen Vibrations. By **Hans Rindfleisch** 273
Refinement of the Bridge Method for Measuring Electrolytic Resistances at High Frequencies. By **W. Geyer** 299
Relativistic Quantum Dynamics of the Problem of Many Bodies. By **Hellmut Seyfarth** 321
Absorbing Power of the Black and White Surfaces of Radiometers. III. By **E. Hasché** 342

COMPTES RENDUS

VOL. 195, NO. 5 — AUGUST 1, 1932

International Electrical Congress of 1932. By **Paul Janet** 348
Quantitative Study of the Adsorption of Metallic Cations by Cellulose. By **P. Pascal and J. Hansot** 349
Prediction of the Action of a Rapidly Varying Wind. Application to the Katzmayr Effect and to the Autorotation. By **A. Lafay** 358
Variations in the Absorption of the Atmosphere. By **G. Rougier** 363
Permeability of a Vacuum and the Theorems of Chipart. By **J. Cayrel** 366
Excitation of Atomic Rays by an Electromagnetic Discharge of High Frequency. By **Armand Bogros and Félix Esclangon** 368
Realization of a Photoelectric Polarimeter. By **G. Bruhat and P. Chatelain** 370
Fluorescence of an Atomic Beam of Zinc. By **P. Soleillet** 372
Partial Absorption in the X-Ray Region. By **F. C. Chalklin and L. P. Chalklin** 374
Response of a Gas-Filled Photoelectric Cell to Rapid Illumination. By **P. Fourmarier** 378
Chemical Inertia. By **Lemarchands and Jacob** 380

Influence of Temperature on the Structure of Nitrocellulose Films. By **Desmaroux and Mathieu** 383
Selective Adsorption by Silica Jel in Ammoniacal Solutions of Heavy Metals. By **Berthon** 384
X-Ray Study of the Chitine d'Aspergillus Niger, of Psalliota Campestris and Armillaria Mellea. By **Y. Khouvine** 396

LE JOURNAL DE PHYSIQUE

VOL. 3, NO. 8 AUGUST, 1932
Chlorides of Nickel and Cobalt in Solution. Magnetic Varieties. Linear Relations between Curie Constants and Curie Points. By **B. Foëx** 337
New Theory of the Flowing of Very Rarefied Gases. By **R. Darbord** 345
Electro-acoustical Lissajous Curves. By **Z. Carrière** 355

REVUE D'OPTIQUE

VOL. 11, NO. 5 MAY, 1932
Visibility of Marks Lighted by a Projector. Part I: Generalities. Elementary Calculation of the Brilliancies and Contrasts. By **Yves Rocard** 193
Measurement of Reflecting Powers. By **M. Duffieux** 212
Arrangement for the Study of Double Refraction of Industrial Glasses. By **J. Escher-Desrivieres** 215
Photometric Apparatus for the Measurement of Transmission and Reflecting Factors of Optical Instruments 222

BUREAU OF STANDARDS JOURNAL OF RESEARCH

VOL. 9, NO. 4 OCTOBER, 1932
Synthesis, Purification and Certain Physical Constants of the Normal Hydrocarbons from Pentane to Dodecane of *n*-amyl Bromide and of *n*-normal Bromide. By **B. J. Mair** 482
Study of Some Ceramic Bodies of Low Absorption Maturing at Temperatures below 1,000°C. By **R. F. Geller and D. N. Evans** 483
Determination of Magnesia in Phosphate Rock. By **James I. Hoffman** 484
Collisions of the First and Second Kind in the Positive Column of Caesium Discharge. By **F. L. Mohler** 485
Areas and Tensile Properties of Deformed Concrete-Reinforcement Bars. By **A. H. Stang, L. R. Sweetman and C. Gough** 486
Calorimetric Method for Determining the Intrinsic Energy of a Gas as a Function of the Pressure. By **Edward W. Washburn** 487
Photographic Emulsion; Variables in Sensitization by Dyes. By **Burt H. Carroll and Donald Hubbard** 488
Method for the Separation of Rhodium from Iridium and the Gravimetric Determination of these Metals. By **Raleigh Gilchrist** 489
Isoelectric Point of Silk. By **Milton Harris** 490
Effective Applied Voltage as an Indicator of the Radiation Emitted by an X-Ray Tube. By **Lauriston S. Taylor, George Singer and C. F. Stoneburner** 491
Column Curves and Stress-Strain Diagrams. By **William R. Osgood** 492

JOURNAL OF THE OPTICAL SOCIETY OF AMERICA

VOL. 22, NO. 9 SEPTEMBER, 1932
Sensitization of Ordinary Photographic Plates to Wave-Lengths below 2500A. By **A. J. Allen and R. G. Franklin** 469
Limitations of a Blanket Calibration Chart for Reading Dispersions of the Abbe Refractometer. By **Laurence Ellsworth Dodd** 477
Simplified Method of Preparing Schumann Plates. By **J. J. Hopfield and E. T. S. Appleyard** 488
Use of Plane Transmission Gratings. By **H. M. Reese** 496

THE REVIEW OF SCIENTIFIC INSTRUMENTS

VOL. 3, NO. 9 SEPTEMBER, 1932

Precision Aperiodic Thermostat. By **Otto H. A. Schmitt and Francis O. Schmitt** 467
Simple Device for Demonstrating Brownian Movement in Gases. By **D. A. Wells and William Lange** 474
New Type of Vacuum or Circulating Pump. By **E. L. Harrington** 476
High-Speed High-Vacuum Diffusion Pumps. By **Immanuel Estermann and Harold T. Byck** 482
Method of Measuring the Maximum Intensity of Light from the Photoflash Lamps or from Other Sources of Short Duration. By **W. E. Forsythe and M. A. Easley** 488
Improved Laue Camera. By **H. Kersten and William Lange** 493
Hydrogen Discharge Tube for the Continuous Ultraviolet Spectrum. By **H. C. Urey, G. M. Murphy and J. A. Duncan** 497
Frequency Requirements and the Control of Frequency for Synchronous Motor Operation of Astronomical Telescopes. By **G. W. Moffitt** 499

PHYSICS

VOL. 3, NO. 3 SEPTEMBER, 1932

Some Measurements on the Vapor Viscosities of the Two Common Pentanes, Two Pentenes and Carbon Tetrachloride. By **William M. Bleakney** 123
Crystal Structure of Black Nickel. By **H. Kersten and Joseph Maas** 137
Capillary Fow Through an Ideal Uniform Soil. By **W. O. Smith** 139
Penetration of Hydrogen Through Steel at Four Thousand Atmospheres. By **Thos. C. Poulter and Lester Uffelman** 147
Semiportable Alternating-Current Susceptibility Meter. By **William M. Barret** 149
Reduced Scale Studies in Armor Penetration. By **L. Thompson** 155

THE AMERICAN INSTITUTE OF PHYSICS

Incorporated

GOVERNING BOARD

Representing The American Physical Society:
KARL T. COMPTON, Massachusetts Institute of Technology, Chairman of the Board
GEORGE B. PEGRAM, Columbia University, Secretary of the Board
JOHN T. TATE, University of Minnesota

Representing The Acoustical Society of America:
H. D. ARNOLD, Bell Telephone Laboratories
HARVEY FLETCHER, Bell Telephone Laboratories
DAYTON C. MILLER, Case School of Applied Science

Representing The Optical Society of America:
PAUL D. FOOTE, The Gulf Companies
LOYD A. JONES, Eastman Kodak Company
F. K. RICHTMYER, Cornell University

Representing The Society of Rheology:
E. C. BINGHAM, Lafayette College
WHEELER P. DAVEY, The Pennsylvania State College
A. STUART HUNTER, du Pont Rayon Company

Representing The American Association of Physics Teachers:
HOMER L. DODGE, The University of Oklahoma
PAUL E. KLOPSTEG, Central Scientific Company
FREDERIC PALMER, Haverford College

ADMINISTRATIVE STAFF

HENRY A. BARTON, *Director*
JOHN T. TATE, *Adviser on Publications*
MADELINE M. MITCHELL, *Editorial Secretary*
Office: 11 East 38th Street, New York, New York

The Institute is a membership corporation whose object is to provide the five Founder Societies, whose representatives form the Governing Board, with an agency suitable for cooperative undertakings. The principal work of the Institute at present is the publication of the journals sponsored by the Societies. The journals will continue to be edited for the most part under the direction of the several Societies, but the mechanical details of editing and the business management of the journals has been, or soon will be, transferred to the Institute.

Journals now, or shortly to be, published by the Institute of Physics:

THE PHYSICAL REVIEW REVIEWS OF MODERN PHYSICS PHYSICS	JOHN T. TATE, *Managing Editor* J. W. BUCHTA, *Assistant Editor*
JOURNAL OF THE OPTICAL SOCIETY OF AMERICA THE REVIEW OF SCIENTIFIC INSTRUMENTS	F. K. RICHTMYER, *Editor-in-Chief*
JOURNAL OF THE ACOUSTICAL SOCIETY OF AMERICA	F. R. WATSON, *Chairman Editorial Board* WALLACE WATERFALL, *Managing Editor*

JOURNAL OF RHEOLOGY—E. C. BINGHAM, *Managing Editor*

The Institute represents about 5000 members and subscribers who are devoting themselves to physics by research, by application of its principles, by teaching or by study. It is part of its purpose to foster cooperative relations between physicists and the science of physics on one hand and allied sciences, the arts and industries on the other. It is empowered to administer grants and endowments.

GEORGE BANTA PUBLISHING COMPANY, MENASHA, WISCONSIN